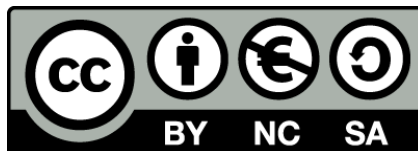




UNIVERSITAT DE  
BARCELONA

# Development of cellular microarrays for stem cell culture and early stage differentiation evaluation

Santiago Andrés Rodríguez Seguí

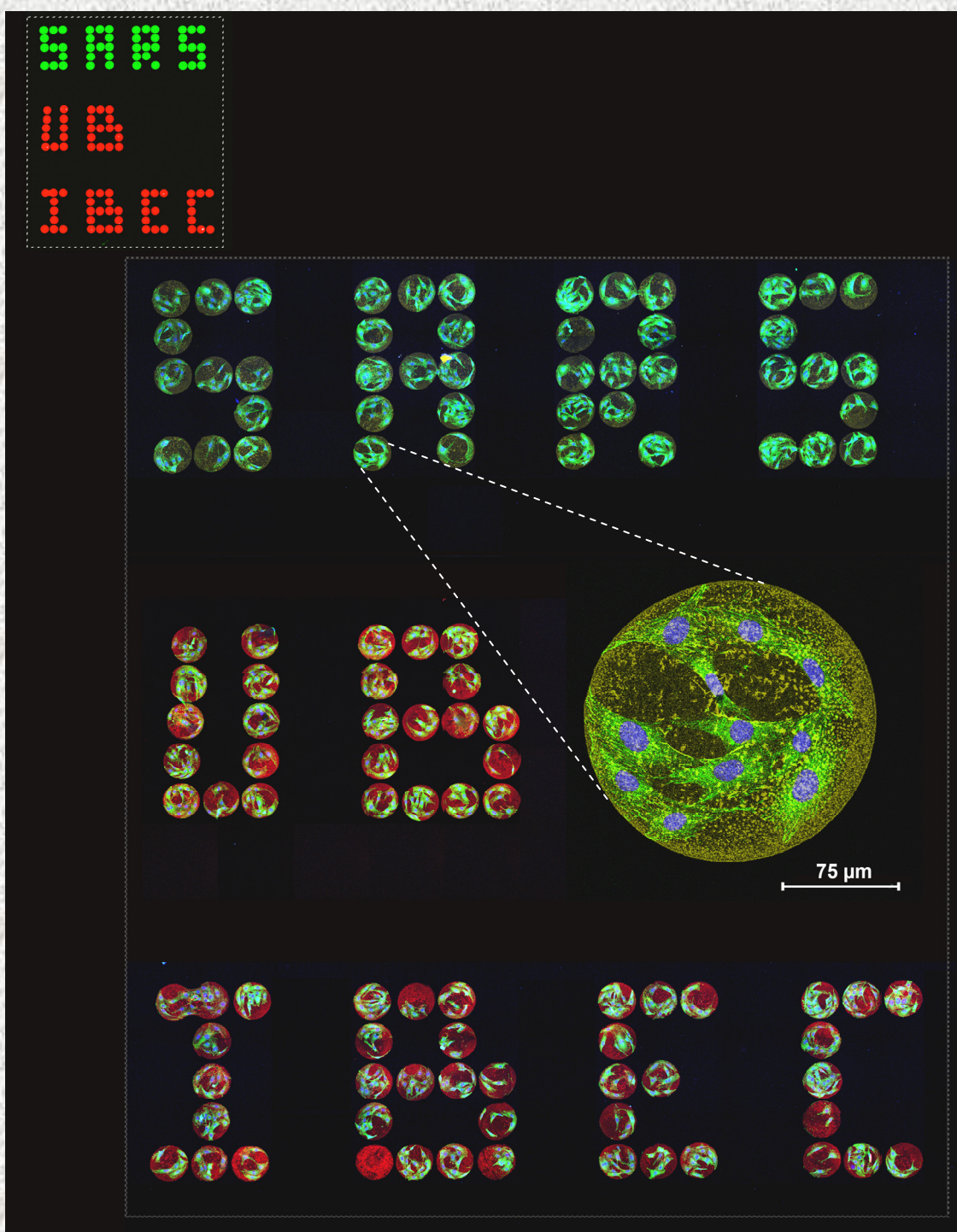


Aquesta tesi doctoral està subjecta a la llicència [Reconeixement- NoComercial – Compartirlqual 4.0. Espanya de Creative Commons](#).

Esta tesis doctoral está sujeta a la licencia [Reconocimiento - NoComercial – Compartirlqual 4.0. España de Creative Commons](#).

This doctoral thesis is licensed under the [Creative Commons Attribution-NonCommercial- ShareAlike 4.0. Spain License](#).

# Development of cellular microarrays for stem cell culture and early stage differentiation evaluation



Santiago Andrés Rodríguez Seguí







# **Development of cellular microarrays for stem cell culture and early stage differentiation evaluation**

*Memoria presentada por*

**Santiago Andrés Rodríguez Seguí**

*para optar al grado de **doctor en Biomedicina***

**Departamento de Electrónica**

Universidad de Barcelona

Programa de Doctorado: “**Biomedicina**”

Bienio 2007-2009

Directores: **Profesor Josep Samitier Martí y Dra. Elena Martínez Fraiz**



**Barcelona, Enero de 2010**

**Front cover image:** Composite image. The top left image was obtained with a fluorescent scanner device and shows protein spots immobilised on a chemically activated glass surface. Spots are composed of unlabelled fibronectin and streptavidin labelled with Alexa Fluor 647 (red fluorescence spots), or fibronectin labelled with Alexa Fluor 555 (green fluorescence spots). The main image in this composition has been produced by the superimposition of several pictures taken using a confocal microscope, and shows C2C12 cell attachment to the spotted protein layout. The fluorescence signal from the Alexa Fluor 555 fluorophore is presented in yellow in this image, cell nuclei are stained in blue and paxillin (a protein of the cytoskeleton) is stained in green. The zoom-in image shows a detail of the attachment of cells to one of the spots. The 75  $\mu\text{m}$  scale bar corresponds to the zoomed-in image.

**Back cover image:** Composite image showing two fibronectin spots (immnostenated in red) seeded with mesenchymal stem cells (with nuclei stained in blue). This image has been superimposed with the silhouette of a muslim man entering at the Al-Karaouine mosquée in Fez, Morocco, recongnised as the oldest continuously operating university in the world. The original image was taken and modified by the author of this PhD thesis, and is presented in the Appendix D.II (Image 3) of this work.

*Life is just what happens to you while you're busy making other plans*

John Lennon, “Beautiful Boy”

*Traducción al castellano: “La vida es justamente aquello que pasa mientras estás ocupado haciendo otros planes”*



*On ne voit bien qu'avec le cœur.*

*L'essentiel est invisible pour les yeux.\**

**A Cynthia,**

**A Bruno,**

\* Antoine de Saint-Exupéry, “Le petit prince”

*Traducción al castellano: “Sólo con el corazón se puede ver bien. Lo esencial es invisible a los ojos”*



# Agradecimientos

Al momento de escribir estos agradecimientosuento ya cuatro años y medio de trabajo en mi tesis doctoral y, como todo en la vida, es una etapa que se acerca a su final para dar lugar a otra. En este punto, me complazco en mirar hacia atrás y ver que la travesía ha valido la pena. Estos últimos años de mi vida han implicado mucho mas que la realización de una tesis doctoral, ya que para mi estarán entrañablemente asociados también con hechos de la vida personal como son el haber partido a vivir lejos de mi tierra, de mi familia, y comenzado una convivencia de pareja que trajo, entre otras alegrías, el nacimiento de mi hijo Bruno hace ya 2 años, y otro hermanito/a en camino. En este espacio quiero dedicar unas palabras a todas esas personas que me han hecho crecer como científico y como ser humano.

A mis directores de tesis, el Profesor Josep Samitier y la Dra. Elena Martínez. A Josep por haber creído en aquel muchacho que cayó un día en su despacho con una idea de tesis distinta a la que en ese momento estaba desarrollando. Gracias también por haber puesto todos los medios que tuvieron a su alcance para que esta tesis sea lo que es, y por haberme apoyado en cada una de mis iniciativas. A Elena por haberme guiado en el día a día del desarrollo de esta tesis. Con ella hemos visto erigirse en trabajos científicos aquellas medidas experimentales muchas veces difíciles de interpretar. Me es imposible dejar fuera de estos primeros agradecimientos al Dr. Abdelhamid Errachid. La historia de esta tesis no es tan lineal, y comenzó con una reunión “de paso” con Erra, en su entonces despacho del laboratorio de Nanobio. Él fue quien en ese primer momento me abrió las puertas para ingresar en este grupo y quien me guió durante el primer año de mi doctorado, cuando aún estaba enfocado en el empleo de la microbalanza de cuarzo. He aprendido muchas cosas de él y, sobretodo, no olvidaré nunca su generoso y desinteresado gesto al haberme permitido cambiar el objetivo de mi tesis, aun sabiendo que eso implicaba una desvinculación profesional, aunque no personal, con él.

A la Dra. Elisabeth Engel, quien ha sido mi instructora inicial en los aspectos biológicos de esta tesis y que, junto con Elena, me ayudó con la redacción de mi primer trabajo científico con los microarrays celulares, me será difícil olvidar esas tardes de discusión científica en la cafetería del Parc. A Miriam Funes quien me enseñó las técnicas básicas de cultivo y tinción biológicas. Al Dr. Francesc Ventura, quien aportó la idea de aplicación biológica que forma parte del capítulo final de esta tesis, y a María José por su colaboración. Al Dr. Xavier

Fernández Busquets, por su colaboración en los trabajos que emprendí al principio. A mis amigos del departamento de electrónica (el Jordi O., Sergio, Oscar, Rubén, Jordi S., Jordi C., Ivón), gracias por haberme recibido con los brazos abiertos en mis comienzos del doctorado.

A mis compañeros del Nanobiolab, Anna, Christian, Coco, David C., David I., Eva, Isabel, Jordi C., Juan Pablo, Juanjo, Marília, Maruxa, Mathias, Mónica, Muriel, Nadia, Patricia, Sabine, Sam y Xavi S. A los que una vez lo fueron y ya han emprendido un nuevo viaje: Javi, Chris, Marc, Jordi, Nacho, Mateu y Ramona.

A ese grupo de amigos de Barcelona, que pasaron a ser mi familia sustituta en muchos casos. Gracias a Romén, María, Mariano, Alicia, Paz, Lorena, Manuel y Goretti, por todos los innumerables buenos momentos que hemos compartido en este tiempo y por haberme hecho sentir como en casa. Y también al grupo extensivo, que he conocido más recientemente: Paolo, Nacho, Braulio, Carlos, Giulia, Davide y Simone.

A mis amigos de la Facultad y de Paraná (Beto, el Colo, Pablo, Diego, el Cordobés, Germán, Nati y Sabi), gracias por los buenos momentos compartidos a lo largo de esa etapa clave de mi vida. A mis amigos de toda la vida, Mauro, Augusto y Fernando. En reconocimiento de los buenos recuerdos y porque a pesar de la distancia los siento parte de este viaje.

A mis padres, por haberme guiado y apoyado siempre en todas las decisiones importantes y gracias a eso he logrado llegar hasta acá. A mis hermanos, Diego y Ale, porque sé que mi lejanía de la familia hizo que muchas cosas recaigan en mayor medida sobre ellos, pero a pesar de todo me apoyaron para seguir con este camino.

Finalmente, mi reconocimiento más especial a Cynthia, mi pareja y compañera de aventuras. Gracias por haber aceptado el desafío de vivir en España, por haber soportado el extrañar a tu familia y tus amigos y también por haberme dado el hermoso hijo que tenemos. Me alegra de haber compartido los buenos y los malos momentos con vos y también gracias por haberme permitido compartir los tuyos. Y claro, tampoco voy a dejar de agradecerle a mi hijo Bruno. Por haber cambiado el centro de gravedad de mi vida y haberme hecho ver mis acciones desde otra perspectiva completamente nueva e inesperada para mí antes. Gracias a esta nueva familia, porque junto a ellos sigo creciendo y madurando día a día.

Al escribir estos párrafos, me dí cuenta de que hice una vista hacia atrás para recordar todos aquellos acontecimientos que de una u otra forma marcaron mi vida y que, puestos en perspectiva, dejan entrever un futuro emocionante en el cual se encuentran escondidos los agradecimientos que hoy, aún, no puedo expresar. ¡Salud!

# Index

Agradecimientos.....	ix
Index.....	xi
Preface .....	xiii
List of abbreviations.....	xv
Chapter 1 Introduction .....	1
1.1 Microarray-based techniques .....	1
1.2 DNA microarrays .....	3
1.3 Protein Microarrays.....	6
1.3.1 Principle of detection.....	8
1.3.2 Immobilisation methods.....	9
1.3.3 Applications of protein microarrays.....	11
1.4 Cellular Microarrays.....	14
1.4.1 Applications.....	19
1.4.2 Scope and aims for this thesis .....	27
Chapter 2 Quantitative characterisation and comparison of protein immobilisation on substrates for cellular microarray applications.....	29
2.1 Introduction .....	29
2.2 Materials and methods.....	33
2.2.1 Proteins and chemicals .....	33
2.2.2 Substrate preparation .....	33
2.2.3 Substrate characterisation previous to the protein microarray fabrication.....	36
2.2.4 Protein microarray fabrication.....	37
2.2.5 Protein microarray characterisation.....	39
2.2.6 Statistics .....	41
2.3 Results .....	42
2.3.1 Substrate characterisation previous to the protein microarray fabrication.....	42
2.3.2 Qualitative protein microarray comparison among substrates .....	45
2.3.3 Analysis of the spot size and morphology of the protein microarrays.....	48
2.3.4 Fluorescence signal calibration curves for the spotted substrates .....	70
2.3.5 Immobilised protein quantification: spots containing Fn only .....	74
2.3.6 Immobilised protein quantification: spots containing Fn and SA protein mixtures....	84
2.3.7 Global analysis .....	91
2.4 Conclusions .....	95
Chapter 3 Cellular microarray fabrication and characterisation .....	97
3.1 Introduction .....	97
3.2 Materials and methods.....	98
3.2.1 Proteins and chemicals .....	98
3.2.2 Cell isolation and culture.....	99
3.2.3 Evaluation of cell differentiation.....	101
3.2.4 Microarray fabrication.....	101
3.2.5 Microarray characterisation.....	104
3.2.6 Statistics .....	106
3.3 Results .....	106
3.3.1 Protein deposition in a microarray format.....	106

3.3.2 Cell culture in the microarrays .....	110
3.3.3 Mesenchymal stem cell differentiation .....	127
3.4 Conclusions .....	132
Chapter 4 Application: Analysis of early differentiation stages using a cellular model .....	135
4.1 Introduction .....	135
4.2 Materials and methods .....	138
4.2.1 Proteins and chemicals .....	138
4.2.2 Cell culture .....	138
4.2.3 Microarray fabrication .....	139
4.2.4 Fabrication of substrates with large-area protein surfaces .....	142
4.2.5 Protein microarray characterisation .....	143
4.2.6 Characterisation of cell cultures .....	143
4.2.7 Statistics .....	144
4.3 Results .....	144
4.3.1 Protein microarray characterisation .....	144
4.3.2 Cellular microarray fabrication and characterisation .....	151
4.3.3 Cell differentiation at 24 h – Osterix gene expression analysis .....	161
4.3.4 Cell differentiation after 4 days – ALP activity analysis .....	176
4.4 Conclusions .....	180
4.5 Future work .....	181
Chapter 5 Conclusions of the thesis .....	183
Appendix A Devices for microarray fabrication .....	185
Appendix B Devices and methods used for microarray characterisation .....	188
Appendix C Suitability of the substrates chosen for cellular microarray fabrication .....	199
Appendix D Miscellaneous .....	201
Appendix E Publications and conference communications .....	211
Resumen en castellano - Desarrollo de microarrays celulares para el cultivo de células madre y la evaluación de estadios tempranos de diferenciación .....	215
Prefacio .....	215
Capítulo 1 Introducción .....	216
Capítulo 2 Caracterización y comparación cuantitativa de la inmovilización de proteínas en substratos para aplicaciones de microarrays celulares .....	220
Capítulo 3 Fabricación y optimización de los microarrays celulares .....	229
Capítulo 4 Aplicación: Análisis de estadios tempranos de diferenciación usando un modelo celular .....	235
Capítulo 5 Conclusiones de la tesis .....	244
References .....	247

# Preface

The topic of this thesis deals with the development of a relatively new technique known as cellular microarrays. In particular, when dealing with stem cell culture, cellular microarrays have been reported from 2004 and on. Despite a broad range of applications could be devised for the cellular microarrays aiming at targeting stem cell differentiation to specific cell types, when turning it to practice it was found that certain limitations appeared in the state of the art of cellular microarray development. Further basic research was needed to yield insights into the technological parameters affecting cell response in cellular microarrays, and this actually leaded to the current aims of this thesis. As an example, the first cellular microarray report that could be found dealing with stem cell differentiation in response to printed extracellular matrix proteins was published in 2005, by the time the work on this PhD thesis was begun. Other reports appeared in the following years, defining the trends and challenges in this area of research. The present work was developed in this context of novelty, and this explains why most of the literature reports cited for cellular microarrays date from the period during which this thesis has been developed. The work presented here is the result of 4 years of research at the Nanobioengineering group of the Institute for Bioengineering of Catalonia (IBEC) and the department of Electronics of the University of Barcelona.

This thesis is divided into 5 chapters. In the introduction (Chapter 1) an overview of the general microarray-based techniques is provided, with special the emphasis in cellular microarrays. The recent achievements and main limitations of this technique are presented to introduce the motivation of this work. The scope and aims for this thesis are presented at the end of this chapter. The following chapters describe the experimental work performed and the results obtained to accomplish each of the proposed aims. In Chapter 2, a characterisation of several substrates for cellular microarray applications has been carried out based on the quantity of protein immobilised by each of them after printing and washing. This is an important issue when dealing with cellular microarrays, since it is the immobilised proteins which are expected to interact with cells attached on top of them, therefore if low or no protein is left, no cell interaction will take place and the microarray application would be void. From this analysis, the substrate appearing as best candidate was chosen to accomplish the following aims of this thesis. In Chapter 3, the cellular microarray fabrication parameters were optimised for culture of

mesenchymal stem cells in the microarray up to 8 days. These cells are a very promising source of stem cells for cell therapies and therefore the adaptation of cellular microarrays for the future study of some of its differentiation stages is highly appealing. In Chapter 4, an approach to the study of stem differentiation using the previously optimised cellular microarray protocol is presented, reporting the early cell differentiation in response to a printed growth factor and identifying new challenges to overcome in the future. In Chapter 5 the conclusions of this thesis are presented. In Appendix A, the devices used for cellular microarray fabrication are described. Appendix B deals with the devices and methods used for microarray characterisation. Appendix C presents a preliminary test of substrates in terms of their suitability for cellular microarray formation. Appendix D includes miscellaneous work that was produced during the development of this thesis, and deals mostly with presenting science in a non-conventional way to approach a non-expert public. In particular, a short commentary on stem cell differentiation and nanotechnology and several scientific images modified to introduce additional “artwork” to make them more attractive to a non-specialized public are presented. Finally, Appendix E presents the scientific publications and the conference communications published.

# List of abbreviations

AD-Agarose: Aldehyde derivatised agarose substrate

AD-Glass: Aldehyde derivatised glass substrate

a-PMMA: Chemically activated (PFP-COOH derivatised) PMMA substrate

BMP-2: Bone morphogenetic protein 2

BMP-4: Bone morphogenetic protein 4

BSA: Bovine serum albumin

BSA-Glass: BSA pre-coated glass substrates

CA: Contact angle

cDNA: Complementary deoxyribonucleic acid

CNTF: Ciliary neurotrophic factor

Col I: Collagen I

Col III: CollagenIII

Col IV: Collagen IV

Ctrl-Glass: Control glass substrate

CV intra: Coefficient of variation intra-slide

DNA: Deoxyribonucleic acid

ECM: Extracellular matrix

EGF-1: Epidermal growth factor 1

FBS: Foetal bovine serum

FGF-2: Fibroblast growth factor 2

Fn: Fibronectin

HEK293: Human embryonic kidney cells

hMSC: Human Mesenchymal stem cells

ITS: Insulin-transferrin-sodium selenite (media supplement)

Ln: Laminin

MDSC: Muscle derived stem cells

NGF-3: Nerve growth factor 3

NT-3: Neurotrophic factor 3

PBS: Phosphate buffered saline

PC12: Rat adrenal phoeochromocytoma cells

PDMS: Poly(dimethylsiloxane)

PEO-like: Poly(ethylene) oxide-like coated glass substrate

PLL. Poly-L-lysine

PMMA: Poly(methyl methacrylate)

PMT: Photomultiplier tube gain

PS: Polystyrene

RNA: Ribonucleic acid

RT: Room temperature

SD: Standard deviation

SNR: Signal to Noise Ratio

tPS: Tissue culture polystyrene

# Chapter 1      Introduction

## 1.1 Microarray-based techniques

High-throughput microarray-based screening techniques have been the focus of intense research in the last decades.<sup>1, 2</sup> Their main advantage is to allow a massive, parallel and miniaturized approach to molecular and cellular biology analysis by detecting multiple analytes in a sample through affinity-binding events at a surface interface. The high-throughput multiplexed data obtained from a single experiment is usually the equivalent of performing hundreds of individual experiments by the standard molecular biology techniques, therefore providing a faster and low sample consumption alternative, with higher quantitative accuracy and sensitivity.

A microarray consists of a substrate on top of which different molecules have been immobilised as separated spots in an array format with a specific and known layout. When this substrate is incubated with a sample solution, specific and parallel reactions take place between the surface-immobilised molecules and the molecules present in the sample. The product of these reactions can be analysed with the help of site-specific reading detectors, thus providing information about the sample solution.

A microarray application usually involves the steps presented in Figure 1.1. First of all, the microarray is fabricated by “printing” (immobilising) the substances of interest on top of a substrate. Next, the spotted substrate is submerged in a solution to passivate non-printed areas and avoid unspecific molecule attachment there, and then it is incubated with the sample. After a certain time of incubation, the sample is removed, the microarray is washed to remove any unspecifically bound material and then it is labelled using appropriate protocols, which usually involve some kind of fluorescent staining,<sup>3</sup> to reveal the recognition events that took place during the incubation with the sample. The last step consists of “reading” the microarray results. For this purpose the slide can be scanned using a fluorescent scanner device, as is usually the case for DNA and protein microarrays, or imaged using a microscope, which is most common for tissue and cellular microarrays.

Microarray technology was initially applied to DNA microarrays and has evolved from there to antibody microarrays and, finally, to other types of microarrays such as carbohydrate,

enzyme, protein (other than antibodies), tissue and cellular microarrays.<sup>4</sup> The main difference between these types of microarrays resides in the substances or molecules that are printed in the spots. Therefore, a carbohydrate microarray consists of an array of different carbohydrates printed on a substrate, while an enzyme microarray deals with enzymes. Analogously, a tissue microarray has complex mixtures of tissue spotted in a microarray format and a cellular microarray has cells attached in isolated spots on top of a surface. The events taking place between the surface-immobilised agents and the sample molecules can be extremely varied, based on the microarray type used, but usually involve DNA or protein recognition from a complex sample.

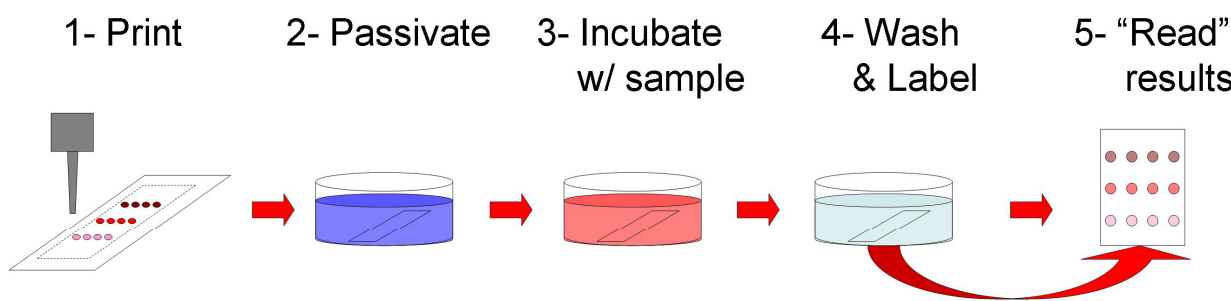


**Figure 1.1** Schematic of a generic microarray application. A microarray application usually involves the fabrication of the microarray by printing the substances of interest (1), passivation of the non-printed surface (2) incubation with the sample (3), washing, to remove any unbound substances from its surface, and labelling (4) to reveal the recognition events that took place. The final step (5) is to “read” the results by using a fluorescent scanner device or a microscope to image the spots.

The nomenclature adopted here to describe the microarray applications uses the term “probe” to refer to known molecules involved, while “target” is used to describe the unknown molecules, which will be recognised through the microarray application. Therefore, the selective interaction taking place between the probes and the targets provides the recognition events which will be assessed.

The approaches used in microarray-based techniques can be broadly classified in 3 types:

- The probes are spotted on the substrate and the microarray is incubated in a complex sample of unknown composition (i.e. the targets). The desired outcome is the **recognition of targets present in the test sample**. Quantitative results using this approach can be obtained by calibration with standardised analytes. This approach is often used in DNA and antibody microarrays.

- The target solution (or sample) is printed in the spots and, then, the spotted microarray is incubated in a solution with a limited number of probes which will selectively attach to spots containing their targets. The desired outcome is the **recognition of targets present in the spots**. This approach is often used for tissue microarrays, but also for DNA and protein microarrays. These microarrays usually provide semi-quantitative information.
- The composition of the printed spots is known and cells are cultured exclusively on top of the printed spots. The desired outcome is a **response of the cells to the printed factors**. This approach is referred to as cellular microarrays and provides semi-quantitative information.

DNA microarrays are by now a well-established technique in biology laboratories<sup>1</sup> and are commercially available from many different sources.<sup>5</sup> Antibody microarrays have also yielded some commercial applications to date.<sup>6</sup> For other types of microarrays, however, mostly proof-of-principle studies have been published in the literature so far.<sup>2</sup> Following the microarray developmental “evolution line”, in the following sections DNA, protein and cellular microarrays are reviewed.

## 1.2 DNA microarrays

The concept of microarray technology dates from the late 1970s.<sup>7</sup> By then Kafatos *et al.* reported the use of a technique, named as “dot blot”, which consisted on spotting multiple samples of cloned deoxyribonucleic acid (DNA) of unknown composition in an array format on nitrocellulose paper.<sup>8</sup> At that time, DNA spotting was performed either manually or by means of a disposable pipette connected to a syringe pump. The array was then hybridised with a radioactive labelled complementary probe (a single DNA of known sequence) and the hybridisation ratio was semi-quantitatively evaluated after autoradiography. A variant of this method, named “reverse dot blot”, was introduced in the late 1980s.<sup>7</sup> In this case, probe DNA sequences of known composition were immobilised on a membrane and the target DNA was labelled. The first DNA arrays created on an impermeable support, in contrast to the membrane supports used until then, were reported by Maskos *et al.* in the early 1990s.<sup>9</sup> Those comprised short oligonucleotides synthesized *in situ* on a glass surface and were covalently attached to the glass.<sup>10</sup> At about the same time, Fodor and colleagues were developing the technology that definitely pushed DNA microarrays towards industry and the commercially available high throughput technique nowadays known.<sup>11, 12</sup> Their particular approach consisted in adapting the

photolithographic techniques, mostly used by the microelectronics industry, to carry out the parallel synthesis of a large number of oligonucleotides on solid surfaces. By this approach, they were able to manufacture arrays containing hundreds of thousands of oligonucleotide probe sequences on glass slides of less than 2 cm<sup>2</sup> in size.<sup>13</sup> Since then, and with the invaluable help of the polymerase chain reaction (PCR) technique to produce a virtually unlimited number of exact copies from specific DNAs, it was only a matter of time for DNA microarrays to become a widely used standard technique for research in genetics and molecular biology.<sup>1</sup> Another important advance into DNA microarrays was reported in 1997 by Lashkari *et al.*<sup>14</sup> In their work, the authors described the development of a complete eukaryotic genome (for the yeast *Saccharomyces cerevisiae*) integrated into a single high-density DNA microarray, and demonstrated its application for the parallel gene expression analysis at the whole genome level.

Nowadays, DNA microarrays are usually fabricated on glass, silicon or plastic substrates and are commercially available from many different providers such as Affymetrix (Santa Clara, CA, USA), TeleChem International Inc. (Sunnyvale, CA, USA), Agilent Technologies (Santa Clara, CA, USA) and others.<sup>5</sup> The most important techniques for DNA microarray fabrication are piezo-based (non-contact) inkjet or pin-based (contact) spotting techniques to print the DNA, and photolithography for the *in situ* microarray synthesis.<sup>5</sup> While the first ones can produce a spot density of up to 100 features per mm<sup>2</sup> (limited by the droplet size or the pin dimensions, Figure 1.2A), the photolithographic approach can yield ~8200 features per mm<sup>2</sup> and is the leader technique in density and quality control (Figure 1.2B).<sup>1</sup> However, the use of photolithography for microarray production results expensive due to the costs associated with the requirement of photolithographic masks and photolithography facilities. Contact and non-contact microarray spotting techniques, on the other hand, provide an easy approach to produce small lots of custom microarrays. Further details on these spotting techniques are provided in Appendix A.

To date, DNA microarrays have been reported for a wide variety of quantitative and semi-quantitative biological applications. Messenger RNA (mRNA) measurements are the most common applications of DNA microarrays due to the information that can be derived from an understanding of the function of genes in cells and tissues. The expression of a group of genes, known as an “expression profile”, can be compared between different tissues, across disease states and across experimental conditions such as drug treatments.

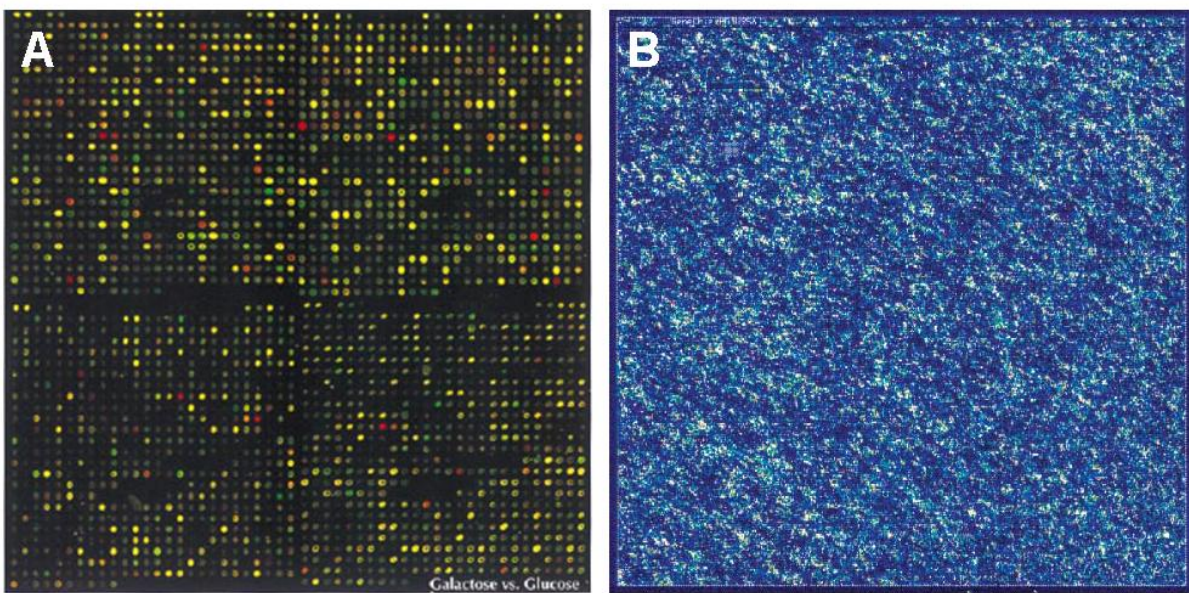


**Figure 1.2** Example of hybridised DNA microarrays. **A.** Image obtained from a two-colour fluorescent scan of a yeast microarray containing 2,479 elements in a  $\sim 1.8 \text{ cm}^2$  area, fabricated using a contact pin arraying robot. The microarray was hybridised to a complementary DNA mixture obtained from yeast cultures grown in either galactose (green signal) or glucose (red signal). Image reproduced from cited reference.<sup>14</sup> **B.** Data from an experiment showing the expression of thousands of genes on a single GeneChip® probe array from Affymetrix. The actual size of the GeneChip® array is  $1.28 \text{ cm}^2$ . Image courtesy of Affymetrix (obtained from the Affymetrix Image Library at [www.affymetrix.com](http://www.affymetrix.com), updated as of June 2009).

Cancer outcome prognosis can significantly benefit from DNA microarray analysis. Clinical treatment decisions based on data obtained from DNA microarrays is foreseen for the near future.<sup>1</sup> As an example, Alizbeth and colleagues fabricated DNA microarrays by spotting more than 17,000 complementary DNA clones, which were selected to recognise genes with preferential expression in lymphoid cells or genes with suspected roles in processes important in immunology and cancer. Using this chip, they reported the finding of predictive markers of survival in patients suffering from B-cell lymphoma.<sup>15</sup> Another report described the identification of 70 transcripts that predicted breast tumour metastasis using microarrays containing more than 25,000 human genes.<sup>16</sup> Weinstein *et al.* used the gene expression profiles of 60 cancer cell lines and combined them with growth inhibition data obtained for these lines under 118 drug treatments, with the aim of finding the mechanisms of drug action and their molecular targets.<sup>17</sup> In order to provide an understanding of the genetic alterations occurring in pancreatic cancers, Jones and colleagues reported the use of microarrays containing probes for  $\sim 10^6$  single nucleotide polymorphisms (i.e. DNA mutations).<sup>18</sup> Using this platform they were able to identify genetic alterations in cellular signalling pathways and processes in the pancreatic tumours analysed.

Hughes and co-workers reported in 2000 the use of microarrays containing more than 6,000 DNA probes (representing ~97 % of the predicted yeast *Saccharomyces cerevisiae* genome) to monitor hundreds of cellular functions simultaneously in samples obtained from mutated or chemically treated cells.<sup>19</sup> In another report, DNA microarrays applied for the analysis of changes in the gene expression profile as a response to compounds of known toxicity allowed the generation of toxicity landmarks in rat liver.<sup>20</sup> This information was shown to be useful for understanding the mechanisms of toxicity.

DNA microarrays can also be used to provide insights into infectious diseases, and aid in its early detection. As an example, Behr and co-workers reported the application of a DNA microarray containing 3,902 DNA selected probes to identify differences in the genomic composition between the *Mycobacterium tuberculosis* and the strain used in the BCG (Bacillus Calmette-Guerin) vaccine.<sup>21</sup>

The number of research reports involving the use DNA microarrays at some stage of the process continues to expand, as new applications are described in the literature. As briefly exposed here, DNA microarrays constitute a mature technique that has already been applied to the study of many different biology questions, from the discovery of biological pathways underlying toxicology responses to genetic alterations involved in cancer disease. New insights into biology pathways are expected to give, in a future, some solutions for these and other health-associated diseases. The current challenge for DNA microarrays resides in increasing the miniaturisation of the assay, which will lead to smaller hybridisation volumes and less reagents use, with the final objective of reducing costs and allow its use as point-of-care techniques in medical diagnosis. Another challenge consists in sharing and standardising the data obtained from DNA microarrays.

### **1.3 Protein Microarrays**

The general paradigm in cell biology is the DNA to ribonucleic acid (RNA) information passage, called transcription, and the RNA to protein information passage, called translation. The DNA is contained inside the nucleus of the cell (for eukaryotic cells); there it is transcript to RNA when adequate signals (proteins or smaller molecules) are provided. The transcript RNA exits the nucleus and is translated into proteins in the cytoplasm of the cell. These newly formed proteins, after going through different chemical and morphological modification steps, can follow different paths. Proteins can stay in the cell to fulfil its function there, either metabolic or as mediators in a signalling pathway. Proteins can also be inserted in the cell membrane and act

as cell-anchoring or as cell signalling receptor or, finally, they can be secreted outside the cell, thus becoming signals in response to a stimulus. Then, it is actually proteins that carry out the work in cells.

Proteins may be referred to in several different ways depending on their biological function and size. Therefore, a peptide is a “small” protein consisting of two or more amino acids; peptides larger than about 50 amino acid residues are usually classified as proteins. When protein function involves catalysis of biochemical molecules, which is an important process in cell metabolism, they are called enzymes. Antibodies (also called immunoglobulins) constitute a specific subset of proteins found in blood, with a molecular mass of ~150kDa, which are used by the immune system as recognition agents for foreign objects such as bacteria and viruses. They show an extremely high affinity-binding constant with their target probes, known as antigens.

Although gene expression profiling is usually performed by DNA microarray analysis at the RNA level, it could also be performed at the protein level. Protein concentration is in fact assumed to be more closely related to cell function than the mRNA is. In an attempt to address this issue, microarray technology has been adapted for the screening of protein-protein interactions by protein microarrays. A key role has been proposed for these microarrays as the link between the genome knowledge and the cell behaviour in healthy and disease states.<sup>4</sup>

Protein microarrays consist of spatially arranged protein spots printed on a suitable surface to create a high density microarray. These microarrays can be used to detect specific proteins present in a test sample by means of protein-protein recognition events.<sup>22</sup> The high affinity recognition binding between antibodies and their target proteins has been the base for the development of this technique.

However, it has proven to be technically much more difficult to achieve the equivalent of genome-wide profiling by using protein microarrays.<sup>4</sup> The main drawback is that identification or generation of protein recognition probes (equivalent of DNA hybridisation probes) is not trivial. While nucleic acids have in common four basic chemical units and a limited folding repertoire, proteins show a much more complex panorama with a wide range of polarities, hydrophobicities, charges, sizes and structures. Additionally, the proteome (i.e. the complete set of proteins that can be expressed by a genome) is much larger than the genome, meaning that there are more proteins than genes. It is expected that 300,000 to 500,000 yet-unknown proteins could be expressed by the 30,000 to 50,000 estimated coding genes within the human genome.<sup>4</sup>

Most important, there is no PCR-equivalent technique for proteins, which means that it is not possible to easily create unlimited exact copies of protein probes.

Protein microarrays find their origins in the early 1980s, as the protein version of a dot-blot hybridisation of immobilised DNA.<sup>4</sup> Interestingly, an antibody array using antibody spots on a solid surface for simultaneous and multiple detection of cell surface antigens was first demonstrated for the capture of cells (thymocytes and mononuclear cells)<sup>23</sup> and, a short time later, for the immunodiagnosis of proteins occurring in plasma.<sup>4, 24</sup> Even more, the first application reported by Fodor and colleagues regarding the use of photolithography for the array formation of biological materials involved a parallel chemical synthesis to produce a 1024 peptide array.<sup>11</sup> As mentioned before, shortly latter this technique showed its potentiality for DNA microarray fabrication.<sup>12</sup>

### **1.3.1 Principle of detection**

Protein microarray assays can be currently approached in two alternative ways:

- Forward-phase protein microarray assays. The substrate is printed with capture probes (usually antibodies), which will interact with specific proteins (antigens) by means of an affinity-binding reaction.<sup>6</sup> The microarray is incubated with a complex protein sample in which the target proteins are recognised, if present in the sample, by the spotted capture probes. This approach is the most commonly used and the detection of the binding events is usually based on comparative fluorescence measurements.<sup>25</sup> In this set-up, two complex protein samples (one test and one control sample) are labelled using different fluorescent dyes and incubated in the protein microarray (steps 1 and 2 in Figure 1.3). After washing and scanning the microarray slide for fluorescence signals, the relative intensity between both dyes (test/control sample) represents the abundance of the protein species recognised by each particular probe spot (step 3 in Figure 1.3).
- Reversed-phase protein microarrays. This approach starts by printing a large set of unknown protein samples, usually obtained from cell or tissue lysates, in a microarray format. Then, the spots are analysed for binding events in the presence of known protein probes, being each single protein probe usually tested at a time.<sup>6</sup> This analysis is accomplished by incubating the microarrays with fluorescently labelled target-specific antibodies. The interactions taking place between the antibody and the proteins immobilised on the microarray spots are identified by the fluorescence detection in each particular feature. Based on these data, the presence of specific proteins in complex

samples such as differentially regulated proteins in treated and untreated cells can be identified.<sup>26</sup>

### **Protein microarrays detect relative protein species abundances between test and control targets.**

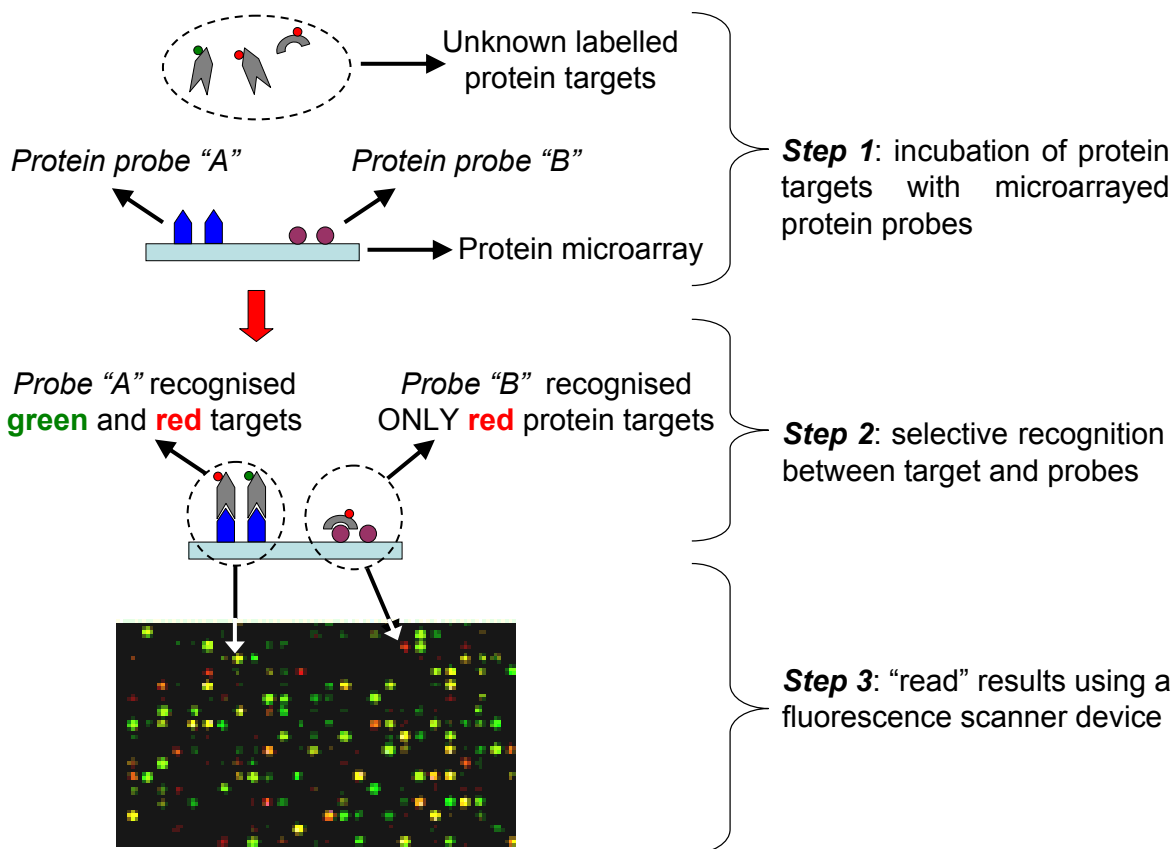


**Figure 1.3** Schematic of a typical protein microarray assay applied for the detection and quantification of protein concentration in an experimental sample based on comparative fluorescence measurements. Spots recognising both the green and red labelled protein targets will emit a yellow fluorescence signal, while spots recognising only one of the labelled targets (e.g. red in the schematic) will only emit the corresponding fluorescence signal. The microarray image used in this schematic has been adapted from cited reference.<sup>27</sup>

#### **1.3.2 Immobilisation methods**

In protein microarray applications, the surface to be spotted must fulfil specific requirements to ensure the proper protein immobilisation:

- In order to yield reproducible results, a controlled surface chemistry must be provided for the linking of proteins to the substrate.
- The surface should provide a low degree of unspecific binding.

- A high degree of protein immobilisation, in an active conformation, on the printed spots is desired.

Protein immobilisation methods reported for protein microarrays can be broadly classified in 3 groups:

- Direct protein immobilisation via non covalent adsorption. This approach has been validated for antibody immobilisation in polystyrene, poly-L-lysine, acrylonitrile-butadiene-styrene (ABS), poly(vinylidene difluoride) (PVDF), polyacrilamide, agarose and nitrocellulose polymer substrates.<sup>2, 3, 25</sup> After microarray spotting, these surfaces have to be passivated to reduce non specific binding on the non-printed areas. Drawbacks of this approach include the elevated background signals due to unspecific protein adsorption on non-spotted areas and the elimination of adsorbed species on the spots during the washing steps, both resulting in reduced signal-to-noise ratios.<sup>2, 28</sup>
- Direct protein immobilisation via covalent binding to chemically activated substrates. This method has been described in a wide variety of substrates including glass derivatised with amines, epoxides, thiols or aldehydes,<sup>3</sup> and agarose derivatised with aldehydes,<sup>29</sup> among other reactive chemistries.<sup>30</sup> After microarray spotting, the non printed area has again to be passivated. This approach has the advantage of retaining larger amounts of the spotted proteins and also yielding higher reproducibility and lower background signals than the previous one.<sup>2, 28</sup> A disadvantage of this option is the possible alteration of the protein activity due to the covalent binding to the surface.
- Indirect binding of proteins. This can be accomplished by pre-coating the surface with an affinity binding protein such as streptavidin. The protein coating acts as mediator of the attachment between the actual spotted biotinylated proteins and the substrate (Figure 1.4).<sup>31</sup> The main advantage of this option resides in the possibility of targeting protein orientation as well as in reducing protein decrease of activity due to direct covalent binding.

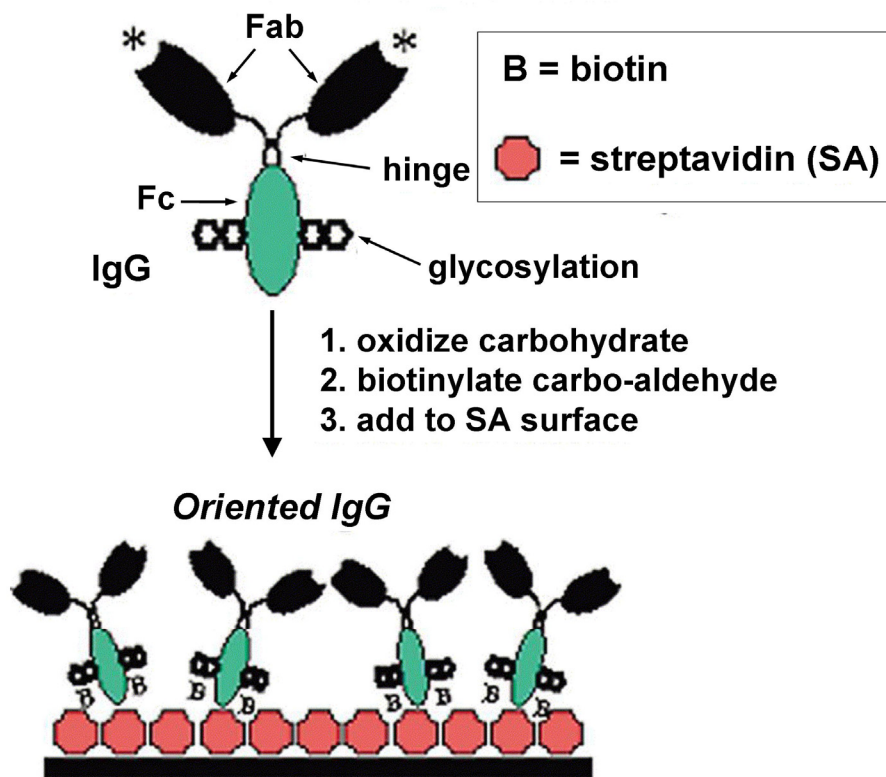


**Figure 1.4** Indirect binding of proteins (antibodies in this case) by means of streptavidin pre-coated surfaces. The structure of the antibody (monoclonal IgG) is shown at the top of the diagram. It consists of two antigen binding (Fab) fragments connected by a hinge region to the Fc portion, which is usually glycosylated. To orient the IgGs, the N-linked glycosylation site on the Fc is oxidized and then biotinylated. The biotinylated antibodies will attach to the streptavidin (SA) pre-coated surface yielding orientated Fab fragments. Image adapted from cited reference.<sup>31</sup>

### 1.3.3 Applications of protein microarrays

Despite ongoing challenges, up to date protein microarrays have proven to be useful in a wide variety of biomedical research applications such as antibody microarrays for antigen detection,<sup>25</sup> detection of protein-protein,<sup>32</sup> protein-nucleic acid<sup>33</sup> and protein-small molecule or drug interactions.<sup>3, 4, 22, 33, 34</sup> Additionally, protein microarrays specialised for protein-lipid (important when analysing transmembrane protein functions) and enzyme-substrate interaction have also been developed.<sup>34</sup> An example of high density protein microarrays was provided by Zhu *et al.*, who printed 6,566 protein samples representing 5,800 unique proteins (an almost complete yeast proteome) on a single nickel-coated microscope glass slide (Figure 1.5).<sup>32</sup> Using this protein microarray they identified many new proteins, which were spotted on the substrate, based on its interaction with a known protein (calmodulin), which was incubated in solution with the microarray.

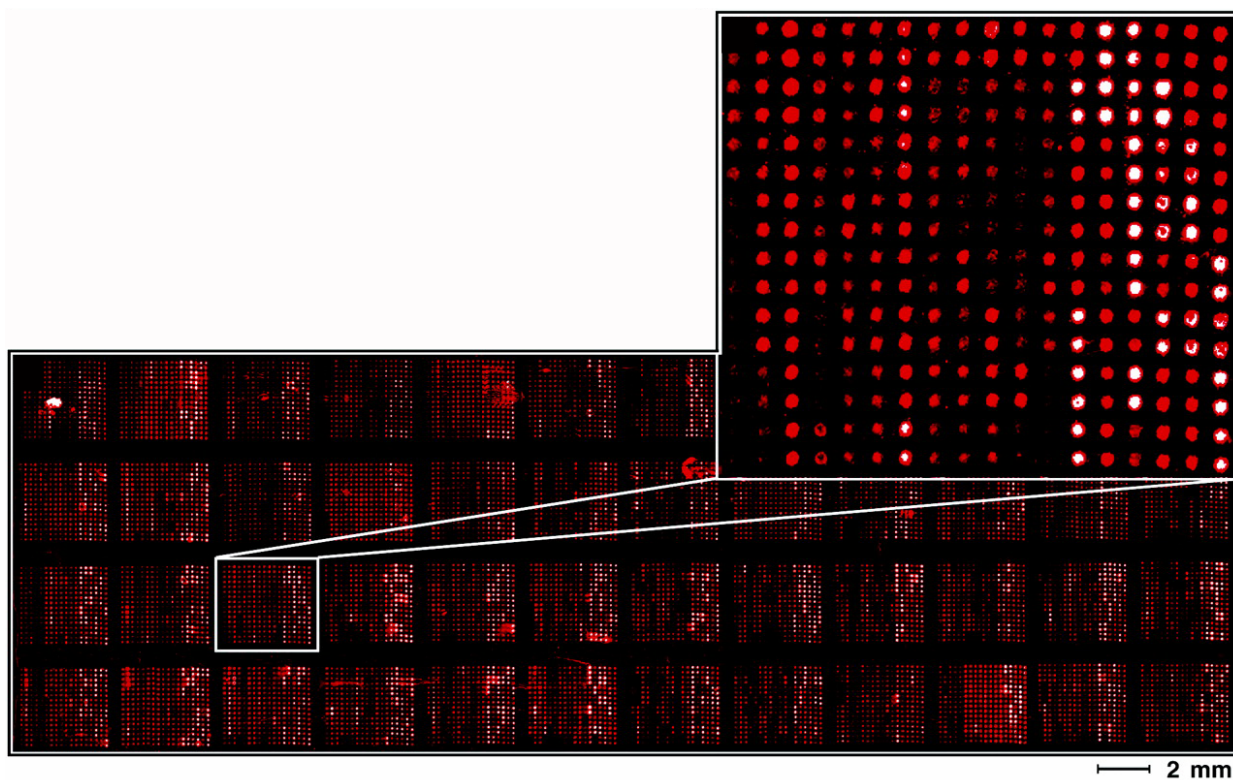


**Figure 1.5** Example of a protein microarray containing 6566 protein samples spotted in duplicates. Fusion proteins (fused with a common GST enzyme tag for detection) were expressed in yeast, purified and subsequently immobilised on a nickel coated glass slide. Once fabricated, the protein microarray was probed with labelled antibodies against GST to determine covalent and reproducible attachment of all sets of proteins spotted. Image adapted from cited reference.<sup>32</sup>

MacBeath *et al.* demonstrated the suitability of protein microarrays for protein-protein and protein-small molecule recognition.<sup>35</sup> They selected three pairs of proteins that are known to interact with a correspondent counterpart protein:

- 1<sup>st</sup> pair: **protein G** and **immunoglobulin G** (IgG)
- 2<sup>nd</sup> pair: **p50** and its inhibitor **IκBα**
- 3<sup>rd</sup> pair: the **FKBP12-rapamycin binding domain** of FKBP-rapamycin-associated protein (FRAP) and the **human immunophilin FKBP12**.

The first two couples interact without special requirements, whereas the interaction of the third couple depends on the presence of the small molecule rapamycin. The first protein of each pair was printed in quadruplicate onto aldehyde derivatised glass slides. After printing and passivation of non-spotted areas, the slides were assayed separately with their fluorescently labelled protein counterparts and also with a mixture of all of them (Figure 1.6). All proteins were successfully recognised by its specific counterparts, and the FKBP12 labelled protein could only be detected if co-incubated with the rapamycin molecule.

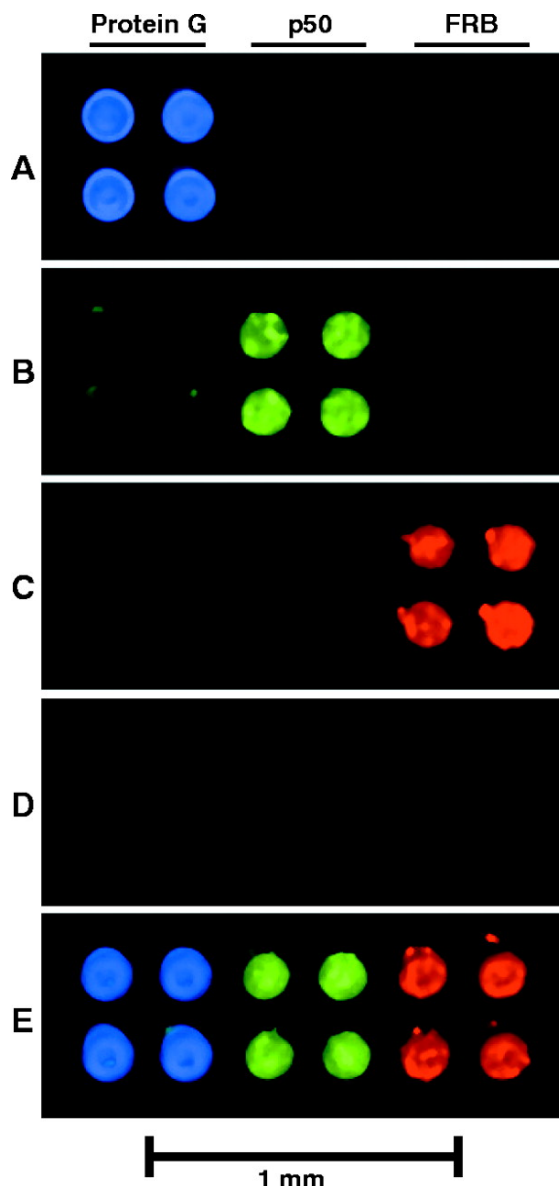


**Figure 1.6** Detecting protein-protein interactions on glass slides. **A.** Slide probed only with blue (BODIPY) labelled IgG. **B.** Slide incubated with green (Cy3) labelled I $\kappa$ B $\alpha$ . **C.** Slide probed with red (Cy5) labelled FKBP12. **D.** Slide incubated with red (Cy5) labelled FKBP12 and no rapamycin. **E.** Slide incubated with all previously described fluorescently labelled proteins and 100 nM rapamycin. Image reproduced from cited reference.<sup>35</sup>

Intense research carried out in the last decade has led to protein microarrays being commercially available from several providers such as TeleChem Interantional Inc. (Sunnyvale, CA, USA), BD Biosciences (San Diego, CA, USA) and Pierce (Rockford, IL, USA). Some of these companies provide not only pre-established sets of antibody microarrays for specific applications but also on-demand customised protein microarrays. These microarrays are used to analyse the level of protein expression as well as protein-protein interactions.

Current challenges in protein microarray development include the optimisation of protein immobilisation in an oriented way and in an active conformation, and the implementation of

fully automated platforms for microarray applications, so that manually executed process is avoided at all possible stages. This will ultimately lead to robust and validated microarray-based results.<sup>2</sup> Future prospects for protein microarray include its use in point-of-care disease diagnosis and also as monitoring systems of water or food samples.

## **1.4 Cellular Microarrays**

One of the latest and more challenging applications of protein microarrays consists of culture cells on them to create the so called cellular microarrays. The aim of these microarrays is to screen the effects in cell behaviour in response to the underlying spotted proteins. These include effects in cell adhesion, spreading, proliferation and differentiation cell behaviour, among other biological parameters of interest such as cell toxicity. This technique has gained a lot of attention quite recently, most applications using surface adhesive cell types dating from 2004 and on.<sup>36-39</sup>

A typical experiment with cellular microarrays is depicted in Figure 1.7 and consists basically of 3 steps:

- Protein microarray fabrication. Protein solutions are spotted onto the substrates, mostly by contact pin or non-contact piezoelectric nozzles linked to a robotic microarray plotter device (see Appendix A for details).
- Cellular microarray formation and cell culture. The formation procedure involves the passivation of the non-printed substrate surface to increase selective cell adhesion to the printed spots, and cell seeding. After a time long enough to allow cell attachment to the spots but not so long as to promote cell adhesion to the non-printed areas, unattached cells are removed. The formed cellular microarray is then ready to be cultured for the desired period of time.
- Cellular microarray characterisation. This intends to evaluate the effects of the printed proteins on the cell behaviour. For this purpose, cells are usually fixed and immuno stained for markers of interest, which detect specific proteins expressed in cells. Finally, the cellular microarray is imaged using fluorescence microscopy.

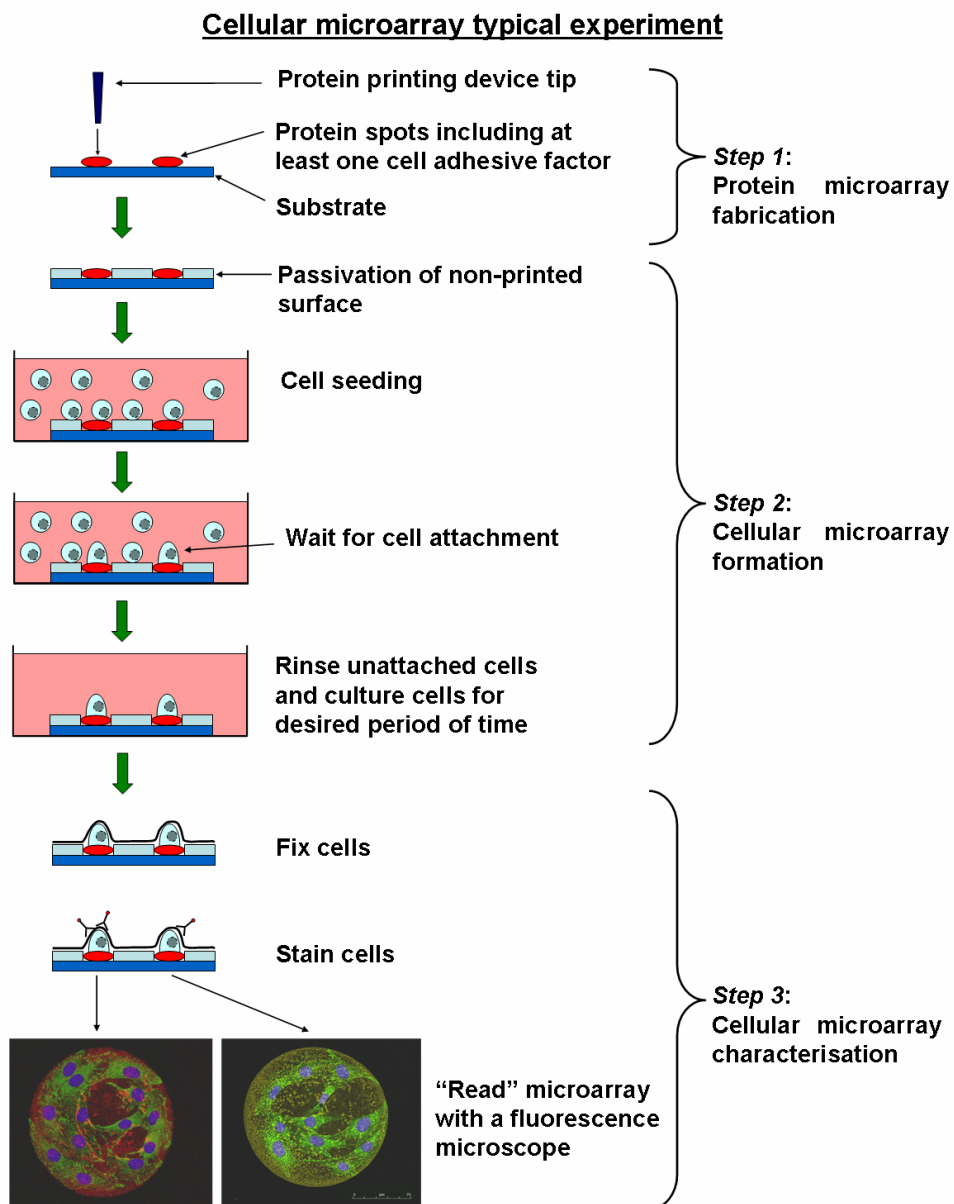


**Figure 1.7** Schematic of a typical experiment with cellular microarrays. Images show C2C12 cells attached on fibronectin spots (yellow and red labelling is due to the inclusion of Alexa Fluor 555 labelled fibronectin (yellow) or Alexa Fluor 647 (red) labelled SA in the spots composition). Stained cells were labelled for focal contacts (paxillin immuno staining, in green) and nuclei (Hoechst staining, in blue).

In contrast with DNA microarrays and even protein microarrays, cellular microarrays are not yet a well-established technique in biology laboratories. This is due to a number of difficulties appearing as a result of the increase in complexity from spotting DNA to spot functional proteins and, then, to allow viable cell culture on these spots. Therefore, the choice of the strategy in the design of cellular microarrays is related to the type of application and specific problem under study.<sup>38, 39</sup> In particular, the cell type used, cell culture time and culture medium required are key issues to be dealt with in each specific application.<sup>40</sup> Most important, the proteins immobilised on the spots might also have different thresholds, both in terms of their

**densities** per cell required for their active signalling, and in terms of their **time of cell exposure** to initiate cell signalling cascades.<sup>41</sup> These thresholds are also cell type dependant.

Currently, there are no standard protocols allowing for universal applications of cellular microarrays. However, a set of challenges have already been identified as the key issues in cellular microarray development. These involve finding solutions for the following issues:

- Avoiding cell attachment outside the microarray spots while allowing for high amounts of spotted protein immobilisation on the substrate. In order to make this possible, a compromise has to be found between the choice of the substrate type, the chemical activation and the passivation strategy used.
- Keeping the spots with attached cells isolated from each other during the whole cell culture period of the experiment. In this case, the most important parameters to be tuned are the passivation strategy of non-spotted areas and the medium used for cell culture. Protein containing mediums (e.g. those supplemented with fetal bovine serum, FBS) tend to damage the microarray layout, while serum free mediums are detrimental for cell viability.
- Maintaining the viability of cells attached on the spots for several days, depending on the experiment time required. This issue imposes a compromise to be struck between the medium used for cell culture and the isolation of spots throughout the culture period assayed.
- Optimising the amount and activity of the proteins immobilised. This issue requires a first step involving the actual quantification of the immobilised proteins. Once this performed, the optimisation procedure is associated with the immobilisation strategy chosen and is strongly affected by the chemical activation of the substrate. In general, chemically activated surfaces will retain larger amounts of strongly bound proteins, but will be more difficult to passivate efficiently.

As exposed, these challenges are addressed by choosing specific values for parameters such as substrate type, surface chemical activation, passivation strategy and the cell culture medium for each particular application (Table 1.1).<sup>39, 42</sup> Additionally, other approaches for cellular microarray fabrication, alternatives to the one presented Figure 1.7, might include direct cell spotting onto the substrate, therefore simplifying the task of cell selective adhesion,<sup>43, 44</sup> or culturing cells in monolayer atop the spotted microarrays,<sup>45-47</sup> avoiding the complexity of

keeping cells isolated on the spots. Some examples of these alternative strategies for cellular microarray fabrication are also included in Table 1.1 as reference.

Substrate used / Surface coating	Surface chemical activation	Agents spotted	Covalent immob.	Passivation	Culture medium	Culture time	Ref
<i>Seed and culture cells in printed spots only</i>							
Glass	Aldehyde derivatised	ECM + growth factors	Y	BSA	Serum free (enriched)	4 d	48
Glass	Silane modified	ECM + growth factors	N*	-	10 % FBS	7 d	49
Polyacrylamide	-	ECM / peptide / antibodies	N	-	4 – 15 % serum	24 h - 6 d	50-52
Nitrocellulose	-	ECM / PLL	N	Stabil Guard®	Serum free	4 h	53
Gold	NHS esters	ECM / peptide + growth factors	Y	BSA	Serum free (enriched)	3 d	54
PEG based	-	ECM / antibodies / PLL / polymers	N	-	2 – 10 % serum	6 h – 7 d	55-58
Agarose	-	ECM	N	-	10 % serum - serum free (enriched)	5 d - 16 d	59
Carboxy-methyl-dextran	NHS esters	Peptides	Y	-	10 % serum	5 d	60
PDMS	-	ECM + growth factors + antibodies	N	Pluronic F108	0.5 % serum	24 h	61
pHEMA	-	Polymers / polymers + small molecules	N**	-	10 – 20 % serum	2 d – 10 d	62-64
Poly(vinyl alcohol)	NaOCl***	NaOCl solution / plasmid DNA	N	-	10 – 20 % serum	4 d	65
<i>Seed and culture cells in monolayer on top of the printed microarrays</i>							
Glass (pre-coated with Fibrin)	-	Growth factors	N*	-	2 % serum – serum free (enriched)	4 d – 9 d	46, 66, 67
Glass	Silane modified	ECM + growth factors / plasmid DNA	N*	-	10 % serum	6 d - 7 d	45, 47, 49
<i>Print cells on top of printed spots</i>							
PS-MA	-	PLL / ECM	Y****	-	5 – 10 % serum	5 d	43, 44

**Table 1.1** Substrates and cellular microarray strategies reported in the literature. Abbreviations: Y: Yes; N: No; PDMS: polydimethyl-siloxane; PLL: Poly-L-lysine; BSA: Bovine serum albumin; ECM: Extracellular matrix protein; NHS: N-hydroxysuccinimide; PEG: Poly(ethylene glycol); PS-MA: Poly(styrene-co-maleic anhydride). \*growth factor immobilisation in the spots in this case has been proposed to be aided by association with ECM or Fibrin proteins. \*\*spot polymerisation on the surface was induced by UV exposure. \*\*\* printed to create cell adhesive spots. \*\*\*\* provided by the coating.

The choice of the substrate defines the amount and efficiency of protein immobilisation on its surface, as well as the stability of the cellular microarray layout over time. Usually, the substrates chosen for these applications have been previously validated for protein microarray applications. A summary of the substrates reported in the literature for cellular microarray applications can be found in Table 1.1.

Cell attachment to the microarray spots is usually accomplished including at least one extracellular matrix (ECM) protein or cell adhesion factor within the spot composition (Table 1.1). Proteins reported in the literature for this purpose include laminin (Ln),<sup>48</sup> fibronectin (Fn)<sup>68</sup> and collagen I (Col I),<sup>59</sup> among others. The use of polymers<sup>62, 63</sup>, antibodies<sup>36</sup>, peptides<sup>52</sup> or other approaches such as creating cell adhesive domains through direct chemical patterning of naturally cell-repellent surfaces<sup>65</sup> have also been reported for cellular microarray formation.

To avoid cell attachment to the non-printed area of the substrate, there are two main approaches:

- Direct printing of the protein spots on naturally cell repellent substrates such as agarose,<sup>59</sup> acrylamide<sup>50</sup> or poly(ethylene)glycol (PEG).<sup>55</sup> In these cases, the spotted protein is generally physisorbed on the surface. As cleverly exposed by Folch and Toner,<sup>40</sup> the fact that it is very difficult to completely remove a physisorbed protein from surfaces, combined with the extreme sensitivity of the cell anchorage machining to trace amounts of ECM proteins, allows the use of these approach. This could explain the success in cellular microarrays where no chemical activation of the substrate is provided for spotted protein anchoring (Table 1.1).<sup>50, 55</sup>
- Spotting protein solutions onto a chemically activated substrate, followed by the passivation of the non-printed surface with suitable reagents. In this case, the chemical groups introduced on the substrate surface react, usually, with amino groups exposed by proteins to create covalent bonds between the protein and the substrate.<sup>25</sup> This approach is most important when, besides the cell adhesion factors, growth factors or other non-ECM protein molecules are included within the protein solution spotted (Table 1.1).<sup>41, 48</sup> For passivation of the non-printed surface, the use of naturally cell-repellent proteins such as BSA<sup>48</sup> or the use of PEG chains (modified to react with the surface chemistry) are the most common approaches reported in the literature.<sup>69</sup>

The medium used to culture cells in cellular microarrays can be broadly classified in serum containing medium and serum-free alternative medium compositions. Medium containing

variable quantities of animal serum (5-20%) is most usually employed to expand and further culture most cell types. Animal serum contains unknown factors (including hormones, growth factors, transport or binding proteins to present hormones to the cell in a non-toxic form, protease inhibitors, etc.), in unknown quantities, that are necessary for cell attachment and growth in experiments *in vitro*.<sup>70</sup> Additionally, serum also plays a role in stabilising and detoxifying the culture environment. The importance of these roles of serum in cell cultures will vary depending on the cell type being studied and the culture conditions used.<sup>40</sup> In particular, when dealing with cellular microarrays, controlled cell growth and behaviour are preferred, so that cultured cells remain on the printed spots and respond in an unbiased way to the factors immobilised. Therefore, the elimination of serum in the culture medium is highly desired. Serum-free medium usually replace serum content with a set of hormones, growth factors, attachment proteins and transport proteins, in quantities optimised for specific cell cultures.<sup>70</sup> However, serum-free alternative medium compositions are not always available for all cell types and culture studies.

### 1.4.1 Applications

The origin of cellular microarrays can be tracked back as far as 1983. By then, T.W. Chang described the binding of thymocytes and mononuclear cells to specific antibody spots arrayed on a solid surface.<sup>23</sup> Until recent years, the affinity between antibodies and T-cells has been the workhorse of cellular microarrays and many researchers have exploited this affinity to optimise and further develop the technique.<sup>36, 71</sup>

Many applications for cellular microarrays have aroused in the last five years, focusing on the high-throughput study of cell-biomaterial interactions,<sup>62, 63</sup> detection of local appearance or loss of phenotype in microarrayed cells,<sup>55</sup> cytotoxicity of specific factors,<sup>44</sup> study of cell adhesion<sup>53</sup> and study of stem cell differentiation.<sup>48, 51</sup> The later is definitely one of the most challenging and interesting applications of cellular microarrays. It is aimed at providing insights into stem cell differentiation pathways, therefore allowing the postulation of activation/inactivation protocols to direct stem cell differentiation along the desired cell fate. In stem cell differentiation applications microarray spots contain ECM proteins and often growth factors<sup>37, 39</sup> As stem cell differentiation has been the driven force at the origin of this work, a short summary considering the basics for this process is included in the following section.

## Stem cell differentiation

Stem cells have become a hot topic of research in the last decade due to its promising applications as unlimited cell source for cell-based therapies.<sup>72, 73</sup> This is because they have two extremely important properties (Figure 1.8):

- They can divide to give rise to cells which are identical to the progenitor
- They can differentiate into many cell types, therefore producing technically unlimited numbers of patient-compatible specialised cells.

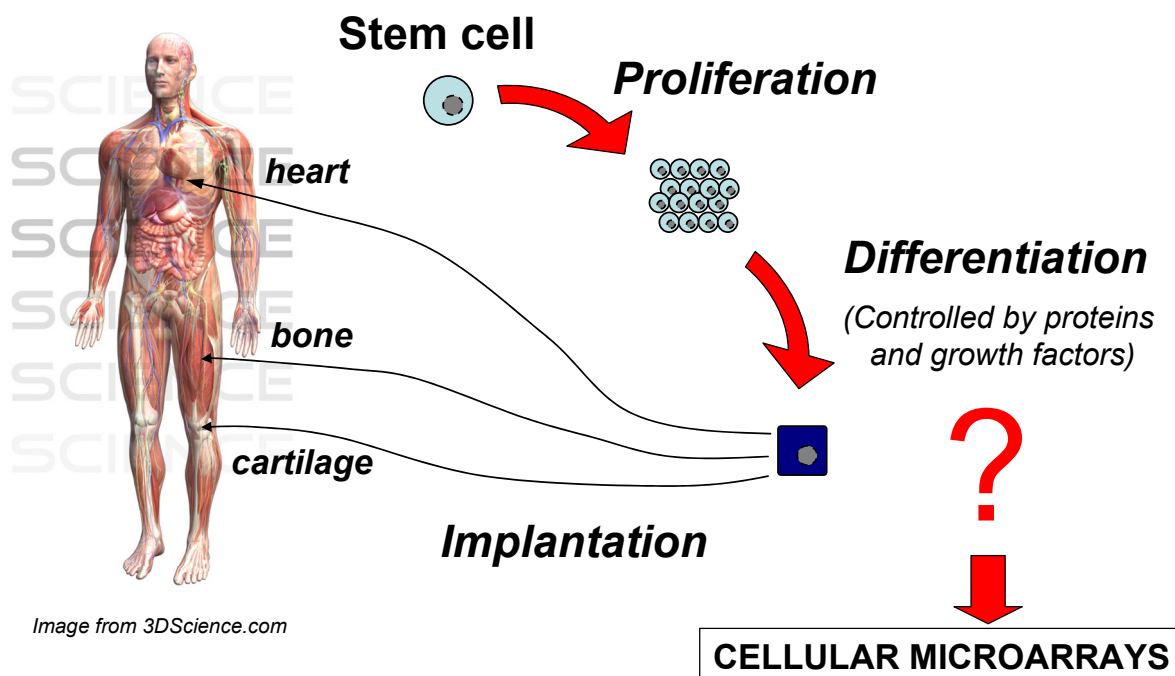


**Figure 1.8** Stem cell properties and cellular microarray niche of application. Stem cells can divide and give rise to cells which are identical to the progenitor, and they can differentiate into many cell types of the human body. Its implantation as part of a cell therapy application is very promising. Cellular microarrays could help to improve the knowledge in the stem cell differentiation process by allowing the large scale screen of protein and growth factor effect on stem cells.

Their differentiation potential depends on the source of the stem cells. Stem cells obtained from the embryo, the so called embryonic stem cells (ESCs), are pluripotent cells. This means that each of them can differentiate into every cell type of the body.<sup>72</sup> Other type of stem cells, called multipotent due to a more restricted capacity of differentiation, can be obtained from different tissues of adult individuals.<sup>73</sup> In particular, the so called mesenchymal stem cells or mesenchymal stromal cells (MSCs), which can be harvested from bone marrow, blood or adipose tissues, have been shown to differentiate into most cells of the mesenchymal lineage

such as osteoblasts, chondrocytes and adipocytes.<sup>74</sup> Transdifferentiation of MSCs to other cell fates has also been reported.<sup>75</sup> Despite MSCs have a more limited differentiation potential when compared to ESCs, they have the advantage of being obtained from adult (not embryonic) tissues. Therefore, differentiated MSCs could be used in autologous implants (re-implant functional cells in an individual after stem cell harvesting and their in vitro differentiation) for cell therapy applications that avoid compatibility issues and ethical issues associated with the use of human embryonic stem cells. Another advantage is that MSCs do not form teratomas (tumours) when implanted into the body, while ESCs do.<sup>76, 77</sup> Another source of stem cells recently reported are obtained from reprogramming of differentiated cells to an undifferentiated phenotype by co-transfection of four genes.<sup>78</sup> These cells are referred to as induced pluripotent stem (iPS) cells and have been shown to have identical differentiation potential as the ESCs.

Stem cell fate and function has been shown to be responsive to a combination of many signalling cues coming from its microenvironment (Figure 1.9).<sup>50, 79</sup> In particular, and with the final aim of stem cell differentiation control, the study of cell-ECM protein interactions that can directly induce cellular signalling through integrins,<sup>50, 80</sup> and the effect of growth factors on cells,<sup>48, 81</sup> both have became the focus of intense research.

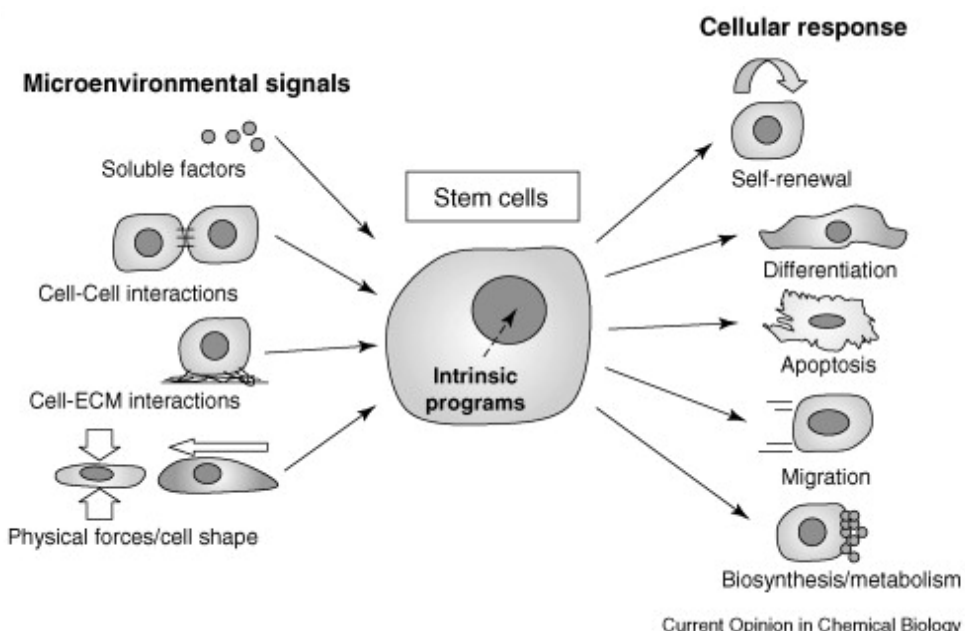


**Figure 1.9** Micro environmental cues affecting stem cell behaviour. Image reproduced from cited reference.<sup>39</sup>

Cell-ECM protein and cell-growth factor interactions have been usually studied by multiwell plate assays, where purified matrix proteins are used as coating and growth factors are added in solution to the cell cultures (alone or in a combination) for multiple screening.<sup>82</sup> This

methodology is expensive and time consuming when the experiments are parallelised to test large combinations of factors. This is mainly due to the high quantities of growth factors required per experiment, resulting from typical well volumes (~200 µL/well) and growth factor concentrations (~200 ng/ml) involved in this approach, and the important amounts of manually executed protocols involved in these studies. Still, the accurate control of stem cell differentiation remains a challenge since standard protocols evaluate the average response of thousands of cells, cultured in each wellplate, to the differentiation cocktails added. This approach produces inhomogeneous cell populations, composed of differentiated and undifferentiated cells, after treatment with the differentiation cocktails. The additional signals that appear in this type of cell cultures, coming from cell-cell signalling, either by direct cell-cell contact or by paracrine signalling (i.e. by signalling factors secreted to the culture medium by the cells), can account for this complex differentiation outcome.

Performing lots of experiments in parallel would allow learning faster and more efficiently details of the cellular differentiation process. These high-throughput experiments could be performed in a relatively easy way if, instead of using protein solutions that require individual well plates, proteins are “printed” (immobilised) on specific locations on a substrate in a microarray format. This layout would ensure that only cells on each spot are interacting with that particular protein (ECM and growth factors) combination. This would allow for systematic and high-throughput studies, where 100s to 1000s factor combinations could be tested in parallel in a single microscope slide. Additionally, this approach allows performing highly accurate statistics where outlier spot responses can be easily identified from replicate conditions. Miniaturization in the format of cellular microarrays also allows working with low protein sample volumes (which are immobilised on the spots), being then time and cost efficient.<sup>39</sup> Obtaining similar results using wellplates could take months or years, when possible. It is important to highlight that cellular microarrays are aimed for the screening of large combinations of factors to find those controlling stem cell differentiation, and not to produce large numbers of differentiated cells for being used in therapeutic applications.

### ***Cellular microarrays applied to the analysis of cell differentiation***

To date, cellular microarrays have been successfully applied to yield light into some biological pathways by the high throughput screening of combinations of surface-immobilised factors affecting stem cell adhesion and differentiation.<sup>37, 39</sup> This technique has allowed “mimicking” at the biomolecular level a large number of individual cell microenvironments,

composed of extracellular matrix (ECM) proteins<sup>50, 53</sup> and even some growth factors,<sup>48, 54, 60</sup> on flat surfaces. However, cellular microarrays are still an emerging platform and application reports have been highly customized for specific cell types and differentiation studies.

One of the earliest reports of cellular microarrays applied to the systematic screening of cell-ECM protein interactions, was provided by the group of S. Bhatia in 2005.<sup>50</sup> They reported the parallel screen effect of 32 combinations of 5 ECM proteins (Fibronectin, Laminin, Collagen I, Collagen III and Collagen IV) on rat hepatocytes and mouse embryonic stem cells (mESC) differentiation. Hepatocytes usually dedifferentiate and lose their phenotype when cultured *in vitro* for several days, which prevents them to be used in liver implants and in toxicology *in vitro* applications. They reported specific protein combinations which allowed sustenance of rat hepatocyte phenotype for 7 days. Other protein combinations (which included Fibronectin and Collagen I) leaded mESC cell differentiation towards an early hepatic fate (Figure 1.10) after 3 days of cell culture in the microarray.

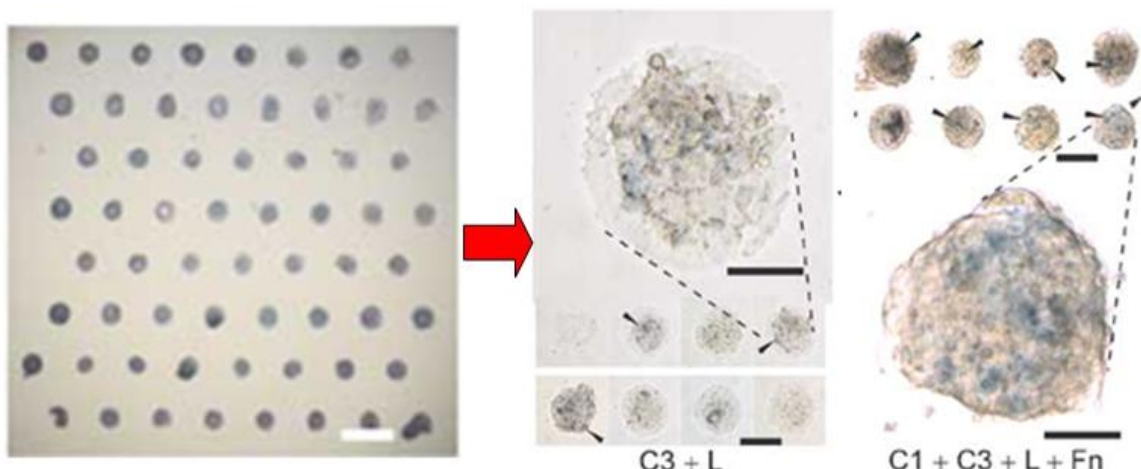


**Figure 1.10** ECM protein microarray for the study of mESC differentiation. Left: Alkaline phosphatase staining of day 1 mESC cultures (scale bar, 1mm). Right: Bright-field images of X-gal stained cells (to detect  $\beta$ -galactosidase activity, linked to *Ankrd17* activity) on selected ECM protein spot compositions (indicated below each image) after 3 days of culture. It can be seen that spots including fibronectin (Fn) and collagen I (C1) induced higher *Ankrd17* reporter activity (arrowheads) than spots without these factors. Scale bars, 250 $\mu$ m. Image adapted from cited reference.<sup>50</sup>

The use of cellular microarrays for the study of MSC differentiation is an appealing application, due to the promising therapeutic applications that could be derived from this knowledge.<sup>83</sup> However, developing cellular microarrays using MSCs represents an additional challenge, since these cells have extremely high adhesive properties and synthesise high quantities of their own ECM proteins. The microarray requirement of keeping cell spots isolated from each other throughout the whole culture time period is then compromised. Because of this,

cellular microarrays using MSCs have just recently been reported (2005 and on). Anderson and colleagues fabricated human MSC cellular microarrays to analyse cell response to more than 6,000 microarrayed polymer compositions in parallel, in a high throughput way.<sup>63</sup> In this study cells were cultured for 48 h and the best polymer compositions allowing and inhibiting cell attachment and spreading were reported (Figure 1.11).

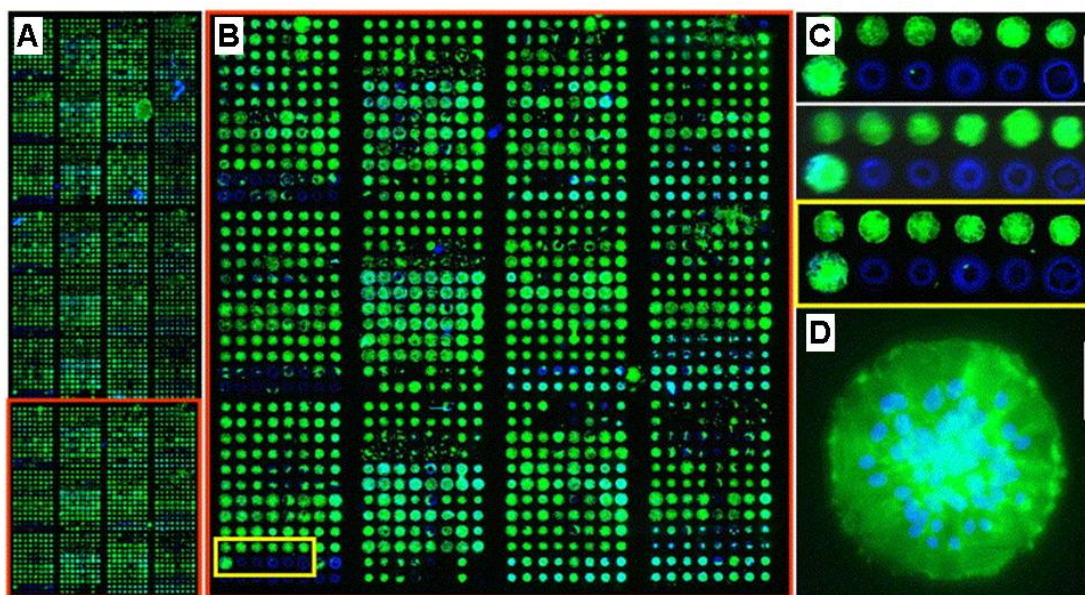


**Figure 1.11** Cellular microarray for the study hMSC-polymer interactions. **A.** Scanner image of a 3456 spot biomaterial microarray seeded with over 1 million hMSC and stained 48h later for actin (green). **B.** Detail from image A. **C.** Close up of triplicates for 12 polymer compositions (6 polymer compositions in 2 rows). It can be seen that reproducible data results in the identification of 5 polymer compositions (bottom row) which clearly inhibit cell attachment. **D.** Close-up of a polymer spot with hMSC, actin is stained green and nuclei are stained blue. 100  $\mu$ m scale bar is shown in white. Image adapted from cited reference.<sup>63</sup>

Benoit *et al.* have reported a cellular microarray application using hMSCs for the screening of small molecules inducing cell differentiation after 10 days of cell culture in the microarray.<sup>64</sup> This approach was based in the use of a non-cell-adhesive surface (poly(2-hydroxyethyl methacrylate), pHEMA) as microarray substrate, on top of which spots composed of mixtures of a polymer (PEG) and several small molecules were immobilised. The cell culture time reported here was extended to 10 days, in comparison with the previous report, and the cellular microarray was used in this study as an intermediate screening stage within the experimental process. Unfortunately, no images of cells growing on the microarray spots after 10 days were included in this report and no information was provided regarding cell proliferation on the spots or cells exceeding the spot premises after a certain time of cell culture.

Cellular microarrays which include ECM proteins together with growth factors in the spot composition with the aim of targeting stem cell differentiation have been reported in the literature from 2006 and on.<sup>48</sup> In their paper, Soen and co-workers printed mixtures of Ln and growth factors in a 44 combination microarray format on aldehyde derivatised glass slides, to provide a covalent linkage between factor and substrate.<sup>48</sup> Neural precursor cell differentiation was evaluated after 3 days of cell culture on these microarrays. They found specific combinations of growth factors that leaded cell differentiation to neurons or glial cells, while spots composed exclusively of Ln produced differentiation to a neuronal fate (Figure 1.12).

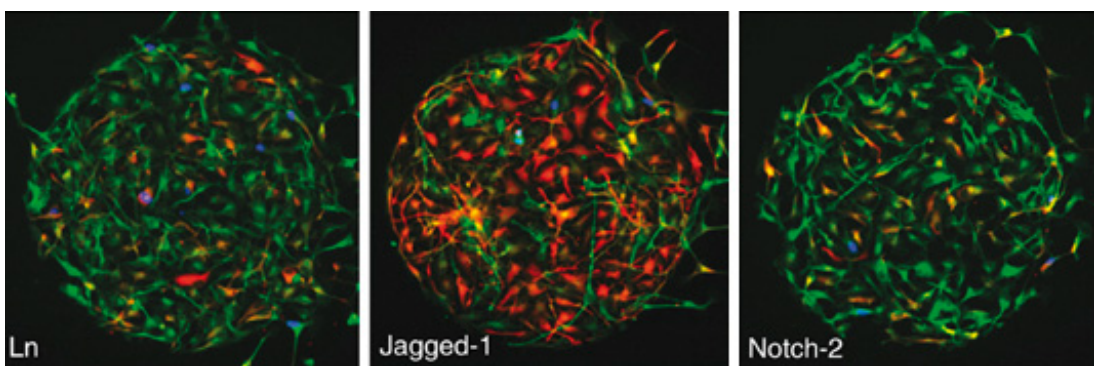


**Figure 1.12** Cellular microarray for the study of neural progenitor cells differentiation. Red staining indicates glial-like cells while red staining marks neuronal-like cells. Ln spots (on the left) and Ln with Notch-2 spots (on the right) produced differentiation to neuronal fates while Ln with Jagged-1 spots (middle) induced glial differentiation. Image adapted from cited reference.<sup>48</sup>

Nakajima and co-workers targeted in their work neural stem cell differentiation in response to natural and artificial ECM proteins with and without growth factors spotted in 25 specific combinations. Using an approach for microarray fabrication based in photo-assisted patterning, they were able to identify combinations of factors that biased cell differentiation towards neurons or glial cells. Most important, this work reported that the growth factor effect was frequently altered depending on the type of co-immobilised ECM protein.

Another report has demonstrated the application of cellular microarrays containing growth factors for the analysis of an early differentiation response in human mammary progenitor cells.<sup>61</sup> Interestingly, in this case cells were cultured only for 24 hours in the growth factor containing microarrays but the differentiation fates found in response to specific factors were predictive of differentiation trajectories that would be sustained for as long as 10 days in standard cell cultures supplemented with these factors.

Noteworthy, cellular microarray applications to date have focused in cell response to a relatively small number of spot conditions, when compared with DNA and protein microarrays. The reason why cellular microarrays have not turned, yet, into a so massively and parallel

approach as protein and DNA microarrays is not due to impossibility of printing growth factors and proteins at high spatial densities, nor to cell seeding onto hundreds or thousands of spots (already proved by Anderson *et al.*<sup>63</sup>), but to the lack of appropriate high throughput devices for characterisation of cell response on each spot. Fluorescence microarray scanner devices and signal processing software, highly customized for DNA and protein microarrays data “reading” and processing, still need to be adapted for their use with cellular microarrays. While DNA and protein microarray spots have mostly uniform fluorescence signals, cellular microarray spots are composed of tens to hundreds of cells, each one having a specific response to the printed factors, making the spot fluorescent signal non-uniform. Moreover, cellular microarrays characterisation usually involves a more complex signal analysis, as cell nuclei are stained in parallel with response-specific factors that often change from one spot to another, thus making the effective interpretation of the staining for the whole microarray a challenge. A recent study demonstrating the feasibility of accomplishing this aim was provided by the group of S. Bhatia.<sup>51</sup> This study reported the high throughput analysis of cell response to spots composed of 32 mixtures of 5 ECM proteins and simultaneous soluble growth factor signalling in separate chambers within a single glass slide, yielding a 240 ECM protein and growth factor treatment conditions. Using a standard DNA microarray scanner device and software, they demonstrated that mESC differentiation efficiency toward the cardiac lineage could be tracked after 48 hours of cell culture. This report highlights the advantages of high-throughput cellular microarray reading and analysis while, at the time, evidences that accomplishing this aim to date resides in a high customisation of cellular microarray platforms to allow standard DNA and protein microarray reading and analysis techniques to be applied.

### ***Technological variations introduced in the implementation of cellular microarrays***

As previously exposed, the cellular microarray fabrication process involves the printing of protein/growth factors onto the substrate, passivation of the non-printed surface, cell seeding onto the spotted protein microarray and further cell culture for time periods ranging from a few hours to several days. Afterwards, cells are fixed and stained for molecular markers of interest. Variations of this protocol might include the direct spotting of protein-cell composites onto the substrate,<sup>44</sup> cell seeding on a monolayer on top of the printed protein microarray<sup>66</sup> and creation of transfected cellular microarrays.<sup>45</sup>

The group of D. Sabatini has pioneered the development of a transfected cellular microarray technique, which consists on printing plasmids into a microarray format and cell seeding in

monolayer atop this array.<sup>45, 84</sup> Using this approach they have demonstrated multiple and parallelized transfection of cells with the spot specific plasmids. A similar variation of cellular microarrays for transfection of hMSC was also reported.<sup>85</sup> In this case, cells were cultured in a monolayer for 3 days on top of a Fn-plasmid printed microarray. Interestingly, the authors propose that the inclusion of Fn within the spot composition increases the hMSC transfection efficiency.

Another variation is the one reported by the group of P. Campbell. Based on a home-made fibrin coated substrate, they created growth factor (FGF-2) microarrays on top and seeded cells in monolayer onto these microarrayed substrates. Using this methodology they demonstrated that spots of FGF-2 with different surface densities proportionally induced cell proliferation.<sup>46</sup> Additionally, in a more recent report, the same group reported that C2C12 cells cultured in monolayer on top of a BMP-2 printed pattern switched their differentiation pathway towards the osteoblast lineage in response to the printed pattern (Figure 1.13).<sup>67</sup>

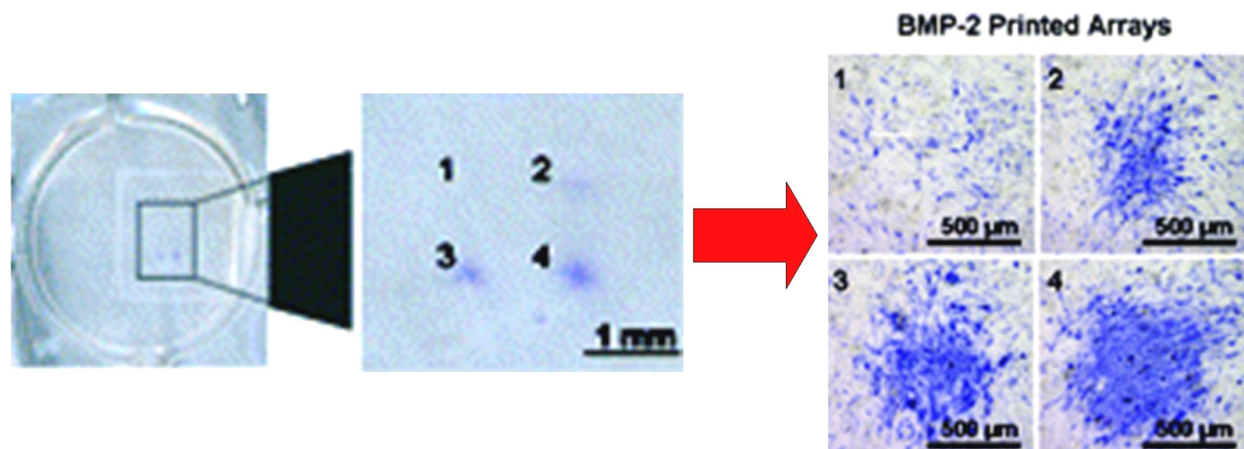


**Figure 1.13** Spatial control over osteogenic lineage progression for C2C12 cells. Left: The BMP-2 printed microarray, placed in a wellplate, was cultured with cells attached in monolayer for 48 h and then cells were stained for alkaline phosphatase (ALP, an osteoblast protein marker). Blue staining indicates ALP production by cells, and therefore osteoblast differentiation. Right: Zoom in of the spots named 1 to 4 in the image of the left. Image adapted from cited reference.<sup>67</sup>

#### 1.4.2 Scope and aims for this thesis

The cellular microarray applications just previously described reported the use of a large variety of substrates, printing buffers and protein concentrations spotted, being these parameters entirely customized for the specific cell types and studies carried out. An integrative study of protein immobilisation throughout several substrates of interest for cellular microarray applications, similar as those extensively reported for DNA and protein microarrays,<sup>86-88</sup> is lacking to date for this technique. This analysis should focus on already validated substrates for

cellular microarray applications, and should study the immobilisation efficiency of cellular microarray-relevant proteins spotted at relevant concentrations. This led to the formulation of the first aim of this thesis, which consists in the evaluation of different substrates for cellular microarray applications. The substrate performance is evaluated in terms of which yielded the largest amounts of protein immobilised on the surface while providing good reproducible results. The evaluation of some protein microarray fabrication parameters (i.e. the buffer composition, the type of protein spotted and the spot size) which affect the amount and density of protein immobilised on each substrate has been a primary concern and has been addressed by a quantitative model to analyse the protein-surface immobilisation. Yielding light about the strengths and weaknesses of each substrate allowed choosing the best candidate to accomplish the following aims of this work.

Previous literature reports described optimised parameters for cellular microarrays applications using several different cell types. As already mentioned, MSC are an attractive cell type to apply the potential capabilities of cellular microarrays. Thus, the second aim of this thesis was to take advantage of the systematic and large scale screening provided by cellular microarrays to find optimum microarray fabrication parameters (i.e. the spot size, printing buffer composition, cell culture medium, cell seeding time and cell seeding density) to achieve MSC culture in a cellular microarray composed of fibronectin spots. Optimum parameters were those allowing the longest cell culture time, while still kept cells in isolated spots in the microarray throughout the whole culture time period.

Finally, the effect of growth factors printed in cellular microarrays has been reported for neural stem cells<sup>48, 54</sup> and most recently for mammary progenitor cells.<sup>61</sup> Cell response to the immobilised factors might be different for different cell types, at the time that different immobilised growth factors could be active to different extends. Therefore, it is foreseen that using other cell types will require specific customization of the cellular microarray experiments to achieve cell differentiation in response to the printed growth factors. The last aim of this thesis consisted in applying the cellular microarrays developed to analyse the effect in cell early differentiation stages when they are cultured on spots composed of a growth factor combined with ECM proteins.

Summing up, among all the possible microarray types and applications introduced, this thesis will deal with the development of cellular microarrays with the final aim of allowing stem cell culture on them and evaluating some early cell differentiation events.

# **Chapter 2      Quantitative characterisation and comparison of protein immobilisation on substrates for cellular microarray applications**

## **2.1 Introduction**

Despite the increasing number of reports regarding cellular microarray applications, this technique is yet far from being well-established and it needs to be improved before it can be routinely applied to study cell biology. Some technological parameters are especially crucial when fabricating the protein microarrays that would be further used for cellular microarrays. In particular, the properties of the substrates used for microarray experiments should be carefully chosen. Substrate surfaces need to be suitable for the strong binding of the desired proteins on the microarray spots (in a covalent way if possible),<sup>41</sup> while they should allow appropriate passivation of the non-spotted areas to prevent cell adhesion there.<sup>42</sup> For this purpose, surface chemistry improvements have allowed the development of surfaces that significantly reduce non-specific protein adsorption from biological fluids such as cell culture medium.<sup>69</sup> These surfaces are usually referred to as “non-fouling”.<sup>89</sup> This effect has been proposed to be due to different chemical properties of the surfaces, as will be exposed in the following paragraph. However, while the best non-fouling surfaces are also the ones that retain immobilised the lowest amount of printed protein (and generally in a denaturalised form), substrates that provide strong protein-surface bindings present a challenge for robust passivation of the non-printed areas.

Many different materials have been tried as substrates for cellular microarrays, including agarose,<sup>59</sup> acrylamide,<sup>50</sup> gold,<sup>54</sup> glass,<sup>48</sup> nitrocellulose,<sup>53</sup> poly(methylmethacrylate)<sup>68</sup> and poly(ethylene glycol) (also called poly (ethylene oxide)),<sup>55, 89, 90</sup> among others.<sup>60, 61</sup> The mechanisms for protein immobilisation on these surfaces differ. Some of these substrates (e.g. agarose and acrylamide) are 3-D hydrogel polymer matrices which have the ability to reduce non-specific adsorption of biomolecules as a result of their chemical composition,<sup>42</sup> therefore no further passivation of the printed surface is needed. Protein binding to these surfaces is mainly due to physical adsorption into the hydrogel matrix. Nitrocellulose surfaces consist also of a 3-D

polymer matrix and bind proteins by physical adsorption,<sup>3</sup> but this substrate requires an additional passivation step after printing to reduce the non-specific adsorption of biomolecules.<sup>53, 71</sup> Poly (ethylene oxide) substrates (abbreviated as PEO) retain proteins when they are deposited,<sup>91</sup> and render the surface protein adsorption resistant (i.e. non-fouling) when it is in a liquid environment mainly due to a self-repulsion of the PEO chains in water.<sup>90</sup> Other substrates such as glass, gold and poly(methylmethacrylate) usually include the coupling of proteins by covalent binding to the substrate through surface functional groups (aldehyde,<sup>48</sup> N-hydroxysuccinimide (NHS)-ester,<sup>54</sup> pentafluorophenol<sup>68</sup>). These surfaces need an additional passivation step after spotting of the proteins which is usually accomplished by incubation of the printed substrate in a BSA solution.

Although several comparisons among substrates performance in protein microarray applications can already be found in literature,<sup>28, 86-88</sup> such a comparison could not be found for cellular microarrays. In particular, no paper was devoted to make a comparison among different substrate performances in cellular microarray applications on the bases of the quantification of the amount of protein immobilised. To date, each cellular microarray report was focused on a specific type of substrate. Lacking quantitative comparative data, however, makes difficult the decision of the most adequate substrate for each individual cellular microarray application.

One of the main challenges when addressing a comparison on the performance of substrates for protein or cellular microarray applications is that, despite protein can be quantified in solution with excellent detection limits (down to the ng mL<sup>-1</sup>),<sup>92</sup> quantification of proteins adsorbed onto surfaces is a non-solved problem yet. Some of the methods used focus on measuring the protein concentration remaining in a solution before and after its incubation with the surface (in this case, a decrease in protein concentration accounts for the amount of protein adsorbed on the surface).<sup>93</sup> Other techniques, such as the quartz crystal microbalance,<sup>92, 94</sup> ellipsometry,<sup>95, 96</sup> surface plasmon resonance<sup>97, 98</sup> or atomic force microscopy<sup>99</sup> also have some problems when trying to give absolute quantitative numbers because of the contribution of water molecules, surface roughness or time limitations. Moreover, these techniques are not suitable for high-throughput screening of samples. The use of fluorescent dyes to label and detect proteins is another alternative and, despite it can affect the conformation of the labelled protein, it has become nowadays the preferred method for the detection of molecules in microarray applications.<sup>3</sup> This methodology is suitable for high-throughput screening by using a fluorescent scanner device and also allows multicolour detection, based on the restricted excitation and emission spectra of the alternative dyes. Microarray measurements using fluorescent labelling

can be either quantified absolutely (through direct labelling of the spotted protein) or relatively.<sup>3</sup> The later approach is the most commonly used in protein microarray applications and relies on making relative fluorescence comparisons between spots or substrates, after the printed slides have been incubated with the labelled target proteins or antibodies.<sup>3, 87</sup> Radiolabelling of proteins can be another choice,<sup>66</sup> although this approach results more complex and expensive than fluorescence labelling due to the requirement of radioactive material handling and detection equipment.<sup>3</sup>

In order to focus our study on the comparison of the most promising substrates used in cellular microarrays, an extensive comparison of the results reported in the literature concerning the use of different substrates was carried out. This revealed that most of the reported works on cellular microarrays deal with specific proteins (antibodies, ECM proteins and growth factors) that are needed for applications such as cell-antibody,<sup>52, 71</sup> cell-ECM protein<sup>50, 53</sup> or cell-growth factor<sup>48, 54</sup> interaction testing.

Usual strategies for cellular microarrays devoted to **cell-ECM protein interaction** studies require the fabrication of ECM protein microarrays and those have been reported to be successful on both chemically activated<sup>48, 68</sup> and non-activated<sup>50, 57</sup> substrates.

On the other hand, cellular microarrays used in **cell-growth factor interaction** studies have been reported to require growth factor microarrays being build on chemically activated substrates to promote the factor anchorage to the surface.<sup>48, 54</sup> Chemically activated substrates can promote a strong binding of growth factors and other signalling ligands, therefore enhancing its effects on cells.<sup>41</sup> The surface chemistry is generally used to directly immobilise the factor on the surface in a covalent manner.

Other appealing strategies to bind growth factors and other proteins reside in using an “intermediate” linker protein (such as antibodies,<sup>100</sup> streptavidin,<sup>31</sup> or fibrin<sup>46</sup>) which will capture the desired signalling ligands by a high-affinity reaction.<sup>25, 101</sup> In these strategies, the intermediate linker protein is immobilised onto the chemically activated substrate and, when the target protein is added, it binds exclusively to spots containing its counterpart (refer to section 1.3.2 in the Introduction of this thesis for a graphical example).<sup>101</sup> In general, strategies based on protein immobilisation through an intermediate linker are a more complex approach that benefit of a reduction on the degree of protein denaturation, therefore improving its biological activity.<sup>31</sup>

Besides the substrate surface chemistry, another parameter which is known to be critical in a cellular microarray application is the printing buffer, this term referring to the solution used to

dilute the proteins that are going to be printed in a protein microarray fashion. Solution additives are usually employed to keep the spot hydrated during protein immobilisation, with the aim of promoting protein attachment in an active conformation, and to generate a homogeneous distribution of molecules.<sup>102, 103</sup> For this purpose, several printing buffers have been described in literature. The most commonly used printing buffer is phosphate buffered saline (PBS), which is used alone<sup>67</sup> or with the inclusion of a variable percentages of glycerol.<sup>35, 48, 50</sup>

The motivation of this work was to set up the bases for the fabrication of cellular microarrays which allow the culture of mesenchymal stem cells and, eventually, the study of some early differentiation stages. Taking into account the state-of-the art, the experimental approach chosen here to fabricate the cellular microarrays consisted in producing protein microarrays built with two components, an ECM protein that was considered spotted alone or mixed with a growth factor on the substrate. Therefore, in this platform cell attachment will be provided by the ECM protein, while the differentiation responses will be induced by the combination of the ECM protein and the growth factor.

Based on the stated election and the considerations mentioned before regarding substrates requirements and assayed approaches, in this chapter it was decided to focus the comparative performance work on four different substrates reported in the literature (and also evaluated here from preliminary assays performed, which are presented in Appendix C) as suitable for cellular microarray formation: aldehyde-derivatised glass (AD-Glass), aldehyde-derivatised agarose (AD-Agarose), poly(ethylene) oxide-like glass (PEO-like) and PFP-COOH –derivatised poly(methylmethacrylate) (a-PMMA). Two more substrates that are not chemically activated have been used as controls: untreated glass (Ctrl-Glass) and BSA-coated glass (BSA-Glass). The first one was chosen as a non-chemically activated control substrate and the last one was chosen as a negative control for its ability of avoiding protein adsorption. The performance of these substrates in protein microarrays for cellular microarray applications was tested by means of quantitative comparisons of the amount of the protein immobilised on the spots, passivation efficiency and other characteristics as spot shape and uniformity. For the purpose of these studies, one of the most common ECM molecules, fibronectin (Fn) was used as an ECM protein model while a smaller protein, streptavidin (SA) was selected as a convenient model for growth factor protein (no real growth factor protein has been used on these experiments because of pricing reasons). Both proteins (fibronectin and streptavidin) were fluorescently labelled with different carefully chosen fluorophore molecules, so that their detection was possible by a fluorescence scanner that provided accurate data suitable for quantification. Solutions of either

single protein or protein mixtures were prepared and tested, covering a broad range of concentrations (chosen taking into account the existing cellular microarray literature) and two buffers (PBS and PBS with 2% glycerol). This set-up provided enough data for a thoughtful comparison among the different substrates regarding their performance on the chosen model of protein microarrays and allowed ending up with conclusions defining the substrate and other experimental parameters (i.e. the protein concentration used for printing, the spot size and the printing buffer) to be used for further cellular microarray applications using stem cells.

## **2.2 Materials and methods**

### **2.2.1 Proteins and chemicals**

Human cellular fibronectin (Sigma, Spain) was fluorescently labelled using the Alexa Fluor 555 protein labelling kit (Invitrogen, Spain) following the manufacturer's instructions. Labelled Fn was checked to be still in its active conformation by a successful cell attachment and viability test at 24 h before being used in the microarrays. Streptavidin Alexa Fluor 647-conjugated was purchased from Invitrogen (Spain). Unless otherwise specified, all other chemicals were purchased from Sigma (Spain).

### **2.2.2 Substrate preparation**

Four chemically modified substrates and two control substrates were used for the experiments in this chapter. Taking into account their surface protein immobilisation properties, the tested substrates can be classified into three categories:

- Substrates with chemically activated surfaces to promote protein covalent immobilisation: aldehyde-derivatised glass (AD-Glass), aldehyde derivatised- agarose (AD-Agarose) and PFP-COOH-derivatised PMMA (a-PMMA) substrates.
- Substrate with a chemically modified non-fouling surface: poly(ethylene) oxide-like glass (PEO-like).
- Substrates with non-chemically modified surfaces (control substrates): untreated control glass (Ctrl-Glass), used as reference, and BSA-coated glass (BSA-Glass) as negative control that avoids protein adsorption.

Table 2.1 summarizes the main characteristics of the surfaces tested regarding their chemical activation to promote protein immobilisation, their availability as commercialised standard

products and their non-fouling properties, together with some literature references in which they have been used for protein microarray and cellular microarray applications.

Substrate	Abbrev. used	Properties			References	
		Non-fouling surface	Chemical activation	Standardised production	Prot. microarray related	Cellular microarray related
Aldehyde derivatised glass	AD-Glass	N	Y	Y	35, 86	48, 68
Aldehyde derivatised agarose	AD-Agarose	Y*	Y	N	29, 104	(non activated agarose) <sup>59</sup>
PFP-COOH-derivatised PMMA	a-PMMA	N	Y	N	105	68
Poly(ethylene) oxide-like coated glass	PEO-like	Y	N	N	90	57, 91
BSA pre-coated glass	BSA-Glass	N.A.	N	N	N.A.	N.A.
Control Glass	Ctrl-Glass	N.A.	N	Y	N.A.	N.A.

**Table 2.1** Substrate information summary. Abbreviations used are, N: NO; Y: YES; N.A.: Not Applicable. \* non-fouling surface when not chemically activated.

AD-Glass slides were purchased from Array It under the trade name “SuperAldehyde 2” slides (Telechem, USA) and were printed as received.

Activated AD-Agarose slides were provided by the Transcriptomics Platform of the Parc Científic de Barcelona (Spain). These substrates were prepared as reported by Afanassiev et al.<sup>29</sup> For this purpose, ethanol-cleaned microscope glass slides (Deltalab, Barcelona, Spain) were first silanised (PlusOne Bind-Silane, Amersham Biosciences, Spain) overnight in agitation at RT. Afterwards, the slides were washed with PBS and dried by centrifugation. An agarose solution (1% in Milli-Q water) was prepared and boiled until completely dissolved. This solution was poured over the silanised slides (2 mL per slide) and a gasket slide (Agilent technologies, Spain) was placed on top to restrict the agarose coating to a ~14.25 cm<sup>2</sup> area (62 x 23 mm). After gelling of the agarose, the gasket was carefully removed and the slides were allowed to dry at RT for 30 minutes. Next, the coated slides were submerged in Milli-Q water for 4 h at RT for hydration, followed by an overnight incubation at 37 °C. This last step allowed for the strong adhesion of the agarose matrix to the substrate. The coated slides were next incubated with a 20 mM NaIO<sub>4</sub> solution for 2 h in agitation at RT, for the chemical activation of the agarose.

Finally, the slides were washed with Milli-Q water and dried by centrifugation (5 minutes at 1000 rpm). Slides were stored at RT until used.

The protocol followed for PMMA activation has been previously reported and is depicted in Figure 2.1.<sup>105</sup> In brief, the PMMA surface was activated by hydrolysing the available methyl esters of the polymer by immersion in NaOH (2 M) for 12 h. After rinsing with Milli-Q water, the newly formed carboxylate anion at the surface was neutralized by briefly dipping the samples in HCl (0.1 M). Following rinsing with Milli-Q water and absolute ethanol, the slides were dried under a stream of argon. The carboxylated surface of PMMA was then further activated by introducing a pentafluorophenol (PFP) group, which makes the carboxylic carbon more reactive to a nucleophilic attack by amine groups, therefore allowing the covalent binding of spotted proteins and of the BSA proteins used for passivation. For this purpose, PMMA sample surfaces were completely covered with an ethanolic solution of N-(3-dimethylaminopropyl)-N'-ethylcarbodiimide hydrochloride (EDC-HCl, 38 mg/mL), N,N-diisopropylethylamine (Atofina EDIPA, 3.5% v/v) and 2,3,4,5,6-pentafluorophenol (36 mg/mL) for 15 min. Finally, PMMA slides were rinsed with ethanol and dried with argon.

PEO-like slides were provided by the group of François Rossi (European Commission, Joint Research Centre, Ispra, Italy). These substrates were produced using plasma-enhanced chemical vapour deposition in a capacitively coupled reactor, using a glow discharge in diethylene glycol dimethyl ether vapour (DEGDME, Sigma), as previously reported.<sup>90, 106</sup>

For BSA-Glass, glass slides obtained from Deltalab (Barcelona, Spain) were ultrasonically cleaned in ethanol absolute for 20 minutes and dried under argon gas flow. Afterwards, they were submerged overnight in a 2% BSA solution in PBS. The following day the slides were washed with PBS, dried under argon and printed.

Control glass (Ctrl-Glass) slides were obtained from Deltalab (Barcelona, Spain). Before printing, control glass slides were ultrasonically cleaned in ethanol absolute for 20 minutes and dried under argon gas flow.

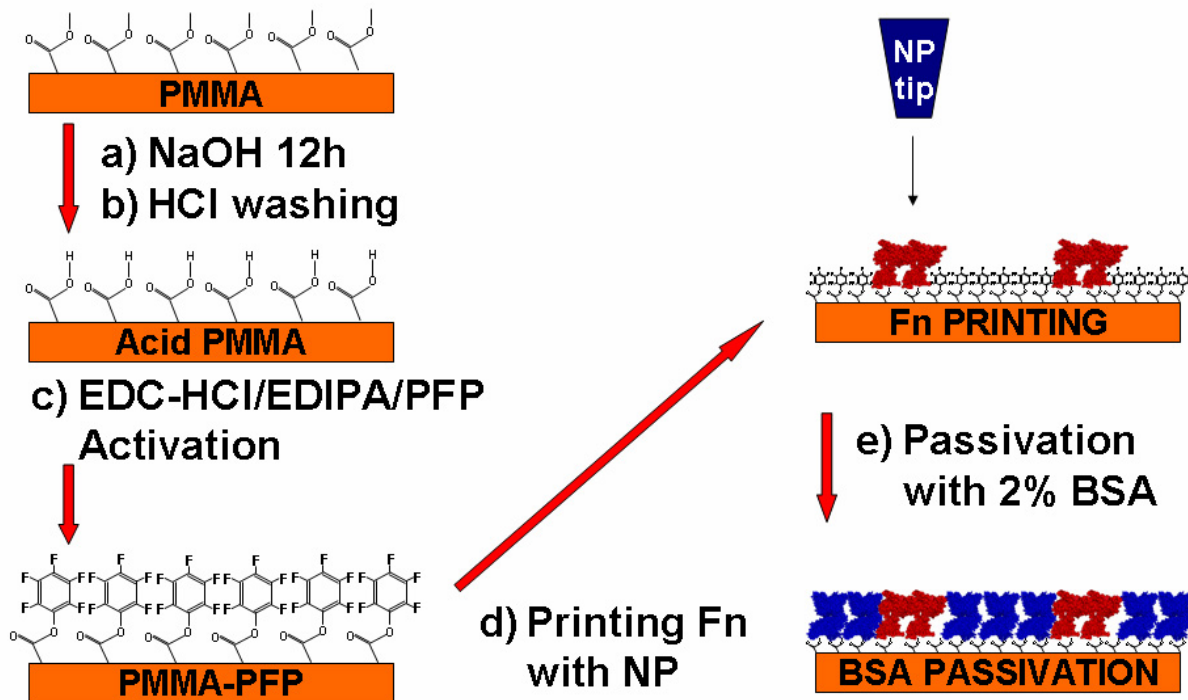


**Figure 2.1** PMMA chemical activation protocol and protein printing. The PMMA was activated by hydrolysing the surface by immersion in NaOH (a) for 12 h, afterwards the surface was washed by briefly dipping the samples in HCl (b) and then it was further activated by incubating the surface in an ethanolic solution of EDC-HCl, EDIPA and PFP (c). After activation, the Fn features were spotted on the surface (d) and then the non-printed surface was blocked with BSA (e).

### 2.2.3 Substrate characterisation previous to the protein microarray fabrication

All the substrates selected for the experiments described in this chapter, including the control ones, were characterised on the surface properties that potentially have the largest contribution to their performance on the protein adsorption or immobilisation and protein spot dimension and morphology. These properties are their wettability (assessed by contact angle measurements) and their roughness, measured by atomic force microscopy.

Contact angles of the printing buffer solution (PBS) on the different substrates were measured by the sessile-drop method with an OCA contact angle system (Dataphysics, Germany). PBS droplets of 3  $\mu$ l in volume were carefully deposited on each sample surface and images of the liquid droplets in contact with the surfaces were captured immediately after droplet stabilization. Droplet profile was automatically fitted with SCA20 software (Dataphysics, Germany) using a circular fitting method. At least ten contact angle measurements were collected from two different samples for each substrate. As protein microarray fabrication was carried out in the substrates while their temperature was fixed at 4°C, it was decided to measure the substrate

wettability properties in the same conditions. For this purpose, all substrates were previously kept overnight at 4 °C, and just taken from the refrigerator immediately before the contact angle measurements.

Atomic force microscope (AFM) measurements were performed by using a commercial MFP-3 (Asylum Research, USA) AFM device. AFM measurements were completed in air, in tapping mode using MPP-12100-50 AFM silicon tips (Veeco, USA) with 123-166 kHz resonant frequency and 5 N/m spring constant. Four measurements were done for each ready-to-print substrate from two different samples on random areas of 40 x 40 micrometers. RMS roughness values were obtained by analyzing the AFM images with the WSxM software (Nanotec, Spain).<sup>107</sup> Roughness values given here represent the average and standard deviation obtained from the 4 measurements performed on each substrate.

#### **2.2.4 Protein microarray fabrication**

For the preparation of printing solutions, labelled Fn (Alexa Fluor 555) was first premixed with unlabelled Fn to yield 1% labelled Fn mixture (Fn 1% A555 in what follows). Protein solutions of Fn 1% A555 at different concentrations ranging from 50 to 360 µg/mL were prepared in the two printing buffers to be tested, namely, PBS and PBS with 2% glycerol (2% v/v). Moreover, mixtures of Fn 1% A555 at different concentrations and Streptavidin Alexa Fluor 647 (SA A647 in what follows) at a concentration of 50 µg/mL were prepared, again in the two buffers assayed. Table 2.2 summarizes the composition of the prepared solutions and the nomenclature selected to refer to them, which will be kept in what follows.

Volumes of 10 µL of all the solutions were placed in wells of a 384 wellplate. A robotic non-contact piezoelectric plotter (Nano-Plotter, GeSiM GmbH, Germany) was used to dispense the protein solutions onto the substrates in a square microarray format following the layout described in Figure 2.2. The volume of the liquid dispensed by each drop, given by the dimensions of the piezoelectric-jet dispenser needle, was set at 0.4 nL. This layout accounts for the different experimental conditions assayed, such as the spot composition printed, spot size and printing buffer used. Spot size was tuned by overprinting multiple drops (1, 5 or 10) consecutively at one single location. The experimental system was placed in a clean room facility, and the environmental humidity was in the range from 40 to 60 % during the printing process. Moreover, the workplate where the substrates were placed for the deposition procedure was cooled down to 4 °C with the aim to delay protein dry-out during the printing process. Once

printed, the slides were incubated overnight at 4 °C to prevent evaporation and allow proteins to react with the surface chemistry (where adequate).

Buffer	Fn 1% A555 concentration spotted [µg/mL]	SA A647 concentration spotted [µg/mL]	Spot condition nomenclature
PBS or PBS 2% glycerol	50	0	Fn50
	100	0	Fn100
	200	0	Fn200
	360	0	Fn360
	50	50	Fn50 SA50
	100	50	Fn100 SA50
	200	50	Fn200 SA50
	360	50	Fn360 SA50

**Table 2.2** Nomenclature adopted to refer to each spot composition printed. Besides the Fn and SA concentrations used for printing the solutions, all conditions were spotted in PBS and PBS 2% glycerol, and in 1, 5 and 10 consecutive drops.

The technical nanoplotter parameters used in the printing process (i.e. the voltage and width of the electric pulse used for delivering the drops from the piezoelectric pipette and the time during which the pipette was washed in between dispensing tasks) were carefully chosen after a previous screening work, to be the optimal for the adequate drop dispensing (i.e. no satellites formed, no clogging of the system and no protein carry over). In between the dispensing of two different protein solutions and in order to avoid cross-contamination among the different mixtures, an additional pipette washing step was configured. By this, the pipette produced a 10 µL uptake of a KOH solution (100 mg/mL) that was incubated within the pipette for 10 seconds and then washed again 30 seconds in Milli-Q water before next protein solution uptake. No protein carryover while dispensing the solutions was detected using this protocol. For each type of substrate a minimum of 3 printed replicas were performed (2 replicas for BSA-Glass and Ctrl-Glass) in independent experiments, meaning that for each batch of microarrays the protein solutions were newly prepared.

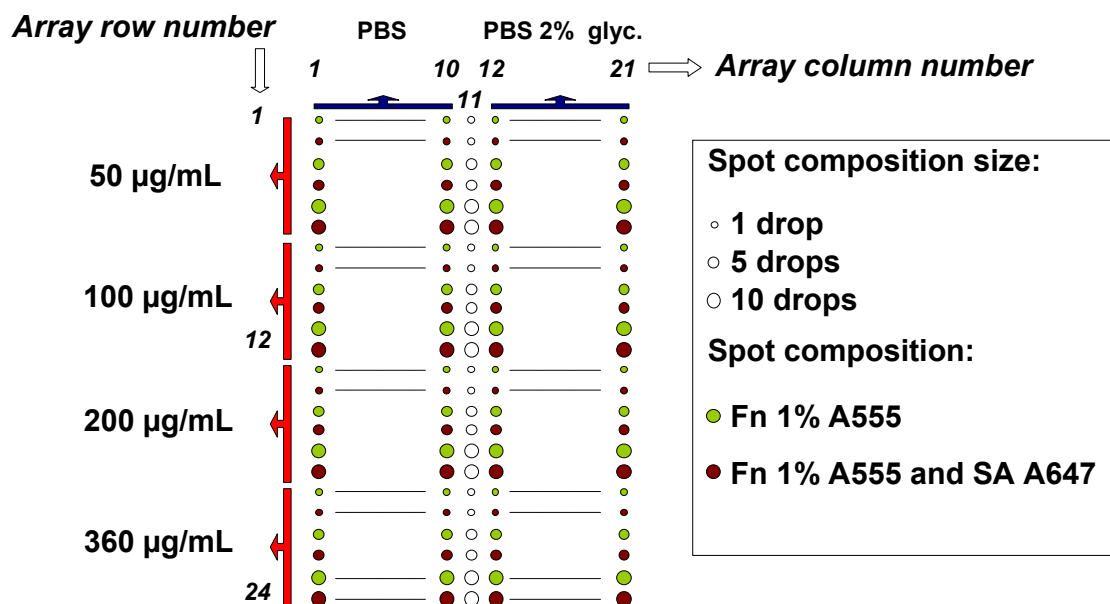


**Figure 2.2** Spotted protein layout. Each spot condition was defined by the number of drops spotted (1, 5 or 10 drops), the buffer composition (PBS or PBS with 2% glycerol), the Fn 1% A555 concentration (50, 100, 200 or 360 µg/mL) and the inclusion or not of SA A647 (50 µg/mL) in the protein solution spotted. Spot conditions were spotted in 10 replicates in each block, as presented here. Two such blocks were spotted in each slide assayed, yielding 20 spot replicates per condition tested.

## 2.2.5 Protein microarray characterisation

A GenePix 4000B fluorescence microarray scanner device (Molecular Devices Corp., USA) was used to measure the fluorescence signal of the protein microarrays built on the different substrates. The scanning resolution was set to 10 µm/ pixel and the laser power used was the same (10%) for all substrates in all scans. The PMT (photomultiplier tube) gain values, that define the amplification of the signal by the scanner fluorescence detector device, were optimised for each individual substrate to get the best signal-to-noise ratio (i.e. the PMT that yielded the highest signal with the lowest background). The fluorophores used in this study have an excitation peak at 555 nm (Alexa Fluor 555) and 647 nm (Alexa Fluor 647), and the emission maxima at 565 (Alexa Fluor 555) and 665 nm (Alexa Fluor 647). These fluorophore signals were successfully detected using scanner lasers that excite at 532 nm (green) and 635 nm (red), with the ~557-592 nm and ~650-690 nm emission filters, respectively.

The experimental procedure followed to quantify the protein mass successfully immobilised on each spot of the different substrates is depicted in Figure 2.3 and it was based on the fluorescence measurements performed with the described scanning apparatus. After overnight incubation of the printed slides, the protein microarrays were scanned “as spotted” and the fluorescence intensity values for each individual spot were measured (Figure 2.3, step 2). By associating the fluorescence intensity measured at this point (background subtracted),  $I_c$ , for

each spot with the theoretical amount of mass deposited,  $m$ , for that spot (calculated by Eq. 2.1), a calibration curve linking the fluorescence signal value with the protein mass producing those intensity levels (Eq. 2.2 and Figure 2.3, step 3) could be established:

$$m = C \cdot \#D \cdot V \quad (\text{Eq. 2.1})$$

where  $C$  is the concentration of the protein solution spotted,  $\#D$  is the number of drops in the spot and  $V$  is the volume of each drop (constant and equal to 0.4 nL for all the experiments presented here).

Being  $I_c \propto m$ , if calibration is linear, then:

$$I_c = A \cdot m + B \quad (\text{Eq. 2.2})$$

where  $A$  and  $B$  are the regression constants that link the fluorescence intensity measured with the amounts of protein mass deposited in each spot condition (linked to the amount of fluorophore deposited in each spot).

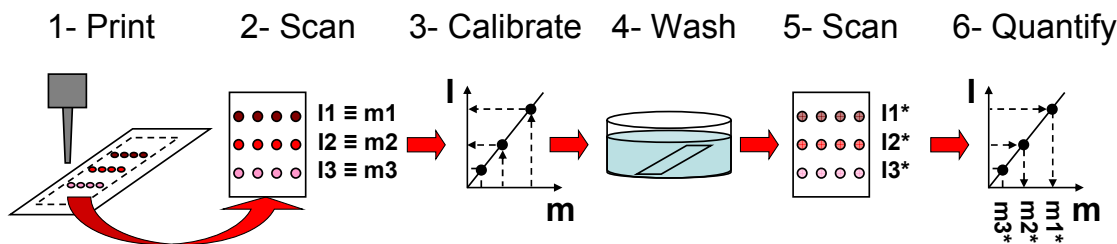


**Figure 2.3** Experimental schematic. The protein solutions were first spotted on the substrates (1) and, after overnight incubation, the slides were scanned “as spotted” with a fluorescent scanner device (2). Data obtained from these scans allowed tracing calibration curves between the spotted mass and the fluorescence intensity obtained for each feature (3). Afterwards the substrates were passivated (according to the case) and washed (4). Finally, the slides were scanned again “after washing” (5) and the fluorescence intensity data was converted to immobilised protein mass using the previously obtained calibration curves (6).

In order to calculate the amount of immobilised protein on each spot, the main parameter on which substrate performance comparison was based, the next steps involved the removal of the unbound protein and the passivation of the areas outside the spots. For this purpose, the fabricated protein microarrays were treated as follows (Figure 2.3, step 4):

- For AD-Agarose and PEO-like glass substrates, no passivation was performed and washing was done with PBS 0.05% Tween for 1 hour in agitation at RT. The washing step was finished by centrifuging the slides at 1000 rpm for drying purposes.

- For all the other substrates (including BSA-Glass), surface passivation was accomplished by incubation in a BSA solution (2% in PBS) for 1 hour in agitation at RT. Afterwards, the substrates were washed twice in PBS and allowed to dry at RT.

For all substrates, data obtained after these passivation and washing steps is referred to as “after washing” data. The substrates were fluorescently scanned again (Figure 2.3, step 5) taking care that the same PMT values were kept. The new intensity data values measured now for each spot,  $I^*$ , were then entered in the calibration curve obtained previously (Eq. 2.2), to obtain the protein mass,  $m^*$ , that would be leading to such intensity values (Eq. 2.3 and step 6 in Figure 2.3). These values were associated with the amount of protein mass immobilised in each spot.

$$m^* = \frac{(I^* - B)}{A} \quad (\text{Eq. 2.3})$$

Additionally, substrate performance was also compared in terms of protein spot size and homogeneity, evaluated “as spotted” and “after washing” for all the substrates and experimental conditions described in the layout of Figure 2.2. Spot size values together with protein mass obtained from Eq. 2.3 were also used to compute and compare spot protein density immobilised on the different substrates.

## 2.2.6 Statistics

Three independent experiments, meaning protein microarray fabrication, were performed for each type of the four chemically modified substrates, while two independent experiments were performed for the two control substrates. All measurements presented here for each spot composition, defined by the protein and buffer combinations and the spot size, represent the average of 20 spots with identical composition and size ( $n = 20$ ), spotted in replicate blocks within each slide printed. Protein microarray measurements and analysis was aided with GenePix Pro 6.0 software. Statistical analysis was performed using MS Excel and SPSS. Comparison between mean values was done using the Student’s t-test, setting a significance level of  $p = 0.05$ . All graphical data is reported as mean +/- standard deviation. Standard deviation values associated to the immobilised protein masses predicted from the calibration curves were estimated using a weighted least squares regression to account for the uncertainties obtained with the calibration method. The R package<sup>108</sup> gplots was used to perform hierarchical clustering on substrates and spot compositions using average linking on Euclidean distance.

Parametric one-way ANOVA tests were performed for statistical analysis of the substrate contact angles ( $n = 10$ ) and roughness data ( $n = 4$ ). Significance levels were set at  $p < 0.05$ .

## 2.3 Results

### 2.3.1 Substrate characterisation previous to the protein microarray fabrication

The substrates chosen for these experiments covered a broad range of surface chemistries, yielding a range of different surface properties. Among these properties, the contact angle (CA) between the printing buffer (PBS) and the different substrates is considered one of the main parameters contributing to the spot size,<sup>109</sup> the amount of protein immobilisation and the protein configuration on the surface.<sup>110, 111</sup> In particular, contact angle values approaching or larger than 90° indicate a hydrophobic surface that is going to confine the protein solution drops on smaller areas and, by this, smaller spot sizes will be expected for these substrates. The results obtained for CA measurements of PBS buffer on all the substrates tested are presented in Table 2.3.

Substrate						
	AD-Glass	AD-Agarose	a-PMMA	PEO-like	BSA-Glass	Ctrl-Glass
CA (°) ± SD	70.9 ± 6.0	44.7 ± 25.1	80.0 ± 2.0	70.7 ± 3.4	63.2 ± 5.4	19.9 ± 3.6

**Table 2.3** Contact angle results (in PBS) for the substrates tested. Measurements performed after overnight incubation at 4 °C of ready-to-print substrates. Each value represents de mean and standard deviation of 10 measurements. AD-Glass and PEO-like CA values are not statistically different at the  $p < 0.05$  level (One-way ANOVA test), CA values for all other substrates are statistically different between each other ( $p < 0.05$ , One way ANOVA Test).

After performing a One-way ANOVA analysis of the CA results, it was found that the order of statistically different substrates in terms of larger to smaller CA values was: a-PMMA>AD-Glass and PEO-like>BSA-Glass>AD-Agarose>Ctrl-Glass. Based on these results, the largest microarray spot sizes are expected for Ctrl-Glass, AD-Agarose and BSA-Glass substrates, in that order. The smallest microarray spot sizes, on the other hand, would be expected for a-PMMA. Based on the CA results presented, AD-Glass and PEO-like are expected to yield similar spot sizes. AD-Agarose slides showed a large dispersion in the contact angle values, which also changed from one to another batch of fabricated slides. Besides, the value obtained for AD-Agarose is considered here only as a qualitative indicator of wettability, since the actual printed spot sizes might be affected not only by the CA but also by the fact of AD-Agarose consisting of a polymer matrix which allows penetration of the solution into the coating.<sup>112</sup> In

this case, the volume of liquid deposited could be distributed in a 3D volume and therefore spot diameters can be different (probably smaller) than equal volumes spotted onto non-permeable surfaces.

On the other hand, other surface property that has been reported to be closely linked to protein adsorption is surface roughness. It is well-known that high surface roughness values amplify hydrophobicity,<sup>113</sup> increase the surface specific area and could act on protein conformation.<sup>110, 114</sup> Therefore, an increase in surface roughness would also increase hydrophobicity and will lead to smaller spot sizes. On the other hand, the effect of surface roughness on protein adsorption on a surface is not so clear. While some authors have reported that surface roughness in the range from 8 to 53 nm did not affect the amount of protein adsorbed,<sup>115</sup> other researchers have reported a marked increase in protein adsorption as the surface roughness increased from 2 to 33 nm.<sup>116</sup> The differences in the results reported in the literature can be attributed to the different types of proteins assayed as well as the material compositions on which the rough surfaces were produced.

The RMS surface roughness values obtained from the AFM images of each substrate (Figure 2.4) are summarised in Table 2.4. After performing a One-way ANOVA analysis of the roughness results, it was found that the order of statistically different substrates in terms of larger to smaller roughness values was: BSA-Glass>a-PMMA>AD-Agarose>Ctrl-Glass and PEO-like>AD-Glass. For the BSA-Glass slides, the results obtained are probably due to a non-homogeneous BSA coating on top of the glass slide, where randomly distributed BSA aggregates produce the increase in average roughness. For a-PMMA, an increase in roughness was expected due to the NaOH overnight incubation step performed for the chemical activation, which erodes the surface of the PMMA. AD-Agarose slides consist of a polymeric matrix and therefore it was also expected to show larger roughness values than those obtained for glass slides. AD-Glass was the substrate with the lowest roughness value. This result was expected since this commercially available substrate is based on ultra-plane, polished glass slides, and it is in accordance with the provided by the manufacturer (average 2 nm for SuperAldehyde 2 microscope slides, data from <http://www.arrayit.com>). Roughness of the Ctrl-Glass substrate was a little higher than AD-Glass, since the first one is just a standard microscope glass slide without any special polish treatment. PEO-like substrates also yielded low roughness values which were not significantly different (at the p<0.05 level) to the values obtained for Ctrl-Glass. Again, this was expected since the PEO-like substrates consist of a uniform, 20 nm thick, polymer layer deposited on top of glass slides.<sup>117</sup>

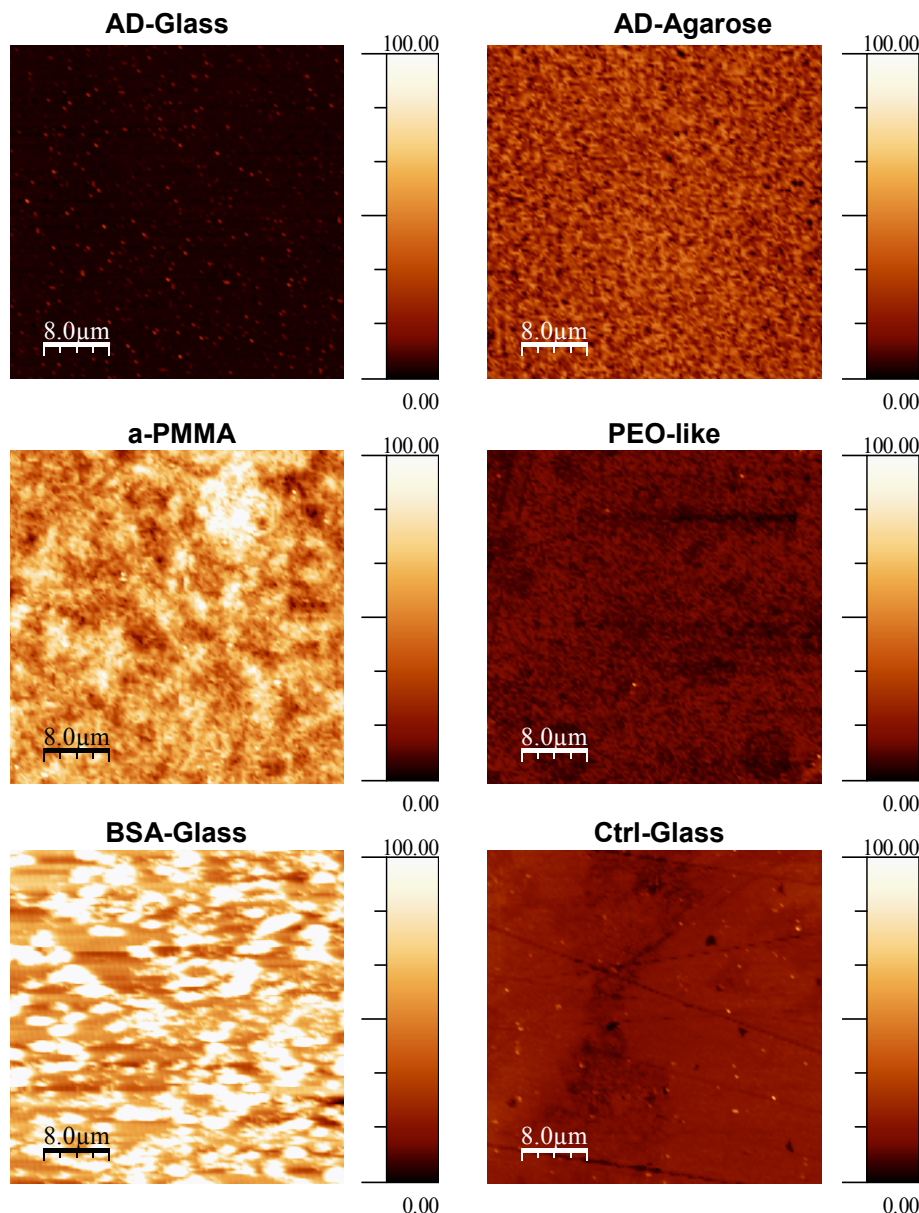


**Figure 2.4** Representative AFM images obtained for each of the substrates assayed. It can be observed that the substrates with the highest roughness values are BSA-Glass, a-PMMA and AD-Agarose, in that order. AD-Glass, on the other hand, is the substrate with the lowest roughness value.

Substrate						
	AD-Glass	AD-Agarose	a-PMMA	PEO-like	BSA-Glass	
Roughness (nm) ± SD	2.6 ± 0.2	11.4 ± 1.6	16.8 ± 1.3	5.0 ± 1.0	26.5 ± 7.8	5.4 ± 1.5

**Table 2.4** RMS roughness values obtained for each of the substrates assayed. BSA-Glass is the substrate with the highest roughness value, followed by a-PMMA and AD-Agarose. AD-Glass is the substrate with the lowest roughness value. PEO-like and Ctrl-Glass roughness values are not statistically different at the p<0.05 level (One-way ANOVA test), roughness values for all other substrates are statistically different between each other (p<0.05, One way ANOVA Test).

Contact angle and roughness values can provide a first estimation of which substrates are going to show smaller and which larger spot sizes. However, an additional parameter should be taken into account to predict the effective size of the protein spots on the microarrays, i.e the protein “fouling/non-fouling” character of the substrate surfaces.

This “non-fouling” property is used to refer to surfaces which resist protein adsorption,<sup>89</sup> and is mainly dictated by the chemical composition of the surface.<sup>118</sup> As an example, PEO-like surfaces are non-fouling when they are in a liquid environment mainly due to a self-repulsion of the PEO chains in water.<sup>90</sup> Therefore, protein solutions spotted in PEO-like slides could not spread so well on the substrate, yielding lower spot sizes than initially expected.

### **2.3.2 Qualitative protein microarray comparison among substrates**

Representative fluorescence scanner images for each substrate tested “as spotted” and “after washing” are presented in Figure 2.5 and Figure 2.6 and have been used to assess an overall qualitative performance of substrates for protein microarrays with the chosen proteins and the layout referred in Figure 2.2. It can be noticed that the images taken for all the substrates “as spotted” faithfully reproduce the intended layout. Comparing both the proposed layout and the “as spotted” experimental data obtained, some interesting qualitative remarks that assess the good quality of the protocol followed for the microarray fabrication can be made. Firstly, the approach of creating larger spots by increasing the number of drops was successful for all the substrates. Secondly, for a given number of drops deposited, increasing the protein concentration in the printing solution resulted in brighter spots, presumably containing increasing mass amounts of the proteins. Thirdly, spots containing one single protein in the printing solution do not show cross-contamination (presence of the other fluorophore) while spots that were designed to contain a mixture of the both proteins assayed present a yellow colour that comes from the mixture of the red and the green fluorophores associated to the individual proteins. At a first glance, it can also be observed that the “as spotted” feature sizes for equivalent spotting conditions significantly differ between the different substrates. The PEO-like glass surfaces yielded the smallest spots while the BSA-Glass and the AD-Agarose substrates showed the largest spots. PEO-like slides also had a strong background signal for the green scanner channel, probably due to an autofluorescence effect of the material.

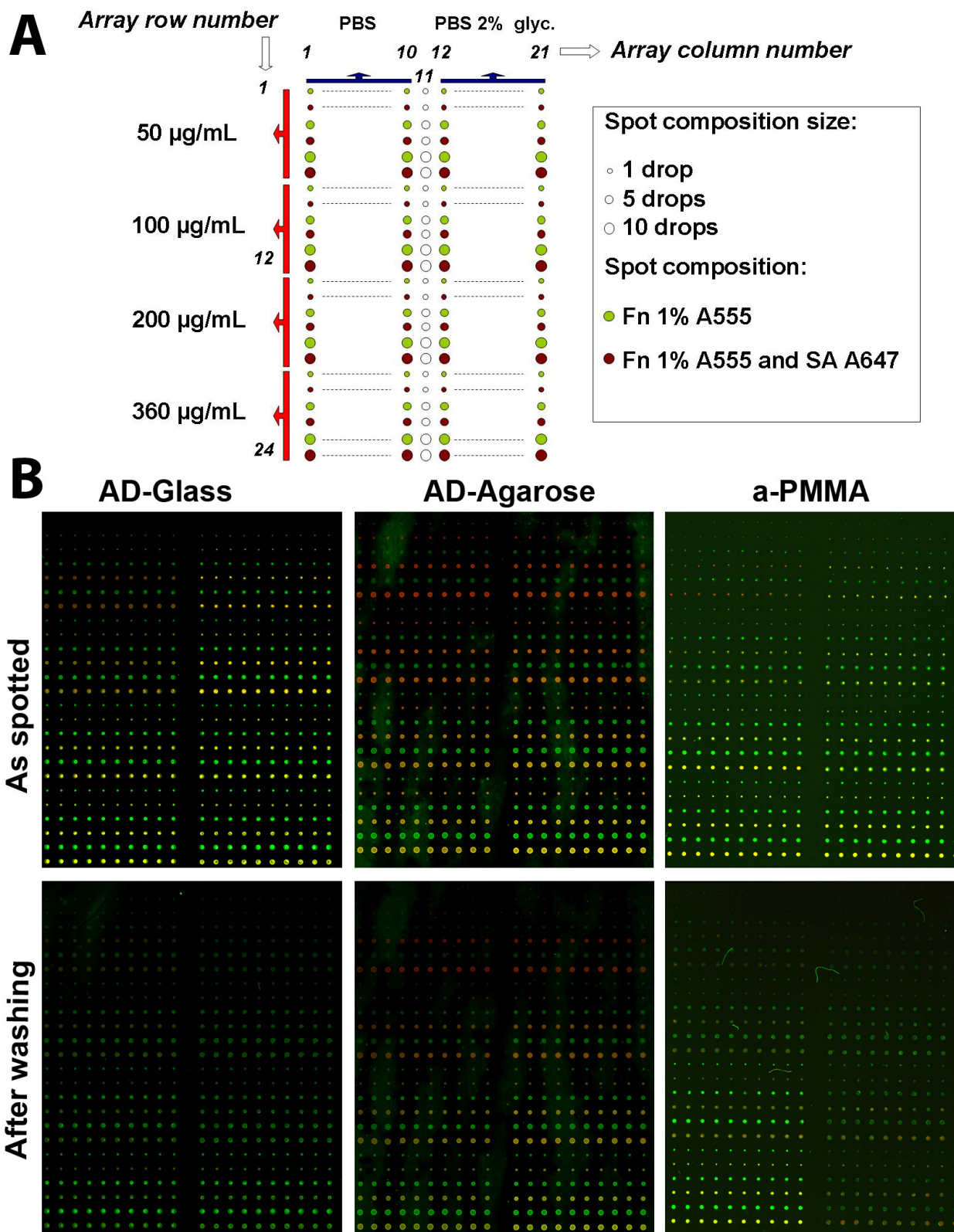


**Figure 2.5 A.** Protein layout spotted, reproduced from Figure 2.2. **B.** Representative scanner images obtained for substrates “as spotted” and “after washing” for AD-Glass, AD-Agarose and a-PMMA substrates. Green spots are Fn 1% A555, red to yellow spots are SA A647 premixed with different concentrations of Fn 1% A555. Distance between spots is 1 mm.

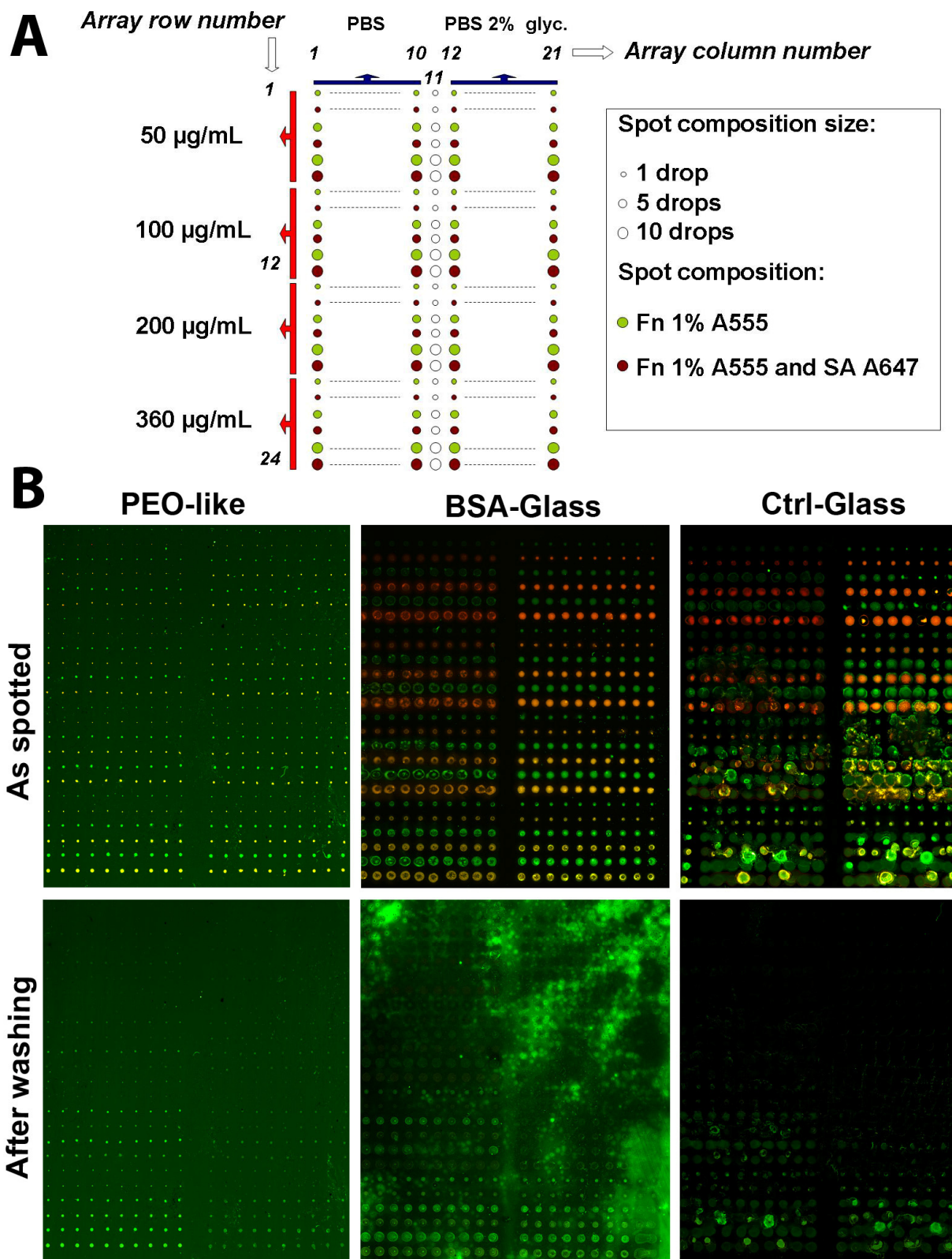


**Figure 2.6 A.** Protein layout spotted, reproduced from Figure 2.2. **B.** Representative scanner images obtained for substrates “as spotted” and “after washing” for PEO-like, BSA-Glass and Ctrl-Glass substrates. Green spots are Fn 1% A555, red to yellow spots are SA A647 premixed with different concentrations of Fn 1% A555. Distance between spots is 1 mm.

However, the most interesting differences among substrates are evidenced after the washing step, with the new fluorescence scanning images now showing the signal coming from the amount of the protein immobilised on the spots and some signal in the background coming from the unspecific adsorption of the unbound proteins to the passivated area (Figure 2.5 and Figure 2.6). These images are then giving comparative qualitative information about how the different surfaces performed on protein immobilisation and on surface passivation. It can be seen that all the chemically activated substrates (AD-Agarose, AD-Glass and a-PMMA) kept the protein microarray layout clearly identifiable “after washing”, although with less fluorescence intensity as it was expected. On the other hand, PEO-like glass substrates showed a dramatic decrease in fluorescence intensity, with the microarray layout lost for the spots with the lowest protein concentrations (top rows of the microarray) and also for almost all the spots made with PBS 2% glycerol (right column of the microarray). Additionally, they showed a negligible signal from SA (i.e. spots are mostly greenish). Other several interesting issues appear when looking at the protein microarrays obtained on the control slides. BSA-Glass slides, on one hand, did not effectively retain any of both proteins on the substrate, which were washed away or diffused over the passivated areas, thus creating an intense green background signal all over the substrate that was even more evident for the substrate part containing the spots made with PBS 2% glycerol buffer. As the green signal comes from the Fn, it can be proposed that this protein is the one adsorbed unspecifically all over the substrate. As no red or yellow signal was found after washing, it can be established that SA had a completely different behaviour and it was just washed away, probably because of being a less “sticky” protein. On the other hand, protein solutions printed on Ctrl-Glass slides yielded an unidentifiable microarray layout “as spotted”, since the spots produced using the highest protein concentrations and sizes merged with its neighbours. “After washing” most of the protein was removed and, interestingly, in comparison with BSA-Glass, the negligible increase in the background signal allows proposing a role of the BSA coating for the attachment of Fn. This effect has been previously noted by other researchers,<sup>119</sup> and consists of an activation of cell adhesion proteins (such as Fn) by BSA, which could modulate the protein conformation.

### **2.3.3 Analysis of the spot size and morphology of the protein microarrays**

#### ***General overview***

A more detailed qualitative analysis of the spot size and morphology yielded interesting insights for each of the substrates. Figure 2.7 to Figure 2.9 show detailed “as spotted” images of

representative spots for all the conditions on the different substrates. As previously seen on the whole layout images, increasing the number of drops of protein solution resulted in an effective increase in spot diameter for all substrates and both printing buffers tested.

At a first glance, it was observed that the order of substrates (classified according to the spot sizes) differed from that expected just from the CA data. A new tentative order of substrates, from larger to smaller spot sizes, can be proposed from visual inspection of Figure 2.7 to Figure 2.9 as follows: Ctrl-Glass>BSA-Glass>AD-Agarose>AD-Glass>a-PMMA>PEO-like. These closer pictures also allowed assessing that, for a given number of drops, the size and morphology of green spots (Fn only, upper spots) and red to yellowish spots (Fn and SA, bottom spots) was not affected by the inclusion of SA in the protein mixture spotted.

In particular, for the control substrates it was observed that spotting protein solutions into Ctrl-Glass slides resulted in spots mixing with its neighbours (Figure 2.9, bottom). This effect occurred both for spots with and without glycerol, and was more important as the Fn concentration of the solution and the number of drops spotted increased. This performance can be explained by the extremely low CA obtained for this substrate, indicating a highly hydrophilic surface that allowed the spotted drops to spread and contact the neighbour spots, which were set 1 mm apart. If the same substrate was pre-coated with BSA, therefore yielding the BSA-Glass substrates, it was previously noted that the hydrophilicity of the glass surface was importantly decreased (from CA data), and this was further confirmed by the smaller spot sizes presented in Figure 2.9.

### ***Feature morphology analysis***

When comparing the AD-Agarose “as spotted” features (Figure 2.7) with those obtained for a-PMMA (Figure 2.8) and AD-Glass (Figure 2.7), it was found that for the lowest Fn concentrations a two-phase concentrical intensity regions were clearly distinguished in a-PMMA and AD-Glass (with a brighter fluorescence signal at the centre of the spot). These two-phase intensity regions had interesting effects on the spots “after washing”, as presented in Figure 2.10.

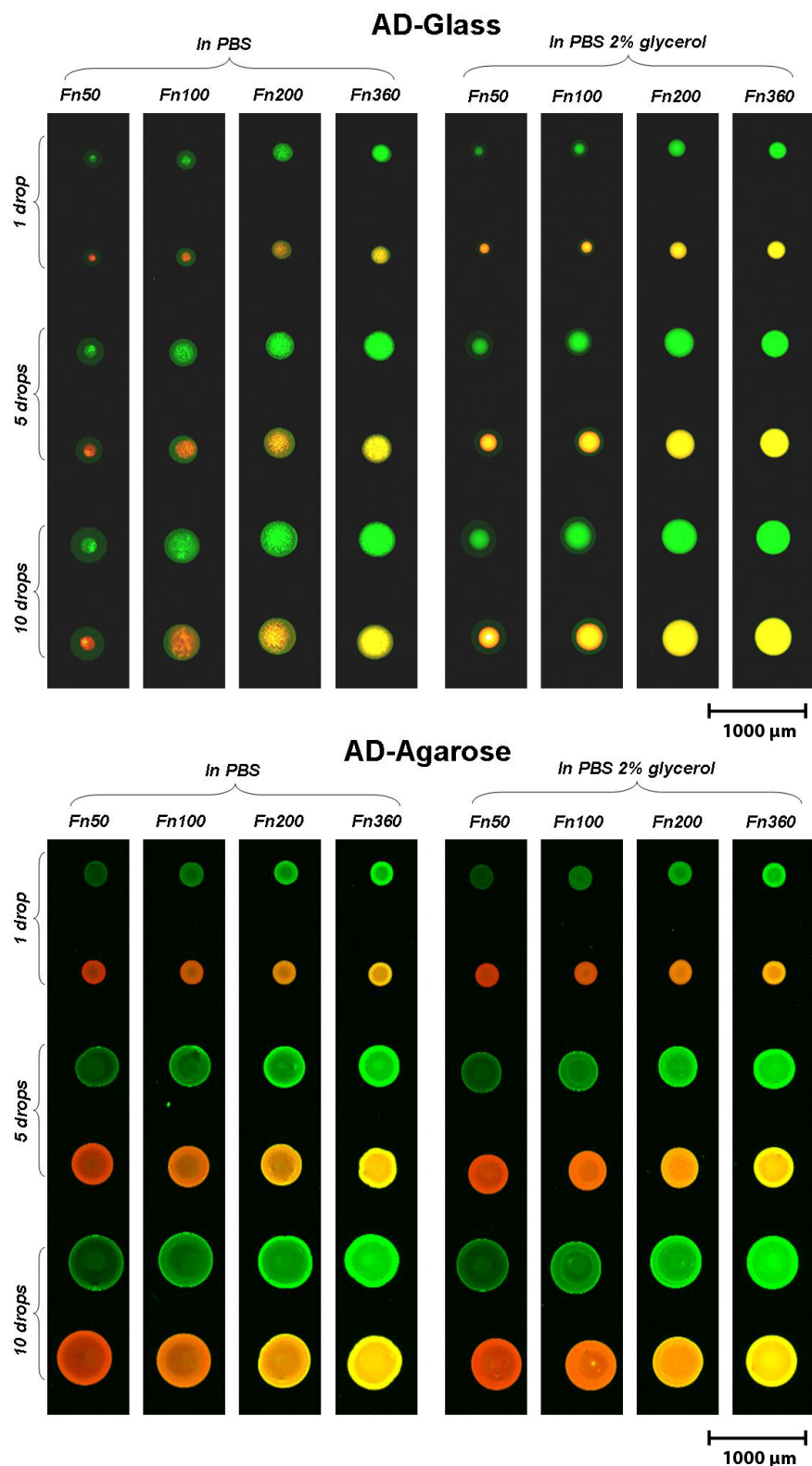


**Figure 2.7** Zoom-in of scanner images for AD-Glass and AD-Agarose substrates “as spotted”. Detail of the spots printed at different Fn concentrations (indicated at the top of the image), with (on the right) and without (on the left) glycerol, at different spot sizes (indicated on the left of the image) and with (bottom, red to yellowish spots) and without (upper, green spots) SA50 included in the protein mixture spotted.

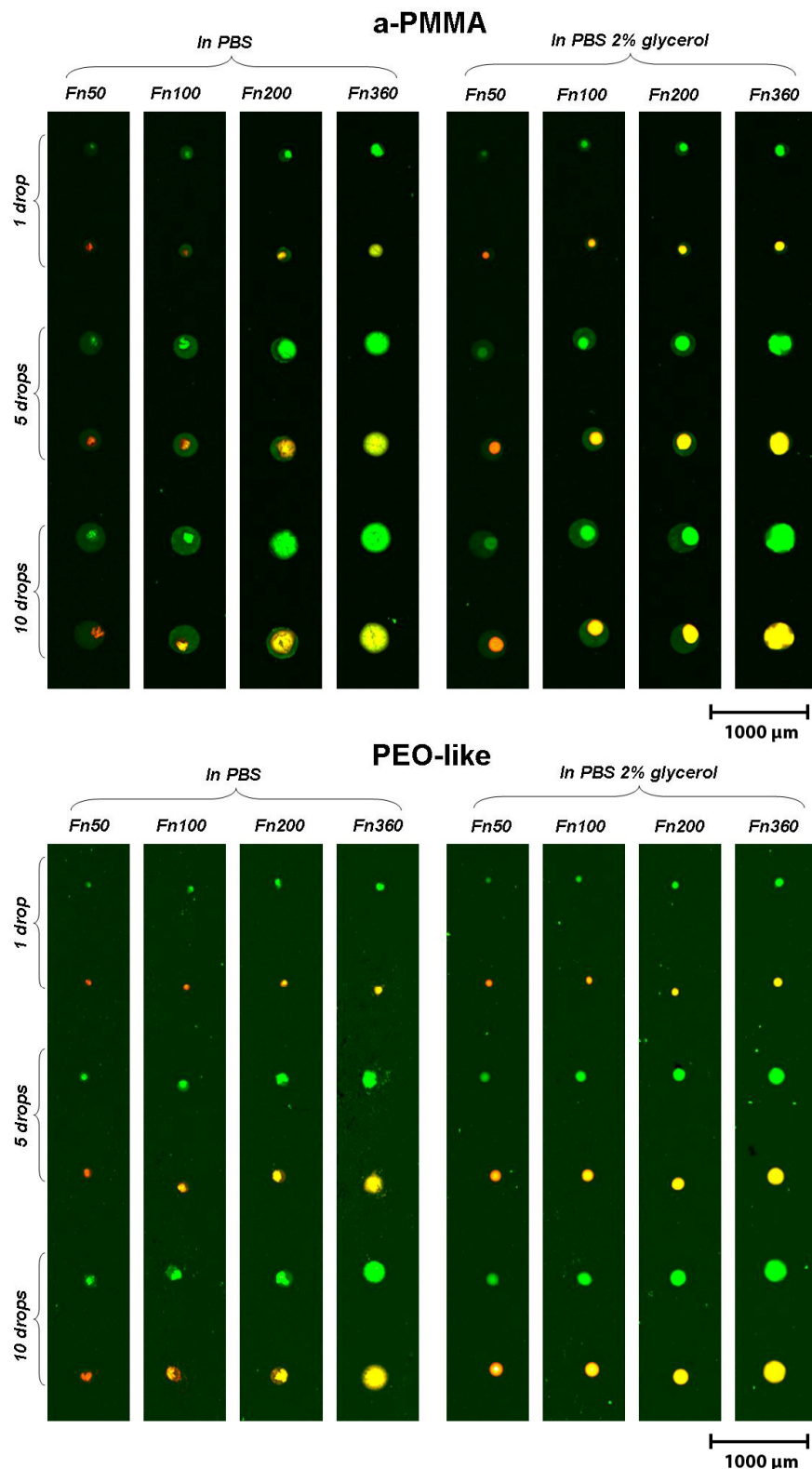


**Figure 2.8** Zoom-in of scanner images for a-PMMA and PEO-like substrates “as spotted”. Detail of the spots printed at different Fn concentrations (indicated at the top of the image), with (on the right) and without (on the left) glycerol, at different spot sizes (indicated on the left of the image) and with (bottom, red to yellowish spots) and without (upper, green spots) SA50 included in the protein mixture spotted.

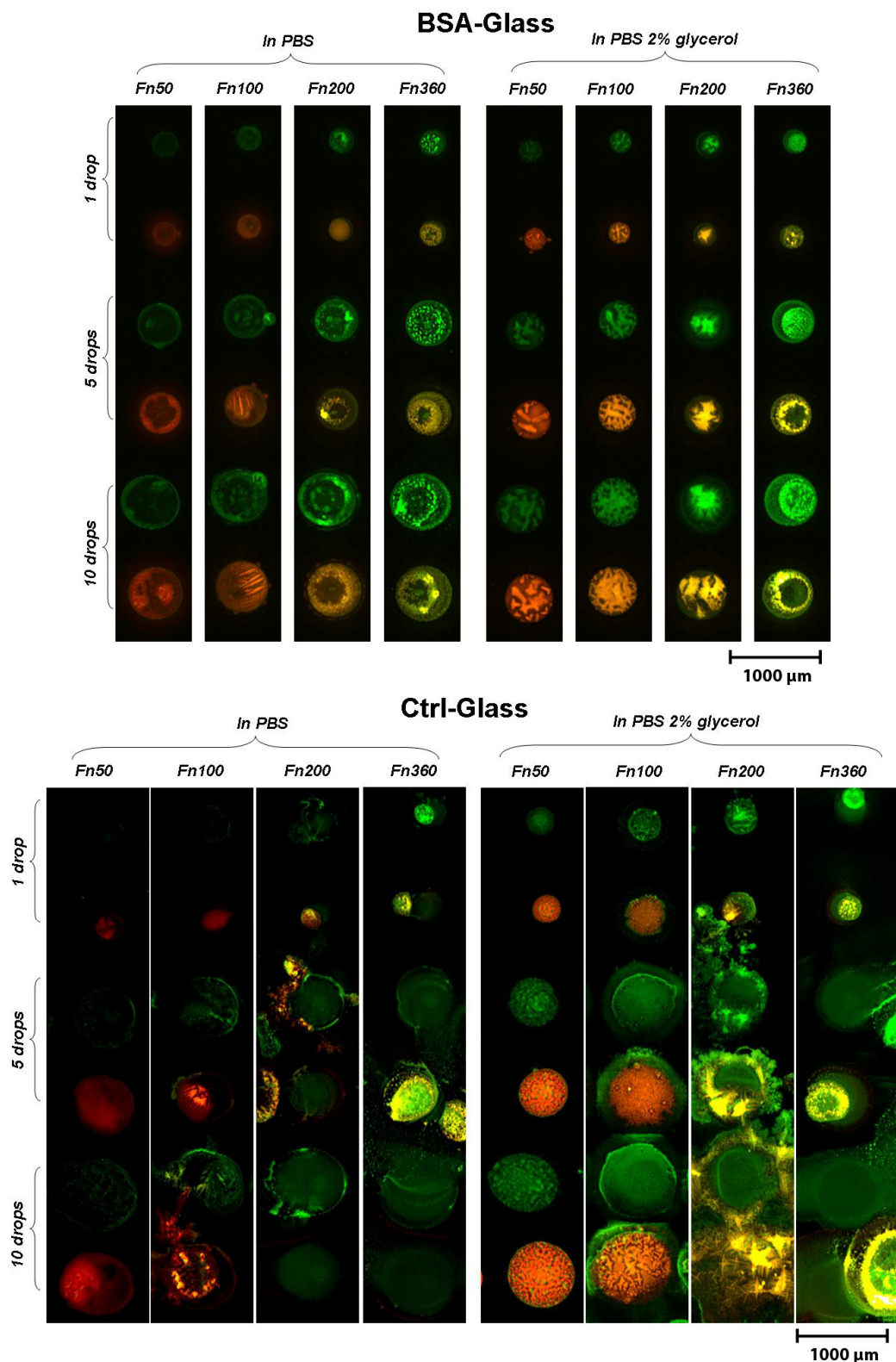


**Figure 2.9** Zoom-in of scanner images for BSA-Glass and Ctrl-Glass substrates “as spotted”. Detail of the spots printed at different Fn concentrations (indicated at the top of the image), with (on the right) and without (on the left) glycerol, at different spot sizes (indicated on the left of the image) and with (bottom, red to yellowish spots) and without (upper, green spots) SA50 included in the protein mixture spotted.

For spots deposited on AD-Glass, the two-phase intensity region appeared in the “as spotted” features printed with Fn50 and a big difference was observed “after washing” between spots with and without glycerol (Figure 2.10). While for spots printed with Fn50 in PBS a trace of the higher intensity region could be observed “after washing”, for glycerol spots a ring effect (with a significantly lower fluorescence intensity region in the centre of the spot, surrounded by a brighter boundary) was observed. This ring effect has been previously noted by other researchers and has been proposed to be due to protein transport at the air/water interface while the spot keeps hydrated.<sup>120</sup> For a-PMMA, the two-phase intensity region was also present in features “as spotted” and traces of the higher intensity region were also visualised in the “after washing” features printed in PBS. However, the ring effect was not so evident for “after washing” glycerol spots. For PEO-like substrates, the two-phase intensity region was only visible to a less extend for the PBS features “as spotted”. Spots printed with glycerol did show a homogeneous intensity feature “as spotted”. “After washing”, no traces of the brighter intensity region were visualised from the features spotted in PBS, and negligible fluorescence signal was detected from the spots containing glycerol indicating that no Fn had adsorbed for these spots. For spots printed on AD-Agarose, no important variations in the spot morphology were observed between features spotted with and without glycerol. Furthermore, spot profiles after washing were extremely similar.

Two-phase intensity regions (with brighter signal in the centre of the spot, similar to those found for AD-Glass and a-PMMA here) have also been noted by other researchers<sup>103</sup> and proposed to be in relation to the drying pattern of the spots. Interestingly, Wu et al.<sup>103</sup> reported rapid evaporation (within a few seconds) of the droplets spotted, even when printing was performed in a 65%-70% humidity chamber. However, other reports suggest that the antibody spots (used without any additive) are kept hydrated when incubated for 1 h in controlled humidity environment and reported ring structure formation as a result of protein transport at the air/water interface.<sup>120</sup> Despite being quite commonly reported, there is not a unique successful explanation to date for the variations observed in spot size, homogeneity and morphology in protein microarrays. This is in part due to the complex combination of variables that interact in the microarray printing process. These variables include substrate properties such as hydrophilicity of the surface, surface chemistry and in some cases also the polymer coating thickness and density. On the other hand, printing condition variables include protein types and protein sources used, print buffers, humidity and temperature settings during the printing process, and the use of contact versus non-contact printing devices.

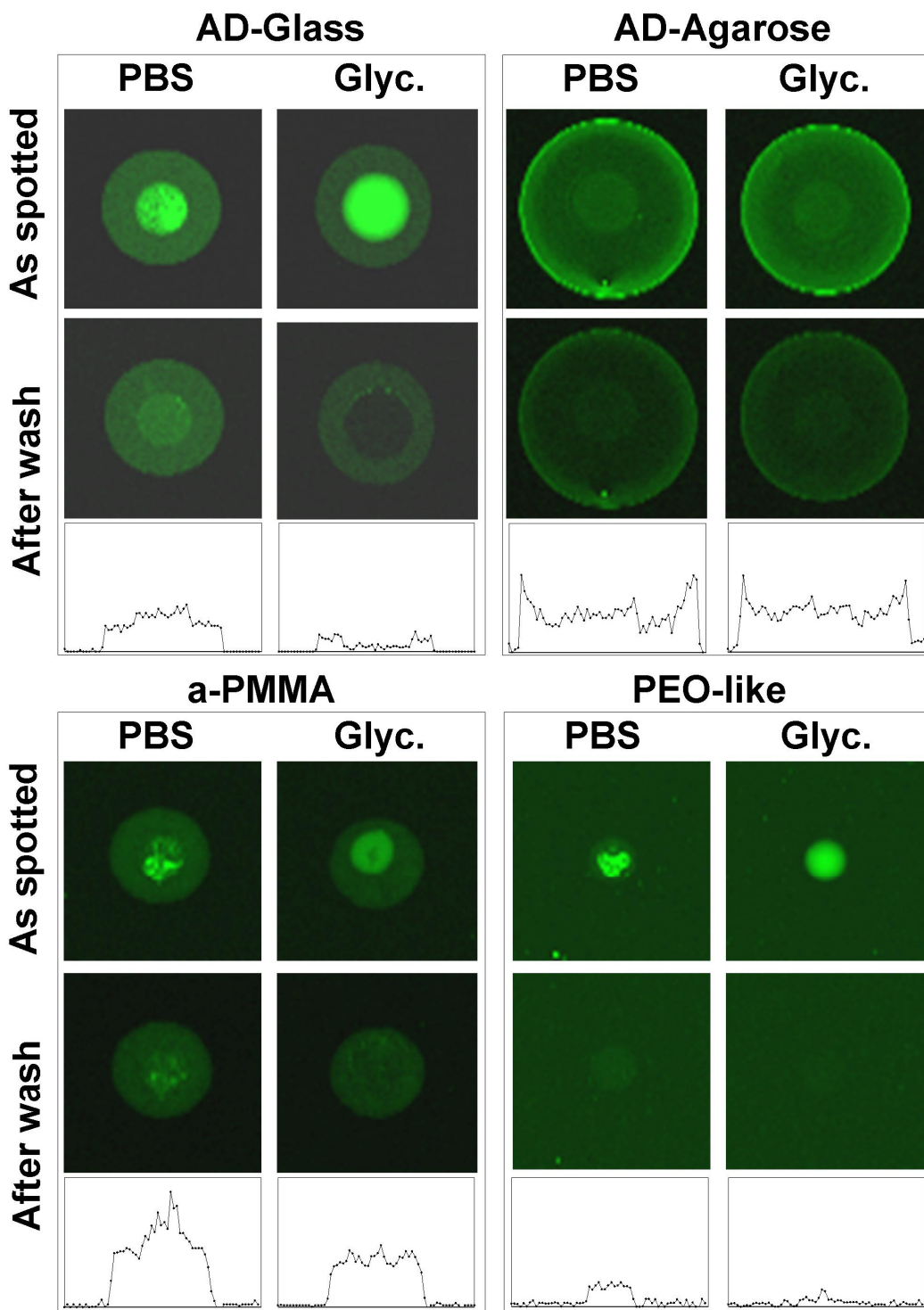


**Figure 2.10** Representative spots (Fn50, 10 drops) printed in PBS only (PBS) or with a 2% glycerol addition (Glyc.). Images obtained from slides “as spotted” (top within each box) and “after washing” (bottom within each box) for AD-Glass, AD-Agarose, a-PMMA and PEO-like substrates. Signal intensity and contrast have been independently optimised for each substrate to allow visualisation of the microarrayed spot morphology. “After wash” image fluorescence intensity profiles (background subtracted) are shown below each image.

### **Protein spot morphology: a complex phenomena described in the literature**

An explanation for these “ring-like” effects, where the centre of the ring yields alternatively higher (for PBS spots) or lower (for glycerol containing spots) fluorescence intensity than the boundaries depending on the spot condition and the substrate, can be suggested from a comparison between features “as spotted” and “after washing” (Figure 2.10). The following analysis centres on spot morphologies observed for AD-Glass, a-PMMA and PEO-like and compares spots containing PBS or PBS with 2% glycerol, for each substrate. This explanation assumed that the following hypotheses were held:

- During the spotting process (which lasted between 1 and 3 hours, depending on the number of replicate substrates printed in parallel), performed with the substrates kept at 4 °C, all spots (those containing PBS with and without glycerol) were kept hydrated. Therefore, proteins in the spotted volume on the substrate remained distributed in a liquid, 3D-environment. This situation would hold during the overnight incubation at 4 °C.
- At the moment of passivation and washing of the substrates, PBS spots were already dried while spots with glycerol did not dry. This can be assumed to be the case here, since 30 minutes to 1 hour elapsed between the moment in which the slides were taken off the fridge and the moment of the scanning. Therefore, after the “as spotted” scanning of the substrates the proteins were distributed on a 3D (non-evaporated) volume for glycerol spots, but were adsorbed on the surface for PBS spots.

If these hypotheses are assumed to represent the real situation, then the observed effect (i.e. the differences in the outer spot diameter and the protein distribution) for AD-Glass, a-PMMA and PEO-like substrates could be proposed to be a combined outcome of 3 complex phenomena already described in the literature:

- Change of the surface hydrophilicity due to protein attachment.<sup>112</sup>
- Protein transport at the air/water interface.<sup>120</sup>
- Protein adsorption at the air/water interface and film formation.<sup>121, 122</sup>

Taking into account these effects, the differences in the **outer spot diameter** found between substrates would be caused by a **combination** of:

- The hydrophobicity of the initial surface (before spotting), where more hydrophobic substrates yield smaller spots.<sup>109</sup> For the substrates considered here, the CA varied

between 70° and 80°. Based in the literature, the outer spot diameter variation for a protein-free solution in response to this change in the CA is expected to be less than 10%.<sup>109</sup>

- The change in the surface contact angle due to protein attachment, where protein adhesive substrates yield larger spots after prolonged incubation in a protein solution (such as overnight incubation). It is known that proteins attach to fouling and non-fouling surfaces (in particular when these surfaces are chemically activated) with different avidity, and that surface hydrophilicity can be changed by a protein coating.<sup>112</sup>

⇒ **Using the sessile-drop method** (Figure 2.11A), here it has been shown for the extremely hydrophilic Ctrl-Glass substrates, that a BSA coating changes the CA from ~20° to ~60°, in this case reducing the substrate hydrophilicity. Another report has shown that a tissue culture polystyrene (tPS) substrate changed the contact angle from 65.9° to 97.6° when coated with Fn.<sup>123</sup> However, **these measurements were performed by deposition of water (or PBS) droplets on dried protein coatings**, and it has been previously noted that many proteins can lose their pronounced hydrophilicity following drying, changing its adsorbed orientation to a much hydrophobic tertiary configuration.<sup>124</sup>

⇒ More recently, it was reported that an adsorbed protein layer on the surface actually increases its hydrophilicity when the protein (Fn in the report) was kept in liquid environment.<sup>112</sup> **Contact angles measured using a liquid-liquid CA technique** (for deposition of an octane drop on a substrate submerged in water, Figure 2.11B) have been reported to vary from 115.9°, for raw tissue culture polystyrene (tPS), to 154.4° for Fn coated tPS (Figure 2.11C, bottom). In this case, **an increase in the contact angle for the octane drop indicates an increase in hydrophilicity of the surface** (i.e. a higher affinity of the surface for the water environment in which the measurements are performed). In other words, a CA variation of up to 33% could be accounted for protein adsorption, therefore showing that the Fn coating did modulate the original hydrophilicity of the surface. Moreover, it was verified that increments in the amount of Fn adsorbed on the surface leaded to increments in hydrophilicity (i.e. increments of the liquid-liquid CA). In the case of study, AD-Glass and a-PMMA are highly protein-adhesive substrates due to its chemical activation, while PEO-like slides are non-fouling surfaces that strongly repel protein adsorption while proteins remain in a liquid

environment.<sup>90</sup> If the hydrophilic variation of 33% for the liquid-liquid CA reported is assumed to result in a “hypothetical” decrease in the CA obtained for PBS droplets measured in air with the sessile drop technique, provided that the Fn coating remains hydrated between the droplet and the surface, then the 80° CA measured here for a-PMMA could be decreased down to 53.6° (33% decrease from 80°). Therefore, the changes in hydrophilicity due to protein attachment will dominate over the CA variation previously presented for the substrates tested here (e.g. a 10° difference between a-PMMA and PEO-like) and would lead the changes observed in the spot diameter.

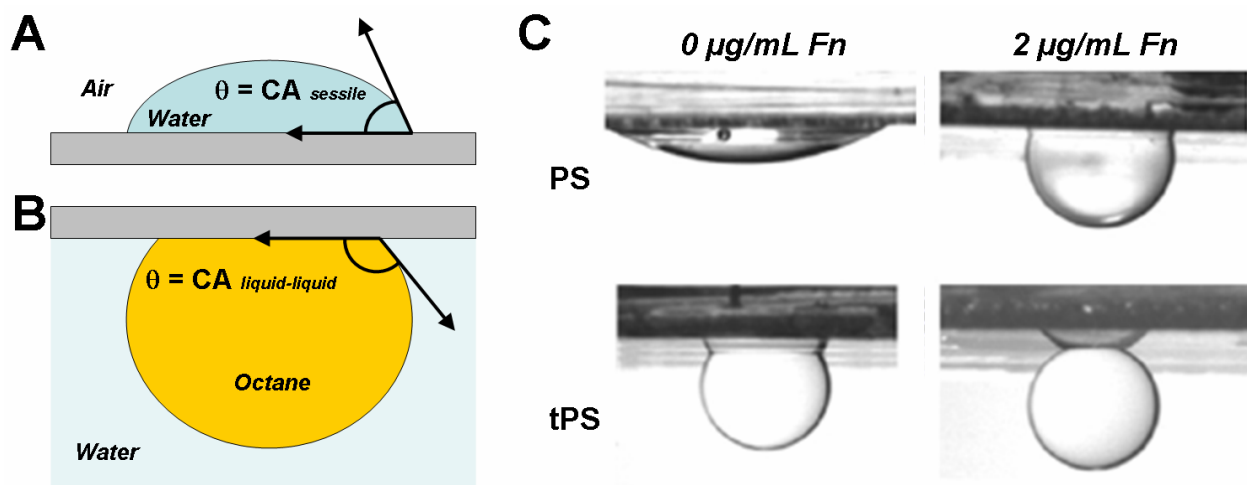


**Figure 2.11** Fn coating increases substrate hydrophilicity. **A.** Schematic showing the contact angle evaluated using the sessile-drop method. **B.** Schematic showing the contact angle evaluated using the liquid-liquid contact angle technique. Note that in this case an increase in the contact angle for the octane drop, submerged in water, indicates an increase in the hydrophilicity of the substrate (i.e. a higher affinity for the water environment). **C.** Liquid-liquid contact angle measurements for Fn coated substrates. Shapes of octave drops deposited the substrates submerged in water. Images obtained for raw (on the left) and Fn coated (on the right) polystyrene (PS) and tissue culture polystyrene (tPS) substrates. Image adapted from cited reference.<sup>112</sup>

- The volume of the protein solution spotted, where larger volumes spotted yield larger spots. This has been experimentally verified here, where spotting 1, 5 or 10 drops yielded larger spot sizes, respectively, on all substrates (Figure 2.7 to Figure 2.9).

The **protein distribution within the spot premises**, on the other hand, could be caused by a **combination of**:

- The ring effect observed in protein spots (understood as a high fluorescence ring appearing at the boundaries of the spot, representing higher protein attachment there, around a lower intensity region), which has been proposed to be due to protein transport at the air/water interface during the time that the spots keep hydrated (Figure 2.12).<sup>120</sup>

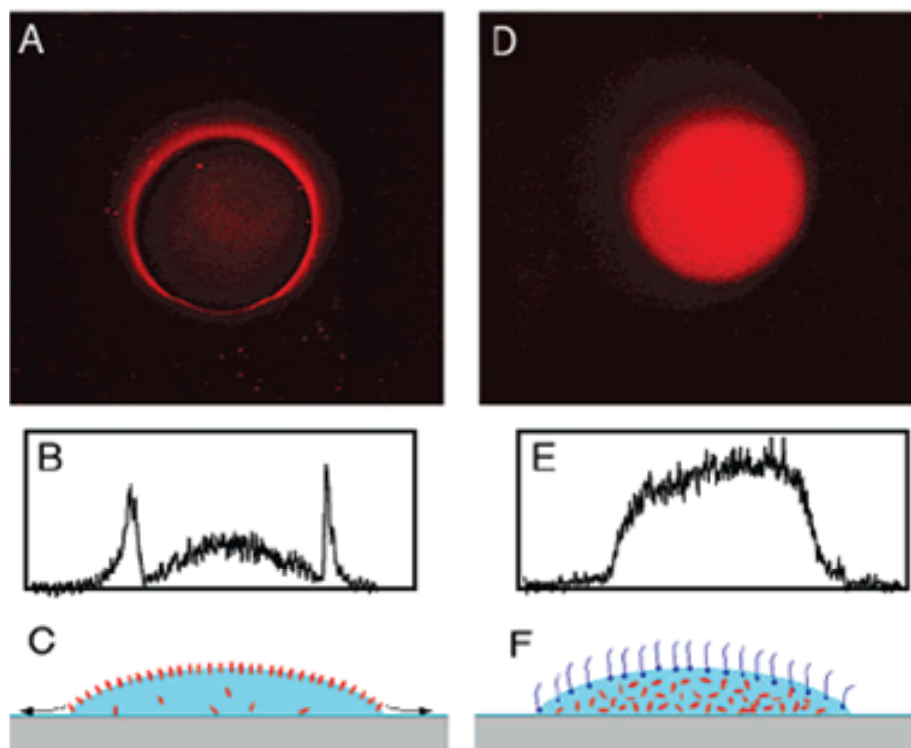


**Figure 2.12** Protein transport at the air-water interface accounts for rings in protein spots: fluorescence images of antibody spots immobilised on an epoxy-functionalised glass slide. The antibody was diluted 1:500 and used directly (**A**) or with a small addition of detergent (0.006% Triton X-100, **D**). The slides were incubated after spotting in controlled humidity environment for 1 hour and then washed 3 times with PBS plus 0.01% Tween 20. The slides were then blocked with 1% BSA in PBS and incubated with a Cy3-labelled secondary antibody. **B, E.** Cross-sectional profiles of images (A) and (D), respectively. **C, F.** Schematic of the droplets (light blue) spotted onto the substrate (in gray) showing the action of protein (in red) transport at the air-water interface in image (C), and its neutralisation by the action of the detergent agent (in dark blue). Image reproduced from cited reference.<sup>120</sup>

- The adsorption of proteins at the air/water interface. This is a widely reported effect which takes place during the process of food emulsification or foaming. The process of protein adsorption and film formation at an interface can be regarded as a two-step process, an initial anchoring step of the protein at the interface and next a conformation change and rearrangement of the adsorbed protein to form a cohesive viscoelastic film. This process has been demonstrated to take place with many proteins under dynamic conditions (BSA, fibrinogen and globulins, among others).<sup>121</sup> In particular, when protein aging takes place in the protein films adsorbed at the interface (i.e. when proteins have

been adsorbed at the air/water interface for some time), a “barrier ring” (such as the one observed for the spots printed with Fn50 and Fn100) has been reported to appear when a capillary pressure is applied to the aqueous film (Figure 2.13). As a result, changes in the adsorbed protein film thickness, which passes to be governed from thick to thin-film forces, take place.<sup>122</sup> Interestingly, the surface activity-compressibility relationship of proteins at the air/water interface has been proposed to affect protein distribution on this interface when the spot is composed of protein mixtures.<sup>121, 125</sup> These phenomena will be further referenced in the following subsection, when the morphology of spots containing protein mixtures is presented.

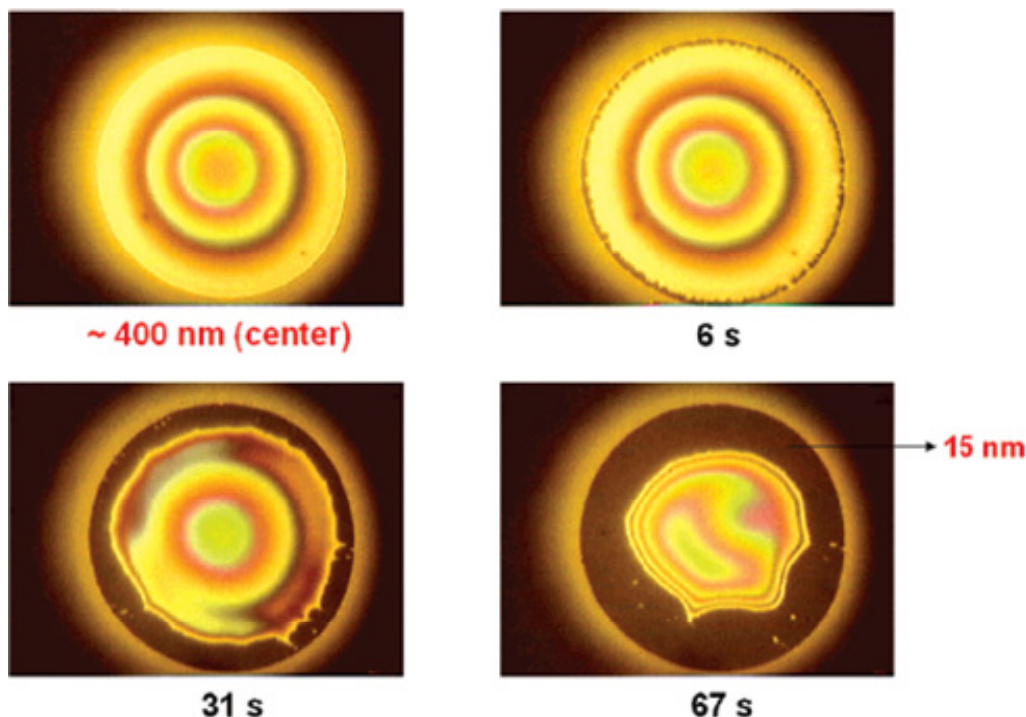


**Figure 2.13** Protein aging at the air-water interface produces a “barrier ring” as a result of a capillary pressure applied to the film to induce changes in the adsorbed protein film thickness. Yellow areas in the photomicrographs denote thick film zones and dark brown areas show thin film formation in response to an applied capillary pressure to the film. Time from the onset of capillary pressure is indicated at the bottom of the images. Steps involved in thin film formation and drainage for a BSA film at 0.1 g/L, pH 5.2 and 1.0 NaCl at 22 °C after aging for 40 minutes. Image reproduced from cited reference.<sup>122</sup>

#### ***Proposed model to account for spot morphologies observed***

Combining the experimentally observed data with the literature reports exposed above suggest that the outer spot size is mainly a product of the “non-fouling” properties of the PEO-like substrates,<sup>90</sup> which contrast with the “fouling” properties of both a-PMMA and AD-Glass.

Right after protein droplet deposition onto the substrates (fouling and non-fouling substrates, Figure 2.14A), it is expected that the initial spot size is mainly affected by the degree of hydrophilicity of the surface and could therefore be predicted by the CA values obtained for each substrate (i.e. larger spots for AD-Glass and PEO-like, and smaller spots for a-PMMA). Next, the printed substrates are incubated overnight at 4°C to promote protein interaction with the surface before the passivation and washing steps. During the time lapse between the spotting and the “as spotted” actual imaging, the changes in the spot sizes would take place (Figure 2.14B and C). These changes are proposed to be leaded by a competition between protein adsorption/attachment to the substrate surface (which would increase the hydrophilicity of the substrate leading to larger spot final diameters)<sup>112</sup> and protein adsorption at the air/water interface (which would deplete proteins form the bulk of the droplet therefore reducing attachment to the surface).<sup>120, 121, 125</sup> Chemically activated surfaces (such as a-PMMA and AD-Glass assayed here), yielding larger amounts of Fn immobilised, will increase their hydrophilicity and therefore the final drop diameter would be the equivalent of the spot diameter found for an initially protein coated surface. Non-fouling surfaces (such as PEO-like slides), on the other hand, will have less protein attached on its surface and therefore this change in spot spreading will not be so evident (Figure 2.14D).

The effects presented in Figure 2.14 would account for the differences found between substrates regarding the actual outer spot diameters observed and those predicted from the CA data. To exemplify this reasoning, a numerical hypothetical situation is provided: raw AD-Glass has a 70° CA, and after Fn coating the CA could change to 46.9° (33% decrease, i.e. increase in hydrophilicity); raw a-PMMA has a 80° CA and after Fn coating could change to 53.6° (33% decrease); finally PEO-like has a CA of 70° but, as Fn hardly attaches to this surface, a smaller decrease in the CA would take place (e.g. 10% decrease, leading to a CA of 63°). The outer spot diameters would represent the final values obtained for the spots after the Fn has coated the surface, and are the outcome of a combination of the CA measured for the raw substrate and the change in CA due to Fn coating. For this hypothesized situation, larger to smaller spot diameters would be those obtained for AD-Glass>a-PMMA>PEO-like, respectively. This explanation allows fitting the new temptative order of substrates in terms of spots size, as evaluated from visual inspection of Figure 2.7 to Figure 2.9, and will be further referenced when a more detailed analysis of the spot size is presented in the following subsection.

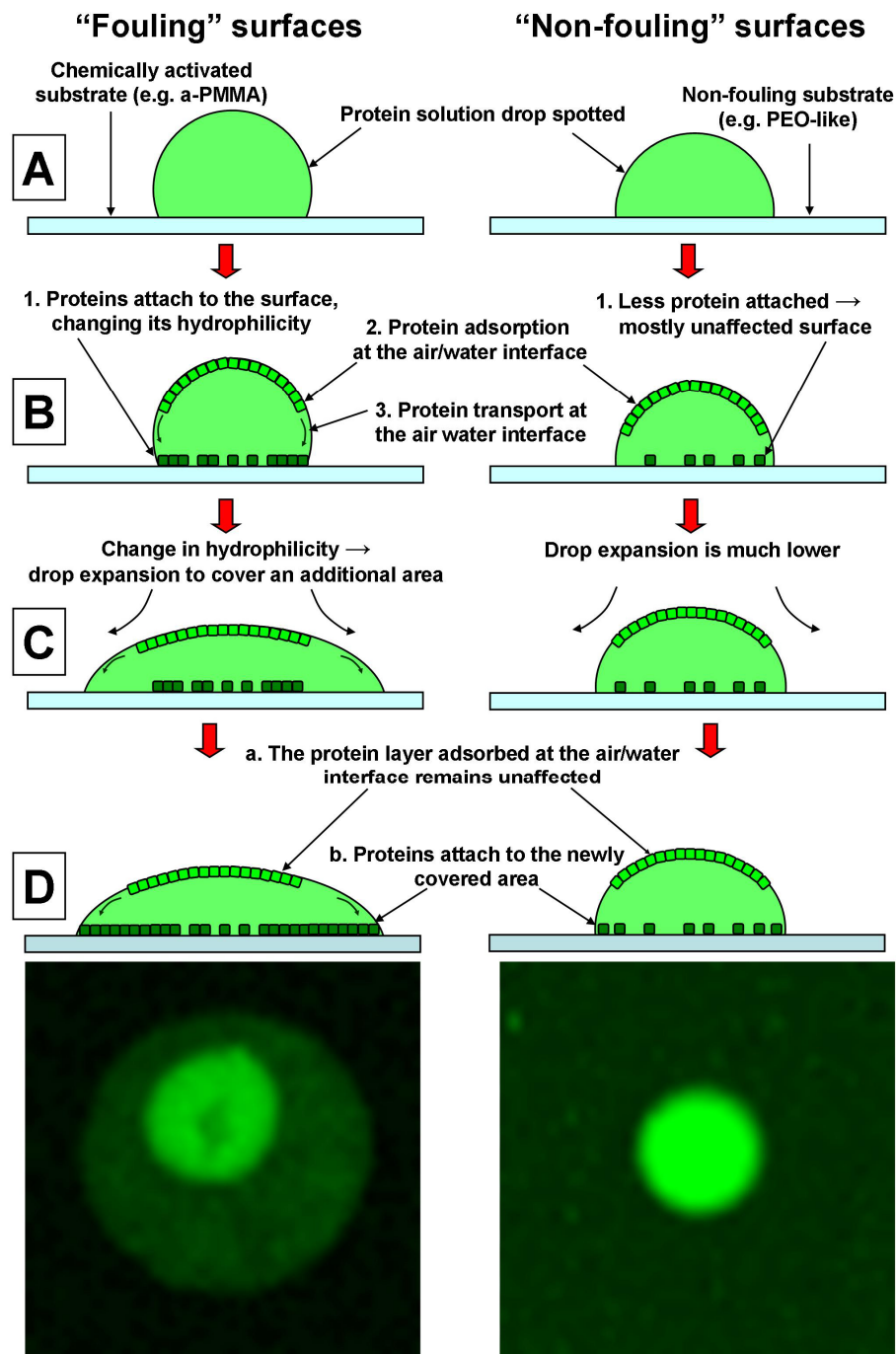


**Figure 2.14** Schematic for spot spreading effect and two-phase intensity regions observed in the “as spotted” images for features printed using Fn at low concentrations. **A.** Right after solution dispensing onto the substrates, the initial spot size is predicted by the contact angle values measures for each surface (in the example, a-PMMA with 80° CA would yield smaller spot diameters). **B.** After some time of incubation of the slide, proteins begin to adsorb at the surface (1) and also at the air/water interface (2). Additionally, protein concentrates on the spot boundaries due to protein transport at the air/water interface (3). **C.** The increase in Fn density attached to the surface would lead to an increase in the contact angle, and therefore surfaces with larger amounts of protein immobilised would yield larger spot sizes due to droplet spreading. **D.** Schematic and fluorescence “as spotted” images of the spots (Fn50, 10 drops) containing 2% glycerol printed on a-PMMA and PEO-like substrates. Note that the adsorbed protein layer at the air/water interface cannot be distinguished from adsorbed protein, but it is suggested in the images as a brighter area in the a-PMMA spot.

On the other hand, an explanation for the differences in the protein distribution within the spot premises (observed for spots printed in Fn50 and Fn100, and specially noted when these spots contained SA) is assayed here as a result of protein adsorption at the air/water interface. This effect would account for the differences in fluorescence intensity regions observed in this case within the spots in the “as spotted” and “after washing” images (AD-Glass and a-PMMA in Figure 2.10). The high intensity regions observed in the “as spotted” features (for Fn50 and Fn100, Figure 2.7, AD-Glass, and Figure 2.8, a-PMMA) are proposed here to be protein layers adsorbed at the air/water interface in spots with glycerol. This is supported by the fact that after substrate passivation and washing steps, the higher fluorescence intensity regions disappear in glycerol spots, which supposedly did not evaporate (Figure 2.15). The same is assumed to happen for “as spotted” features with PBS although, as previously noted, spots are dried before the passivation and washing of the slides (Figure 2.16B). Therefore, despite no big differences were observed in the fluorescence distribution within the “as spotted” features printed with and without glycerol, a striking change took place when comparing the same spots “after washing” (compare PBS and glycerol spots for AD-Glass and a-PMMA in Figure 2.10). It is proposed here that for spots printed in PBS the protein layer originally formed by adsorption at the air/water interface is retained in the surface due to either adsorption or to protein interaction with the substrate chemistry (Figure 2.16C). In contrast, in glycerol containing spots (which did remain hydrated) this layer is washed-off during the passivation and washing steps (Figure 2.15B). This would account for the brighter fluorescence intensity regions remaining (for Fn50 and Fn100) in the “after washing” spots printed with PBS and absent in the glycerol spots. The rings observed in the “after washing” spots printed with 2% glycerol (more evident in AD-Glass substrates, Figure 2.10) could be explained, as previously mentioned, by protein transport at the air/water interface (Figure 2.14B). Moreover, the width of the ring observed for AD-Glass and a-PMMA would be given by the gradual expansion of the spot as more protein attaches to the surface.

### For glycerol containing spots

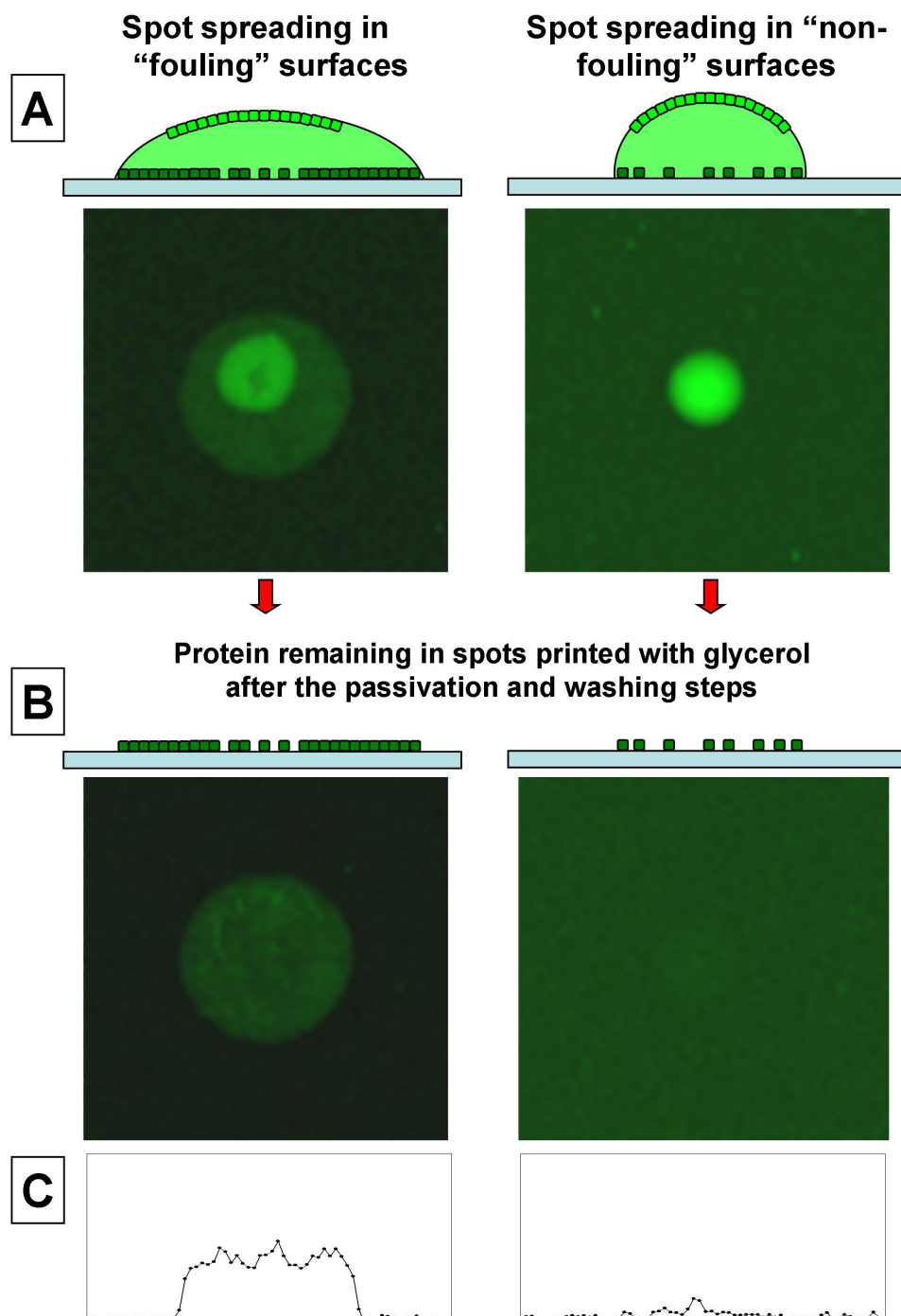


**Figure 2.15** Schematic for the two-phase intensity regions observed in the “as spotted” and “after washing” images for spots (Fn50, 10 drops) which included glycerol in the printing buffer. Left images correspond spots on a-PMMA and right images to spots on PEO-like. **A.** Schematic and fluorescence “as spotted” images of the spots containing glycerol. Note the adsorbed protein layer at the air/water interface. **B.** Schematic and fluorescence “after washing” images of the same spots. Note in this case that the adsorbed protein layer at the air/water interface has been completely washed-off. **C.** “After wash” image fluorescence intensity profiles (background subtracted) are shown below each image. Signal intensity and contrast have been independently optimised for each substrate to allow visualisation of the microarrayed spot morphology.

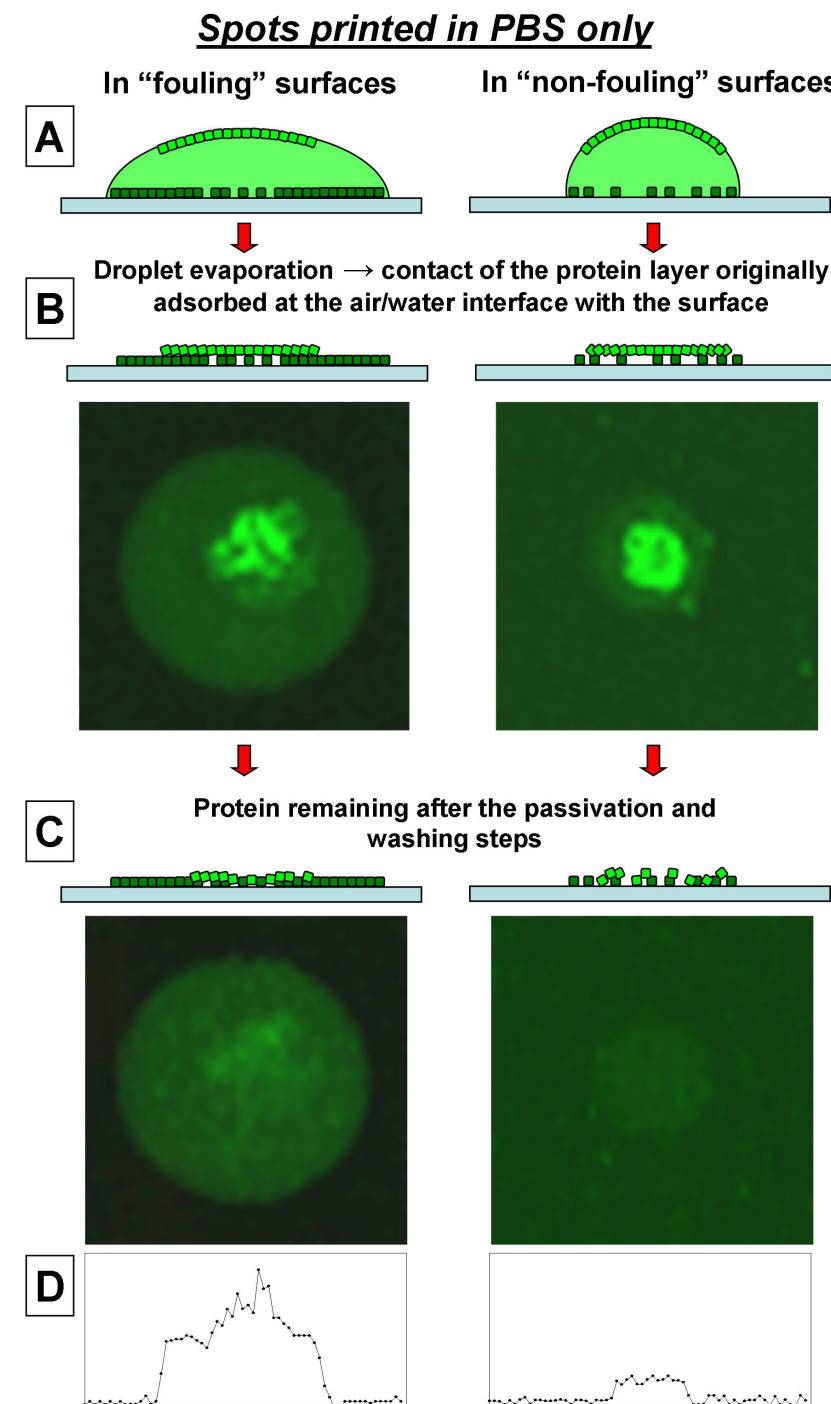


**Figure 2.16** Schematic for the two-phase intensity regions observed in the “as spotted” and “after washing” images for spots (Fn50, 10 drops) which did not include glycerol in the printing buffer. Left images correspond spots on a-PMMA and right images to spots on PEO-like. **A.** Schematic of the spots before buffer evaporation, indicating the formation of the adsorbed protein layer at the air/water interface. **B.** Schematic and fluorescence “as spotted” images after taking the slides off the fridge and during scanning, the buffer is probably evaporated. Note that the adsorbed protein layer at the air/water interface contacts with the surface. **C.** Schematic and fluorescence “after washing” images of the same spots. Note in this case some traces of the adsorbed protein layer at the air/water interface remain attached to the surface. **D.** “After wash” image fluorescence intensity profiles (background subtracted) are shown below each image. Signal intensity and contrast have been independently optimised for each substrate to allow visualisation of the microarrayed spot morphology.

Interestingly, the two-phase fluorescence intensity regions observed in the “as spotted” features became less evident as the Fn concentration spotted increased, until being practically neutralized for Fn200 and Fn360 (Figure 2.7 (bottom), Figure 2.8 (top) and Figure 2.17A, right box). This can be due to a change in the dynamics of protein adsorption both at the substrate surface and the air/water interface, as a result of the excess of protein in the drop volume (resulting from the increased concentration). This could cause a thicker protein layer formed at the air water interface and also a higher protein density coating on the surface before spot dry out. Therefore, a larger protein layer originally formed at the air/water interface would adsorb/attach to the surface after spot dry out (for PBS spots) covering most of the spot area, as observed in Figure 2.17A (right box, “after wash” images). For spots containing glycerol, on the other hand, a thinner ring size was observed (compare glycerol spots “after wash” produced by Fn50 and Fn360 protein concentrations, Figure 2.17A), suggesting that the final spot size is reached faster (as a result of an enhanced protein attachment to the surface due to the increase in Fn concentration). Therefore, the transport of proteins at the air/water interface would accumulate proteins mostly on a thinner region on the borders of the spot.

### ***Feature morphology for spots containing Fn and SA protein mixtures***

The two-phase intensity regions which appeared for Fn spots (for Fn50 and Fn100 spotted in AD-Glass and a-PMMA, green colour in Figure 2.7 and Figure 2.8) did also appear for SA containing spots (red to yellowish colour in the figures). Interestingly in the latter case, it was observed that SA remained mainly in the centre of the “as spotted” features (Figure 2.17B, left box, upper images). It can be argued that the difference in protein size (~550 kDa for Fn and 52.8 kDa for SA) and structure (rod-like, 15.5 nm x 8.8 nm with 2:1.1 axial ratio for Fn;<sup>126</sup> and β-barrel structure with dimensions 5.4 x 5.8 x 4.8 nm for SA<sup>127</sup>) provide a competition effect for protein adsorption at the air/water interface.<sup>121</sup> It has been previously reported that phase separation in protein films formed at the air/water interface can take place even for extremely similar proteins (e.g. α<sub>S</sub>-Casein and β-Casein), and that this separation effect is dependent on the concentration ratio of the assayed proteins in the bulk of the film.<sup>125</sup> In this line of reasoning, if high protein adsorption takes place at the air/water interface (as suggested for SA in the “as spotted” fluorescence images of Figure 2.17B, left box, upper images), the protein concentration in the bulk of the droplet will be depleted.<sup>120</sup> This could justify the extremely low SA (red to yellowish) signal observed in the “after washing” spots printed with Fn50 SA50 both with and without glycerol (Figure 2.17B, left box), the only red fluorescence remaining in the centre of the features for PBS spots due spot dry out and surface contact of the SA layer initially adsorbed

at the air/water interface. As the Fn concentration spotted increased (therefore changing the Fn to SA concentration ratio in the bulk of the droplet), it could be assumed that the Fn competes more strongly with SA for adsorption at the air water interface and therefore the SA in the bulk solution would not be significantly depleted.

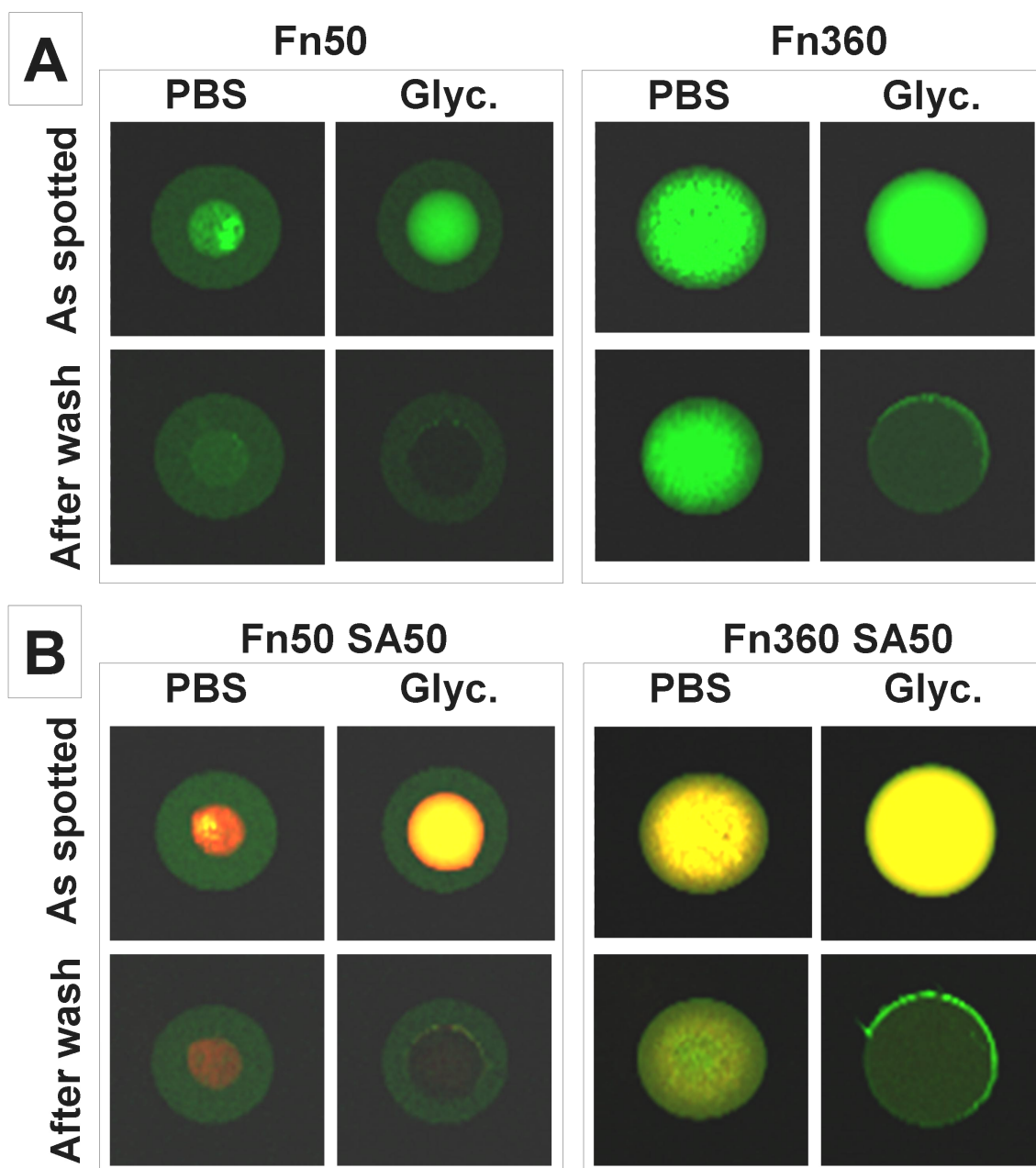


**Figure 2.17** Two-phase intensity effect observed in AD-Glass substrates “as spotted” for Fn printed at the lowest (left boxes) and highest (right boxes) concentrations. **A.** Spots printed with Fn only (green fluorescence signal). **B.** Spots printed with Fn (green signal) and SA (red signal). Yellow fluorescence signal is due to overlapping of Fn and SA signals. It can be observed that the two-phase intensity effect is neutralised increasing the Fn concentration.

Another explanation for the extremely low SA signal observed in Fn50 SA50 “after washing” spots (discarding the red layer in the centre of PBS spots which should still be associated with

the protein layer initially adsorbed at the air/water interface) could be assayed based on observations that the orientation of adsorbed proteins on a surface, and the strength of this interaction, depends upon protein structure and concentration.<sup>128, 129</sup> At low concentrations proteins can maximize its interactions with the surface, generating a stronger attachment. In this context, longer proteins (such as Fn here) could elongate on the substrate therefore providing more contact points for anchorage. So, for Fn and SA spotted at equal concentrations, Fn would competitively displace SA binding on the substrate surface. Further research, falling out of the scope of this chapter, should be made to corroborate the previously exposed theories.

### ***Spot size analysis***

For the quantitative analysis of the spot size, the outer spot diameter was measured from the scanner images taken “as spotted” and “after washing”.

No significant differences were found between the spot diameters “as spotted” and “after washing” for each spot condition and substrate. As a graphical example, Figure 2.18 shows the spot diameters obtained for all the substrates “as spotted” and “after washing” when printing Fn360 in PBS.

A considerable difference was found for identical spot conditions printed on the different substrates tested (Figure 2.18). A statistical analysis of the results presented yielded that the order of statistically different substrates in terms of larger to smaller spot diameter values was: BSA-Glass>AD-Agarose>AD-Glass>a-PMMA>PEO-like. This order held for all drop numbers spotted and spot compositions printed. As a graphical example, Figure 2.18 shows spot diameters for Fn360 in PBS. Taking an AD-Glass average diameter of ~415 µm (for a spot size of 10 drops of Fn360) as reference, diameters for other substrates were 284, 339, 581 and 689 µm for PEO-like, a-PMMA, AD-Agarose and BSA-Glass respectively.

When comparing these results with the CA results previously presented, a good agreement was found with the predicted spot sizes for BSA-Glass (CA=63.2°), AD-Glass (CA=70.9°) and a-PMMA (CA=80°), which had larger to smaller spot sizes, respectively. Ctrl-Glass (CA=19.9°) spot diameters could not be quantified, however CA data was in good agreement with the qualitative analysis previously done for this substrate, yielding large spot sizes which merged with its neighbours, consistent with the extremely low contact angle value reported here. In this context, PEO-like substrates (CA=70.7°) showed diameters much smaller than those expected from CA data (which predicted spot diameters larger than a-PMMA ones and close to those of AD-Glass). This observation can be accounted by the increase in the surface hydrophilicity

when larger amounts of Fn are attached to the chemically activated substrates, as previously exposed when analysing the spot morphology.

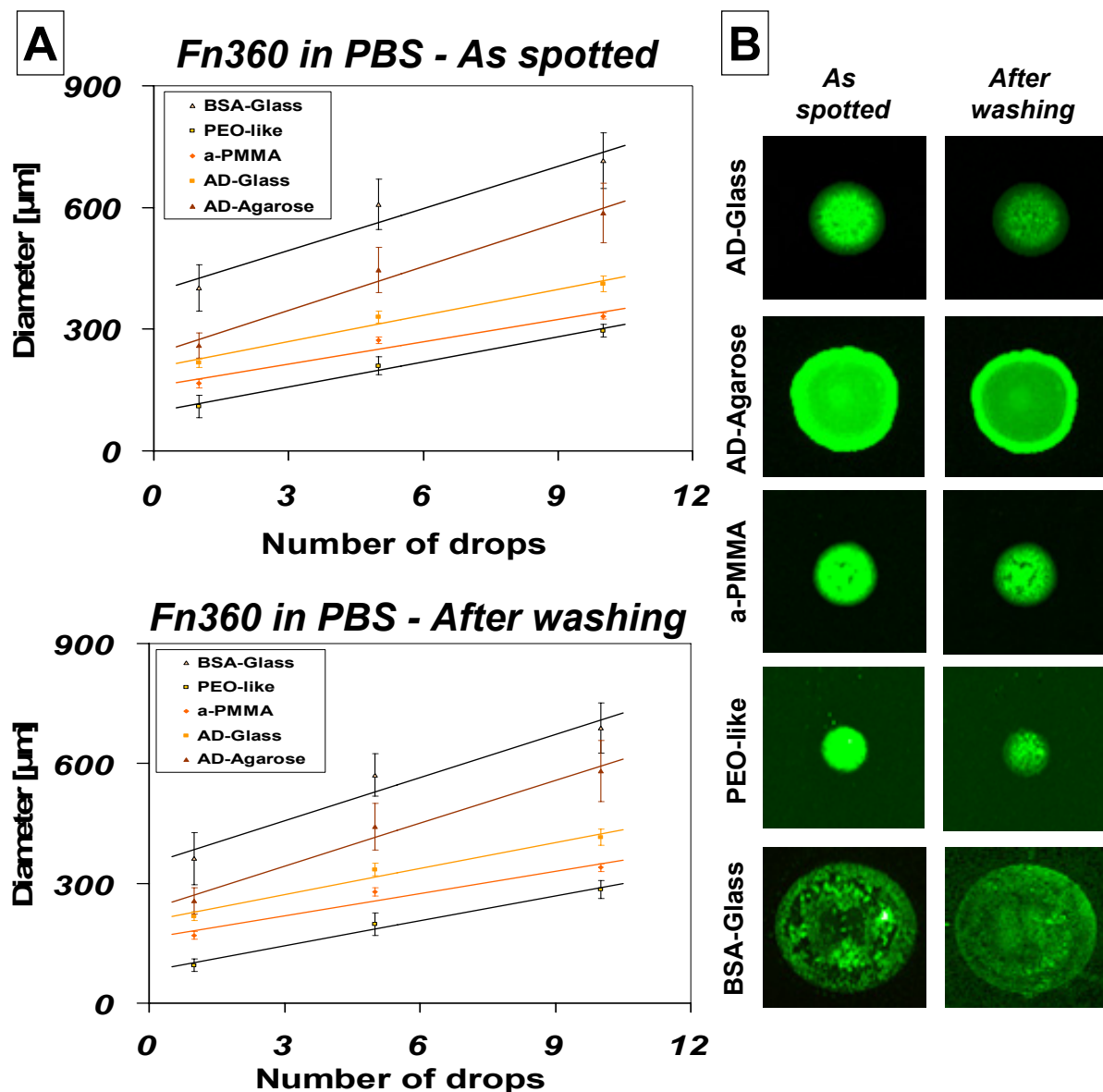


**Figure 2.18** **A.** Spot diameters for different substrates, measured “as spotted” and “after washing”, for Fn360 in PBS. Lines represent a linear fitting of the data points (for 1, 5 and 10 drops) obtained for each substrate and are used here as guide only. **B.** Representative spot images “as spotted” and “after washing” for Fn360 (10 drops spot size) printed on different substrates.

The inclusion of SA in the protein mixture spotted did not significantly affect the feature diameter, therefore average values (independent of the SA content of the spot) were calculated to evaluate the effect of varying the Fn concentration spotted.

For all substrates but PEO-like ones, the feature diameter when spotted in PBS did not show important changes from spotting Fn50 to spotting Fn360 protein solutions, for identical number of drops. PEO-like slides, however, showed an increase in the spot diameter as the protein

concentration increased from Fn50 to Fn360. This increase was more evident for the 10 drops spot size, and can be visualised in the plots presented in Figure 2.19 (left plot) by the increase in the slope of the linear approximation found for PEO-like slides when spotting Fn360. In contrast, AD-Glass diameters for the same spot conditions are presented in Figure 2.19 (right plot). It can be observed that the spot diameter for this substrate yielded extremely close values for all the Fn concentrations spotted, indicating that the spot size in this substrate is mainly affected by the number of drops spotted. Similar results to AD-Glass were found for a-PMMA and AD-Agarose substrates.

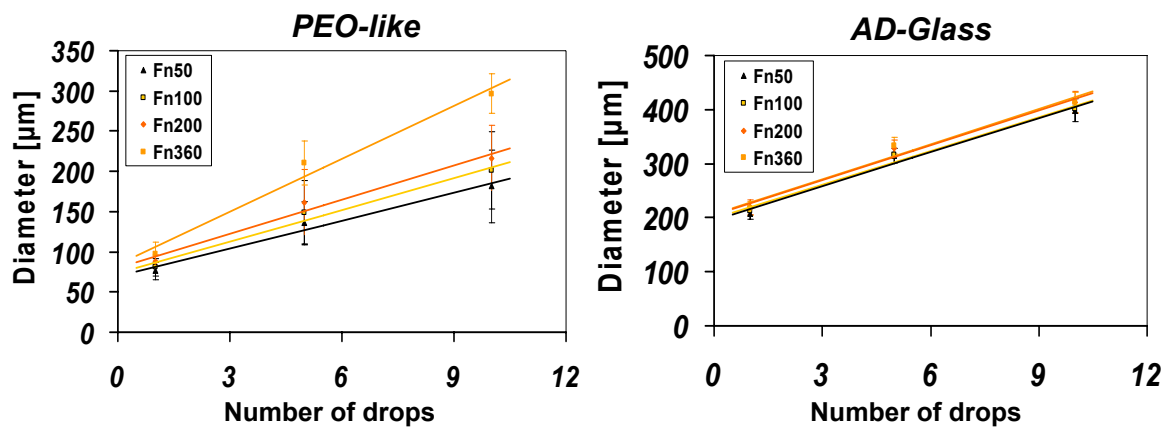


**Figure 2.19** Fn concentration effect. Spot diameters (averaged for spots w/wo SA) measured “after washing” for the different Fn concentrations spotted in PBS. Data presented is for PEO-like (left plot) and AD-Glass (right plot) substrates. Lines represent a linear fitting of the data points (for 1, 5 and 10 drops) obtained for each substrate and are used here as guide only.

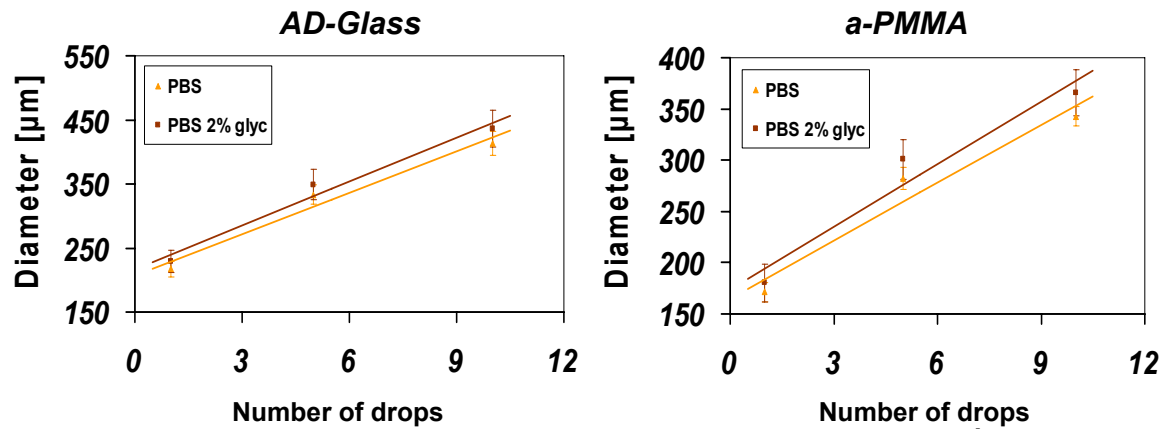


**Figure 2.20** Glycerol effect. Spot diameters (averaged for spots w/wo SA) measured “after washing” for Fn360 spotted in PBS with and without glycerol. Data presented is for PEO-like (left plot) and AD-Glass (right plot) substrates. Lines represent a linear fitting of the data points (for 1, 5 and 10 drops) obtained for each substrate and are used here as guide only.

The inclusion of glycerol in the printing buffer resulted in a slight increase in the spot diameters which was significantly different only for the largest spots (i.e. 5 and 10 drops) in AD-Glass and a-PMMA substrates (Figure 2.20). All other substrates yielded smaller variations which were not significantly different when statistically evaluated.

Overall, two preliminary conclusions can be extracted from the results presented in this section:

- The differences found for the spot diameters indicate that, while the amount of mass spotted on the substrates for an identical spot condition was the same, the area on which the mass was deposited was much smaller for PEO-like slides (leading to higher protein densities deposited on the spot) and much larger for BSA-Glass (yielding lower protein densities on the spots).
- A non-homogeneous protein distribution was found in spots printed with the smallest Fn concentrations (Fn50 and Fn100) for some of the substrates assayed. This effect was most relevant for the distribution of SA, and was found to significantly decrease when increasing the co-spotted Fn concentration. For this reason, in the following sections dealing with the quantitative analysis of the protein immobilised on each substrate, special emphasis is put on spots printed with Fn200 and Fn360 and the “outer” spot diameters are used to assess the protein densities in each case.

#### **2.3.4 Fluorescence signal calibration curves for the spotted substrates**

First of all, the average background signal and signal-to-noise ratio (SNR) were calculated for all substrates. These are important parameters that should be taken into account when analysing quantitative data obtained from the fluorescence signal for the scanned substrates. The background signal has to be compensated when measuring the fluorescence intensity from each spot. This has been taken into account in this work by subtracting the local background value (obtained from a surrounding area of identical size to that of the corresponding spot) to each of the spot intensities measured. The SNR, on the other hand, gives an estimation of the quality of the spot signal and depends of the substrate. A larger SNR indicates a higher signal over the background noise. The results obtained are presented in Table 2.5. It can be observed that for the 532 nm channel signal (green signal, corresponding to Fn), the best substrates (i.e. the substrates with the highest average SNR) were AD-Glass, followed by a-PMMA and AD-Agarose slides. A similar relation was found for the 635 nm channel signal (red signal, corresponding to SA), with AD-Agarose slides holding the best SNR, followed by a-PMMA, AD-Glass and PEO-like

slides. PEO-like slides presented a high background signal for the 532 nm channel, probably due to an autofluorescence effect of the PEO-like layer when excited at this wavelength, yet the SNR for this substrate was larger than the BSA-Glass signal. Due to the low SNR obtained for BSA-Glass, many of the spots from this substrate could not be accurately quantified and were not taken into account for the analysis. For Ctrl-Glass substrates, no data could be obtained for background nor SNR since most spots were unidentifiable “as spotted”, and therefore it was not possible to define the spot premises for further calculation.

	Substrate					
	AD-Glass	AD-Agarose	a-PMMA	PEO-like	BSA-Glass	Ctrl-Glass
Avg. background signal 532 nm	46 ± 12	146 ± 92	94 ± 40	702 ± 552	123 ± 58	NA
Avg. SNR 532 nm	64.9	33.7	38.2	7.7	2.8	NA
Avg. background signal 635 nm	29 ± 1	55 ± 35	29 ± 1	38 ± 16	30 ± 2	NA
Avg. SNR 635 nm	21.8	120.2	34.7	13.5	2.4	NA

**Table 2.5** Average background ( $\pm$  standard deviation) and SNR values of all spots and three slides per substrate (two for BSA-Glass) found for each substrate “after washing”. Background 532 nm and SNR 532 nm are the values measured for the green scanner channel (Fn signal) and background 635 and SNR 635 represent the values measured for the red scanner channel (SA signal). The best substrates in terms of SNR were AD-Glass, a-PMMA and AD-Agarose. The worst SNR ratio was obtained for BSA-Glass slides. PEO-like slides revealed the highest background signal for the 532 nm channel. NA: not available.

To trace the fluorescence signal calibration curves, the scanner fluorescence signal obtained from the images of the substrates “as spotted” was used. The total signal intensity obtained for each spot (i.e. the signal integrated over the whole spot area, already extracting the local background) was expected to be proportionally correlated with the amount of protein mass deposited on each spot (calculated from the drop volumes and the protein concentration of the solution spotted, and exposed in the materials and methods section of this chapter and presented in Table 2.6). It is worth noting in Table 2.6 that there are “equivalent conditions” in terms of protein mass spotted, such as 5 drops of Fn200 and 10 drops of Fn100 (both yielding a 400 pg Fn mass deposited per spot). Calibration curves for each of the tested substrates were traced by

plotting the spot signal intensity (compensated by the background signal and averaged for each spot condition) vs. the spotted protein mass (Figure 2.21A and B).

Number of drops spotted												
	1				5				10			
	Fn conc [µg/mL]				Fn conc [µg/mL]				Fn conc [µg/mL]			
	50	100	200	360	50	100	200	360	50	100	200	360
<b>Fn mass [pg]</b>	20	40	80	144	100	200	400	720	200	400	800	1440
<b>SA mass [pg] (SA conc is 50 [µg/mL])</b>	20	20	20	20	100	100	100	100	200	200	200	200

**Table 2.6** Relationship between the amounts of protein mass spotted, the Fn or SA concentration and the number of drops printed.

As previously noted, spots printed using the highest Fn concentrations were unidentifiable on Ctrl-Glass slides. No accurate calibration curve could be traced for this substrate and therefore it was not included in the following analysis. For all other substrates, the measured intensity was found to follow a linear relationship with the protein mass spotted within the range analysed, thus meaning that measurements were outside the scanner saturation region. Linear regression method was applied to all the substrates, therefore extracting calibration functions that were substrate dependant (Figure 2.21A and B, tables), mainly due to the use of different PMT settings (optimised for the scanning of each slide) which yielded specific background-corrected signals (sometimes lower PMT values were preferred to diminish the background contributions). Results show that calibration curves fitted well the linear approximations, with  $R^2$  values ranging from 0.93 to 0.99.

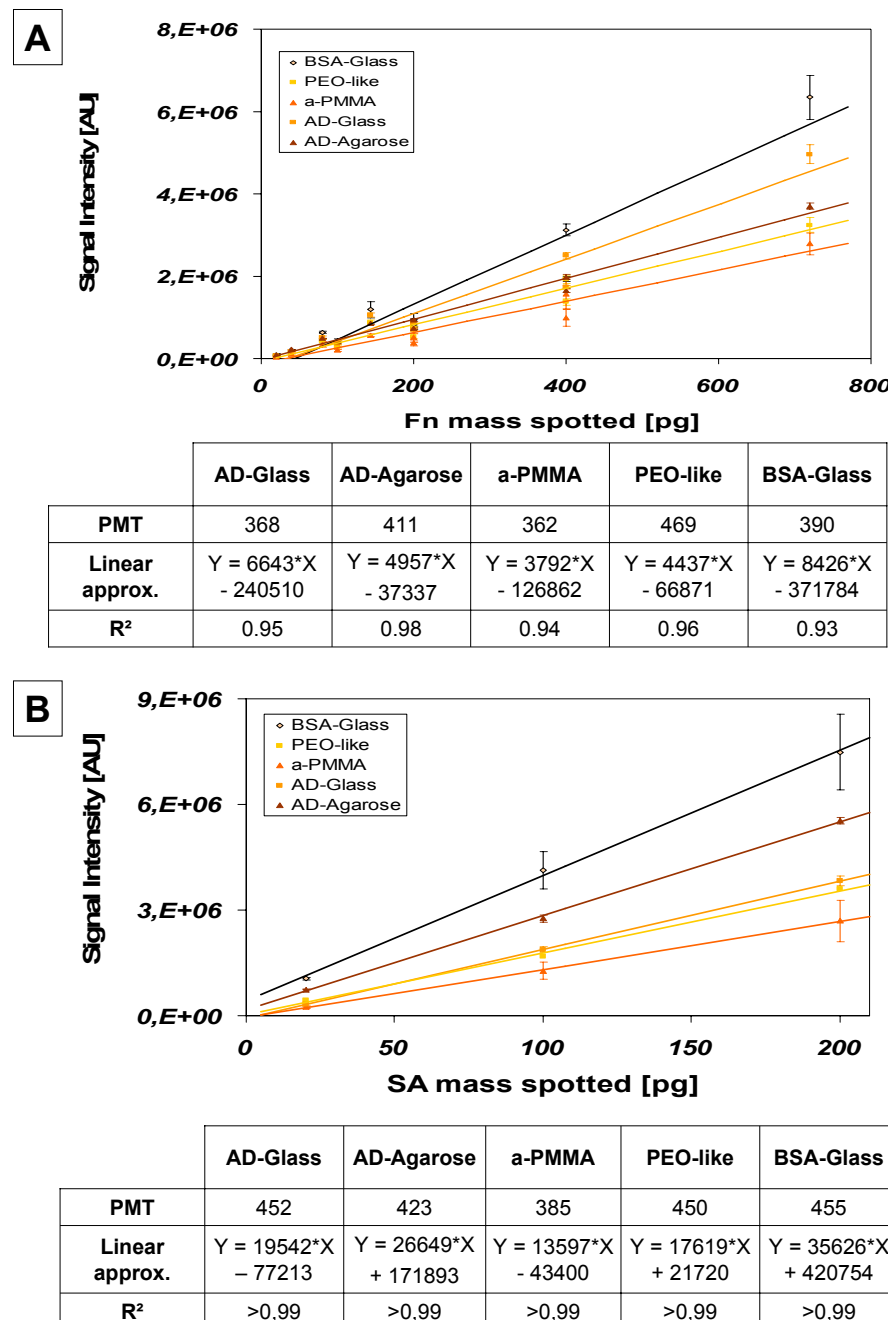


**Figure 2.21** Substrate calibration curves. Plot for the fluorescence signal intensity measured with the scanner and the Fn (A) or SA (B) mass deposited. Each point in the calibration curve represents the mean value of 20 spots and the SD deviation associated. Lines represent the linear approximation for the given values. Tables below the plots indicate the PMT values used for scanning each substrate, the linear approximation equation found for each slide and the R<sup>2</sup> value associated.

Despite the linear correlation found between the spot fluorescence intensity and the amount of protein mass deposited on each spot within each substrate, the calibration curves obtained for different substrates did not overlap, as could be expected since the same amounts of mass were deposited on all of them. When taking into account the PMT values used for scanning, expecting that larger PMT values would lead to larger slopes of the linear approximation curves, the order

of substrates in terms of larger to smaller slopes did not coincide with the results presented in Figure 2.21. As an example, BSA-Glass (scanned with a PMT value of 369) had a larger slope than AD-Agarose and PEO-like substrates (scanned with a PMT value of 411 and 469, respectively, Figure 2.21A). This was mainly attributed to the different substrate compositions assayed. One explanation could be attributed to slight differences introduced in the focus distance of the laser, those having coatings on top (PEO-like and AD-Agarose, with thickness ranging from 20 nm to 1 µm, respectively) leading to lower intensities when scanned, even when using the same laser power. Other effects related to the high background signals obtained from these substrates (refer to Table 2.5) cannot be ruled out. However, since the quantitative data for each slide was obtained from scanning the same substrate “as spotted” and “after washing” using the same PMT values, and the average background signal variation between scans “as spotted” and “after washing” was less than 20%, the linearity found was assumed to hold independently of the actual slope obtained for each substrate. Additionally, any quenching effect was discarded since, for the scan of a given substrate, the linearity held throughout the protein mass ranges fitted (from 20 to 800 pg, which is the range experimentally used for quantification of the protein mass “after washing”). The calibration curves fitted best in the central range of the protein masses evaluated, and the uncertainty resulting from quantification of protein mass using these calibration curves was taken into account as described in the materials and methods section of this chapter (Statistics subsection). It is worth noting that, despite PEO-like slides had the higher background signal for the scanner 532 nm channel, extracting the local background from the PEO-like fluorescence signal resulted in a linear relation between the spotted protein mass and the compensated fluorescence signal, as exposed in Figure 2.21A.

### **2.3.5 Immobilised protein quantification: spots containing Fn only**

Quantitative analysis of the immobilised proteins was performed on the substrates for which accurate calibration curves could be traced, therefore Ctrl-Glass slides were discarded from this analysis. The calibration curves of the intensity measured and the amount (in mass) of spotted protein (Figure 2.21A and B) were used to quantify the protein remaining on each spot on the surface “after washing”. This value was assumed to be the amount of protein immobilised on the spots. To ensure quantification of immobilised protein in the linear range covered by the calibration curves (i.e. mass values larger than 20 pg), the lowest protein masses spotted (1 drop of Fn50 and Fn100) were not included in this analysis. The conditions analysed are the most relevant according to cellular microarray previous reports.<sup>48, 50, 53</sup>

### **Immobilised Fn mass**

Figure 2.22 shows the relationship found between the total protein mass spotted and the immobilised protein mass on each substrate. Three slides (named A, B and C) were quantified for each assayed substrate (two slides for BSA-Glass). The linear approximation equations and the  $R^2$  values for all slides assayed for each substrate are shown in Figure 2.22 (bottom right table).

Several interesting findings were derived from a detailed analysis of these results. On one hand, it was verified for all substrates that for the equivalent spot conditions in terms of amount of protein mass deposited (e.g. 400 pg spotted as 5 drops of Fn200 or 10 drops of Fn100, refer to Table 2.6 for other cases) yielded slightly larger amounts of mass immobilised for the higher Fn concentrations spotted (Fn200 for the example exposed). On the other hand, it was observed that the spots printed in 1 drop could not be linearly fitted (data marked as “not fitted” in the plots presented, corresponding to 80 and 144 pg mass deposited) with the rest of spot conditions. This observation help for all substrates but AD-Agarose slides. This behaviour could be due to a faster evaporation rate for spots printed in 1 drop only, leading to an increase in adsorbed mass on the surface as a result of aggregated multilayers of proteins (independently of the chemical activation of the substrate), as suggested by other authors.<sup>103</sup> Eliminating these data points from the linear approximation allowed finding a linear relation between the spotted and immobilised Fn mass for all the chemically activated substrates, with  $R^2$  values larger than 0.95. PEO-like data could also be adjusted by a linear approximation, but with lower  $R^2$  values (0.87 to 0.92). Data obtained from BSA-Glass substrates could not be linearly fitted.

The slope for the linear equations presented in Figure 2.22 was used as index of the Fn immobilisation ratio for each slide, and this value (expressed in percent) is presented in Table 2.7 (last column). The variations found in the slope between slides of the same substrate could be attributed in part to variations in the substrate properties from one batch to the other. From the results presented, it can be seen that the substrates retaining the highest amounts of Fn immobilised on the surface were AD-Agarose, a-PMMA and AD-Glass, in that order. PEO-like had a lower quantity of Fn retained on its surface, probably due to the lack of a specific chemistry to immobilise proteins. As expected, the rate of protein immobilisation on BSA-Glass was the lowest one.

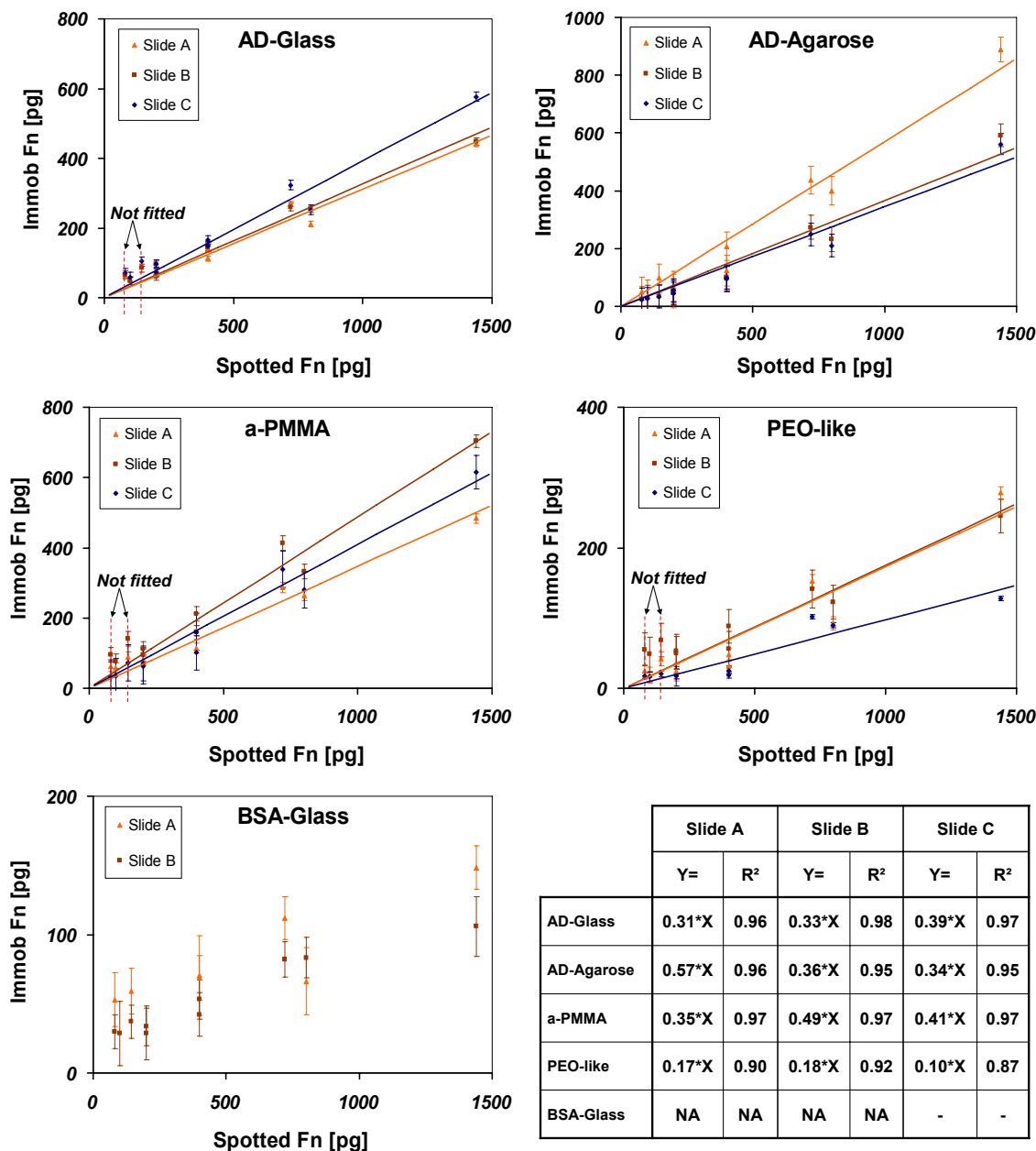


**Figure 2.22** Plots of the immobilised Fn mass as a function of the spotted Fn mass, for spots composed of Fn in PBS. In each plot, data from three experiments (namely slides A, B and C) is presented for each substrate (only 2 slides for BSA-Glass). Lines represent the linear approximation for the given values. The linear approximation equations found for each slide and the R<sup>2</sup> value associated are indicated in the bottom right table. NA: Not applicable.

To assess the intra-slide variation, independent coefficient of variation (CV) values and their associated confidence intervals were calculated for the three slides assayed for each substrate and for each spot condition spotted in PBS. Each of these CVs was calculated by:

$$CV_{int\ ra} (\%) = \left( \frac{\text{standard deviation}}{\text{mean immob mass}} \right) \times 100$$

Table 2.7 presents the CVs obtained for the spot condition of 10 drops of Fn 360 in PBS, as an example. For each substrate, the largest and smallest CVs and its respective confidence intervals are presented. Substrate performance in terms of smaller to larger CVs was similar for the other conditions spotted, although CVs increased as the spotted Fn concentration decreased (Figure 2.23). Additionally, to provide a more general parameter describing the intra-slide variation, all the CVs obtained for each slide were averaged. The largest CVs obtained in this way for each substrate and the standard deviation associated are presented in Table 2.7.

Substrate	Largest CV intra-slide – Fn360 [%]	Smallest CV intra-slide – Fn360 [%]	Largest Average CV intra-slide [%]	Fn immobilisation ratio
<b>AD-Glass</b>	2.5 [1.9, 2.8]	1.7 [1.3, 1.9]	11.7 ± 7.1	31 - 39 %
<b>AD-Agarose</b>	6.7 [5.1, 7.4]	4.7 [3.6, 5.2]	74.8 ± 59.6	34 – 57 %
<b>a-PMMA</b>	7.9 [6, 8.8]	2.6 [2, 2.9]	62 ± 47.3	35 - 49 %
<b>PEO-like</b>	9.8 [7.5 10.9]	2.6 [1.9, 2.8]	33.9 ± 14.1	10 - 18 %
<b>BSA-Glass</b>	20.3 [15.4, 22.6]	10.6 [8.1, 11.8]	37.9 ± 21.6	<10 % (non linear relation)*

**Table 2.7** Largest and smallest intra-slide coefficients of variation (CV) found for each substrate (for the 10 drops Fn360 in PBS spot condition), listed with their corresponding 95% confidence intervals. To provide a wider overview of the intra-slide variation for each substrate, an average CV and the standard deviation associated were calculated using data from all conditions spotted without SA and in PBS. The last column of the table shows the Fn immobilisation ratio, expressed as percent of total Fn mass spotted. This value was obtained from the slopes for the linear approximation equations presented in Figure 2.22.

\* value calculated using data from spot conditions Fn200 and Fn360 spotted in 10 drops in PBS.

In terms of intra-slide variation, the lowest CV (calculated for 10 drops of Fn360 in PBS, presented in Table 2.7) and the smallest change between extreme CVs were obtained for AD-Glass slides, indicating that this substrate yielded the most intra-slide reproducible results. AD-Agarose, a-PMMA and PEO-like had close CV values and ranges. Comparing the intra-slide CV calculated using only data from one spot condition (10 drops Fn360 in PBS) and the average value of CVs obtained from all spots conditions (without SA and in PBS) showed that intra-slide CV are spot condition-dependant, since including several spot compositions resulted in severe increase in the CV intra-slide and its standard deviation. This is further evidenced in Figure 2.23, where it is seen that spotting Fn at 50 µg/mL yielded up to 90% intra-slide variation

in some substrates. Overall, AD-Glass slides were found to yield high rates of Fn mass immobilisation while showing the best reproducibility of results (Table 2.7).

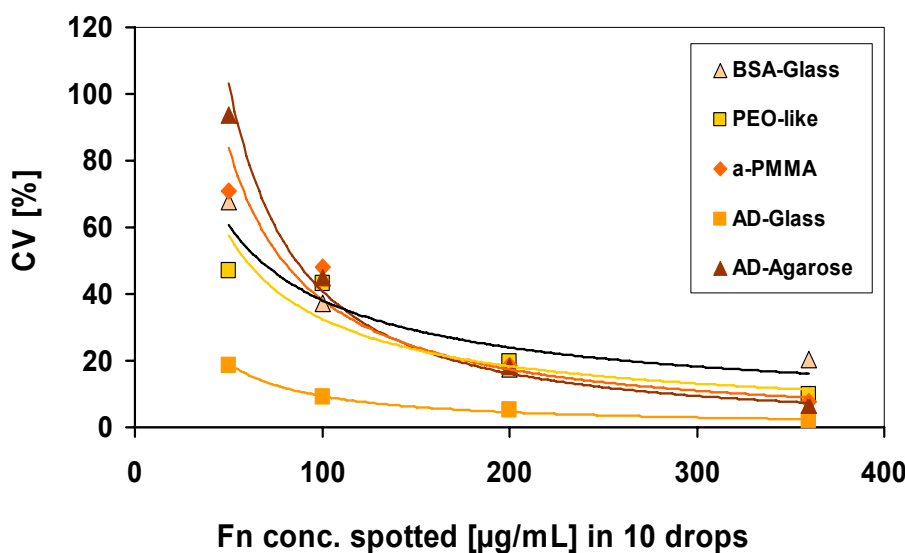


**Figure 2.23** Plot of the coefficients of variation obtained for several Fn concentrations spotted in 10 drops in PBS. Curves represent potential fittings for the data points.

### Immobilised Fn density

To analyse in more detail the effect of printing Fn in different spot conditions (defined by the spot size and buffer composition), slides with the highest and lowest rates of Fn immobilisation were selected based on results presented in Figure 2.22. As an example for AD-Glass, slides C and A were chosen for further analysis, referred to from here on as AD-Glass (up) and AD-Glass (low), respectively. A similar nomenclature was followed for the other substrates.

To look at the surface-bound protein density, the area of each spot was calculated from the measured diameters exposed in the previous section. As a representative example, the results obtained for Fn360 in PBS are presented in Figure 2.24. The immobilised Fn density on each spot condition was then evaluated using this data (Figure 2.25). It was found that important changes took place in the PEO-like (increase in Fn density) and AD-Agarose (density decrease) substrates, bringing them closer to AD-Glass and a-PMMA slides in terms of Fn density immobilised. As previously noted, this can be explained by the fact that despite the same amount of mass was spotted on all substrates for a given spot condition, the area onto which the spotted mass spread was different, therefore yielding different Fn densities. As expected from the diameter results, the increase in Fn density did not show up for BSA-Glass slides (with spot areas considerably larger than those measured for PEO-like slides), which continued to be the substrates with less Fn density on the spots “after washing”.

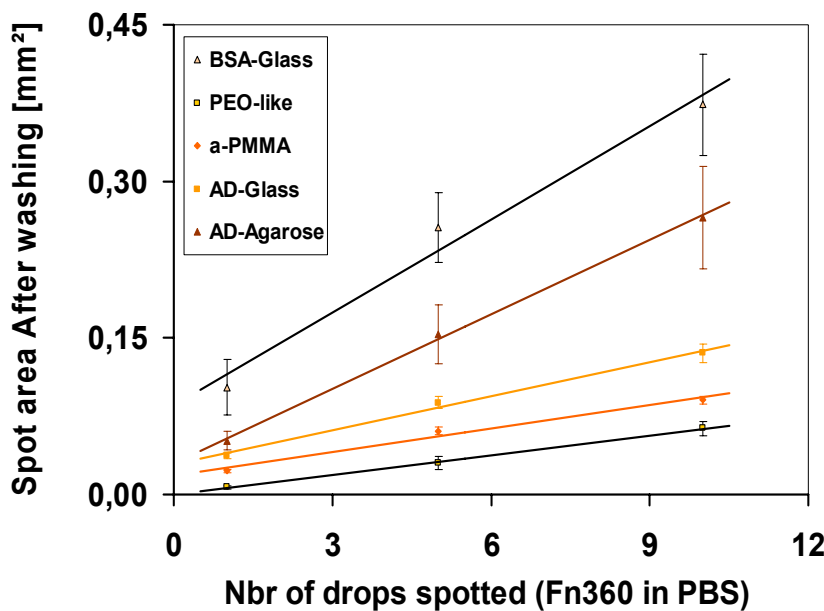


**Figure 2.24** Plot for the spot area “after washing” (for spots printed with Fn360 in PBS) vs the number of drops spotted. Lines represent the linear fitting of the data points (1, 5 and 10 drops) obtained for each substrate. Spot area was found to increase linearly for all substrates, with  $R^2$  values larger than 0.98.

Interestingly, when comparing one-to-one (for the same slide) the groups of bars (1, 5 and 10 drops) for Fn200 in PBS (Figure 2.25A), it was found that the Fn density was almost the same, despite the fact that when spotting 10 drops (800 pg) the mass deposited was the double of that deposited in 5 drops (400 pg) and 10 times larger than the mass spotted in 1 drop (80 pg). The same outcome was found for spots of Fn360 in PBS (Figure 2.25B). Therefore, printing spots in 1, 5 or 10 drops resulted in an increase in immobilised mass, as presented previously (Figure 2.22), but this increase was compensated by an increase in area of the spots (as evidenced in Figure 2.24), yielding similar immobilised Fn densities on the spots. When comparing bars one-to-one (for the same slide) between Fn200 and Fn360 for an equal number of drops (for example, 5 drops Fn200 in Figure 2.25A and 5 drops Fn360 in Figure 2.25B), it was found in this case that a higher protein density was immobilised for the highest Fn concentration spotted. This performance was more evident for AD-Glass, a-PMMA and AD-Agarose slides and is further illustrated for AD-Glass by the spot images presented in Figure 2.25C, where Fn360 (1, 5 and 10 drops) yielded spots with higher fluorescence intensity than Fn200 spots. As a result, these data demonstrates that while an increase in the quantity of Fn mass immobilised on the substrates can be targeted both by increasing the Fn concentration spotted or the number of drops printed (Figure 2.22A), it is mainly the Fn concentration in the solution spotted that significantly impacts the Fn density immobilised on the chemically activated substrates (Figure 2.25).

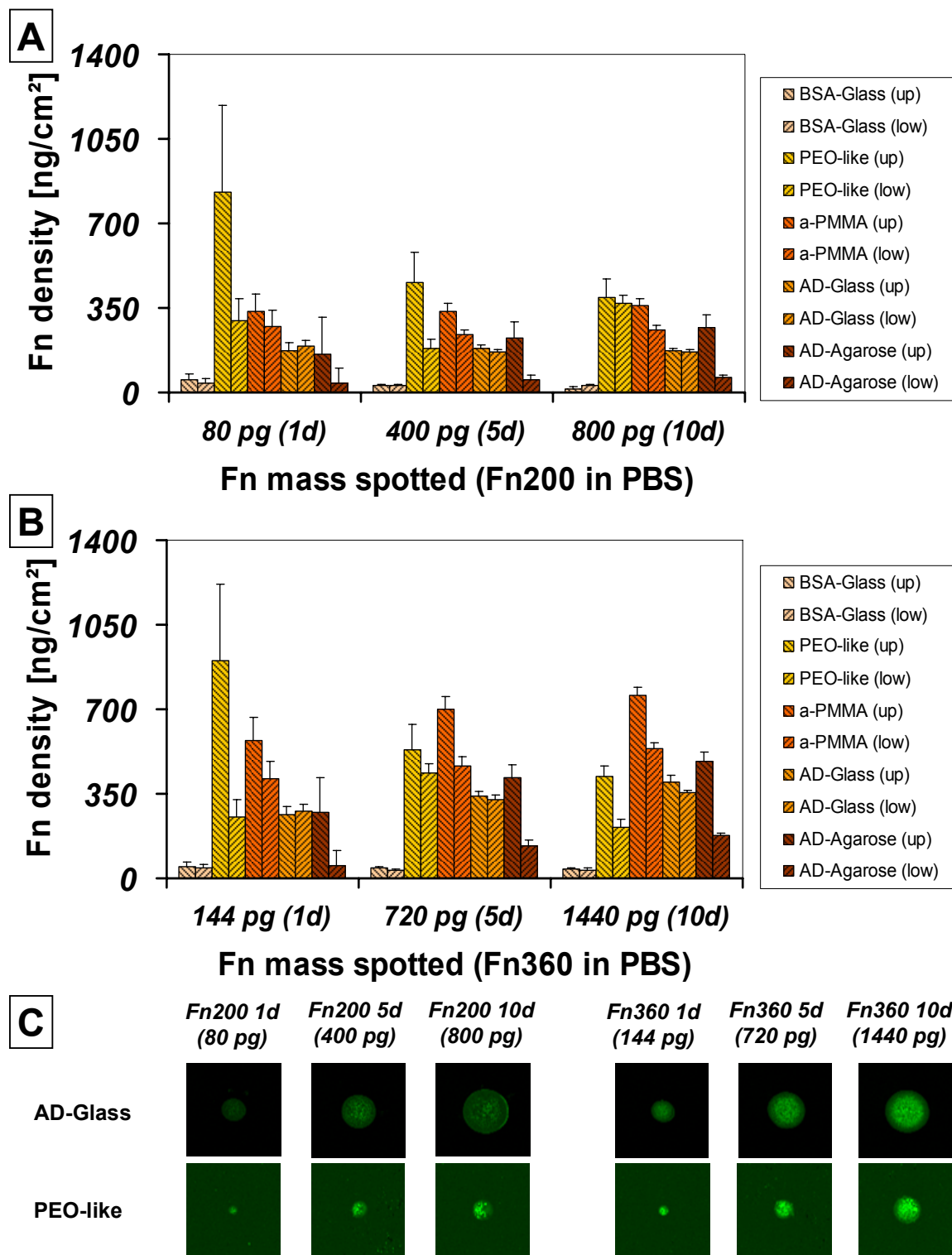


**Figure 2.25** Immobilised protein density plot for Fn200 (A) and Fn360 (B) spotted in PBS. Two representative slides per substrate (indicated as (up) and (low)) are presented. Results show that spotting Fn at higher concentration resulted in a higher density of immobilised Fn, while increasing the number of drops for a fixed Fn concentration did not. **C.** Representative spot fluorescence images for AD-Glass and PEO-like substrates are presented as example. Images show that Fn 360 spots yielded spots with higher intensities. Signal intensity and contrast have been independently optimised for each substrate to allow visualisation of the microarrayed spots, therefore intensity comparison should only be made between spots for the same substrate.

In this study, PEO-like slides showed a high variability in the density of protein immobilised on the spots. These variations were larger between slides for each Fn concentration (e.g. between PEO-like (up) and PEO-like (low) for 1 drop of Fn200 in PBS, Figure 2.25A) than between Fn concentrations spotted, suggesting that either this substrate was more susceptible to slight variations in the experimental protocol followed for slide printing and washing or that the immobilisation of proteins on the PEO-like layer can vary from different batch of slides. PEO-like slides have been previously reported to show a protein saturation trend at  $112\text{ ng/cm}^2$ , based on conversion of ellipsometry data to Fn mass density by theoretical calculation.<sup>57</sup> The Fn densities immobilised on PEO-like substrates reported here were considerably larger. This can be mainly accounted by the differences in the printing buffer used for spotting the proteins. While Ceriotti and colleagues<sup>57</sup> used an acidic buffer with pH 5 (containing ethylenediaminetetraacetic acid (EDTA), Triton-X and glycerol), data presented here corresponds to Fn printed in PBS at pH 7.4. It has been reported that electrostatic interactions (defined by the protein electrostatic properties, the solution pH and its ionic strength) can affect protein adsorption.<sup>128</sup> In particular, Fn has an acidic isoelectric point ( $\sim 5$ )<sup>130</sup> and it has been reported that when the solution pH is close to the protein isoelectric point the protein adsorption, as a result of electrostatic interactions, is minimal.

Despite AD-Agarose slides showed a clear trend to increase the Fn density on the spots as the Fn concentration spotted increased (compare Figure 2.25A and B), for this substrate it was also observed that the protein density variations were larger between slides for each Fn concentration than between Fn concentrations. In this case, however, protein density data is only presented as reference since the matrix-like structure of this substrate could allow protein embedding and therefore the amount of protein retained within the matrix could be distributed in a 3D volume.

An equivalent comparison of the protein density obtained for spots printed with Fn50 and Fn100 could not be accomplished due to the uneven protein distribution on the spot area, as previously exposed. As a result, an average protein density calculated using the spot diameter would not accurately represent the real situation for these spots.

### ***Effect of glycerol inclusion in the printing buffer***

Including glycerol in the printing buffer resulted in spots with a lower quantity of Fn immobilised “after washing” and the loss of linearity between the quantity of immobilised Fn mass and the initial Fn mass spotted, as presented in Figure 2.26. The only exception for this behaviour was for the AD-Agarose slides which continued to show a linear relationship between

spotted and immobilised Fn mass, and similar rates of Fn immobilisation (35 to 54%, data obtained as percent from the highest and lowest slopes presented in Figure 2.26, bottom right table). The results obtained for the other substrates can be explained by the wash-off of the protein layer initially adsorbed at the air/water interface, as previously noted. This effect would account for the decrease in Fn immobilised mass observed for spots containing glycerol. For AD-Agarose substrates, on the other hand, probably its hydrogel nature allows protein embedding in the polymer matrix and therefore avoiding the formation of the protein layer at the air/water interface.

On the other hand, it has been recently reported that glycerol, despite being one of the most commonly employed additives in the printed buffer for protein and cellular microarrays, might interfere with the mechanism of protein attachment to the chemically activated substrates.<sup>131</sup> This mechanism usually involves the nucleophilic attack on the surface bound moiety by the amine-terminated protein. The presence of hydroxyl groups in the glycerol molecule could generate a competition for the surface reactive groups. This competition effect could also account for the loss of linearity observed for AD-Glass and a-PMMA in Figure 2.26.

To look in more detail at the effect of including glycerol on the immobilisation rate of Fn, data from spots printed with Fn360 in 10 drops in PBS with and without glycerol was plotted for all substrates (Figure 2.27, two slides per substrate were chosen as previously described). Substrates were classified in 2 groups, on one hand, there were slides which showed a significant decrease, larger than 50%, in the immobilised protein mass when compared to PBS buffer (indicated with an \* in Figure 2.27). AD-Agarose slides, on the other hand, showed no important impact by the glycerol inclusion (with mass changes oscillating between ~8% decrease for AD-Agarose (up) to ~7% increase in AD-Agarose (low), data from Figure 2.27). The spot images presented in Figure 2.27 (bottom) further illustrate this effect. It can be seen that spots printed with PBS including 2% glycerol had extremely lower intensities when compared to spots printed in PBS. This effect was more evident for PEO-like, a-PMMA and AD-Glass. AD-Agarose slides, on the other hand, showed spots with similar intensity.

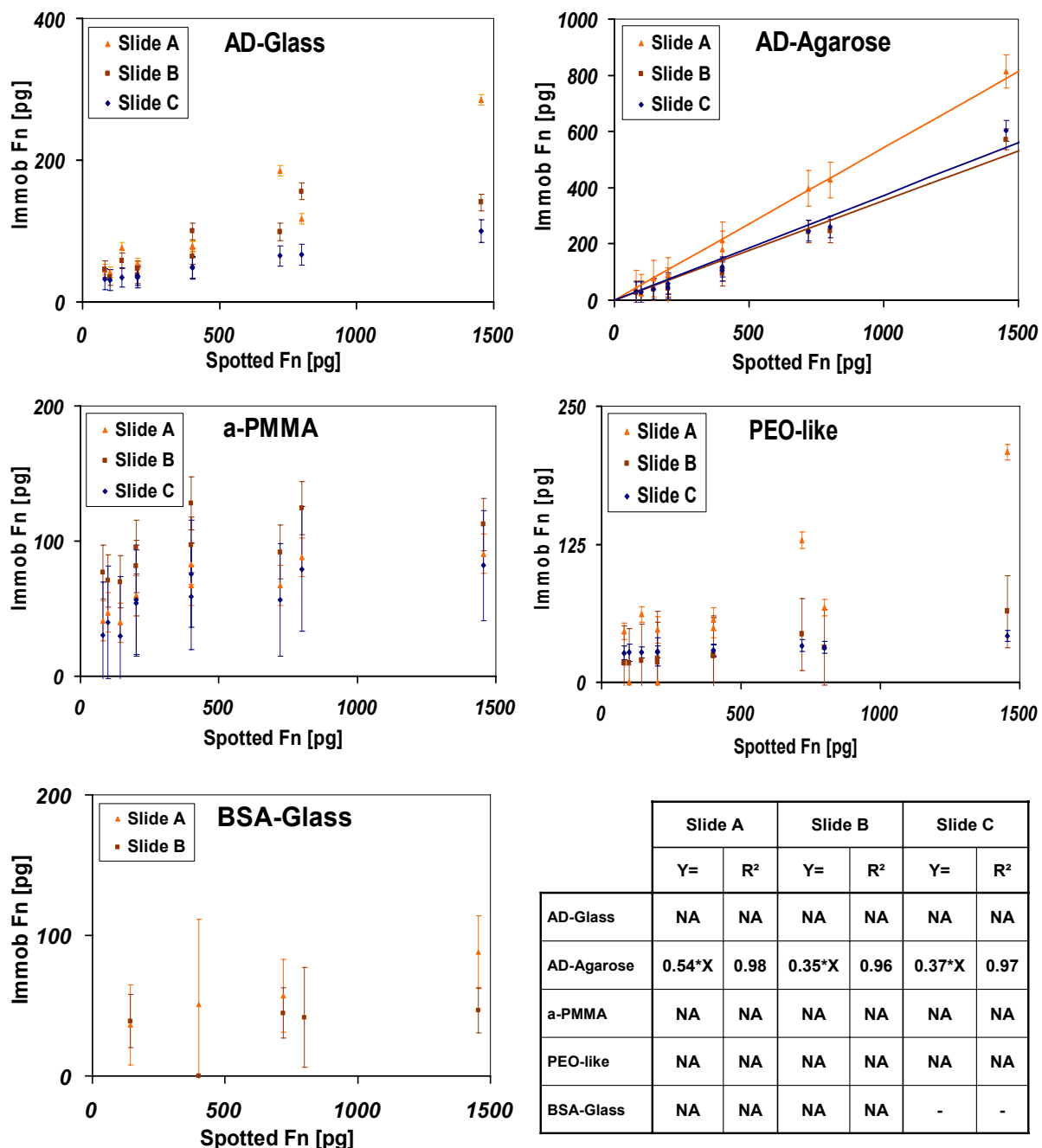


**Figure 2.26** Plots of the immobilised Fn mass as a function of the spotted Fn mass, for spots composed of Fn in PBS 2% glycerol. In each plot, data from three experiments (namely slides A, B and C) is presented for each substrate (only 2 slides for BSA-Glass). Lines represent the linear approximation for the given values. The linear approximation equations found for each slide and the R<sup>2</sup> value associated are indicated in the bottom right table. NA: Not applicable.

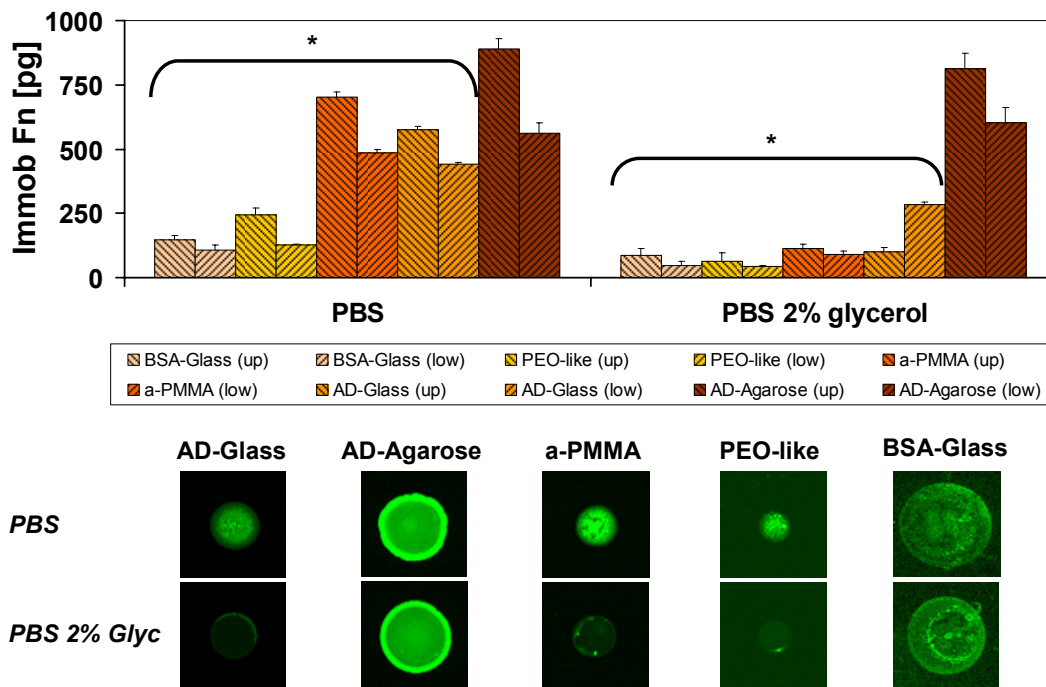


**Figure 2.27** Printing buffer effect on the quantity of immobilised Fn mass. Data plotted for spots printed with Fn360 in PBS w/wo 2% glycerol, and 10 drops spot size. Two independent experiments (indicated as up and low) are presented for each substrate. \* indicates slides for which the amount of Fn mass immobilised was statistically different between printing buffers. The effect of including glycerol in the printing buffer had no important impact on AD-Agarose slides. Bottom: Representative spot fluorescence images for all substrates quantified and for the two buffers assayed. Signal intensity and contrast have been independently optimised for each substrate to allow visualisation of the microarrayed spots, therefore intensity comparison should only be made between spots for the same substrate.

### 2.3.6 Immobilised protein quantification: spots containing Fn and SA protein mixtures

#### Immobilisation of Fn in the spots

For spots containing protein mixtures of Fn and SA, an analysis of the immobilised Fn mass as response of the spotted Fn mass (Figure 2.28) yielded similar results to those presented in Figure 2.22 for spots with Fn only. Comparing the results presented in the bottom right table in Figure 2.28, it was found that for printing Fn premixed with SA, the Fn immobilisation ratio (indicated by the slope of the linear approximation equations) was close to that of printing Fn only. As previously noted, spots printed in 1 drop could not be linearly fitted with the rest of spot conditions by any substrate but AD-Agarose slides. Eliminating these data points from the linear approximation allowed finding a linear relation between the spotted and immobilised Fn mass for all the chemically activated substrates, however, the linear approximation equations presented fitted data with lower  $R^2$  values. The lower  $R^2$  values obtained could be attributed to a

“competition effect” between the co-spotted Fn and SA for attachment to the substrate surface, as previously discussed in section 2.3.3, which could introduce an additional variable accounting for the deviation from the linear fitting.

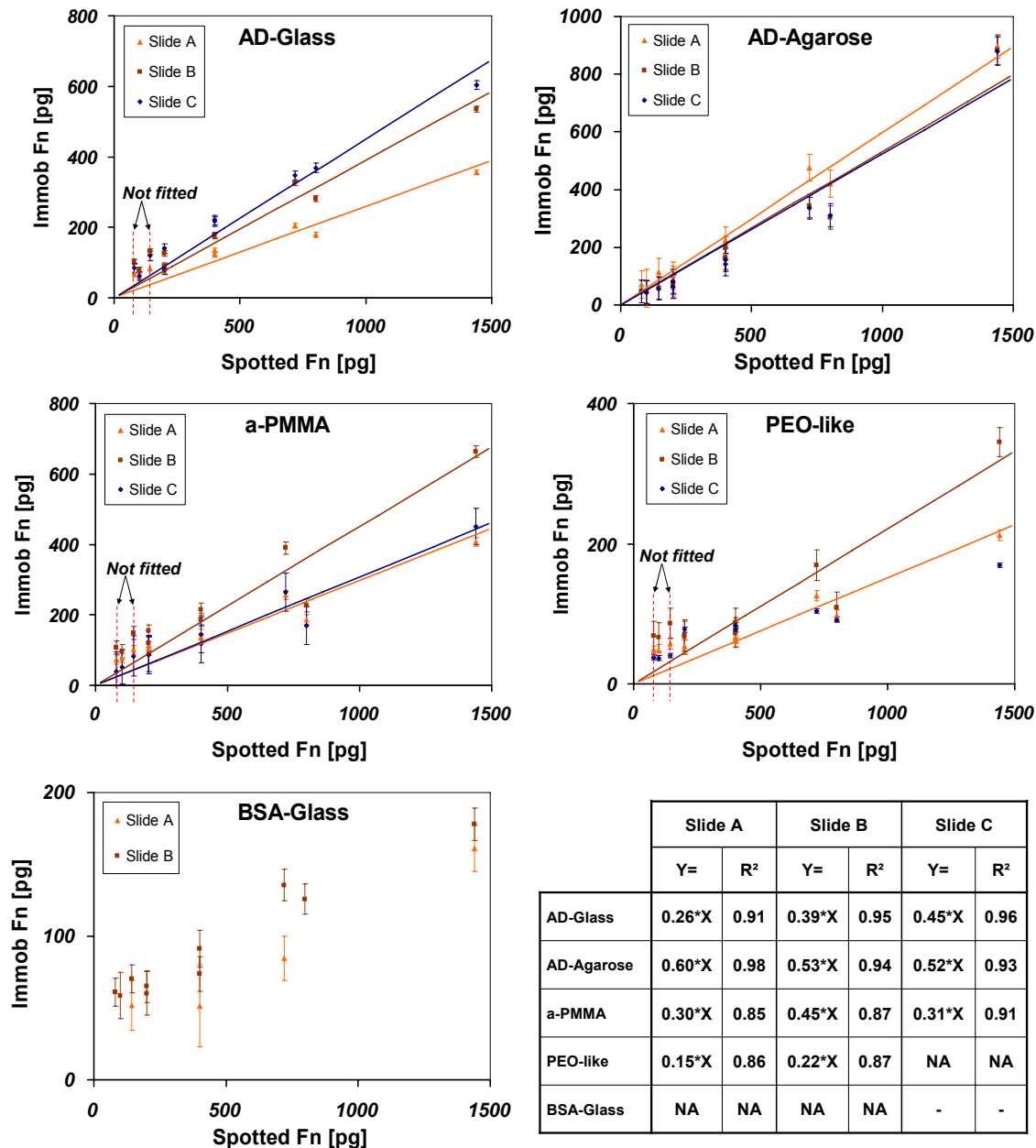


**Figure 2.28** Plots of the immobilised Fn mass as a function of the spotted Fn mass, for spots composed of Fn and SA in PBS. In each plot, data from three experiments (namely slides A, B and C) is presented for each substrate (only 2 slides for BSA-Glass). Lines represent the linear approximation for the given values. The linear approximation equations found for each slide and the  $R^2$  value associated are indicated in the bottom right table. Slide C for PEO-like slides could not be linearly fitted. NA: Not applicable.

The order of substrates in terms of larger to smaller Fn mass immobilisation ratio continued to be AD-Agarose (52 – 60 % of the total Fn mass spotted, data expressed as percent of the slopes presented in Figure 2.28), a-PMMA (30 – 45 %), AD-Glass (26 – 45 %), PEO-like (15 –

22%) and BSA-Glass (less than 10 % for Fn360 spotted in 10 drops), respectively. As expected, the order of slides assayed for each substrate, in terms of highest and lowest Fn immobilisation, was maintained (e.g. AD-Glass, slides C and A in Figure 2.28 were the slides with highest and lowest Fn immobilisation rate, respectively).

### ***Immobilisation of SA in the spots***

Regarding the immobilisation of SA mass, to ensure quantification of immobilised SA in the linear range covered by the calibration curves (i.e. mass values larger than 20 pg, refer to Figure 2.21A and C), the lowest SA masses spotted (i.e. spots printed in 1 drop for all the Fn concentrations) which could not be accurately quantified were not included in this analysis. Moreover, as previously noted, SA signal did not present a homogeneous distribution within the spot area for spots printed with Fn50 SA50 and Fn100 SA50. This effect was shown to be neutralised when increasing the Fn concentration. Therefore, the following analysis of SA immobilised on the substrates is focused in spots printed with Fn200 SA50 and Fn360 SA50.

For all the spot conditions quantified, it was found that some of the spotted SA mass was immobilised on the chemically activated substrates (Figure 2.29A and Figure 2.30A). PEO-like and BSA-Glass slides had negligible SA mass retained on its surface “after washing”. In fact, most of the background-corrected fluorescence intensity values obtained for spots with SA on these substrates were negative, indicating that the averaged (red) signal associated with SA in the surroundings of the spot was higher than the signal from the spots. Therefore, in this study, all the negative values obtained were presented as “zero” to indicate that the spots for these conditions did not effectively immobilise SA. This is further illustrated by the spot images presented in Figure 2.29C, where the inclusion of red labelled SA (mixed with green labelled Fn) yielded yellow spots “as spotted” on the substrates. “After washing”, yellowish spots only appeared in AD-Agarose, a-PMMA and AD-Glass slides. PEO-like and BSA-Glass slides had predominantly green spots.

For the slides retaining SA, it was observed that a-PMMA and AD-Agarose had a similar performance when printing 5 drops of Fn360 SA50 in PBS, keeping around 35% of the total mass spotted (average ~35 pg from a total mass spotted of 100 pg, data from Figure 2.29A). When spotting 10 drops of the same protein mixture solution, AD-Agarose continued to immobilise around 35% of the printed SA, but a-PMMA immobilisation of SA was slightly lower. For AD-Glass slides, on the other hand, spotting 100 pg of SA yielded ~10 % of this mass immobilised (~10 pg out of 100 pg spotted, average data from Figure 2.29A), and

increasing the mass spotted to 200 pg (10 drops of Fn360SA50) provided again ~10 % of mass immobilisation (in this case ~20 pg in average, out of 200 pg spotted). A similar behaviour was observed for SA immobilisation when spotting a Fn200 SA50 solution in PBS (Figure 2.30).

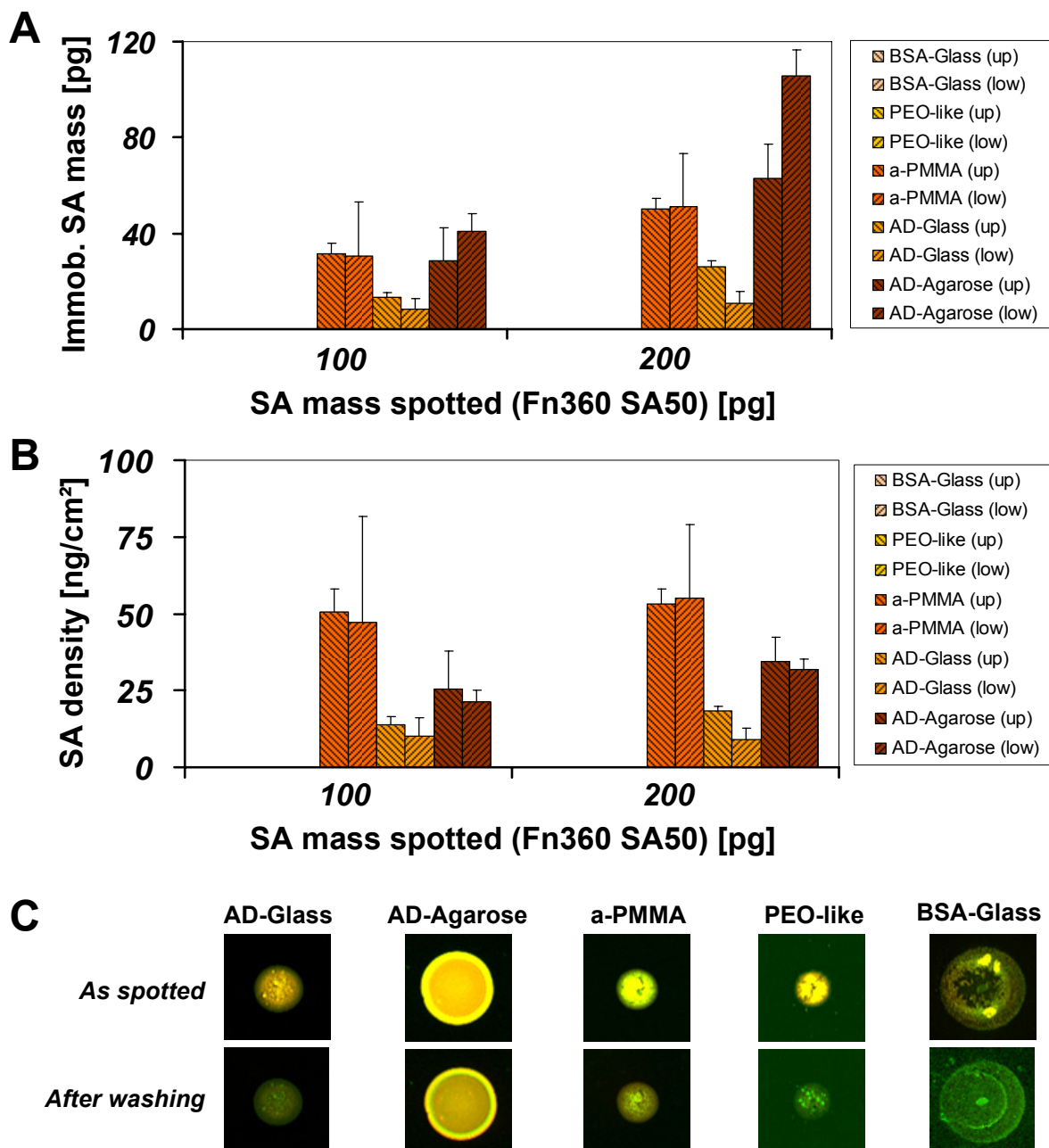


**Figure 2.29** Immobilised SA mass (A) and density (B) bar plots. Data plotted for spots composed of Fn360 SA50 in PBS and 5 drops (yielding a 100 pg total SA mass spotted) or 10 drops (for a total SA mass of 200 pg) spot sizes. Two independent experiments (indicated as up and low) are presented for each substrate. C. Representative spot fluorescence images (for 10 drops in PBS spots) obtained “as spotted” (top row) or “after washing” (bottom row) for all substrates. Yellow spots indicate the presence of both Fn 1% A555 (green) and SA A647 (red). “After washing”, BSA-Glass and PEO-like slides retained negligible quantities of SA (green spots). Signal intensity and contrast have been independently optimised for each substrate to allow visualisation of the microarrayed spots, therefore intensity comparison should only be made between spots for the same substrate.

AD-Glass and a-PMMA share many similarities in terms of surface properties, they are both chemically activated to provide covalent immobilisation of proteins, and they are both non-permeable (non-matrix like) surfaces. Therefore, it could be proposed that a-PMMA immobilises larger amounts of SA than AD-Glass (when spotting equal SA mass on the substrates) because it has a freshly activated chemistry which is more reactive than the one provided by the AD-Glass slides. However, larger standard deviation values are associated with the amounts of SA immobilisation in a-PMMA substrates (Figure 2.29A and Figure 2.30A), indicating that the intra-slide immobilisation rate is more reproducible in AD-Glass slides. Intra-slide reproducibility in the amount of protein immobilisation is a highly important issue in cellular microarrays, since it will allow evaluating cell response (attached on the spots) to a more accurate set of replicate spot conditions. For this reason, AD-Glass substrate was preferred to a-PMMA, despite the lower amount of SA immobilisation.

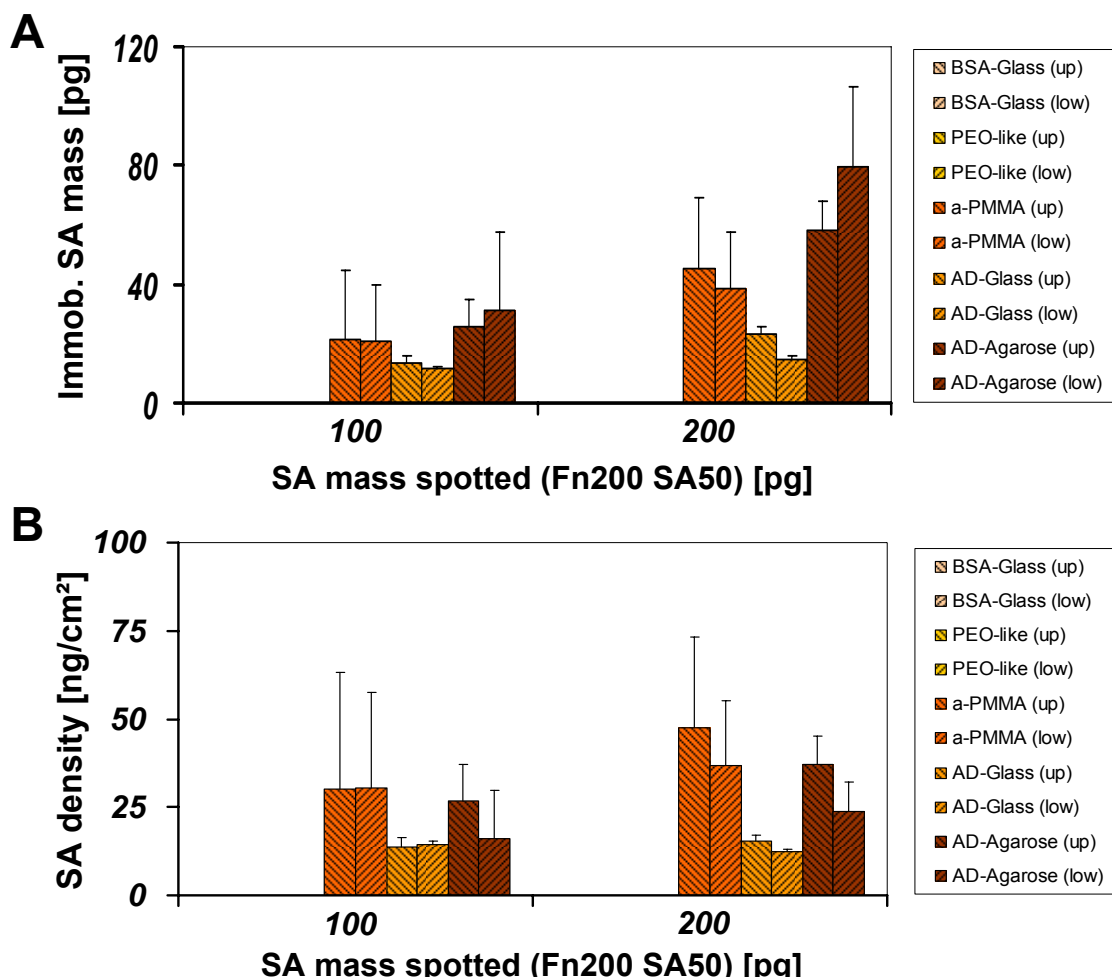


**Figure 2.30** Immobilised SA mass (A) and density (B) bar plots. Data plotted for spots composed of Fn200 SA50 in PBS and 5 drops (yielding a 100 pg total SA mass spotted) or 10 drops (for a total SA mass of 200 pg) spot sizes. Two independent experiments (indicated as up and low) are presented for each substrate.

The immobilised SA density was also assessed as a function of the SA spotted mass. Interestingly, it was found that a similar SA density outcome was attained when spotting 5 or 10 drops of SA (i.e. 100 or 200 pg), suggesting that the increase of spotted mass is compensated (as previously noted also for Fn density) by the increase in spot size (Figure 2.29B and Figure 2.30B). This held for all chemically activated substrates.

Overall, these data underlines the importance of using an activation chemistry to successfully retain proteins other than ECM proteins, which could have different sizes and structures resulting in changes of the “affinity” of the protein for the substrate. The differences in protein-surface affinity can be dictated by protein size, structure and amino acid composition.<sup>128, 129</sup> As previously mentioned, Fn has been described as a rod-like, 550 kDa protein<sup>132, 133</sup> with a length of 15.5 nm, a width of 8.8 nm and an axial ratio of 2:1.1.<sup>126</sup> On the other hand, SA is a β-barrel structure ~50 kDa protein with dimensions 5.4 x 5.8 x 4.8 nm.<sup>127</sup> Therefore, these differences in size and protein structure could account for lower affinities of SA for the PEO-like and BSA-Glass surfaces. Additionally, since the mechanism proposed for protein attachment to PEO-like slides is by adsorption, protein competition effects could favour Fn attachment in detriment of SA. Altogether, this explains why most cellular microarray reports dealing with growth factors included in the spotted solutions used chemically activated substrates.<sup>48, 54</sup>

### ***Effect of glycerol inclusion in the printing buffer***

The effect of including glycerol in the protein mixtures of Fn and SA is presented in Figure 2.31. In Figure 2.31A it can be observed that the substrate performance for Fn immobilisation, when co-spotted with SA in PBS with 2% glycerol, is similar to printing spots with Fn only (refer to Figure 2.27), with an important decrease (>50% when compared to spots printed in PBS) for the immobilised Fn mass spotted in PBS with glycerol. The only exception for this performance was again noted for AD-Agarose slides.

More dramatic changes were observed for the SA immobilised mass (Figure 2.31B). While no important variations were noted for AD-Agarose slides, the inclusion of glycerol in the spot composition had extreme consequences in AD-Glass and a-PMMA, practically reducing to zero the immobilisation of SA on the spots. These data suggests that despite the inclusion of glycerol could be desirable for immobilisation of proteins in a biologically active conformation, by avoiding spot dry out, special care should be taken because depending on the type of protein spotted few or no protein could remain on the printed substrate. Differences in protein-surface affinity and protein adsorption at the air/water interface, as previously noted when discussing

the spot morphology for spotting protein mixtures (subsection 2.3.3), could account for this effect.

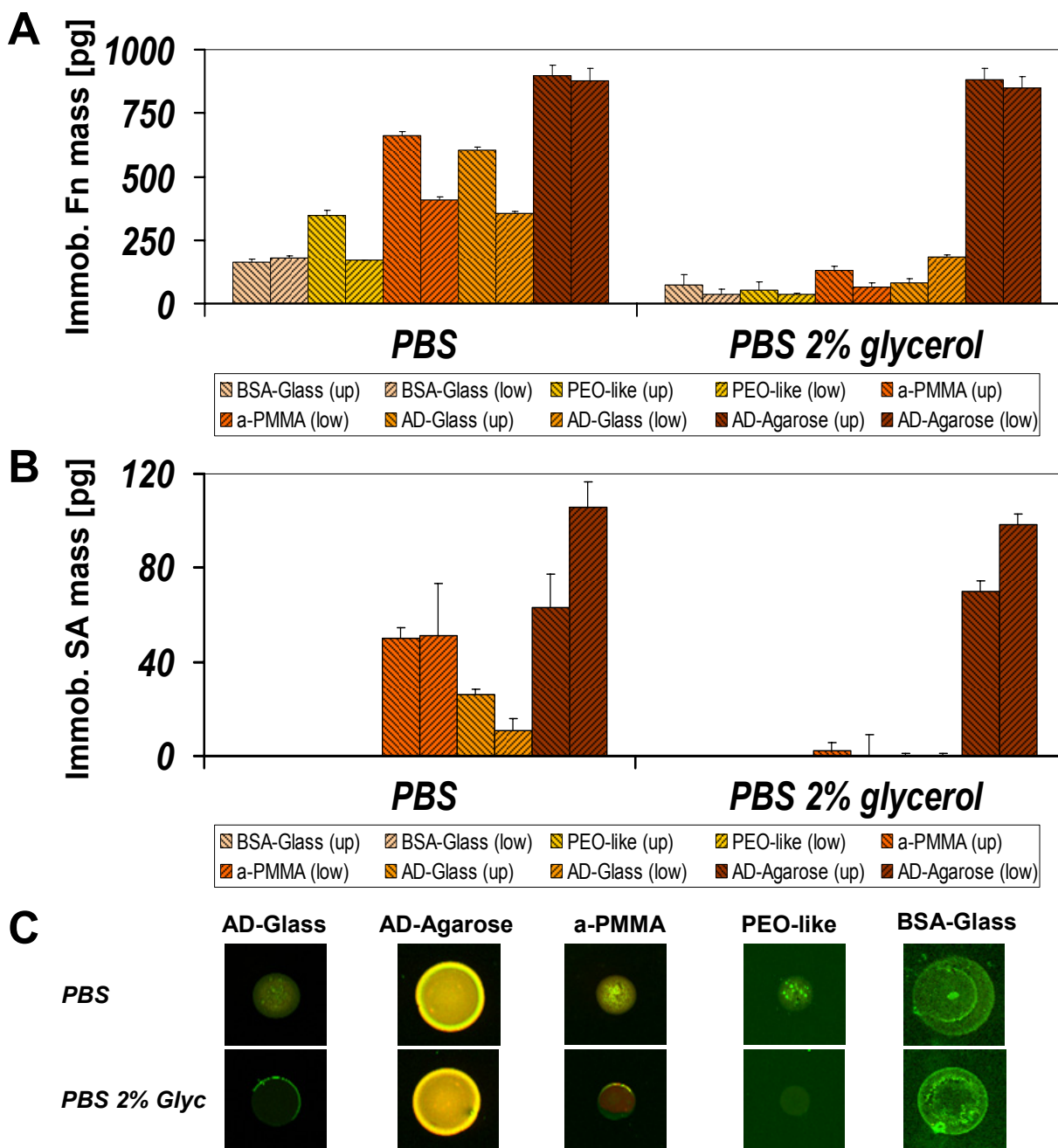


**Figure 2.31** Printing buffer effect on the quantity of immobilised Fn (A) and SA (B) mass. Data plotted for spots printed with Fn360 SA50 in PBS w/wo 2% glycerol, and 10 drops spot size. Two independent experiments (indicated as up and low) are presented for each substrate. The effect of including glycerol in the printing buffer had no important impact on AD-Agarose slides, while dramatically decreased SA immobilisation on AD-Glass and a-PMMA. **C.** Substrate-representative spot fluorescence images for spots printed in PBS and in PBS with 2% glycerol. Signal intensity and contrast have been independently optimised for each substrate to allow visualisation of the microarrayed spots, therefore intensity comparison should only be made between spots for the same substrate.

### **2.3.7 Global analysis**

To provide a broad representation of the results obtained from the spotted microarrays, a cluster analysis was done to roughly classify substrates in terms of similarity in protein immobilisation. Additionally, this allowed assessing the performance of replicate slides for each substrate, and also provided some insights into the effect of spotting different protein concentrations and buffer conditions.

The analysis implemented consisted in doing a hierarchical clustering between substrates, which had as inputs the immobilised protein mass values obtained for all the spot conditions quantified. Also, a clustering between spot conditions was performed. The results are shown in Figure 2.32 (for immobilised Fn mass) and Figure 2.33 (for immobilised SA mass). In these images, the spot conditions are presented as rows and its identity appears in the right side of the plot. The slides assayed for each substrate are presented as columns and its name is shown at the bottom of the plot. Each combination between a slide column and a spot composition defines a rectangle which is colour coded according to the immobilised protein mass value obtained “after washing” for that slide and spot condition. In these plots, reddish to blueish boxes indicate larger to smaller amounts of protein immobilised, respectively. The key for this coding is presented in the upper left box of the figures.

The hierarchical clustering analysis performed consisted in grouping slides by similarity in overall protein immobilisation outcome, assessed by means of the Euclidean distance. Further details for the building of these plots can be found in the Appendix B.II. As a result, the slides are grouped by similarity in performance in terms of immobilised protein mass. These results are presented by means of the hierarchical trees which appear at the top of the plot, where the slide grouping is indicated by the horizontal lines which link the columns of the plot. The grouping is done from bottom to top, therefore slides grouped by lines closer to the plot edge are more similar slides. In these trees, the length of the vertical branches indicates dissimilarity, therefore shorter branches indicate slides with a more similar performance. As an example, AD-Agarose.B and AD-Agarose.C columns in Figure 2.32 were grouped in the first place, and the vertical branches for this group were quite short, indicating that these two slides showed an extremely similar performance. This new group was then clustered with AD-Agarose.A. In this case it can be observed from the Figure that the vertical branches are much larger than the previous ones. This new cluster indicates that, despite AD-Agarose.A performance was more different than the one obtained for the other two slides, it was still closer to the other AD-Agarose slides than to any other slide analysed. All the other slides presented were first

clustered together between them, and the final clustering level occurred between AD-Agarose slides (A, B and C) and the general cluster formed by the other substrates. This indicated that AD-Agarose slides showed the most different performance in terms of Fn immobilisation, a fact which could be explained by AD-Agarose being a 3D polymer matrix that allows protein embedding and therefore yielding higher rates of protein immobilisation when spotted in PBS w/wo glycerol.

An important result that is highlighted from Figure 2.32 and Figure 2.33 is that the replicate slides analysed for each substrate were clustered together in the first place. The only exceptions for these observations occurred for AD-Glass and a-PMMA slides on one hand (the AD-Glass.B and C group being first clustered with the group of a-PMMA.A and C, and only then this new group clusters with AD-Glass.A, Figure 2.32), and for PEO-like and BSA-Glass slides on the other hand (PEO-like.C first clustered with the BSA-Glass group, Figure 2.32). This indicated a highly correlated performance of these substrates in terms of Fn mass immobilisation. This is further confirmed by the next order clusterings, according to substrate similarity in overall response in terms of protein immobilisation. As can be seen, chemically activated AD-Glass and a-PMMA (indicated as group 2 in Figure 2.32) were clustered together, the same occurred for PEO-like and BSA-Glass (indicated as group 3 in Figure 2.32). As previously mentioned, these two groups first were grouped together before clustering with AD-Agarose, suggesting a very different performance for this substrate (indicated as group 1 in Figure 2.32). A similar analysis, applied to SA immobilisation (Figure 2.33), showed a more evident clustering. In this case, all slides for each substrate were first clustered between them, indicating the existence of clear differences between these substrates in terms of SA immobilisation.

From a global point of view, visual inspection of Figure 2.32 and Figure 2.33 shows that AD-Agarose slides were the substrates with the largest quantity of protein (both for Fn and SA) immobilised “after washing”, evidenced by more reddish squares (larger amounts of Fn or SA mass detected “after washing”) in this substrate column. A general tendency draw from Figure 2.32 is that the order of substrates, in terms of larger to smaller Fn immobilisation, is AD-Agarose slides, followed by the a-PMMA, AD-Glass slides, PEO-like and BSA-Glass slides, respectively. These observations are consistent with the conclusions extracted from data presented in the previous sections. Results from the cluster analysis for SA data expose a similar relation to that found for Fn clustering. The best substrates in terms of SA immobilisation were the AD-Agarose slides, followed by a-PMMA and AD-Glass, respectively. PEO-like and BSA-Glass had negligible immobilised SA mass “after washing”, as previously exposed.

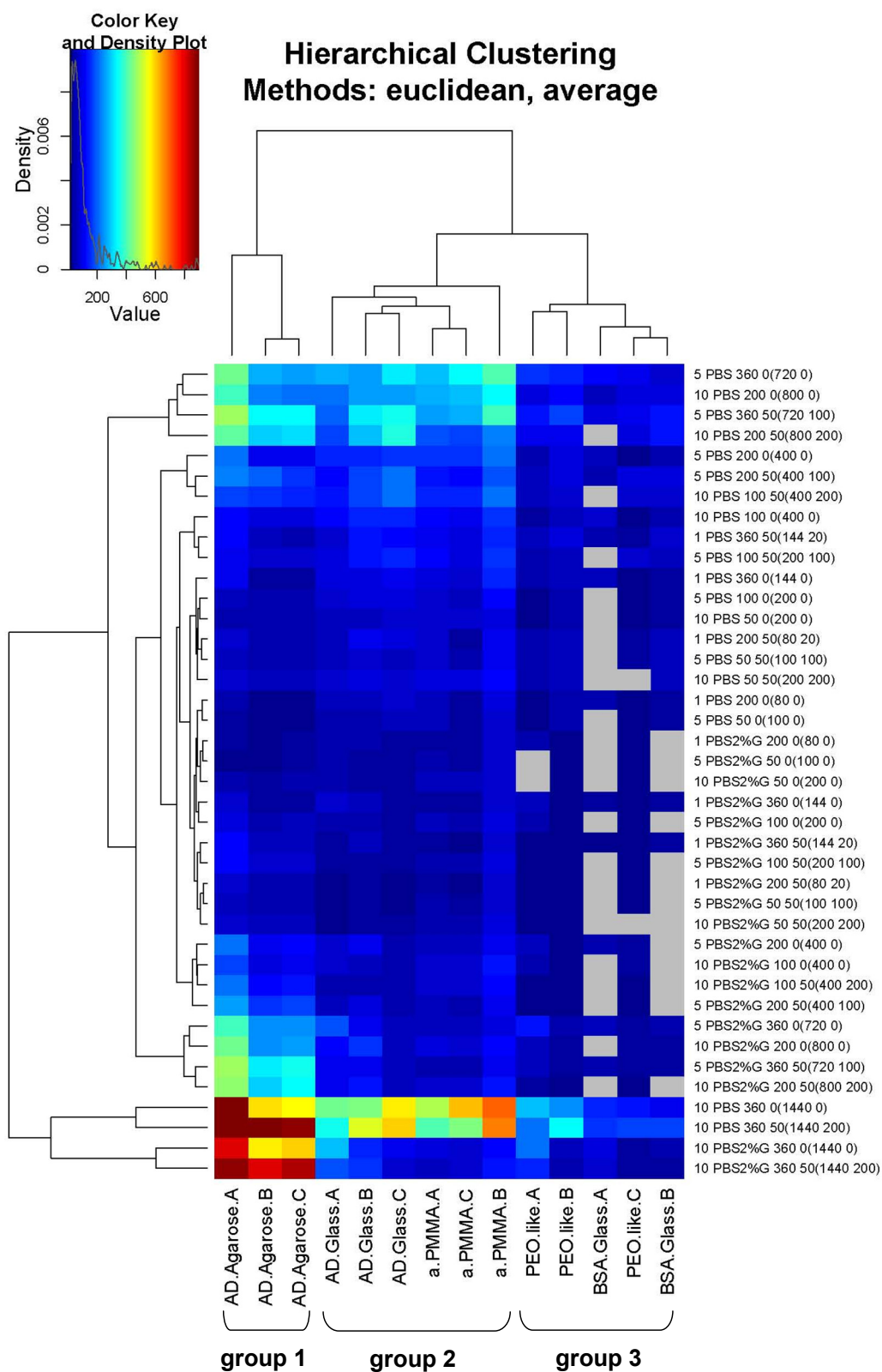


**Figure 2.32** Immobilised Fn mass hierarchical cluster analysis for the five substrates compared. Three slides per substrate (two for BSA-Glass) are presented (A, B and C). Spot compositions on the right side of the image are indicated in the following order: number of drops, buffer, Fn concentration spotted, SA concentration spotted (Fn mass printed, SA mass printed). Colour coding is indicated in the upper left box. The gray boxes represent unavailable values due to extremely low SNR for these conditions and substrates.

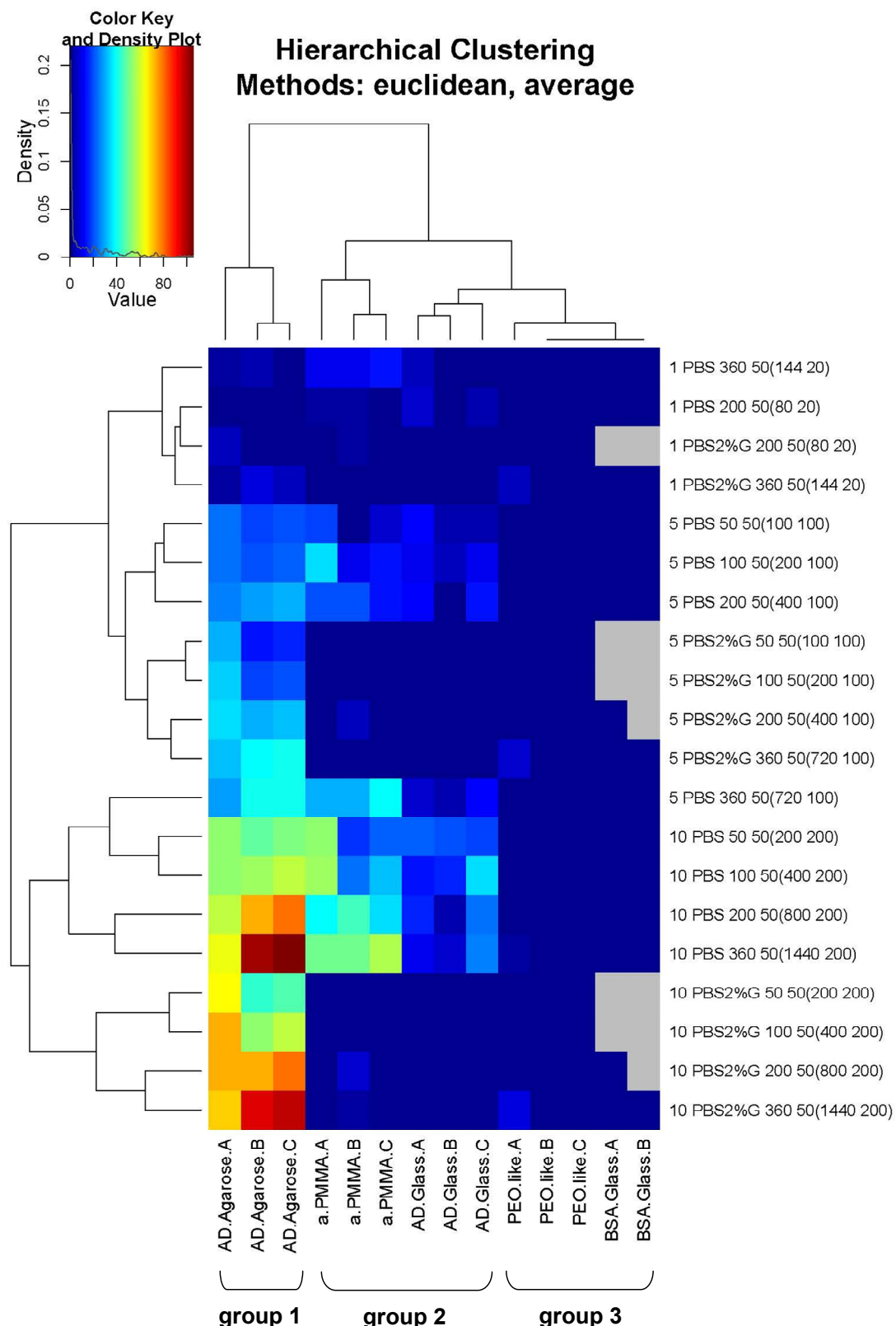


**Figure 2.33** Immobilised SA mass hierarchical cluster analysis for the five substrates compared. Three slides per substrate (two for BSA-Glass) are presented (A, B and C). Spot compositions on the right side of the image are indicated in the following order: number of drops, buffer, Fn concentration spotted, SA concentration spotted (Fn mass printed, SA mass printed). Colour coding is indicated in the upper left box. The gray boxes represent unavailable values due to extremely low SNR for these conditions and substrates.

A second clustering analysis was performed to group the spot conditions by similarity in outcome. These results are presented by means of the hierarchical trees which appear at the left of the plot. As expected, the most important factor determining the quantity of Fn immobilisation (and therefore generating the clusters of first and second orders, i.e. the rows grouped closer to the plot, Figure 2.32) was the total Fn deposited mass, independent of the substrate type and regardless the quantity of drops printed. This can be seen by the (horizontal) clustering of spots with 1440 pg (bottom rows in Figure 2.32, corresponding to 10 drops of Fn360), followed by spots with 800 and 720 pg (corresponding to 10 drops of Fn200 or to 5 drops of Fn360, respectively), and finally spots with 400, 144 and 80 pg were clustered between them.

For the SA hierarchical clustering of the spot conditions, on the other hand, the most important parameters defining the SA immobilisation were the total SA mass spotted and the buffer composition (e.g. 200pg and 100 pg amounts of spotted SA were first clustered together by buffer composition and then by the amount of mass spotted, Figure 2.33).

## **2.4 Conclusions**

In this study, the immobilised Fn and SA mass and density were qualitatively and quantitatively analysed for 4 substrates of interest in cellular microarray applications,<sup>48, 55, 57, 59, 68</sup> and for a negative protein adhesion control substrate. The main objective of this chapter was to elucidate the best substrate for further analysis of cellular microarray fabrication. For this purpose, a number of crucial factors were considered and quantitatively evaluated, these included the amount of Fn and SA immobilised and the intra-slide reproducibility of the protein immobilisation results.

The overall rating in terms of protein immobilisation for the substrates assayed was, from larger to smaller Fn immobilisation ratio, AD-Agarose, a-PMMA, AD-Glass, PEO-like and BSA-Glass. In particular, AD-Glass Fn immobilisation was in the range of 25-45%. Regarding the immobilisation of SA mass, it was observed that a-PMMA and AD-Agarose immobilised ~35% of the total SA mass spotted, AD-Glass retained ~10 % of the total SA mass spotted, and neither PEO-like nor BSA-Glass retained SA on its surface. However, in terms of the intra-slide reproducibility, the best results were obtained for AD-Glass slides both for Fn and SA mass immobilised. These reasons allowed choosing this substrate to perform the cellular microarray optimisation process described in the following chapters of this thesis.

A second objective of this chapter was to report on the best experimental parameters to be used for further cellular microarray fabrication, these including the Fn concentration spotted, the spot size (tuned here by overprinting 1 to 10 drops at a single location) and the printing buffer choice.

It was observed that spots printed with Fn50 and Fn100 produced an uneven Fn distribution, and this effect was neutralised when spotting Fn at higher concentrations (Fn200 and Fn360). For this reason spotting Fn at 200 or 360 µg/mL will be preferred in the further optimisation of cellular microarray fabrication.

The immobilised protein density is an important factor regarding cell adhesion and signalling, since usually 20 to a hundred cells can colonize a spot, depending on its size, and each cell will “sense” and interact with proteins on its area of attachment and the surroundings. Here, it was reported that increasing the spot size does not necessarily impact the protein density (both for Fn and SA), since the increase in mass spotted is compensated by the increase in spot size. As a result, the desired spot densities of Fn (relevant for cell adhesion to the microarrays) or SA (used here to model other co-spotted protein or growth factor) can be targeted mainly by the protein concentration, leaving the choice of a variable spot size for testing, in future cellular microarray applications, other kind of effects on cell behaviour by controlling the number of cell-cell interactions on the spots.

Finally, results found in this study show that spots printed with Fn in PBS 2% glycerol had lower amounts of Fn immobilised “after washing”. Most importantly regarding other proteins which could be included in the spots for future applications targeting other cell signalling pathways (such as cell differentiation), despite the use of glycerol appears as a suitable alternative to enhance protein immobilisation in an active conformation, here it was shown that SA immobilisation was extremely low, even for the chemically activated substrates (except for AD-Agarose). Therefore, printing microarray spots in PBS only will be preferred in the further optimisation of the cellular microarray fabrication process, although PBS with 2% glycerol will continue to be evaluated because of the advantages provided by printing with this buffer (better spot homogeneity and protein immobilisation in an active conformation).

# Chapter 3      Cellular microarray fabrication and characterisation

## 3.1 Introduction

Results obtained in the previous chapter suggested AD-Glass as the best substrate to fabricate cellular microarrays based on the relatively high amounts of fibronectin and streptavidin immobilised by this substrate as well as the intra-slide reproducibility of results. The only report that could be found on cellular microarrays using AD-Glass as a substrate described the use of laminin as cell capture agent and the study of neural precursor cell differentiation after 4 days of cell culture in the arrays.<sup>48</sup> This chapter deals with the fabrication of cellular microarrays on AD-Glass substrates using mesenchymal stem cells (MSCs), aiming to achieve cell culture for several days.

MSCs constitute a highly attractive cell type to explore the potential capabilities of cellular microarray technology. MSC differentiation to several cell fates has been extensively characterised using standard cell biology approaches.<sup>74, 134</sup> As a result, commitment to the osteoblast fate can be currently tracked at several stages of the differentiation process, ranging from a few days to several weeks.<sup>135-137</sup> A detailed state of the art in cellular microarrays has already been exposed in the introduction of this thesis. In particular, when dealing with MSC culture on isolated microarray spots, the only reports that could be found in the literature involved cellular microarray formation on spots composed of polymers (i.e. no proteins) onto poly(2-hydroxyethyl methacrylate) (pHEMA) substrates, in which cells have been cultured up to 10 days. These reports evaluated different polymer compositions supporting cell spreading<sup>63</sup> and inducing differentiation.<sup>64</sup> Mesenchymal stem cell cultures on isolated fibronectin patterns have been reported in the literature using PDMS as substrate for the study of the effects of cell shape on cell differentiation.<sup>138</sup>

Previous studies on cellular microarrays report a large variation in the parameters affecting the fabrication process.<sup>48, 53, 54, 139</sup> Parameters such as the passivation of the non printed surface, the cell seeding time and density, and the medium used for cell culture are usually optimised for particular cell types and periods of cell culture. This is in part due to the known fact that not all cell types behave equally with respect to cell attachment, even for the same amount of protein

immobilised on the surface.<sup>50</sup> Cell properties such as adhesion behaviour, migration, proliferation rate and ability to invade the passivated non-spotted surface areas are cell-type specific and must be considered for each particular cell model.<sup>48, 53</sup> Moreover, an important remark when building cellular microarrays, which is not such a crucial factor for protein microarrays, is the time-dependence of the microarray properties while the cell culture is progressing for several days and, sometimes, weeks. Cells will alter the initial chemistry achieved on both the spots and the passivated areas. Cell dynamic behaviour over the culture period will produce the uptake, release and replacement of the initial protein spot compositions and passivation conditions in part by the secretion of new ECM proteins and protease release. Ideally, the cellular microarray to be built should be then robust enough to allow for cell culture periods ranging from a few hours to several days in such a way that its final characterisation is still feasible.

In the cellular microarray fabrication process described in this chapter, fibronectin (Fn) spots were used as cell adhesion agents that will capture MSCs. Protein microarray fabrication was accomplished following the experimental procedure set in the previous chapter. A range of parameters affecting cellular microarray formation and further cell culture on them is presented. These include the protein concentration of the spotted solutions, the printing buffer used, the strategy for passivation of the non-printed areas, the protein spot size, the cell seeding density, the cell seeding time and the cell culture media.

The results obtained for each of these experimental conditions have been used to set up optimal technological parameters that allowed the successful fabrication of MSCs cellular microarrays suitable for cell culture time periods up to 8 days. After this period of cell culture, spontaneous cell differentiation was observed in some of the spots. The conclusions obtained with the experiments described in this chapter have set the bases that will allow for the future use of such MSCs microarrays in differentiation experiments.

## **3.2 Materials and methods**

### **3.2.1 Proteins and chemicals**

Human cellular fibronectin was obtained from Sigma (Spain). Unless otherwise specified, all other chemicals were also purchased from Sigma (Spain).

### 3.2.2 Cell isolation and culture

Rat MSCs were obtained as primary cultures from the bone marrows of healthy 10 to 12 weeks old rats by means of standard procedures.<sup>140, 141</sup> Briefly, rat femurs (obtained from the Animal Research Centre of the Parc Científic de Barcelona) were first cleaned in PBS and the bone distal ends were removed using a scalpel. Provided of a syringe, cell culture medium composed of Advanced DMEM (GIBCO), 1% penicillin/streptomycin, 1% L-Glutamine and 15% FBS, supplemented with heparin (10 units/mL), was run through the bone cavity to remove the bone marrow. This process was repeated with 4 to 6 femurs. Bone marrow extracts were resuspended several times in the same medium and, after no aggregates were visible, extracts were seeded in a new Petri dish and cultured overnight. These extracts contained several different types of cells, including non-surface adhesive blood cells such as erythrocytes and the MSCs. Of these, the cells adhered to the plastic surface on the following day have been shown to contain mostly the MSC population.<sup>134, 140, 141</sup> At this time, the culture medium was replaced, removing the unattached erythrocytes and other blood cells, and cells were further cultured until reaching semi-confluence. At that time, cells were detached from the surface by incubation with a trypsin solution and seeded at lower densities for further expansion.

Primary cells were expanded by a series of passages, which involved cell seeding on flasks until semi-confluence and then trypsinisation of cell cultures and seeding again at lower densities, with the objective of multiplying the number of cells obtained from one extraction. For the experiments presented here, special attention was paid to use only early passaged cells (passages 3 to 6), which did not reach confluence during the cell expansion process. This was due to the widely reported loss of differentiation potential in MSCs after a high number of passages, or when cells reached confluence.<sup>81, 142</sup> Either of these reasons could block MSC differentiation to other lineages, most commonly triggering spontaneous differentiation to the osteoblast fate and, by this, biasing the results of the experiments<sup>134</sup>

MSC differentiation can be tracked at many stages of the differentiation process. Differentiation to the osteoblast lineage can be followed at 24 to 48 h (Osx gene expression),<sup>135,</sup><sup>136</sup> 7 to 15 days (alkaline phosphatase, ALP, expression)<sup>74, 137</sup> or 21 days (matrix mineralization)<sup>137</sup> (Figure 3.1). Adipocyte differentiation, on the other hand, could be tracked by the expression of the peroxisome proliferator-activated receptor  $\gamma$  (PPAR- $\gamma$ ) transcription factor (after 24 to 48 h of cell culture)<sup>143</sup> and by the presence of lipid droplets, typically assessed after one week of cell culture.<sup>134, 144</sup>

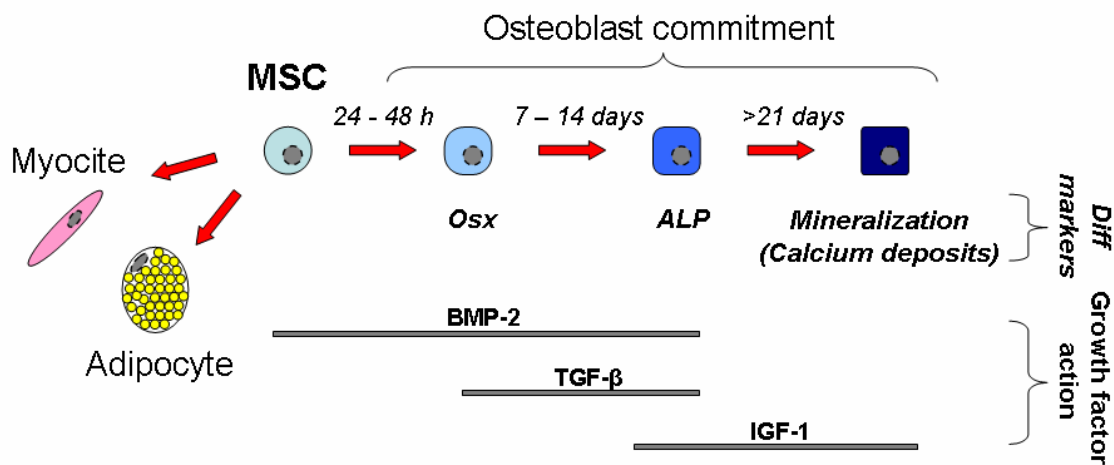


**Figure 3.1** MSC differentiation to osteoblasts can be tracked at several stages of the process, through the expression of characteristic differentiation markers. In the figure, the proposed action of some growth factors during this temporal differentiation pathway is also indicated. Abbreviations used are, BMP: Bone morphogenetic protein, TGF: Transforming growth factor, IGF: Insulin-like growth factor. Data obtained from cited reference.<sup>81</sup>

Before any cellular microarray work was performed, the primary MSCs used here were assessed in terms of their potential to differentiate to osteoblasts and adipocytes in conventional well-plate format cultures. For this purpose, confluent MSCs were cultured in wells of 24-wellplates for two weeks in medium containing standard differentiation inducing cocktails.<sup>74, 134</sup> The differentiation cocktail for osteoblast induction consisted of control medium (Advanced DMEM (GIBCO), 1% penicillin/streptomycin, 1% L-Glutamine and 10% FBS, subsequently called “FBS medium”) supplemented with 0.1  $\mu$ M dexamethasone, 50  $\mu$ g/mL L-ascorbate and 10mM  $\beta$ -glycerophosphate. The differentiation cocktail for adipocyte induction consisted of FBS medium supplemented with 0.1  $\mu$ M dexamethasone, 0.5 mM 3-isobutyl-1-methylxanthine and 10  $\mu$ g/mL insulin for the first 2 days, then the treated cells were maintained in FBS medium enriched with 10  $\mu$ g/mL insulin only.

When culturing cells in a microarray format, the use of a completely defined medium appears as a very important issue in order to avoid undesired signalling coming from medium containing FBS.<sup>70</sup> Therefore, the effect on osteoblast and adipocyte differentiation when MSCs were cultured in a completely defined medium was also assessed for standard cell cultures. A suitable serum replacement, ITS (abbreviation for insulin, transferrin and sodium selenite, the basic composition of this solution), was previously reported for studies of chondrocyte differentiation because FBS contains factors that block cell differentiation towards this fate.<sup>145, 146</sup> ITS consists of a completely defined serum substitute that prevents the adverse effects of unknown factors present in the culture medium which could bias MSC differentiation. In order to assess the effect

on cell differentiation when substituting FBS by ITS in the culture medium, FBS medium was replaced by “ITS medium”, composed of Advanced DMEM, 1% penicillin/streptomycin, 1% L-Glutamine and 1% ITS (composed by insulin, transferrin, sodium selenite, BSA and linoleic acid, acquired under the trade name “ITS+1 Liquid media supplement” from Sigma).

Osteoblast and adipocyte differentiation cocktails were tested using ITS medium. Therefore, to induce osteoblast differentiation the ITS medium was supplemented with 0.1 µM dexamethasone, 50µg/mL L-ascorbate and 10mM β-glycerophosphate. For adipocyte differentiation induction, ITS medium was supplemented with 0.1 µM dexamethasone, 0.5 mM 3-isobutyl-1-methylxanthine and 10 µg/mL insulin for the first 2 days, and then the treated cells were maintained in ITS medium enriched with 10 µg/mL insulin only.

### 3.2.3 Evaluation of cell differentiation

Induced MSC differentiation in wellplate cell cultures was assessed after 2 weeks of culture in differentiation inducing media. For this purpose, osteoblast differentiation was assayed by the determination of alkaline phosphatase (ALP) activity,<sup>81</sup> and adipocyte differentiation was assessed by fluorescence staining of lipid droplets.<sup>147, 148</sup> For ALP activity determination, cells were fixed in 10% formalin for 1 hour, then a solution of naphthol AS-MX phosphate (2 mL) and fast blue RR (1 capsule) in Milli-Q water (48 mL) was used to stain the cells according to the manufacturer instructions (Sigma Kit #85, Spain). Cells were incubated with this solution in the dark for 30 minutes and subsequently rinsed with water. The resulting blue, insoluble, granular dye deposits indicate sites of ALP activity. The stained cells were imaged using a bright field microscope.

For the detection of lipid droplets, the fixed cells were incubated with a Nile Red (diluted 1:1000, Sigma, Spain) and Hoechst (diluted 1:500) solution in PBS for 1h. The nile red dye is strongly fluorescent when it is in the presence of a hydrophobic environment and provides an excellent stain for the intracellular lipid droplets.<sup>148</sup> Dried samples were mounted in Mowiol and imaged using a fluorescence microscope.

### 3.2.4 Microarray fabrication

Cellular microarrays were fabricated on AD-Glass substrates (SuperAldehyde 2, Telechem, USA) by printing Fn spots in a microarray format as described in Chapter 2. Microarray printing was followed by passivation of the non-printed surface and cell seeding (Figure 3.2A). For the

production of cellular microarrays using MSCs, several parameters affecting the microarray configuration and cell survival were assayed and optimised (see below).

### **Protein deposition in a microarray format**

In Chapter 2, based on a qualitative and quantitative analysis of the spot morphology and the amount of protein immobilised, Fn spotted at 200 or 360 µg/mL appeared as the best concentrations to be further assayed. Taking this into account, together with budget considerations regarding the amount of protein used for microarray printing, Fn spotted at 200 µg/mL was chosen as the concentration to be used in the experiments presented in this chapter. Fn spotted at 40 and 100 µg/mL were also printed for comparison to further evaluate cell adhesion behaviour on these spot compositions.

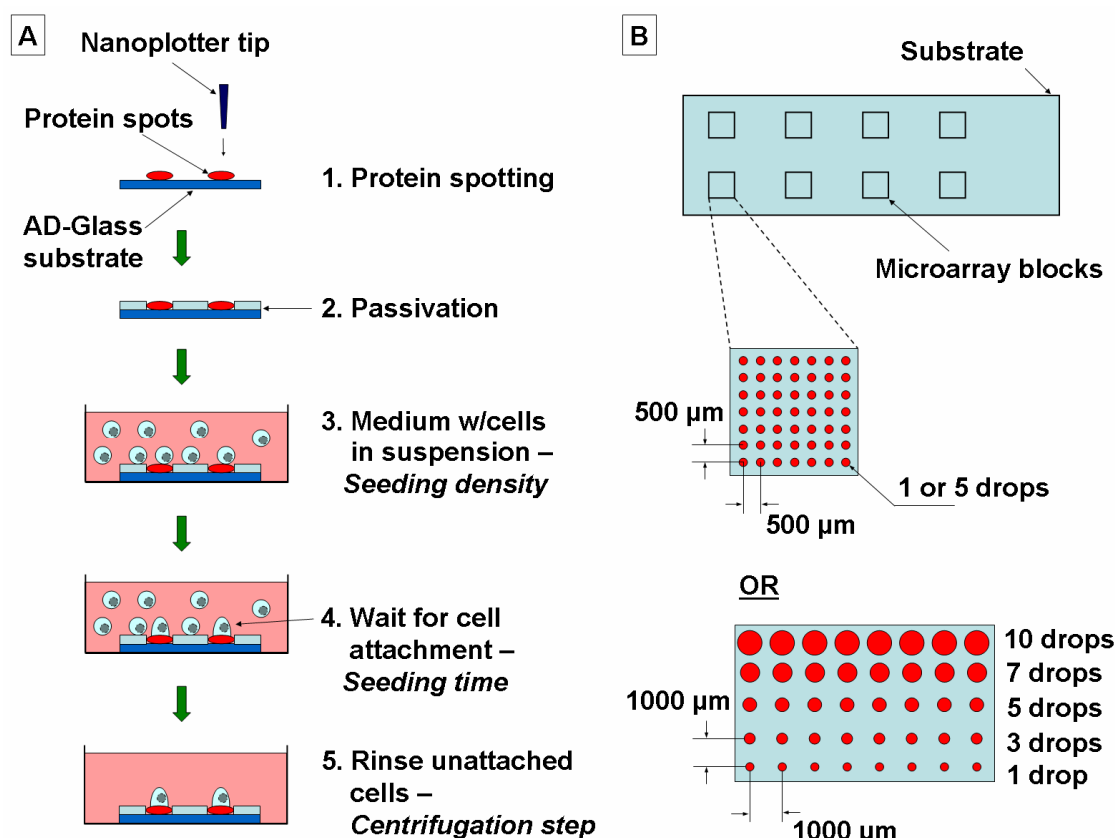


**Figure 3.2** Cellular microarray preparation. (A) Cellular microarray fabrication steps (indicated as 1 to 5 in the schematic). (B) Printed protein microarray layouts.

In cellular microarray reports found in the literature, spotting features in PBS with glycerol (0.1 to 20 %) has been a preferred trend,<sup>48, 50, 57</sup> aiming to improve protein immobilisation on the substrates in an active conformation by delaying or eliminating drying of the printed droplets. However, spotting proteins in PBS (without any additives) has also been reported in the literature, specially when robust proteins such as ECM proteins were printed.<sup>47, 49, 58</sup> In these

cases, the printed proteins were shown to retain its functionality, most usually by supporting cell adhesion and culture on the printed features. The present chapter involves cellular microarray fabrication using spots composed of Fn only, but was it conceived as an intermediary step towards the inclusion of a growth factor in the spot composition (which will be presented in the next chapter). Since data from Chapter 2 suggested that proteins other than ECM ones (e.g. streptavidin in the previous chapter) could be barely immobilised on spots printed with glycerol, both buffers continued to be assayed here to further evaluate cell adhesion and viability concerns.

Taking into account the previously exposed observations, for the studies presented in this chapter, protein solutions of Fn in PBS with and without glycerol (2% v/v) were prepared at different concentrations: 40, 100 and 200 µg/mL; subsequently called Fn40, Fn100 and Fn200. The procedure followed for protein microarray fabrication was similar to the one described in Chapter 2, Section 2.2.4. A robotic non-contact piezoelectric plotter (Nano-Plotter, GeSiM GmbH, Germany) was used to dispense the protein solutions onto the activated glass slides (step 1 in Figure 3.2A) in a square microarray format (8 blocks of 7x7 or 5x8 spots, Figure 3.2B) and the borders of each microarray block were marked with a diamond pen. Spotting of the solutions was performed at room temperature. Different spot sizes were produced by overprinting single and multiple drops (1, 3, 5, 7 and 10 consecutive drops, 0.4 nL in volume each, Figure 3.2B). The distance between spots was set to 1 mm to avoid spot overlapping due to the increasing spot diameter. The printed slides were transferred to a light-tight sealed box and kept at 4 °C for 24 hours to ensure a proper protein-surface interaction.

### ***Surface passivation***

A flexiPERM gasket (Greiner Bio-One GmbH, Germany), previously immersed for 20 minutes in 70% ethanol and exposed to UV light for 15 minutes for sterilisation purposes, was placed on top of the printed slides and aligned with the microarray blocks to create 8 individual wells per slide (Figure 3.3). This allowed testing several parameters in the same slide in independent experiments.

In order to passivate the non-printed surface area, two passivation strategies were tested (step 2 in Figure 3.2A). Either a 2% BSA solution in PBS or, alternatively, an amino-PEG 6000 (O,O'-Bis(2-aminoethyl)polyethylene glycol M.W. = 6000, obtained from Sigma) solution in PBS (38 mg/mL) were added to the wells created by the FlexiPERM gasket. These solutions

were incubated for 90 minutes. Afterwards, the blocking solutions were removed, the slides were washed twice in PBS and cells were immediately seeded as described next.

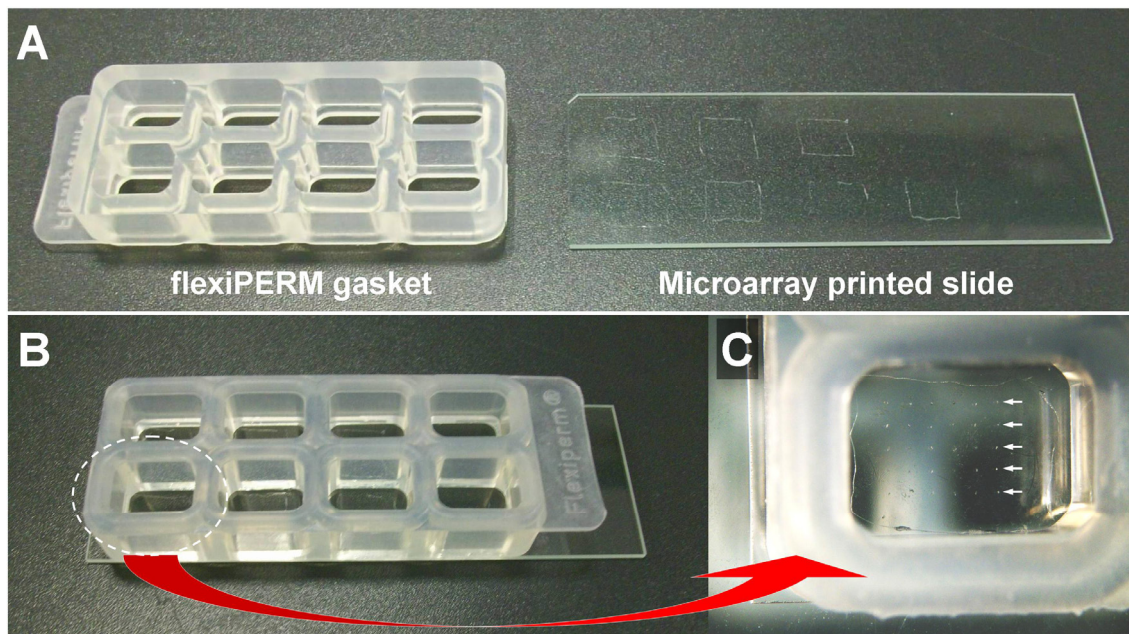


**Figure 3.3** FlexiPERM gasket. **A.** Detail of the flexiPERM gasket used and the printed microarray slide before mounting. **B.** FlexiPERM mounted on top of the printed slide to create 8 individual chambers for cell culture. **C.** Zoom in of one of the chambers. Position of printed protein spot rows is indicated by the white arrows.

#### ***Cell culture on the protein microarrays***

Each flexiPERM well was seeded with cells at densities ranging from 5,500 cells/cm<sup>2</sup> to 110,000 cells/cm<sup>2</sup> (step 3 in Figure 3.2A) and cultured over different seeding times ranging from 5 to 45 minutes (step 4 in Figure 3.2A). After the seeding time was over, the flexiPERM was removed and the slide was placed into a Falcon tube filled with pre warmed ITS medium. Then, it was centrifuged at 1000 rpm for 5 minutes to remove unbound cells between spots (step 5 in Figure 3.2A). Cellular microarrays were further cultured in Petri dishes for periods of time ranging from 1 to 8 days. Cell culture medium, either FBS or ITS medium, was replaced every 2 or 3 days. No differentiation cocktails were assayed with the cellular microarrays.

#### **3.2.5 Microarray characterisation**

Printed protein microarrays were characterised immediately after overnight incubation to ensure protein interaction with the surface. In contrast with the spot characterisation presented in the previous chapter, which involved the detection of Fn directly labelled using a fluorescent dye, in this chapter the indirect immunostaining of the immobilised Fn was chosen for the evaluation of spot morphology and protein distribution. For the Fn immunostaining, the slides

were passivated with BSA (1% in PBS) for 20 min. Afterwards, the slide was incubated with the primary antibody (rabbit anti-fibronectin diluted 1:400, Sigma), followed by incubation with the secondary antibody (goat anti-rabbit Alexa Fluor 568 diluted 1:100, Molecular Probes, USA). Dried samples were either imaged directly using a fluorescence scanner device (GenePix 4000B, Molecular Devices Corp., USA) or mounted in Mowiol plus anti-fade and imaged using a fluorescence microscope, as indicated in the caption of each figure. More details about the immunostaining technique are presented in Appendix B.III.

For cellular microarrays, microarray layout and cell morphology were examined by bright field microscopy during cell culture. Cellular microarrays were also characterised by immunostaining of Fn and cell nuclei immediately after fabrication (at day 0). For this purpose cells were fixed (3% paraformaldehyde), permeabilised for 10 minutes in Triton 100X (0,05% solution in PBS-Glycine) and the slides were blocked with BSA (1% in PBS-Glycine) for 20 min. Afterwards, the slide was incubated with primary antibodies (rabbit anti-fibronectin diluted 1:400, Sigma), followed by incubation with secondary antibodies (goat anti-rabbit Alexa Fluor 568 diluted 1:100, Molecular Probes, USA) and Hoechst (diluted 1:500) for nuclei staining. Dried samples were mounted in Mowiol plus anti-fade and imaged using a fluorescence microscope.

### ***Cell viability***

At days 0 and 8, viability of cells attached on the spots was evaluated by using a cell Viability/Cytotoxicity Assay Kit For Animal Live & Dead Cells (Biotium Inc., USA). This kit is suitable to be applied to substrate-attached cells, and provides a two-colour fluorescence staining, which allows identifying live and dead cells using two probes (calcein AM and ethidium homodimer-III (EthD-III)) that measure recognised parameters of cell viability. The principle of the cell viability measure resides in the intracellular esterase activity of live cells, which allows the conversion of the non-fluorescent cell-permeant Calcein AM to the intense fluorescent calcein. This converted dye is well retained within live cells, producing an intense uniform green fluorescence (with excitation peak at ~495 nm and emission peak at ~550 nm). On the other hand, the measurement principle of EthD-III is related to plasma membrane integrity. EthD-III enters cells with damaged membranes and binds to nucleic acids, undergoing with this event a 40-fold fluorescence increase, which produces a bright red fluorescence in dead cells (with excitation peak at ~530 nm and emission peak at ~635 nm). EthD-III is excluded by the intact plasma membrane of live cells. The protocol followed for applying the viability kit

consisted in incubating the cellular microarrays under culture conditions (i.e. in a humid incubator at 37 °C and 5% CO<sub>2</sub>) for 30 minutes in a 4 µM Eth-D and 2 µM calcein AM solution prepared in PBS. Afterwards, cells were imaged using a fluorescence microscope.

### ***Cell differentiation evaluation***

Spontaneous MSC differentiation in the cellular microarrays was assessed at day 8 after culture in ITS medium, without any additional differentiation cocktail. For this purpose, cellular microarrays were fixed and stained for ALP and lipid droplets following the same procedures explained in section 3.3.2 of this chapter. Additionally after ALP staining, cells were further incubated with Hoechst (diluted 1:500) for nuclei fluorescence staining.

### **3.2.6 Statistics**

All measurements of cell survival were performed on duplicate samples of two separate experiments (n=4) and the data presented consist of representative results. Cell counting and spot size measurements were completed with the aid of Photoshop and GenePix Pro 6.0 softwares. Parametric one-way ANOVA tests were performed on the statistical analysis of variables plotted. All graphical data is reported as mean +/- standard deviation. Significance levels were set at p<0.05.

## **3.3 Results**

### **3.3.1 Protein deposition in a microarray format**

Prior to cell culture, the fabricated protein microarrays were characterised by the indirect immunostaining of Fn. The image presented in Figure 3.4A shows a representative fluorescence image (obtained with the scanner device) of the immunostained arrays printed with all Fn concentrations, buffers and spot sizes assayed. In this case, the fluorescence of the spot was shown in green due to an internal preset of the scanner device (the fluorescence signal for the 555 nm channel, which successfully excited and detected the Alexa Fluor 568 labelled antibodies used, was shown in green). Figure 3.4B shows detailed images for 5 drop spots obtained with the fluorescence microscope.

As expected from the results presented in Chapter 2, the Fn200 spots were the features that yielded the highest and most homogeneous fluorescence intensity. In the results presented here, it was qualitatively observed that the Fn density immobilised on the spots increased with the

concentration of the spotted Fn solution for both printing buffers assayed. This is seen in Figure 3.4 as an increase in the fluorescence signal for spots printed using Fn40, Fn100 and Fn200.

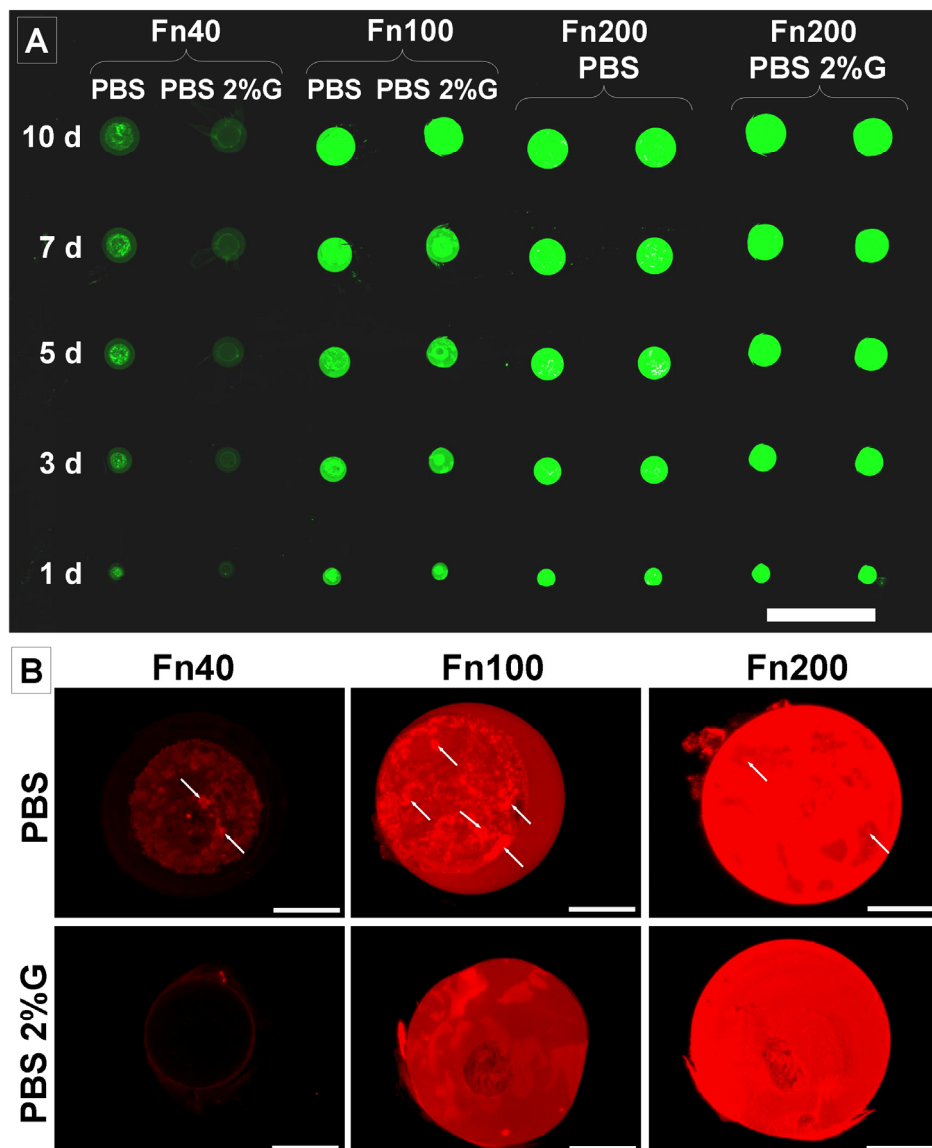


**Figure 3.4** Immunofluorescence images of the microarray layout and details of the different spot compositions. **A.** Scanner image of the immunofluorescence stained slides composed of Fn spots (in green, preselected colour of the scanner for the signal obtained from the 555 nm channel) printed at 40, 100 and 200 µg/mL in PBS w/wo glycerol and in 1 to 10 drops, as indicated in the image. 1000 µm scale bar is shown in white. **B.** Detail of the immunofluorescence images (obtained with the fluorescence microscope) for 5 drop spots printed from Fn40, Fn100 or Fn200 solutions in PBS or in PBS with 2% glycerol, as indicated in the figure. All images were taken using the same exposure time. White arrows suggest sites of high amounts of Fn adsorption. 100 µm scale bars are shown in white.

In the previous chapter, Fn spots printed with glycerol retained immobilised less than 50 % of the Fn mass in comparison with equivalent spots printed in PBS only. In the experiments presented here, spots printed with 2% glycerol showed slightly lower fluorescence intensity when compared to spots printed in PBS only (Figure 3.4). However, since the images presented

here were obtained from an indirect immunofluorescence assay, fluorescence intensity between spots could not be quantitatively compared due to the signal amplification produced by this type of assay (refer to Appendix B.III for further details on the indirect immunofluorescence staining technique).

Regarding the homogeneity of the Fn distribution on the spots, two-phase intensity regions, previously discussed in Chapter 2, were observed in Fn40 and Fn100 spots (Figure 3.4A). The inner, high intensity region was observed to increase as the Fn concentration increased until, for Fn200, a mostly homogeneous staining was observed (Figure 3.4A). A more detailed analysis was made based on the images obtained with the fluorescence microscope (Figure 3.4B). These images were captured at a higher resolution ( $0.3376\text{ }\mu\text{m} / \text{pixel}$ ) than those obtained with the scanner ( $5\text{ }\mu\text{m} / \text{pixel}$ ). The spot images obtained at a higher resolution evidenced that the protein coating in the centre of the Fn40 and Fn100 spots was actually composed of smaller features of high fluorescence intensity (Figure 3.4B, white arrows). These irregularities, which were most importantly observed in the spots printed in PBS only, could account for adsorbed Fn aggregates resulting from the drying of the printing buffer, as previously discussed in Chapter 2. Regarding the Fn200 spots, a more homogeneous Fn distribution was noted for the spots that were printed in PBS with 2% glycerol (Figure 3.4B). Fn200 spots printed in PBS showed some irregularities in the fluorescence intensity within the spot area (white arrows in Figure 3.4B). Based on these findings, the lower intensity obtained from the spots printed in PBS with 2% glycerol was proposed to account mostly for covalently immobilised Fn, while the higher and more irregular fluorescence intensity regions observed in spots printed in PBS only would account for Fn aggregates adsorbed on top of an underlying, covalently immobilised, Fn layer. These observations did not invalidate the conclusions obtained in Chapter 2, since both the adsorbed Fn as well as the covalently immobilised Fn actually accounted for protein mass immobilised. However, in terms of cell adhesion to the spots, the strength of the interaction between the immobilised Fn and the substrate surface could play an additional role. This effect will be presented in the following section.

Figure 3.5 shows the spot sizes obtained for the printing buffers assayed as the number of drops increased. For each printing buffer, data obtained for each number of drops were significantly different at the  $p<0.05$  level (One-way ANOVA test), therefore corroborating that increasing the number of drops spotted in each microarray position was an effective approach to increase the spot size, with diameters in the range 150 to 350  $\mu\text{m}$ . These features would allow

for the culture of small numbers of cells (10s to 100s of cells, depending on the cell type) in isolated spots.<sup>53, 57</sup>

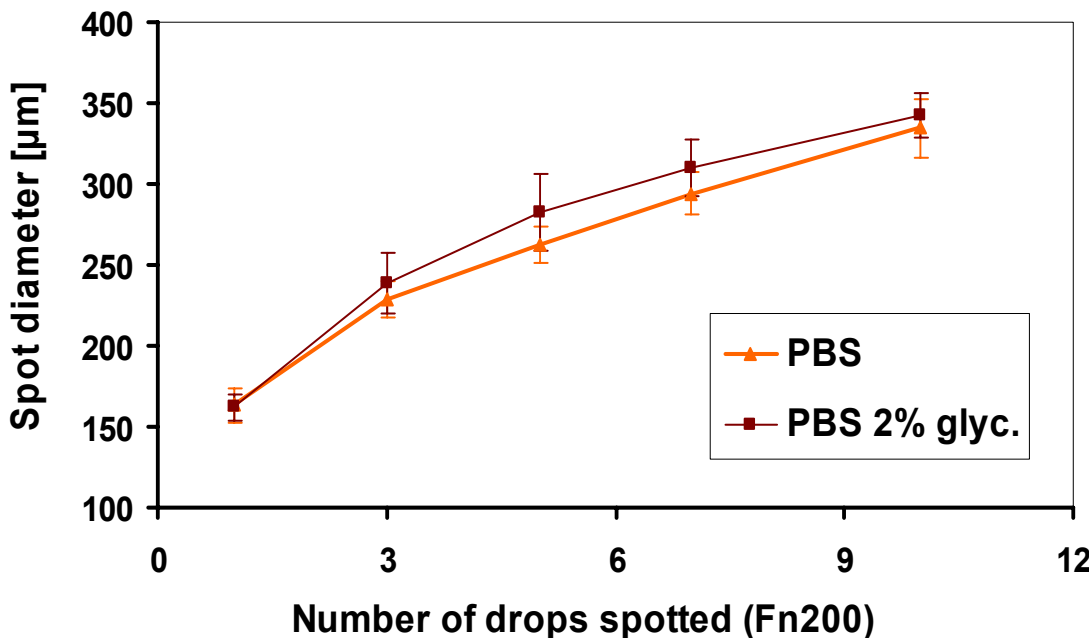


**Figure 3.5** Relationship between the number of printed drops and the spot area for Fn200 printed in different buffers. Each data point represents the average and standard deviation calculated from 16 spots. For each buffer, the spot sizes obtained by overprinting increasing number of drops were significantly different between them ( $p<0.05$ , One-way ANOVA test). Lines are included as a guide only.

As seen in the previous chapter, the inclusion of glycerol in the protein solution resulted in a slight enlargement of the printed spots. In this case, despite the diameter increase was found for spots larger than 1 drop, these differences were significantly different only for 5 and 7 drops, when statistically evaluated (One-Way Anova test). This behaviour was in part due to a smearing effect observed on some of the larger glycerol containing spots (Figure 3.6), resulting from the addition of the BSA solution used for passivation of the non-printed surface, following the standard immunostaining protocol. This effect has been previously noted by other researchers when using chemically activated substrates.<sup>88</sup> In contrast with the passivation approach presented in the previous chapter, which included passivation of the whole slide using larger volumes of the BSA passivation solution (10 mL added to Petri dishes) and agitation during the passivation step, the smearing behaviour observed in this case was related to the smaller volume of the wells created by the FlexiPERM (400 μL of passivation solution were added to each well) as well as the lack of agitation during this step. Therefore, the non-reacted Fn from glycerol spots was more difficult to remove and reacted in the area surrounding the spots, producing an increase in area which was detected by the scanner device during the analysis of the features. Agitation of the slides during passivation was not possible in this case

because the adhered FlexiPERM would detach from the slide, therefore extreme care was taken to try to reduce this smearing effect to a minimum.

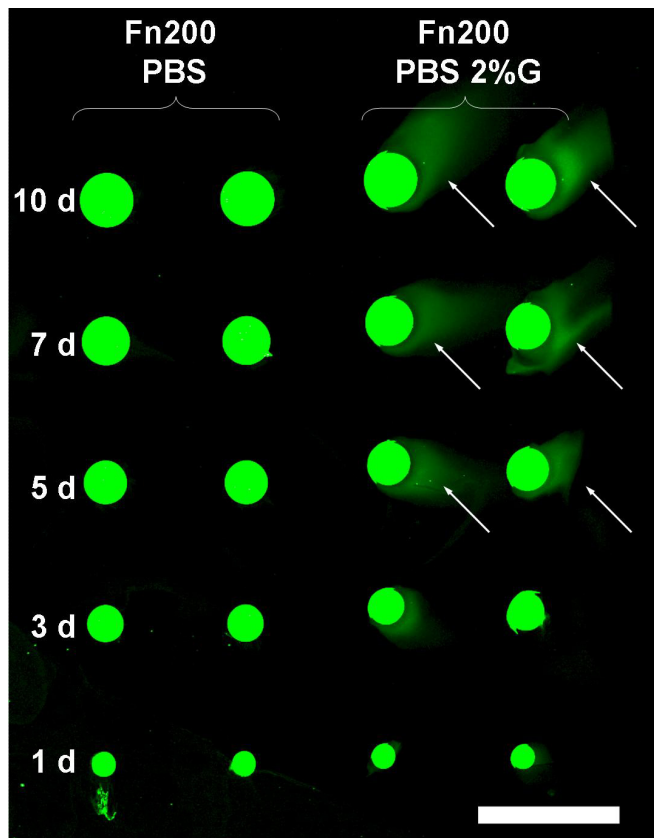


**Figure 3.6** Smearing effect in glycerol containing spots (indicated by white arrows). Scanner image of the immuno fluorescence stained slides composed of Fn spots (in green, preselected colour of the scanner signal for the 555 nm channel) printed at 200 µg/mL in PBS w/wo glycerol and in 1 to 10 drops, as indicated in the image. The brightness and contrast of the image have been forced to visualise the smearing effect. This effect was more important for larger spots. 1000 µm scale bar is shown in white.

### 3.3.2 Cell culture in the microarrays

#### *Surface passivation*

The efficiency of 2% BSA and amino-PEG 6000 solutions as passivation agents was tested for a cell seeding time of 15 minutes and two cell seeding densities (11,000 and 110,000 cells/cm<sup>2</sup>). For this purpose cells were cultured on a microarray formed using Fn200.

It was found that BSA efficiently blocked cell adhesion outside the printed area for both cell seeding densities assayed. Figure 3.7 (top) shows that cell adhesion was strongly localised on the 16 Fn spots presented. Also, for 110,000 cells/cm<sup>2</sup> seeding density it was observed that the Fn spots were crowded with cells, while for the lowest cell seeding density cells attached distributed on the spot area. These observations will be further analysed in the following subsections.

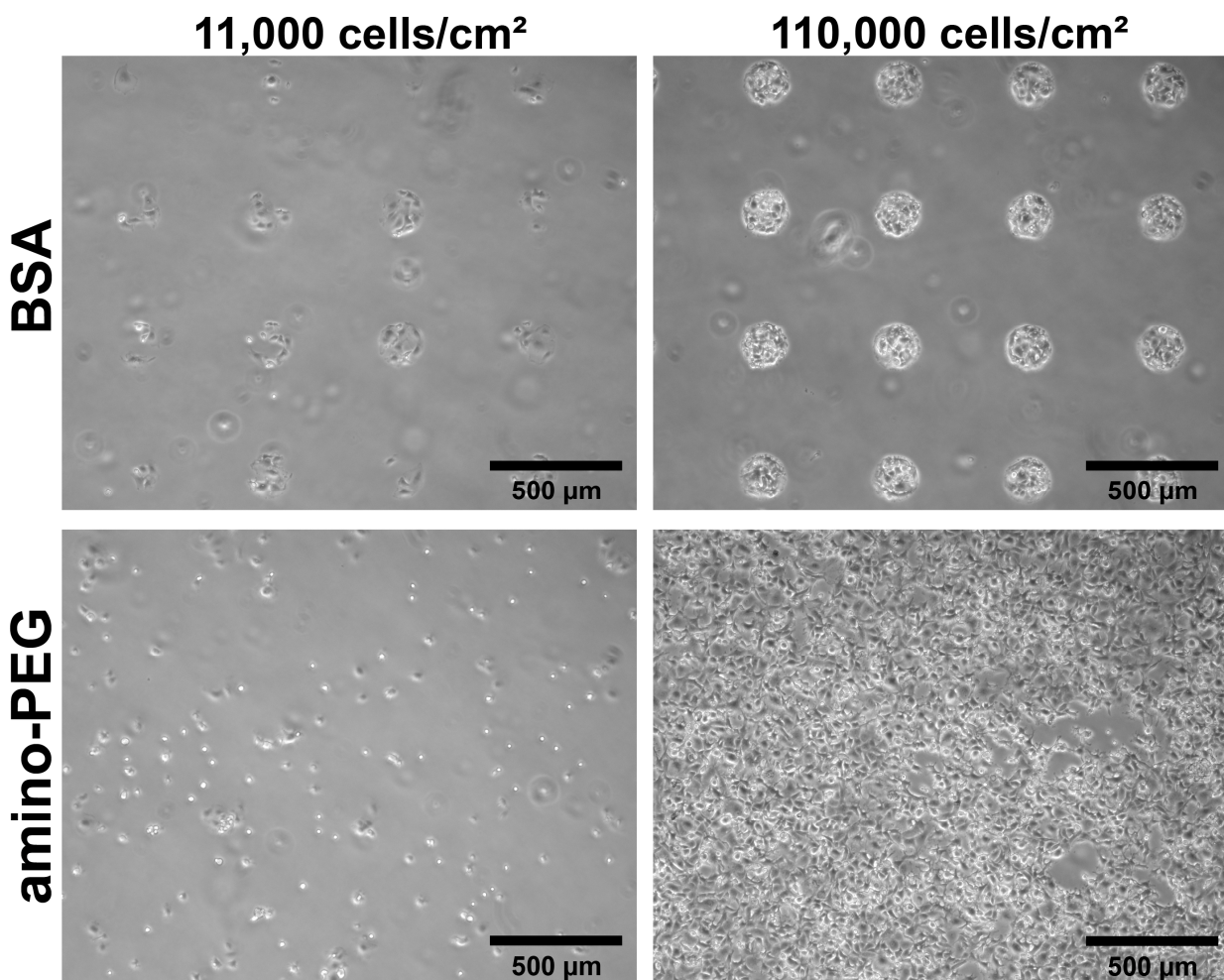


**Figure 3.7** Passivation strategies assayed. Cellular microarray formed using BSA (top images) or amino-PEG 6000 (bottom images) as passivation agents. Printed spots are 1 drop of Fn200 in PBS with 2% glycerol, the cell seeding time was 15 minutes. Two cell seeding densities were assayed: 11,000 (left) and 110,000 cells/cm<sup>2</sup> (right). Amino-PEG 6000 failed to appropriately passivate the substrate surface.

BSA has been widely reported as passivation agent used to prevent protein adsorption in protein microarray applications.<sup>28, 35</sup> Passivation of the non-printed areas using a BSA solution has been also reported for cellular microarrays fabricated on AD-Glass.<sup>48</sup> In the results presented here, the BSA served to quench the unreacted aldehyde groups on the slide and also formed a layer that reduced non-specific binding of other proteins, therefore also reducing cell attachment on the BSA-passivated areas.

The use of PEG coatings has also been widely reported in the literature as an excellent non-fouling and cell repelling agent.<sup>89</sup> However, in the experiments presented here, the use of amino-PEG 6000 did not prevent cell colonization outside the spots (Figure 3.7, bottom). In particular, cell attachment outside the printed area was extremely high for the highest cell seeding density presented in the figure.

The ability of PEG coatings to inhibit protein adsorption and, therefore, to avoid cell attachment on the coated areas, is not fully understood yet, but it is believed that the PEG molecular weight and the polymer chain architecture are involved in the efficiency of this process.<sup>149</sup> These parameters, together with the approach followed for PEG anchoring (adsorption or covalent attachment), control the PEG grafting density on the surface. It has been reported that the final PEG density on the surface is the most important factor for suppression of protein adsorption.<sup>149, 150</sup> In the case presented here, individual PEG molecules with amino groups at their ends were used to block the non-spotted surface. In contrast, other researchers have reported a better PEG blocking efficiency when the PEG molecules are deposited and polymerised to form a denser coating with a high surface coverage on a glass surface.<sup>90, 91, 149</sup> However, for the cellular microarray fabrication approach presented here, which involved the use of a chemically activated substrate for protein immobilisation, the use of individual PEG molecules was a requirement, since the polymerisation of a PEG layer on top of the chosen substrate once the protein microarrays were printed appeared as an extremely difficult task. This impediment resulted from the conditions needed for PEG polymerisation and stable layer attachment to the substrate, which impose the use of UV radiation and specific surface chemistries different than the one presented here.<sup>90</sup>

Besides the passivation agent used, the washing step that follows had to be customized in such a way that it removed many of the cells attached to the passivated area, while leaving cells attached to the protein spots. This prevented cells adhered to the passivated area from corrupting the microarray layout.

Notable spreading in cells attached on the spotted Fn features in contrast with little or no spreading in cells attached on the passivated area is highly desired to selectively eliminate cells weakly attached (i.e. poorly spread) during the washing step. For the same purpose, homogeneous cell spreading within the spot premises is highly desired when cells are initially seeded in cellular microarrays, in order to obtain a uniform cell distribution in the spots after the washing step.

Centrifugation as a method to enhance cell seeding has been previously reported for cellular microarray fabrication.<sup>151</sup> Here, an adapted centrifugation strategy was used to remove loosely attached cells, allowing to standardize the washing step. The schematic in Figure 3.8 shows the proposed effect of the centrifugation step on cells attached to Fn200 spots (in brown) and passivated areas (light blue), which showed differential cell spreading when incubated during the same seeding time (Figure 3.8A and B). After the seeding time was over, the slide was

placed in a Falcon tube filled with preheated ITS medium (Figure 3.8C) and centrifuged (Figure 3.8D). Under these conditions, the centrifuge force removed loosely attached cells (on passivated areas) while better spread cells (Fn200 spots) remained on the spots (Figure 3.8E).

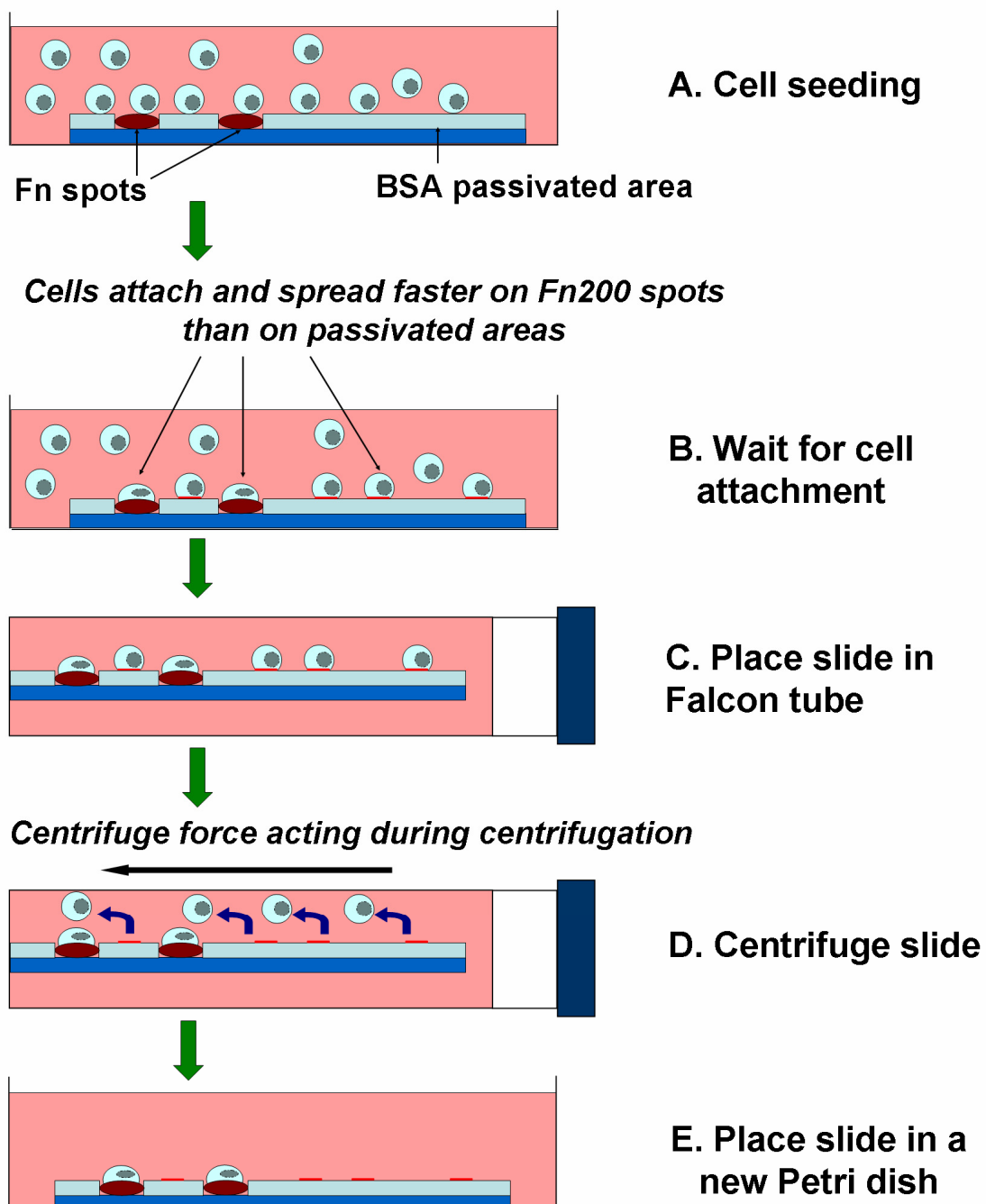


**Figure 3.8** Schematic showing the effect of the centrifugation step on cells attached to Fn spots (in brown) and passivated areas (light blue), which showed differential cell spreading. Cells were seeded (A) and allowed to attach for some time (B). Cells spread faster on Fn spots. Afterwards the slide was placed in a Falcon tube filled with preheated ITS medium (C) and centrifuged (D). The centrifuge force removed loosely attached cells (on passivated areas) while did not affect better spread cells (Fn spots, step E). After centrifugation, the slide was placed again in a Petri dish and further incubated for the desired periods of time.

This method was found to be extremely effective and did not damage cells attached in the spots, as shown in Figure 3.9, which remained viable after this procedure.

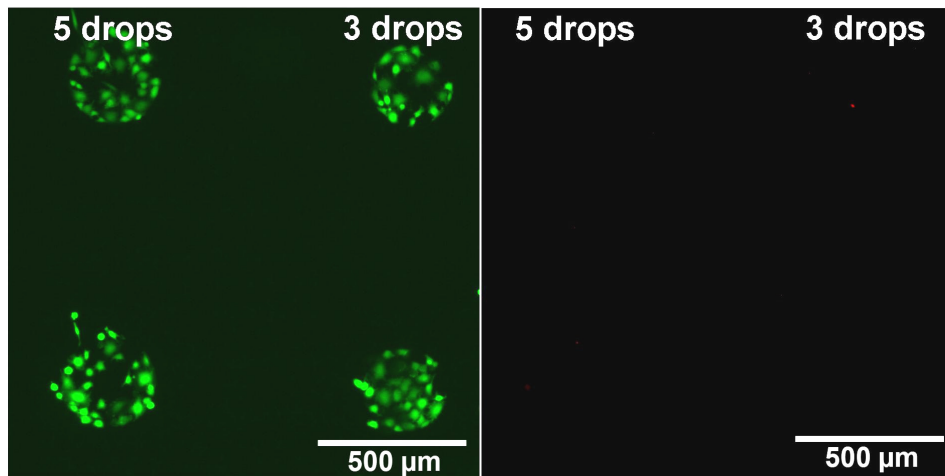


**Figure 3.9** Cell viability on the microarrays at day 0, after centrifugation of the slide. Fluorescence images of live (stained green, left image) and dead (stained red, right image) cells. The images presented are for 3 and 5 drop spots of Fn200 in PBS with 2% glycerol, 110,000 cells/cm<sup>2</sup> seeding density and 15 minutes seeding time. Cell viability was higher than 99% at day 0 for all spot conditions and cell seeding densities assayed.

Based on the results presented, **BSA** as passivation agent and microarray **centrifugation after cell seeding** were chosen for the following experiments.

#### *Effects of the Fn concentration spotted*

Fn200 and Fn360 were suggested in the previous chapter as the best option for further analysis of the fabrication of cellular microarrays. When cellular microarrays were built on Fn spots printed from 40, 100 and 200 µg/mL Fn solutions (w/wo glycerol, using 11,000 cells/cm<sup>2</sup> seeding density and 15 minutes seeding time), it was observed that after the centrifugation step few to none cells remained in the Fn40 (printed w/wo glycerol) and Fn100 (printed in PBS) spots (Figure 3.10). Spots printed in PBS retained less cells attached on them, probably as a result of the non-uniform protein coating, as noted in the previous section. On the other hand, Fn200 spots (and Fn100 to a less extend) printed in PBS 2% glycerol showed a more uniform cell spreading on the spots after the centrifugation step (Figure 3.10), probably due to the more uniform protein density. This suggested that the cells attached better during the relatively short seeding time on more uniformly coated Fn surfaces.

A general trend extracted from these experiments was that as the Fn concentration spotted increased, more cells remained attached on the spots. These results could be accounted by a combination of the amount of Fn mass immobilised and the type of immobilisation (i.e.

adsorption or covalent immobilisation), the Fn distribution within the spots and the effect of the centrifugation step on the recently attached cells. In this context, larger amounts of Fn immobilised allowed for a larger number of cells attached on the spots and a uniformly coated, covalently bound, Fn spot favoured a more uniform and stable cell spreading. Ultimately, better spread cells would be the ones that support the effect of the centrifugation force acting during the centrifugation step (as illustrated in Figure 3.8), and therefore would remain attached on the spots after this step.

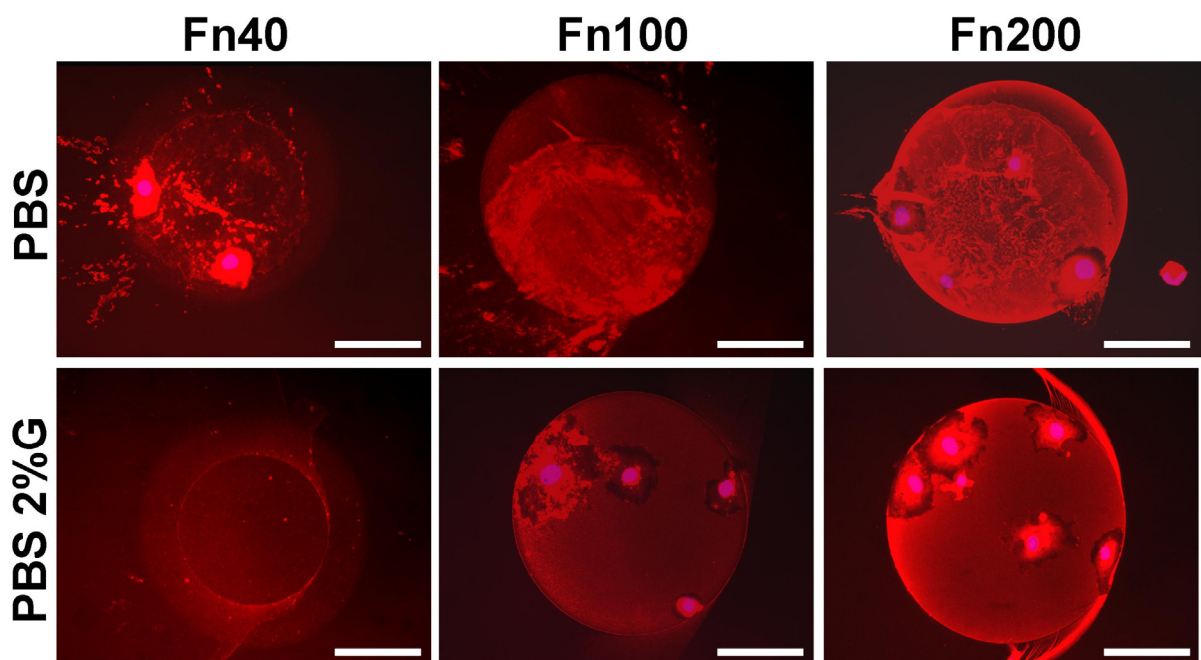


**Figure 3.10** Composed fluorescence microscopy images showing cell attachment (cell nuclei stained in blue) to Fn spots (red immunostaining) printed at 40, 100 and 200 µg/mL in PBS w/w 2% glycerol (5 drop spot size). Images taken at day 0 after cell seeding at 11,000 cells/cm<sup>2</sup> (15 minutes cell seeding time). Cell attachment was best for Fn200 spots, and cell spreading was more uniform when glycerol was included in the spot composition. 100 µm scale bars are shown in white.

Spotting of Fn at 100, 200 and 500 µg/mL have been previously reported by other researchers as the optimum values to fabricate cellular microarrays on a self-assembled monolayer build on gold (allowing covalent protein immobilisation)<sup>54</sup>, nitrocellulose<sup>53</sup> and polyacrylamide substrates,<sup>50</sup> respectively. On the other hand, a broad range study of the Fn concentrations (21 to 333 µg/mL) spotted using a non-contact printing device similar as the one employed here, yielded that concentrations higher than 84 µg/mL were needed for the successful cell attachment and culture of the non-hematopoietic fraction of human umbilical cord blood cells in microarrays printed on PEG pre-coated slides.<sup>57</sup> The variations in the concentration of the Fn solution spotted reported in the literature can be attributed to the printing protocol (i.e. the

device used for spotting proteins and the printing buffer chosen) as well as the type of substrate and cells used for cellular microarray fabrication.

The data presented here supported the choice of **Fn200** for further cellular microarray fabrication with MSCs under the chosen set-up.

#### ***Effects of cell seeding time and density on the initial attachment of cells on the spots***

The cell seeding density plays an important role in cellular microarray formation and, together with the cell seeding time and once the Fn concentration has been fixed, defines the number of cells attached per spot. In the cellular microarray literature,<sup>48, 53, 57, 60</sup> the cell seeding density was found to vary in the range from 7500 cells/cm<sup>2</sup> to more than 40,000 cells/cm<sup>2</sup>. Usually, high cell densities were used to produce almost confluent cell spots.

Cellular microarrays were analysed with respect to the number of cells attached for three different cell seeding times and two cell seeding densities. For this purpose, each of these parameters was changed at a time, i.e. cells were seeded at 11,000 or 110,000 cells/cm<sup>2</sup> in separate wells of the FlexiPERM, and allowed to attach for 3 different cell seeding times (5, 15 and 45 minutes, one for each well). Representative images of the cellular microarray spots obtained are presented in Figure 3.11.

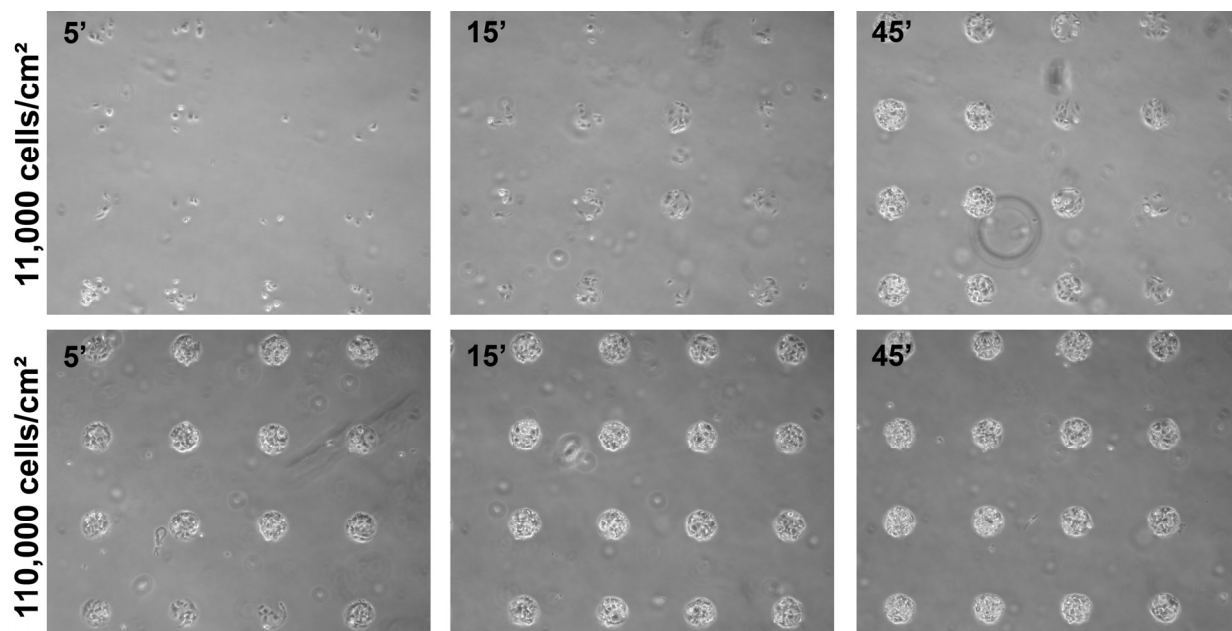


**Figure 3.11** Effect of cell seeding times at day 0. Bright field microscopy images of the cellular microarray formed for different cell seeding times (5, 15 and 45 min.) and 11,000 or 110,000 cells/cm<sup>2</sup> seeding density. As the seeding time and density increased, the number of cells attached per spot did also increase, yielding spots crowded with cells for the highest seeding density. The images presented are for 1 drop spot of Fn200 in PBS with 2% glycerol. 500 µm scale bar is shown in black.

When cells were seeded at the lowest density (i.e. 11,000 cells/cm<sup>2</sup>), the number of cells adhered to the spots was largely dependant of the seeding times:  $5 \pm 3$  cells/ spot for 5',  $7 \pm 3$  cells/ spot for 15' and  $20 \pm 7$  cells/ spot for 45' were attached on the microarrays, Figure 3.12. In particular for the 45' seeding time, it was noticed that the Fn spots were crowded with cells, and apparently some cells were beginning to attach on top of other cells (as indicated by a round, non-spread morphology), which were themselves directly immobilised on the spot. This effect is indicated by the black arrows for this seeding condition in Figure 3.12. From the images presented in Figure 3.11, it can be observed that using a higher cell density (i.e. 110,000 cells/cm<sup>2</sup>) resulted in an important increase in the number of cells attached on the spots, when compared to the lowest seeding density and equal seeding times (Figure 3.12). Increasing the cell seeding time did also produce an increase in the number of cells attached per spot (with more than 20 cells/ spot, as indicated in Figure 3.12). However, the attachment of cells on top of other cells was extremely high and it became more important as the seeding time increased (indicated by the black arrows in Figure 3.12). This effect was extremely important for the 45' seeding time. For this condition, cells on the spots could not be accurately quantified due to the evident overlapping of cell layers.

Crowded cell spots, sometimes with more than one layer of cells attached on them, were not preferred in this study since cell spreading was limited by the spot dimension and the culture medium assayed (ITS medium), as observed after 2 days of cell culture (Figure 3.13). On the other hand, using a lower cell seeding density (11,000 cells/cm<sup>2</sup>) and lower cell seeding times (5 or 15 minutes) allowed for a better cell spreading on the spots. As it was previously noted, a 45' seeding time did produce overpopulated cell spots, with cells attached on top of other cells. However, a seeding time of 15 minutes yielded a slightly larger number of cells per spot.

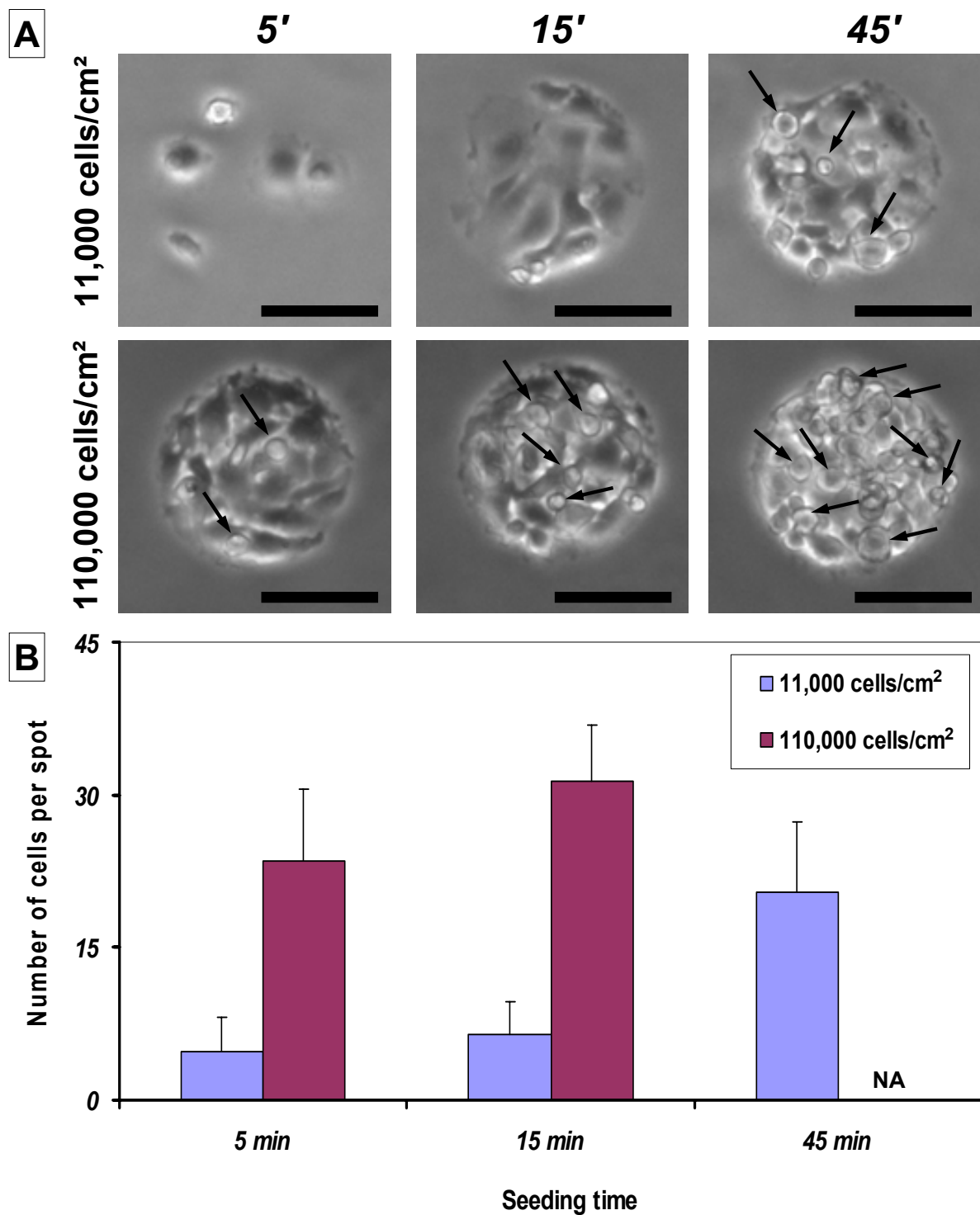


**Figure 3.12** The number of cells attached on the spots increased with increasing cell seeding times. **A.** Zoom in of representative spots for the 2 seeding densities and the 3 seeding times independently assayed, as indicated in the image. Note that as the seeding time increased, more cells attached on the spots until, for a 45' seeding time, cell-cell attachment took place (indicated by the black arrows). The images presented are for 1 drop spot of Fn200 in PBS with 2% glycerol. 100  $\mu$ m scale bars are shown in black. **B.** Number of cells attached on the spots for the cell seeding times and densities assayed. Data obtained from Figure 3.11. NA: Not available.

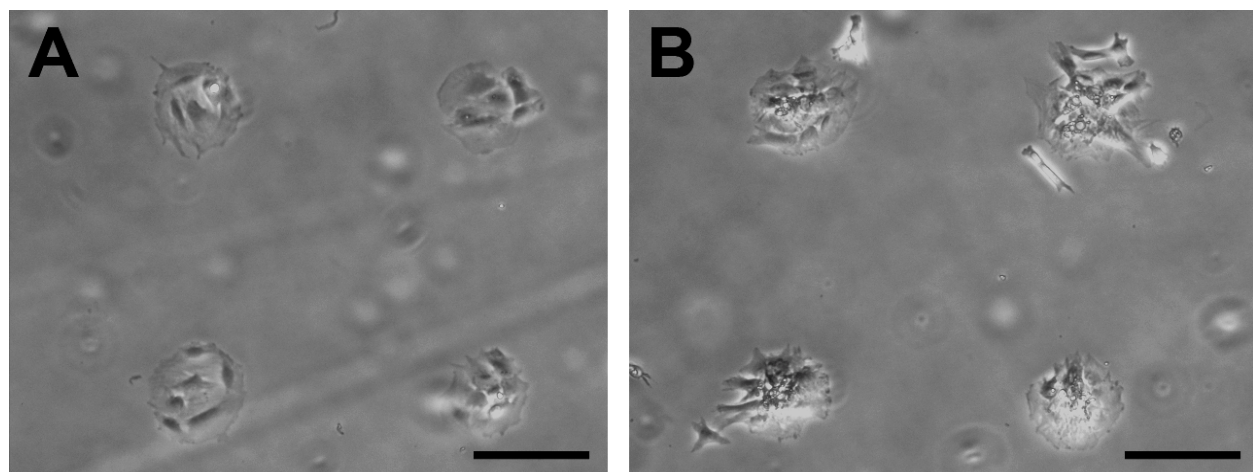


**Figure 3.13** Cell seeding density effect for (A) 11,000 and (B) 110,000 cells/cm<sup>2</sup> (15 minutes cell seeding time). Crowded cell spots in image B showed limited cell spreading after 2 days of cell culture in ITS medium. The images presented are for 1 drop spot of Fn200 in PBS with 2% glycerol. 200 µm scale bars are shown in black.

The results presented here allowed choosing a cell seeding time of **15 minutes** and suggested a **11,000 cells/cm<sup>2</sup>** seeding density to analyse in more detail the rest of parameters affecting cellular microarray formation and culture. However, further insights regarding the effect of the cell seeding density on cell survival will be provided at the end of this section.

### ***Effects of cell culture medium***

A key point of concern when analysing cell response to surface immobilised factors is to avoid undesired signalling from animal serum. It is well known that Foetal Bovine Serum (FBS) contains ECM proteins, growth factors and hormones in unknown and variable quantities.<sup>152</sup> Subtle variations are inevitable in FBS, and other serums, obtained from different sources and at different time. For these reasons, its omission is highly desirable when dealing with cellular microarrays. After formation of the cellular microarrays, two cell culture media were evaluated in their performance for cell culture while keeping the microarray layout over time: FBS medium and ITS medium.

The results obtained showed that FBS medium had undesired effects from day 1, since cells proliferated, exceeding the printed spot premises and invading the passivated area. After 2 days, the cellular microarray layout was lost (Figure 3.14). It has been previously reported that BSA can activate cell adhesion proteins such as Fn by the modulation of its conformation,<sup>119</sup> thus increasing its biological activity (i.e. producing an enhancement of cell attachment) and promoting cell adhesion even when the concentrations of Fn in the culture medium are too low to support cell attachment alone. Therefore, cell corruption of the BSA passivated area in the

experiments presented here was presumably due to the presence of adhesive proteins (Fn, vitronectin, collagen, etc) at low concentrations in the FBS, which attached to the BSA layer facilitating cell adhesion there. Moreover, other growth factors present in the FBS could enhance the synthesis of ECM proteins by the cells, therefore facilitating cell attachment and proliferation.

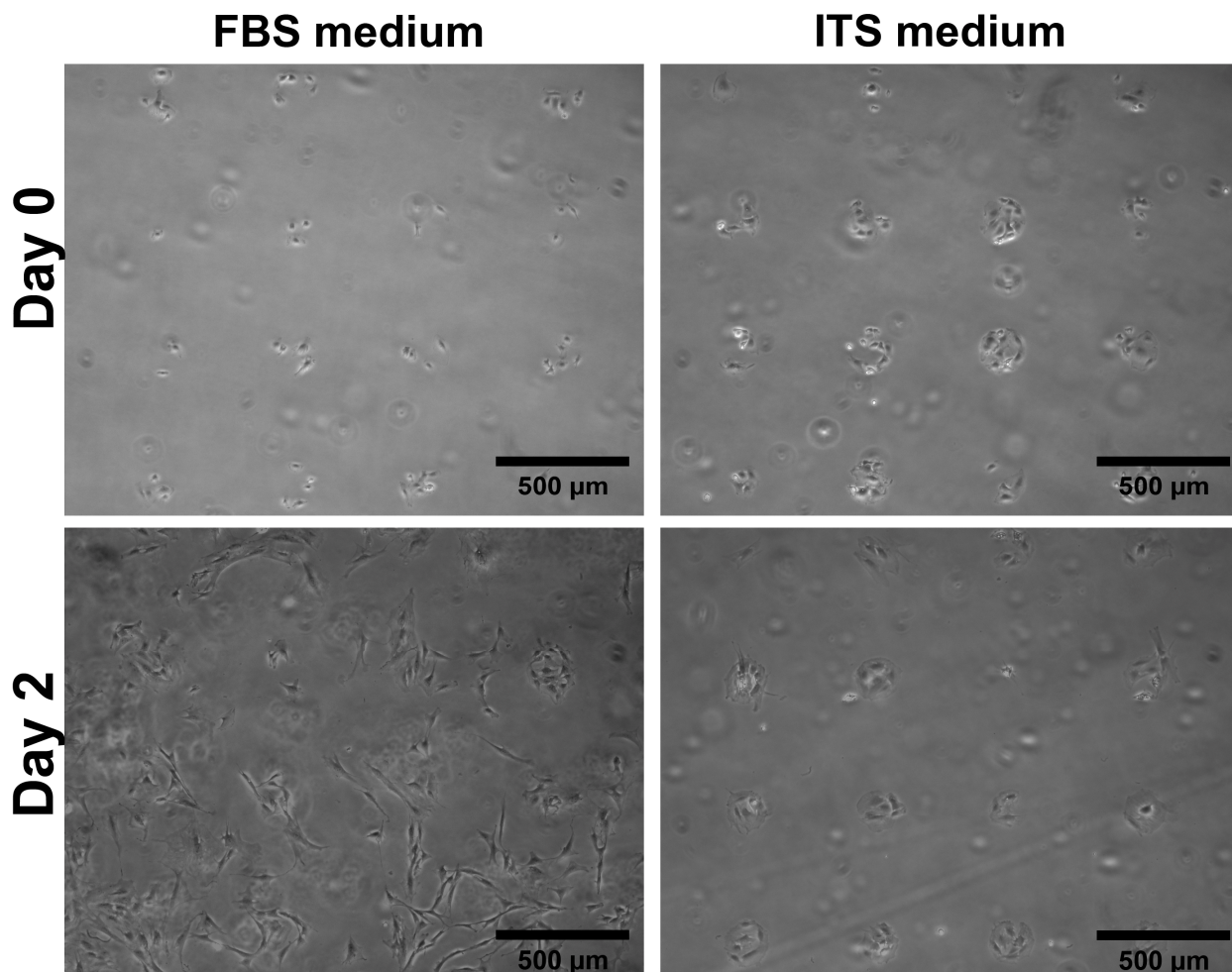


**Figure 3.14** The effect of FBS medium in the culture of the arrays. Cells attached on 16 spots right after cell seeding (day 0) and after 2 days of culture in FBS medium (left) or ITS medium (right). Microarray layout was lost after 2 days of cell culture in FBS medium. The images presented are for 1 drop spot of Fn200 in PBS with 2% glycerol, 11,000 cells/cm<sup>2</sup> seeding density and 15 minutes cell seeding time.

However, when using a completely defined protein-free medium, ITS medium, cells remained on the protein printed spots (Figure 3.14) for the cell culture periods assayed (up to 8 days).

The replacement of FBS by ITS in the culture medium has the advantage of eliminating the undesired signalling coming from the former supplement. However, ITS also lacks many of the growth factors and hormones that are present in unknown and variable quantities in the FBS and that are needed for the optimum expansion and culture of cells. For this reason, ITS has been

previously used in the literature when the elimination of some of the unknown factors present in the FBS was a strict requirement (e.g. for the study of MSC differentiation to chondrocytes).<sup>145</sup>,<sup>146</sup> In the experiments presented here, ITS was found to be a suitable alternative medium, which provided a very basic buffer for cell sustenance and culture detoxification while limiting cell corruption of the microarray layout and impeding the viability of attached cells on the passivated area due to the absence of cell adhesive proteins.

For the reasons exposed above, **ITS medium** was used in the experiments presented in the following sections of this chapter.

### ***Effect of the printing buffer composition***

In Chapter 2 it was observed that glycerol inclusion in the printing buffer resulted in lower amounts of protein mass immobilised, with a >50% of mass reduction. In contrast with what was expected by this observation, spots printed with glycerol kept more cells attached on them at day 0 after the centrifugation step (average 11 cells), when compared with spots printed in PBS only (average 4 cells, Figure 3.15 and Figure 3.16). This was attributed to the more homogeneous Fn coating of the glycerol printed spots, which allowed for a more uniform cell spreading on the spots and ultimately resulted in a stronger cell attachment that allowed cells to remain on the spots after the centrifugation step. Additionally, while the drying dynamics of PBS spots probably caused part of the immobilised Fn to be adsorbed on the surface (as previously discussed in section 3.4.1),<sup>103</sup> the inclusion of glycerol would provide a more suitable environment for Fn covalent immobilisation, reducing importantly the amount of protein adsorption due to the drying effects. This effect could not be evaluated from the fluorescence images presented in Chapter 2, since the signal emitted by the labelled Fn immobilised on the spots was not distinguished by the type of interaction taking place between the Fn and the surface. Taking this into account, together with the observation that cells seeded on PBS printed spots (yielding partly adsorbed Fn) were removed after the centrifugation step, suggested that Fn immobilisation by means of Fn spotting in PBS 2% glycerol provided a more stable strategy for cell attachment.

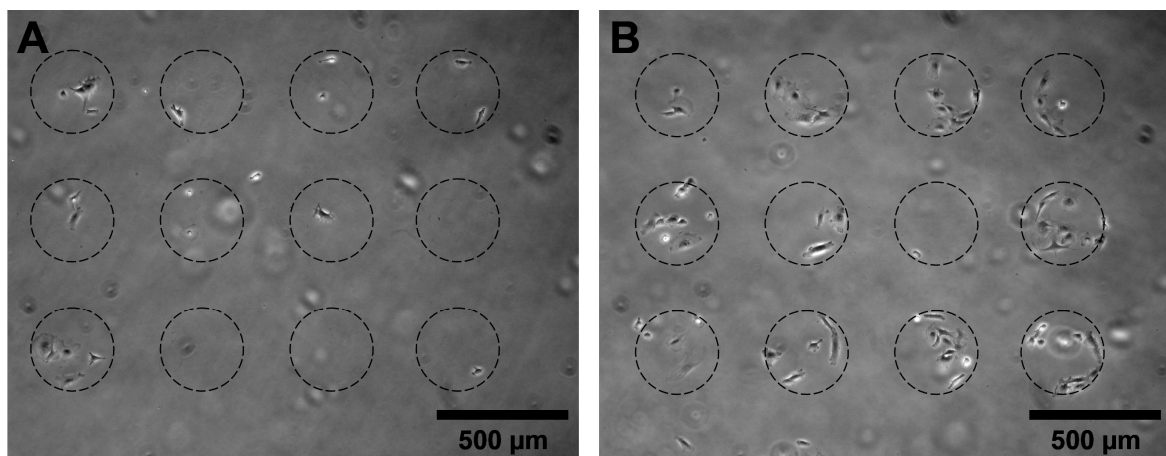


**Figure 3.15** Printing buffer effect on cell attachment at day 0. The images presented show cell attachment to 12 spots composed of 5 drop spots of Fn200 in PBS (**A**) or PBS with 2% glycerol (**B**), 11,000 cells/cm<sup>2</sup> seeding density and 15 minutes seeding time. Approximate spot position is indicated by the black, dashed circles. Glycerol containing spots retained more cells on them after the centrifugation step.

After an 8 days follow up (Figure 3.16), spots produced by both printing buffers (i.e. Fn200 spotted w/wo glycerol) yielded a good cell survival up to 6 days, as more than 50 % of cells attached at day 0 survived in these spots at day 6. However, the large variability obtained for the number of cells attached in Fn features spotted in PBS pointed out that, under the conditions used here for cellular microarray formation, the printing buffer allowing more reproducible number of cells per spot in the features at day 0 was PBS with 2% glycerol.

For the reasons exposed above, printing Fn spots in **PBS with 2% glycerol** has been chosen to perform the following cellular microarray experiments.

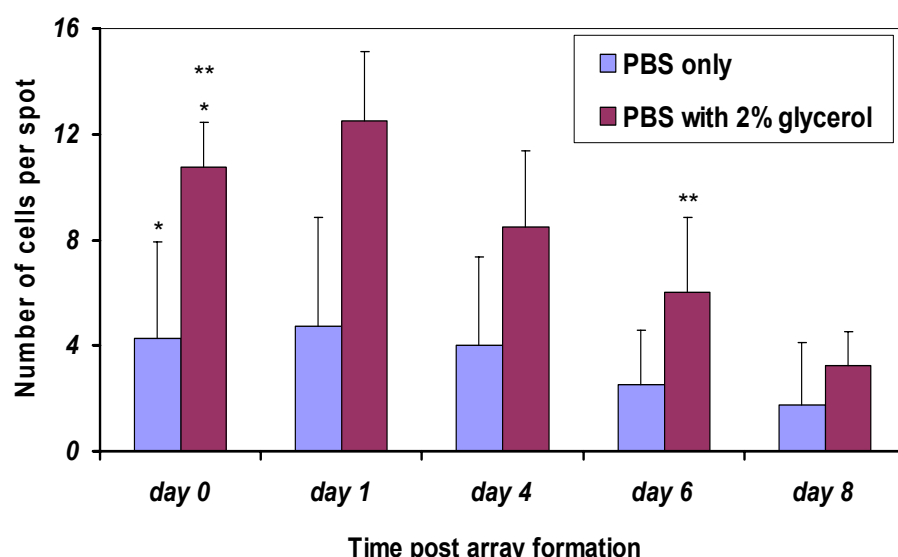


**Figure 3.16** Temporal plot showing cell survival for the different printing buffers assayed (Fn200, 5 drops spot size, 11,000 cells/cm<sup>2</sup> seeding density), 8 days follow-up (n=4). Bars marked with \*, and \*\* denote a statistical difference of p<0.05 (One-way ANOVA test).

### **Effect of the spot size**

Results for cell survival, assessed by the number of spread cells per spot, related to the spot size are shown in Figure 3.17. Interestingly, spot sizes larger than 5 drops yielded more cells remaining attached on the passivated area at day 0, as observed in Figure 3.17B for a microarray printed with spot sizes from 1 to 10 drops within the same array. This was not observed when seeding cells in microarrays composed exclusively of 5 drop spots (as shown in Figure 3.15), and suggested that some of the Fn spotted in the larger spots (e.g. 10 drop spot size) could be removed from the spot premises and attach unspecifically on the passivated area. This effect was already noticed in the immunostained microarray analysis as a protein smearing in some of the glycerol containing spots and, combined with the highly adhesive properties of the cells used,<sup>140</sup> could account for the attachment of cells outside the spot premises.

For a spot size of 1 drop, few cells attached to the spots and cell survival was impeded beyond 4 days. For 3 and 5 drops, cells attached to the spots (9 to 11 cells at day 0, average data from Figure 3.17D) and formed well defined cell spots at day 6 (Figure 3.17C), where ~40% of cells survived up to day 8 (Figure 3.17D). Larger spot sizes (7 and 10 drops) resulted in a larger number of cells attached per spot at day 0 (average 15 cells) but also yielded important variations (~50%) among spots. At day 8 only 20% of the cells survived (Figure 3.17D). A large variability in the number of cells attached on the spots at day 0 is an undesired effect in a cellular microarray application, introducing an additional uncertainty in the analysis of cell response to the printed factors, which could be affected by the number of cell-cell interactions.

Spotting ECM proteins for cellular microarray applications has been reported in the literature to be accomplished by overprinting 1 to 10 drops (~0.4 nL each),<sup>48, 57</sup> when non-contact printing devices similar to the one employed here were used. The optimum value within this range depends on a wide range of variables, these including the substrate used, the cell type assayed and the parameters used for cellular microarray fabrication (cell seeding density, seeding time, culture medium and passivation strategy). Based on the results obtained here, a spot size of 5 drops was revealed to result in the feature dimension allowing for the best MSC survival on the spots. This spot size allowed to initially capture ~11 cells in 0.063 mm<sup>2</sup> spot area, leading to an average density of cells actually seeded in the spots in the range of 200 cells per mm<sup>2</sup>.

The results presented here allowed choosing a **5 drop** spot size for the experiments presented in the following sections.

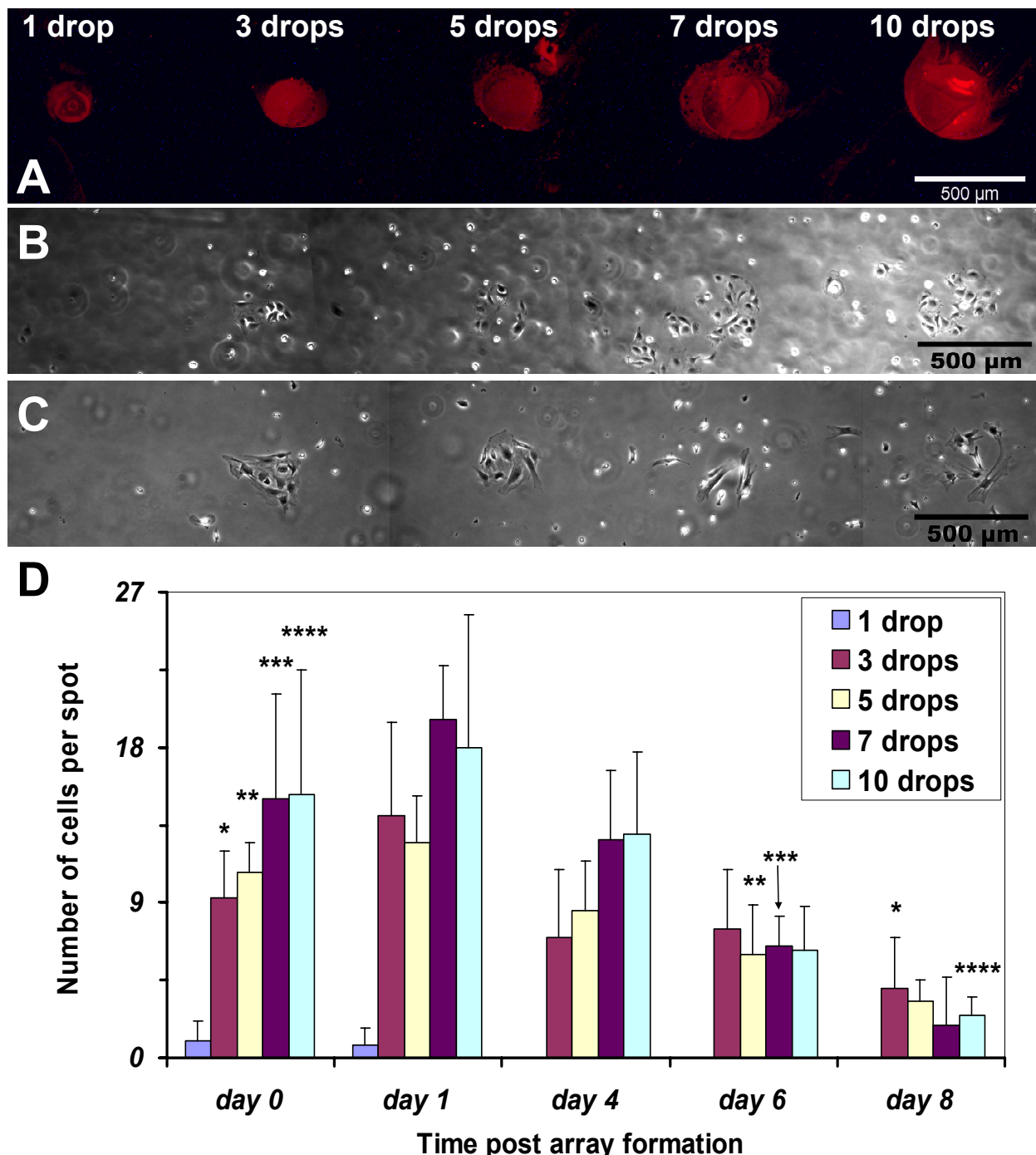


**Figure 3.17** Effect of spot size on cell survival. Cellular microarray formed for a 11,000 cells/cm<sup>2</sup> seeding density and a cell seeding time of 15 minutes. **A.** Fluorescence microscopy images of the microarray for increasing spot sizes of Fn200 in PBS 2% glycerol. **B, C.** Phase contrast images showing cell adhesion to each of the spots at day 0 (B) or at day 6 (C). **D.** Temporal plot of cell survival for the 8 days follow-up (n=4) for different spot sizes. Bars marked with \*, \*\*, \*\*\* and \*\*\*\* denote a statistical difference of p<0.05 (One-way ANOVA test).

#### Effects of cell seeding density and ITS medium on cell survival

The purpose of the experiments presented in this subsection was to provide a further insight into the effect of the cell seeding density and ITS medium on cell survival on the spots, once all

the other cellular microarray parameters have been optimised. With this objective in mind, MSCs were seeded at densities of 5,500, 11,000 and 110,000 cells/cm<sup>2</sup>, keeping all the previously optimised parameters: spots printed with Fn200 in PBS 2% glycerol, 5 drop spot size, BSA passivation, 15 minutes cell seeding time and cell culture in ITS medium. The evolution of the number of cells attached on the spots is shown in Figure 3.18.

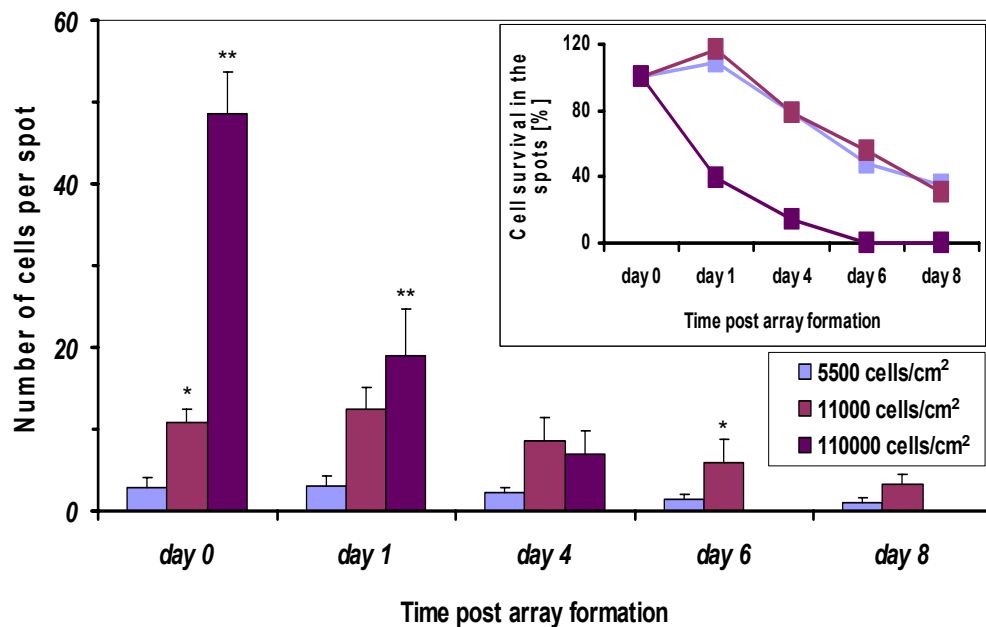


**Figure 3.18** Effect of cell seeding densities on cell survival. Temporal plot of the number of cells per spot for increasing cell seeding densities, 8 days follow up (n=4). Results are for a spot size of 5 drops of Fn200 in PBS 2% glycerol. Bars marked with \* and \*\* denote a statistical difference of p<0.05 (One-way ANOVA test). Inset: Cell survival temporal plot expressed as a percentage of the initial number of cells attached per spot at day 0.

The initial number of cells attached per spot at day 0 was found to increase as the cell seeding density increased. For a 5,500 cells/cm<sup>2</sup> seeding density only a few cells ( $3 \pm 1$  cells) were attached on the spots at day 0. For a cell seeding density of 11,000 cells/cm<sup>2</sup>, the number of cells attached per spot at day 0 was  $11 \pm 2$  cells, and for 110,000 cells/cm<sup>2</sup> it was  $49 \pm 5$  cells. In the latter case, the number of cells per spot can be considered enough to produce a confluent cell spot (Figure 3.19, top right image), in which cell attachment on top of other cells is not so evident as previously noted for longer cell seeding times (Figure 3.12). However, for the highest cell seeding density, the number of cells attached per spot rapidly decreased in the days following seeding (a 60% decrease at day 1, Figure 3.18, Inset). After 6 days of cell culture in the microarray no cells spread on the spots were found, round cells remaining attached everywhere (Figure 3.19, bottom right image). Therefore, this high cell seeding density was not appropriate for cell culture beyond 4 days. This effect has been previously noted by other

researchers for the culture of smooth muscle cells on agarose printed slides.<sup>59</sup> Probably, for the highest cell seeding density assayed here, the attached cells compete in searching room for spreading and, as this is not supported by the culture medium and substrate passivation, many of them die. Limitation of cell spreading has been previously reported to be associated with an increase in cell apoptosis.<sup>153</sup> This association seems to be related to changes in the type of focal adhesion complexes formed by the cells which are mediated by several cell adhesion receptors, mainly different types of integrins. Adhesion complexes ultimately integrate mechanical signals, associated with changes in cell shape, with chemical signals generated directly by integrin binding and, therefore, modulate downstream cell signalling pathways which could lead to cell apoptosis if cell spreading is restricted.

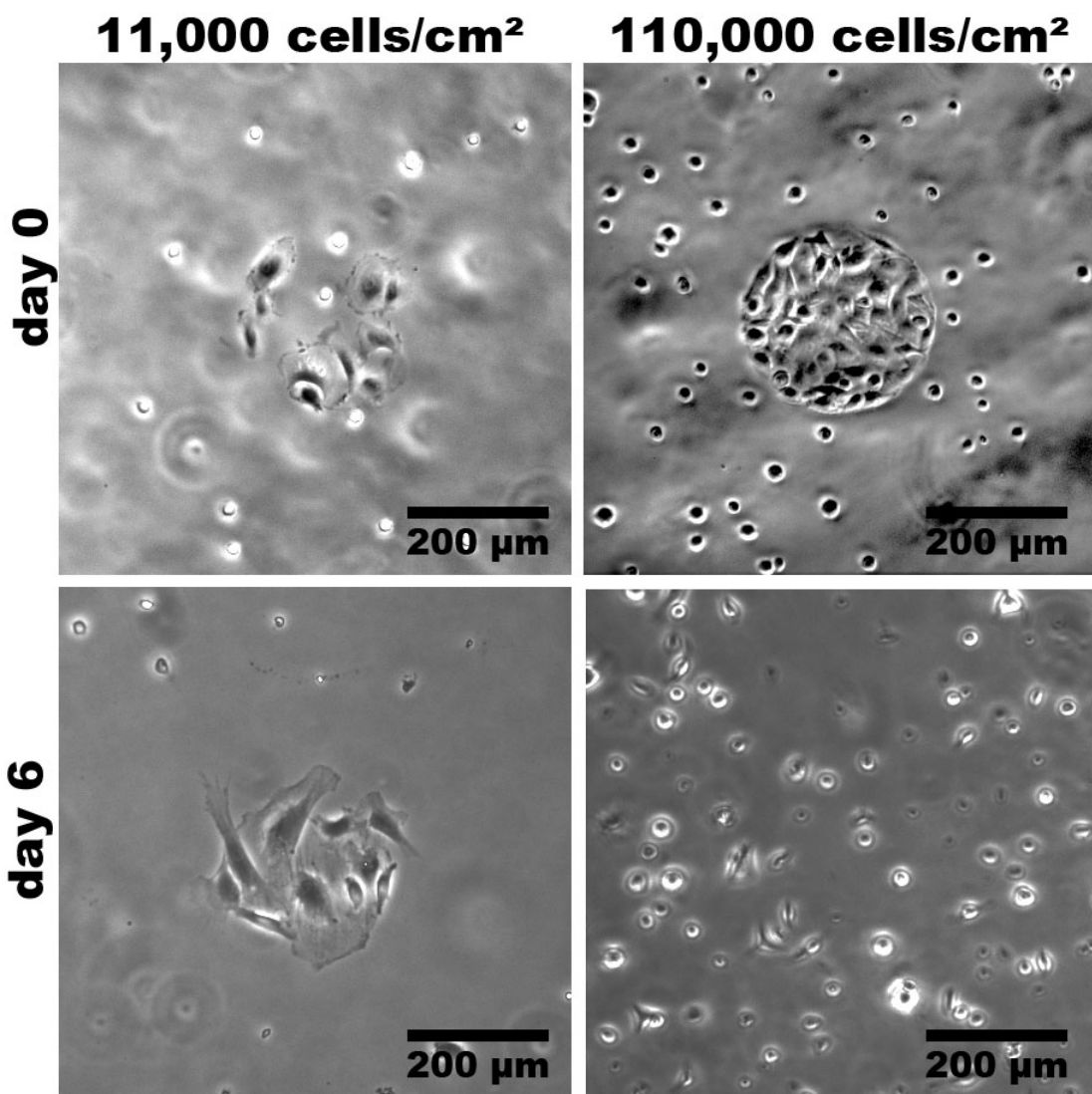


**Figure 3.19** Effect of the cell seeding density on cell survival in the spots. Results obtained for spots printed using a spot size of 5 drops and Fn200 in PBS 2% glycerol. Images show cell attachment at day 0 (top) and at day 6 (bottom) for a cell seeding density of 11,000 cells/cm<sup>2</sup> (left) or 110,000 cells/cm<sup>2</sup> (right).

For the lowest cell seeding densities assayed in these experiments, good cell survival values were observed up to 6 days of cell culture (average 50 % of cell survival, Figure 3.18 and Figure 3.19, bottom left image). From the two lowest densities assayed, more cells remained on the spots after 6 days of cell culture for a cell seeding density of 11,000 cells/cm<sup>2</sup> (average 1 cell for 5,500 cells/cm<sup>2</sup> and 6 cells for 11,000 cells/cm<sup>2</sup>). These results verified the choice initially made of using 11,000 cells/cm<sup>2</sup> seeding density, at the time that supported the choice of the previously optimised parameters.

### 3.3.3 Mesenchymal stem cell differentiation

#### *Primary MSC culture characterisation*

To characterise the adipocyte and osteoblast differentiation potential of the MSCs used, its differentiation to these cell fates was assayed by standard protocols. It was found that the MSCs used were responsive to standard differentiation cocktails after 15 days in culture. Figure 3.20B shows positive ALP expression in response to the osteoblast inducing cocktail, while Figure 3.20C shows lipid droplet staining and adipocyte morphology appearance in response to the adipocyte inducing cocktail. In contrast, control cell cultures revealed a high number of ALP unstained cells (Figure 3.20A), presumably undifferentiated.

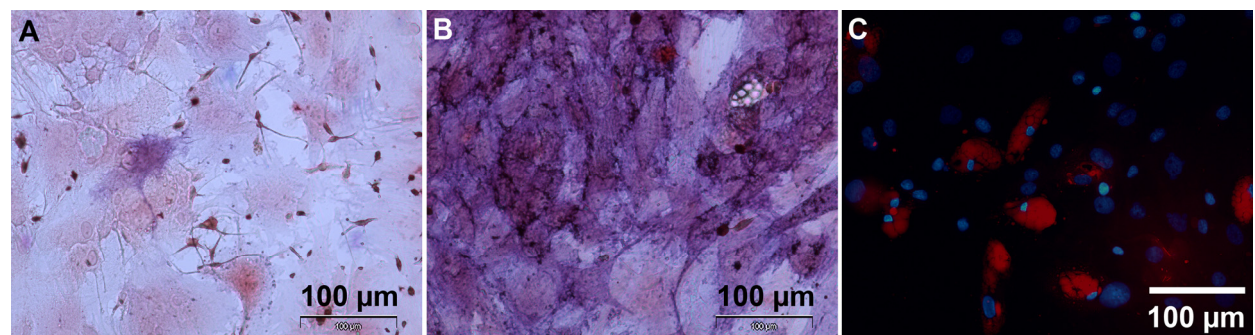


**Figure 3.20** MSCs cultured for 15 days in FBS medium only (**A**) and supplemented with the osteoblast (**B**) or adipocyte (**C**) differentiation cocktails. **A, B.** Histological staining for ALP (violet staining) and Nuclear Fast Red (red nuclei staining). **C.** Fluorescence staining for Nile Red (red staining of lipid droplets) and Hoechst (nuclei stained in blue).

Noteworthy, it can be observed in Figure 3.20B that not all cells expressed ALP in response to the osteoblast differentiation cocktail neither differentiated to adipocytes (Figure 3.20C) in response to the adipocyte inducing cocktail. The complexity of the signalling taking place in these wellplate cultures, which includes not only unknown signalling from the FBS added to the culture medium but also cell-cell signalling and paracrine signalling from attached cells in different places of the wellplate, could account for this fact.

Concerning MSC differentiation in a completely defined medium, it was verified that using ITS as replacement of FBS did not impair osteoblast nor adipocyte differentiation in response to the standard differentiation cocktails. The results are shown in Figure 3.21 and Figure 3.22. It can be seen that in untreated cell cultures (i.e. cell culture in ITS medium only) little to no ALP expression (Figure 3.21A) or adipocyte morphology (Figure 3.22A) were detected at day 15. In contrast, positive staining for ALP (Figure 3.21B) and adipocyte morphology (Figure 3.22B, arrows) were clearly evidenced after 15 days of cell culture in ITS medium supplemented with osteoblast or adipocyte inducing cocktails, respectively.

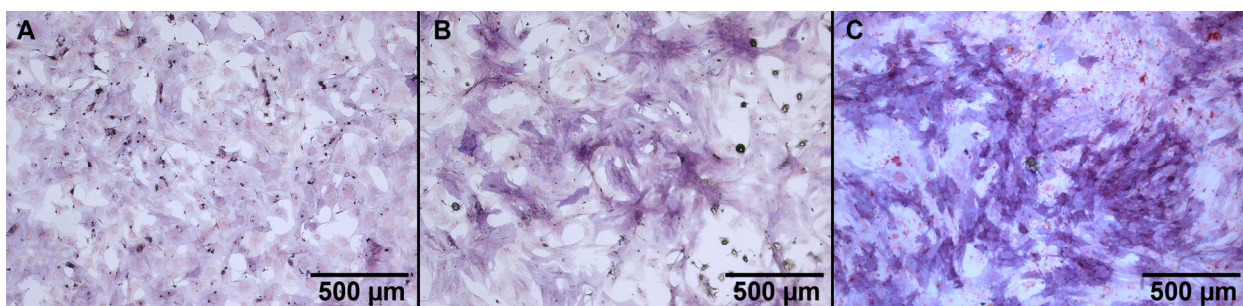


**Figure 3.21** Osteoblast differentiation in ITS medium. MSC response to the osteoblast differentiation cocktail after 15 days of cell culture. Images show the histological staining for ALP/Nuclear Fast Red. **A.** Control cell culture in ITS medium. **B.** Cell culture treated with the differentiation cocktail, using ITS medium. **C.** Cell culture in response to treatment with the standard differentiation cocktail using FBS medium.

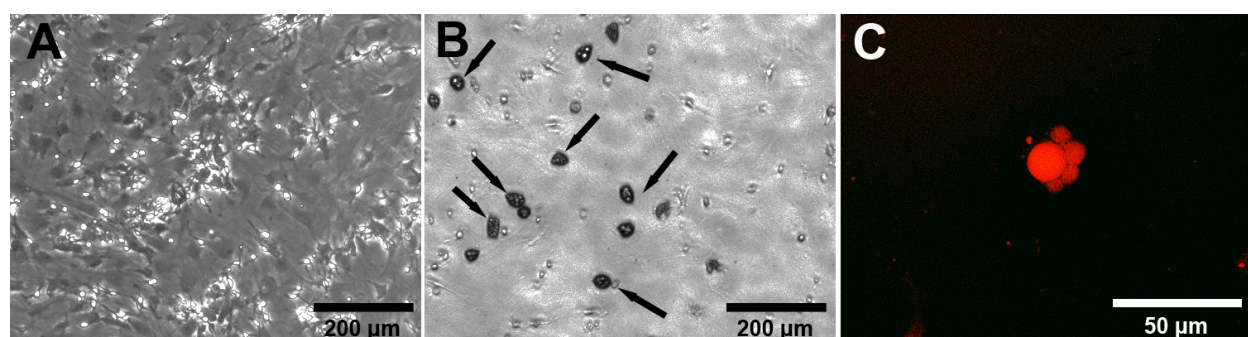


**Figure 3.22** Adipocyte differentiation in ITS medium. **A, B.** Bright field images of cells cultured for 15 days in ITS medium only (A) or supplemented with the adipocyte differentiation cocktail (B). Typical adipocyte morphology (indicated by the black arrows in image B) was observed in cell cultures supplemented with the differentiation cocktail. **C.** Nile red staining of lipid droplets, corroborating adipocyte differentiation in ITS medium supplemented with the adipocyte differentiation cocktail.

Additionally, it was observed that the ALP expression when cells were cultured in ITS medium was slightly lower when compared with the positive differentiation control using FBS medium and the same osteoblast inducing cocktail (Figure 3.21C). However, using a completely

defined medium for the cell culture allowed ensuring that no unknown factor included in the medium was influencing cell differentiation.

### ***MSC spontaneous differentiation in the cellular microarrays***

MSC were seeded on the microarrays using the optimised parameters previously described: Fn200 in PBS with 2% glycerol, 5 drops per spot, BSA passivation, cell seeding at 11,000 cells/cm<sup>2</sup>, 15 minutes seeding time and cell culture in ITS medium for 8 days. No differentiation cocktails were added to the culture medium, so any differentiation outcome would be taking place spontaneously. Cell viability was assessed after this period of time. It was observed that viability of cells attached on the spots after 8 days of cell culture was higher than 99% (Figure 3.23). Interestingly, it was found that some of the viable cells attached on the spots showed an adipocyte morphology (indicated by the white arrows in Figure 3.23), so spontaneous differentiation this fate could have taken place.

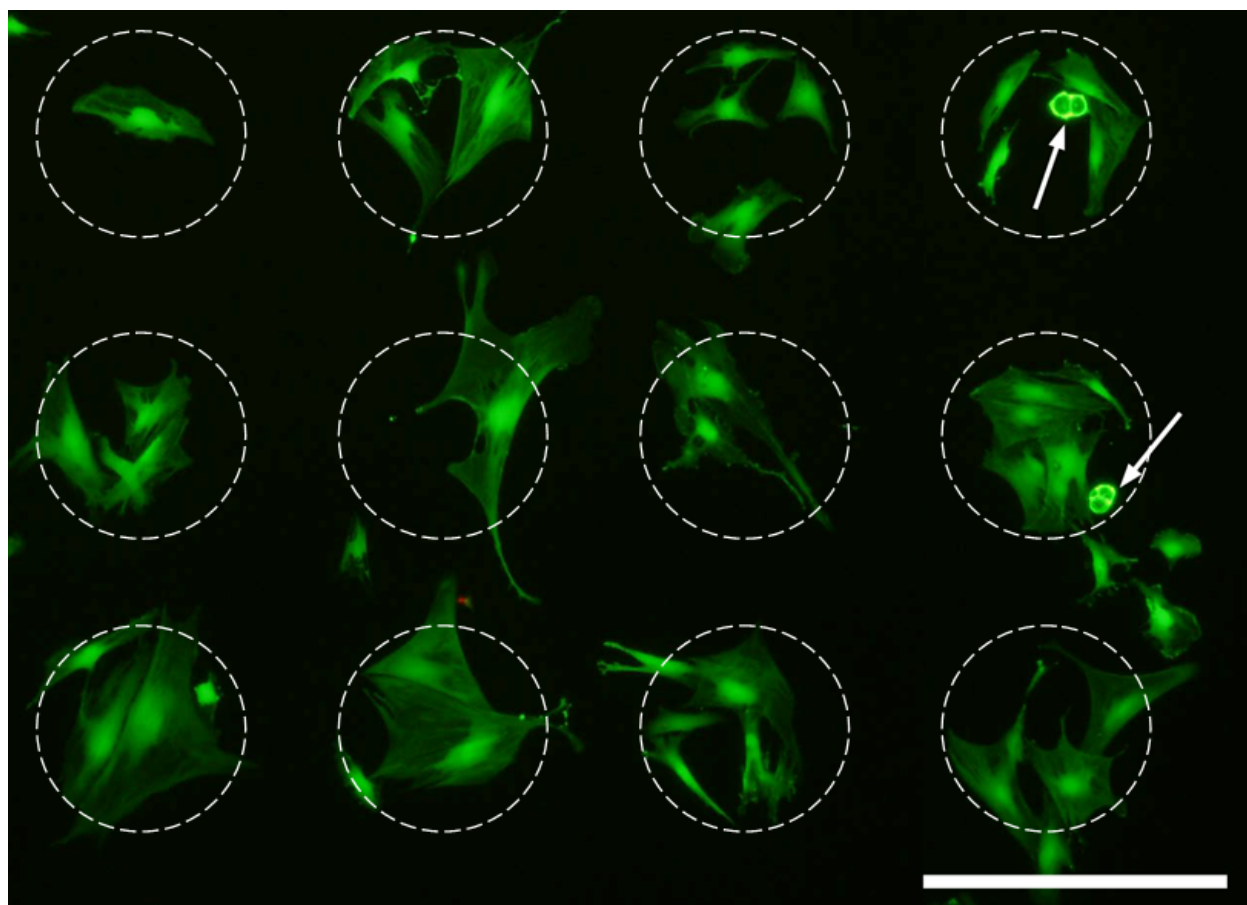


**Figure 3.23** Viability of cells attached on the spots after 8 days of cell culture in ITS medium was higher than 99%. Image shows cells attached on 12 microarray spots (approximate spot position is indicated by the white dashed circles). Viable MSCs were stained in green (Calcein AM) and non-viable cells were stained in red (EthD-III). Note that some of the viable cells in the spots showed adipocyte morphology (indicated by the white arrows). 500 µm scale bar is shown in white.

To further assess spontaneous MSC differentiation, cellular microarrays were fixed and stained for ALP, to assess osteoblast differentiation, and lipid droplets, indicating adipocyte differentiation, after 8 days of cell culture in ITS medium. Results showed that MSCs attached on some of the microarray spots expressed ALP (Figure 3.24 and Figure 3.25A), while most cells did not express this marker (presumably undifferentiated cells). Adipocyte differentiation of cells showing adipocyte morphology (Figure 3.24 and Figure 3.25B) was confirmed by the staining of lipid droplets (Figure 3.25C) in these cells.

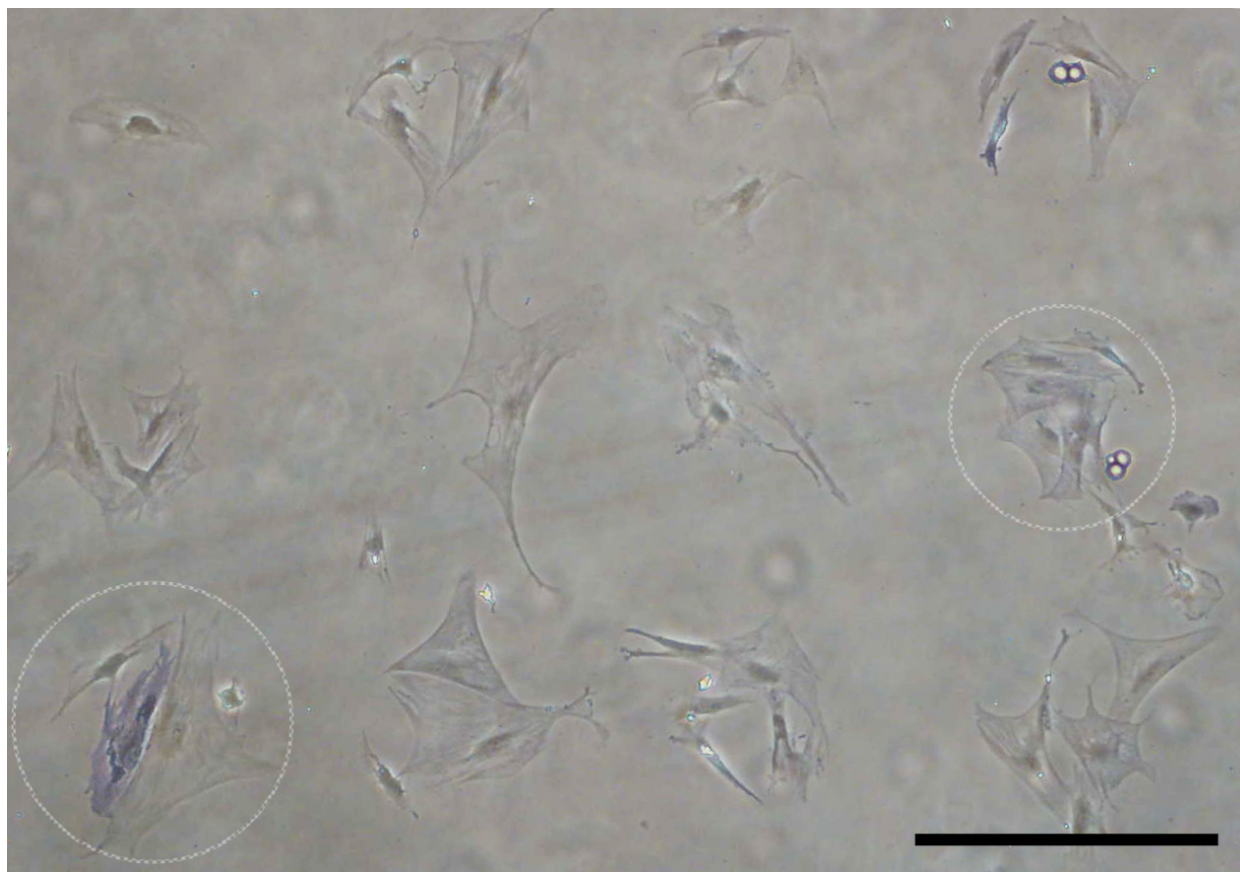


**Figure 3.24** Cellular microarray stained for ALP after 8 days of cell culture in ITS medium. Bright field image showing MSCs attached to 12 spots composed of Fn200 in PBS 2% glycerol, 5 drop spot size. Cell seeding was 11,000 cells/cm<sup>2</sup> during 15 minutes. Some cells were found to spontaneously differentiate to osteoblasts (blue staining, in bottom left spot, indicated with a white circle) or to adipocytes (top right spots, based on cell morphology). 500 µm scale bar is shown in black.

These results showed that MSCs cultured in the cellular microarrays spontaneously differentiated to osteoblasts or adipocytes at a very low rate. This finding was not expected as a response to the spot composition, since all microarray spots were initially composed of Fn only. However, it was also noted in Figure 3.21A, which can be regarded as a wellplate control experiment of osteoblast spontaneous differentiation.

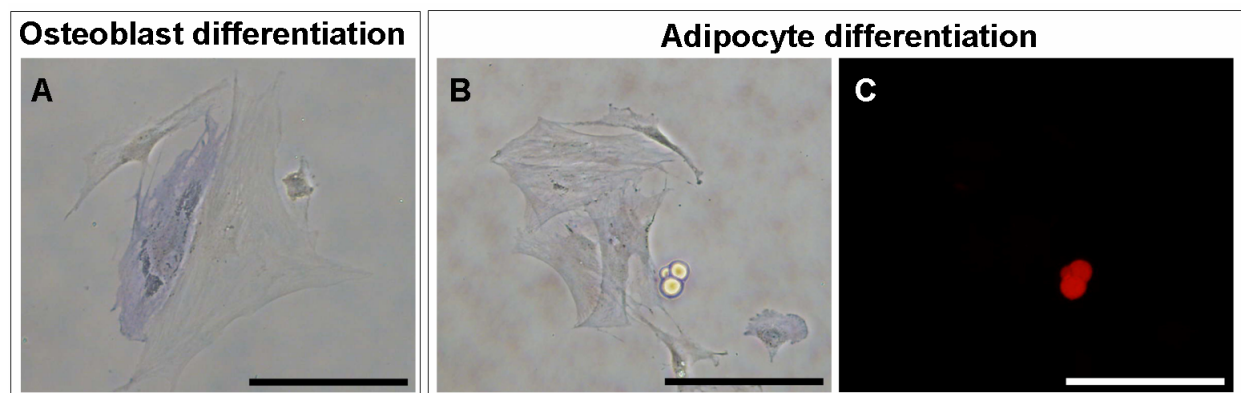


**Figure 3.25** Detail of cells differentiated to osteoblast or adipocytes after 8 days of cell culture in some of the microarray spots presented in Figure 3.24 (marked with white circles). After cells were fixed and stained for ALP, microarrays were further stained with Nile Red. **A.** Bright field image showing ALP staining in some of the cells in the spots (blue staining in the image) indicating osteoblast spontaneous differentiation. **B.** Bright field image of equally stained cells. In this case, no cell was stained for ALP and therefore no osteoblast differentiation occurred. Adipocyte differentiation is suggested by morphology of some of the cells. **C.** Fluorescence image of the same spot shown in B. Lipid droplets are stained in red, indicating adipocyte spontaneous differentiation in the spot presented. 200 µm scale bar is shown in black (images A, B) or white (image C).

It has been previously reported that MSCs initially seeded are composed of a heterogeneous population.<sup>81, 154</sup> This represents an additional parameter which adds complexity for a cellular microarray application, as ideally cells seeded should have identical differentiation potential at the beginning of the experiment. The schematic presented in Figure 3.26 shows that MSCs with limited differentiation potential (e.g. bi- and tripotent cells giving rise to osteoblast, adipocytes and some of them also to chondrocytes) can coexist within a cell culture. In this context, it has been previously reported that osteoblast lineage is the most robust differentiation pathway in MSCs obtained as primary cultures.<sup>134</sup> Therefore, MSCs obtained as primary cultures constitute a heterogeneous population which could show a restricted differentiation potential, biased towards some of the possible cell fates.<sup>134</sup> If these cells are cultured for several days, some of them could show spontaneous differentiation.<sup>155</sup> This fact would account for the osteoblast and adipocyte differentiation of cells cultured in the cellular microarrays presented here. Other effects coming from cell-cell interaction within the spots and the simplified cell culture medium used, which possibly lacks many factors needed for cell proliferation and undifferentiated phenotype sustenance, however, can not be ruled out. For these reasons, the choice of a better characterised cell line, which has a more robust differentiation response, will be preferred for further analysis of cell differentiation in cellular microarrays containing growth factors.

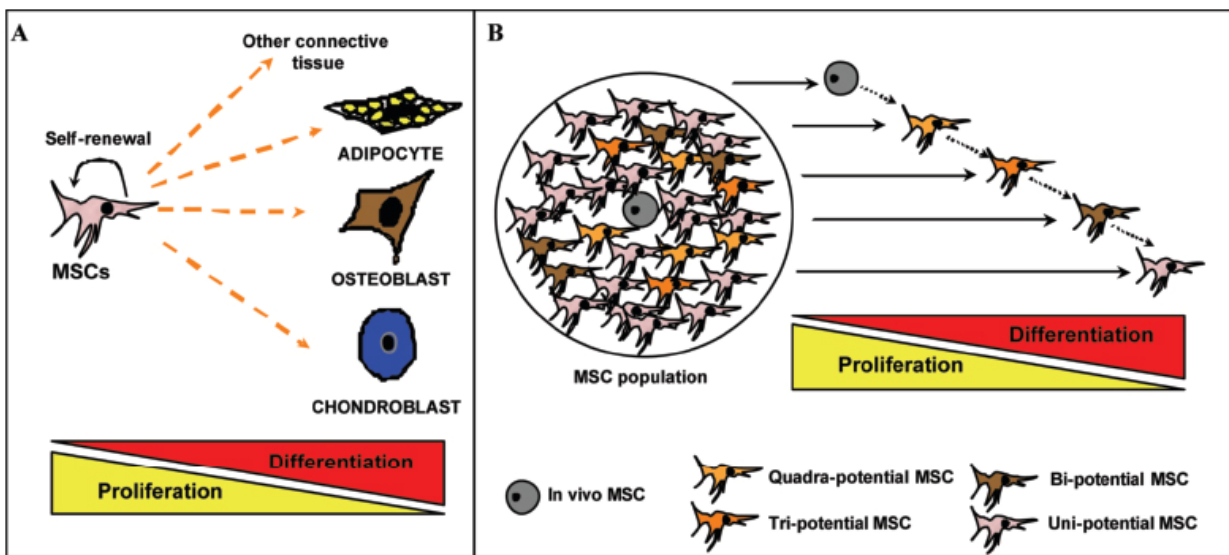


**Figure 3.26** Schematic diagram presenting (A) the most usual mesenchymal stem cell differentiation pathways (osteoblast, adipocyte, chondrocyte and other connective tissue cell types) and (B) the heterogeneous composition of a MSC population. The bottom triangles beyond each image indicate that the proliferation potential of these cells decreases as its differentiation stage advances. Image reproduced from cited reference.<sup>156</sup>

### 3.4 Conclusions

In this chapter, cellular microarray fabrication using five different spot sizes, three Fn concentrations, two buffer compositions and three different cell seeding densities have been analysed.

The results obtained leaded to an optimised set of parameters which were found when spotting 5 drops of Fn200 in PBS 2% glycerol, seeding cells at 11,000 cells/cm<sup>2</sup> density during 15 minutes, and cellular microarray culture in ITS medium. These parameters allowed for cell culture in the microarrays for periods up to 8 days. After this period of time, spontaneous cell differentiation to the osteoblast and adipocyte fates was detected in some of the spots at a very low rate, evidencing that under the adequate stimuli this platform would be viable to assess the differentiation of MSCs. MSCs obtained as primary cultures represent a heterogeneous population in terms of differentiation potential. This should be taken into account when analysing stem cell differentiation by means of cellular microarrays, since the response of cells attached to spots with the same composition can be different according to the differentiation stage of cells initially attached in each spot. For this reason, in order to initially test the effect of the growth factor inclusion in the cellular microarray set-up presented, the choice of a better characterised cell line would be desired.

Overall, the results obtained here were used as a base for the fabrication of cellular microarrays presented in the next chapter, aiming to provide a deeper understanding of how the inclusion of a selected growth factor in the microarray spots can affect the cell differentiation process.



# **Chapter 4 Application: Analysis of early differentiation stages using a cellular model**

## **4.1 Introduction**

When applying cellular microarrays to the study of the effects of growth factors on cell differentiation, an important issue to be taken into account is that the cells initially seeded on the microarray spots should have the most homogeneous phenotype or differentiation stage. Therefore, the spotted factors could be assumed to be the predominant source of cell response and not an acquired state previous to cell seeding. In the previous chapter, the results obtained on the spontaneous differentiation of MSCs suggested that the cells used had an initial heterogeneous phenotype. Due to the complexity associated in performing further characterisation and/or cell sorting to get an homogeneous population of MSC from primary cultures,<sup>73, 154, 157</sup> the choice of a better characterised cell line was preferred for the experimental work presented here.

Cellular microarrays including growth factors and not only extracellular matrix proteins represent an additional challenge. This is because growth factors, which usually signal to the cell from solution (liquid) phase, will be immobilised on the surface and, therefore, its activity might differ to the one they have in solution.<sup>41</sup> This issue adds to the need of a cell model whose response to growth factor stimuli in the soluble phase is well-characterised. Previous reports on cellular microarrays for the study of stem cell differentiation by immobilisation of growth factors were mainly focused on bipotent stem cells (i.e. cells leading to two possible cell fates upon differentiation). This provides a simplified cell differentiation model for the analysis of the immobilised growth factor effects. In these systems, bipotent neural stem cell differentiation to neuronal or glial cells was studied after 4 days of cell culture in the microarrays.<sup>48, 54</sup> Also, bipotent human mammary progenitor cell differentiation to myoepithelial or luminal lineages was studied after just 24 h of cell culture in the microarray.<sup>61</sup> In this last report, it is highlighted the fact that differentiation trends observed at 24 h of cell culture in the microarrays were predictive of the differentiation trajectories that would be sustained for up to 10 days in the presence of the inducing molecules.

For the experiments presented in this chapter, the well-characterised C2C12 cell line was chosen. These are embryonic cells of mesenchymal origin, pre-differentiated to myoblasts (pre-muscle cells).<sup>50</sup> The key aspect that makes them an ideal model for the experiments presented here is that these cells differentiate to myocytes (muscle cells) when reducing the serum content of the culture medium. However, in the presence of BMP-2 (Bone Morphogenetic Protein 2) this pathway of differentiation is altered. The C2C12 cells will then differentiate to osteoblasts (Figure 4.1A).<sup>158, 159</sup> In other words, this system can be regarded as a cell line with two possible differentiation pathways, where a single factor (BMP-2) serves as the key to decide which pathway is followed.<sup>160</sup> This property is already well known and has been demonstrated through traditional biology techniques.<sup>158, 161, 162</sup> C2C12 osteoblast differentiation in response to BMP-2 can be evaluated by histological staining for ALP after 4 days, but it can also be detected earlier, at 24 hours, by analysing the expression of Osterix (Osx) gene (Figure 4.1B).<sup>135, 136</sup>

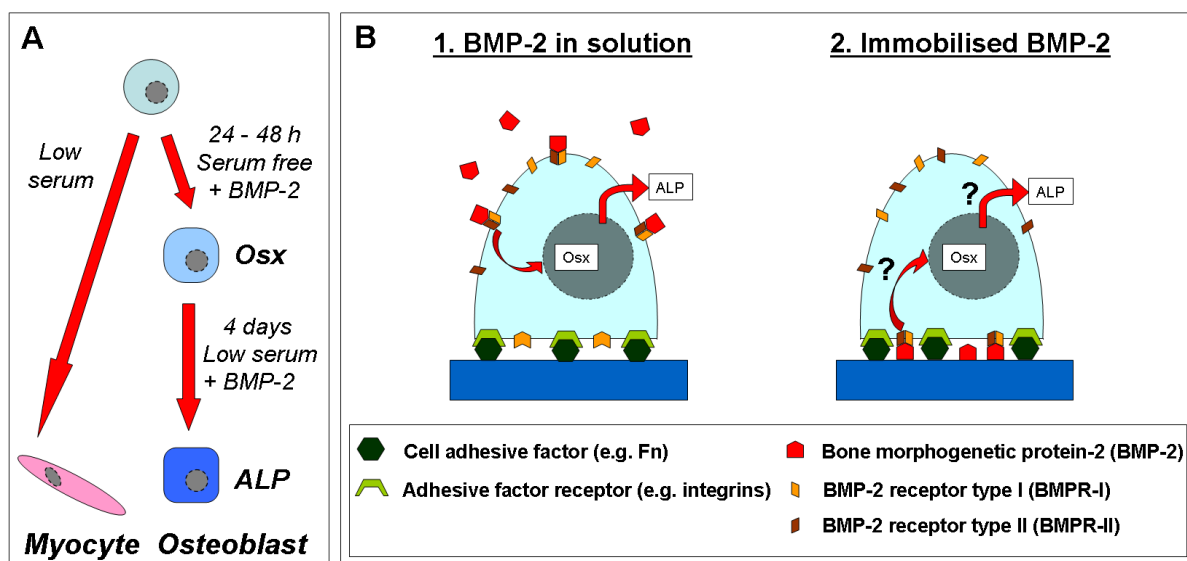


**Figure 4.1 A.** C2C12 cell differentiation pathway is switched from myocyte to osteoblast when BMP-2 is added to the low serum cell culture medium. **B.** Schematic representing a cell attached on a microarray spot (by means of the immobilised cell adhesive factor). The interaction of soluble (1) or immobilised (2) BMP-2 with its receptors initiates an intracellular signalling cascade that induces Osterix (Osx) expression in the nucleus (at 24 h) and alkaline phosphatase (ALP) production (after 4 days).

BMP-2 usually signals to the cell from the liquid phase, when added in solution to the culture medium. It exerts its biological effects through two types of transmembrane receptors (Figure 4.1B): BMP receptor type-I (BMPR-I) and type II (BMPR-II). Clustering of the two BMP receptors together with BMP-2 is indispensable for signal transduction.<sup>163</sup> BMPR-I and BMPR-II possess intrinsic serine/threonine kinase activity, this meaning that they are capable of triggering intracellular signalling pathways when the BMP-2 is recognised.<sup>160</sup>

Recently, it has been demonstrated that BMP-2 can also signal to cells when immobilised on a surface. C2C12 cell differentiation in response to immobilised BMP-2 has been described by the group of P. Campbell.<sup>67</sup> This report described the generation of BMP-2 arrays printed onto uniformly fibrin pre-coated glass slides and the culture of cells in a monolayer fashion atop these arrays for up to 72 h. ALP staining demonstrated that cells differentiated towards the osteoblast fate in response to the BMP-2 printed. This approach profited of the strong interaction between fibrin and BMP-2 to immobilise the later for several days. Still, a cellular microarray approach based on cell culture on mutually isolated spots instead of a monolayer will allow for the parallel study of the influence of multiple protein combinations on cell differentiation response. In order to focus the present study on the complex response of cells to an immobilised growth factor when the cell culture is limited to the restricted spot premises, however, a restricted number of protein combinations were assayed here.

In Chapter 2, a study of different substrates in terms of the amount of spotted protein immobilised on the surface suggested AD-Glass as the best candidate for cellular microarray applications targeting cell differentiation. Several parameters affecting cellular microarray fabrication using MSCs were optimised in Chapter 3 for this substrate, to allow cell culture for periods of time ranging from 6 to 8 days. Based on these results, cellular microarrays were further tested here. The final aim of the present chapter was to characterise the cell response to an immobilised growth factor in the cellular microarray platform developed, and to compare its efficiency with the cell response to the same growth factor when it was added in solution. For this purpose, C2C12 cell differentiation to osteoblasts was analysed in response to different combinations of BMP-2 co-immobilised with fibronectin (Fn) and laminin (Ln) ECM proteins on the microarray spots. For the evaluation of cell differentiation on the microarrays, the main checkpoint used to assess for short term cell response to printed BMP-2 was the Osx gene expression at 24 hours. This marker allowed validating the initiation of the BMP-2 signalling pathway.

In order to provide a comprehensible interpretation of the results obtained with the cellular microarrays in which BMP-2 was immobilised on the spots, several control experiments were designed as follows:

- To validate previously reported osteoblast differentiation of C2C12 cells, the effect of soluble BMP-2 on standard wellplate cell cultures was assessed.

- To evaluate the effect of immobilising the BMP-2 *per se*, cells were cultured on top of control substrates composed of large-area surfaces with immobilised proteins: Fn/BMP-2 and Ln/BMP-2 (i.e. not in a microarray layout).
- To separately evaluate the effect of culturing cells in isolated spots from the effect of immobilising the BMP-2, control cellular microarrays with protein spots composed only of Fn or Ln, in which BMP-2 was not printed, were exposed to soluble BMP-2.

The immobilised BMP-2 was found to induce the initiation of the osteoblast differentiation pathway on some of the cells attached on the BMP-2 containing spots. However, its effectiveness was reduced when compared to the control experiments. Additionally, at the end of this chapter, a medium term cell differentiation checkpoint was assessed by the activity of ALP at 4 days. The cell differentiation outcomes obtained in this case were extremely low. These results could be accounted, in part, by the restricted size of the cell culture, highlighting that this is an extremely important issue to deal with when cellular microarrays are used for the study of cell differentiation.

## **4.2 Materials and methods**

### **4.2.1 Proteins and chemicals**

Human cellular fibronectin and laminin from Engelbreth-Holm-Swarm murine sarcoma were obtained from Sigma (Spain). Recombinant human BMP-2 (expressed in chinese hamster ovary, CHO, cells) was obtained from R&D (USA). This growth factor was provided by the manufacturer as a lyophilized powder containing 50 µg of BSA per 1 µg of BMP-2 (the total BMP-2 mass provided in the vial was 10 µg, and 500 µg of BSA). It was reconstituted to a stock solution of 227 µg/mL of BMP-2 (which also contained BSA at a concentration of 11.35 mg/mL) using a sterilised 4 mM HCl solution prepared in Milli-Q water, following the provider suggestions. When subsequently referring to the BMP-2 concentrations used in the experiments presented in this chapter, it is understood that these solutions also contain BSA in a 50:1 relation (i.e. 50 µg of BSA per 1 µg of BMP-2), as previously exposed. Unless otherwise specified, all other chemicals were purchased from Sigma (Spain).

### **4.2.2 Cell culture**

C2C12 mouse cells were a kind gift of Professor Francesc Ventura, from the Bellvitge Hospital, Hospitalet, Spain. They were expanded in Dulbecco's modified Eagle's medium

(DMEM, provided by GIBCO, Spain) containing 10% fetal bovine serum (FBS), 1% penicillin/streptomycin, 1% L-Glutamine and 1% sodium piruvate, subsequently called “growth medium”.

In order to characterise the short-term cell differentiation towards osteoblasts, Osx gene expression was evaluated on semi-confluent C2C12 cell cultures incubated for 24 h in “serum free medium” (composed of DMEM, 1% penicillin/streptomycin, 1% L-Glutamine and 1% sodium piruvate) supplemented with BMP-2 (50 ng/mL). For the medium-term differentiation analysis, evaluated by the ALP activity, semi-confluent cell cultures were incubated for 4 days in the subsequently called “low serum medium” (composed of DMEM containing 2% horse serum (HS), 1% penicillin/streptomycin, 1% L-Glutamine and 1% sodium piruvate) supplemented with BMP-2 (50 ng/mL). Medium was changed every 2 or 3 days.

#### 4.2.3 Microarray fabrication

Based on results exposed in the previous chapters of this thesis, AD-Glass slides (SuperAldehyde 2, Telechem, USA) were chosen to fabricate cellular microarrays containing mixtures of BMP-2, fibronectin and laminin for cell differentiation experiments. The procedure followed for printing of protein microarrays has been previously exposed in Chapter 2, Section 2.2.4.

The parameters that yielded the best cell survival rate in the 8 days follow-up performed in Chapter 3 were: Fn200 solution printed in PBS 2% glycerol, spotted in 5 drops, passivation of the printed slides using a 2% BSA solution and cell seeding at 11,000 cells/cm<sup>2</sup> during 15 minutes. Despite according to these results protein spots deposited from a solution composed of Fn in PBS with 2% glycerol performed the best for the fabrication of cellular microarrays with MSCs, data from Chapter 2 also suggested that factors different to ECM proteins (such as SA) were very sensitive in terms of their strong attachment after washing. As this issue is strongly dependant on the buffer solution used for the printing, it was decided here to investigate both buffer strategies (i.e. PBS and PBS 2% glycerol).

##### ***Fabrication of protein microarrays with BMP-2 immobilised on the spots***

Protein solutions of Fn or Ln at different concentrations (200 or 360 µg/mL, subsequently called Fn200, Fn360, Ln200 and Ln360) were prepared in PBS. Fn360 and Ln360 protein solutions were also prepared in PBS with glycerol (2% v/v, final concentration). All the protein solutions assayed were prepared with and without BMP-2 (100 µg/mL of BMP-2, subsequently

called B100, which also contained BSA at a concentration of 5 mg/mL). The BMP-2 concentration spotted was of the same order of magnitude of the values previously reported in the literature (70 µg/mL) for the immobilisation of a similar growth factor (BMP-4) in AD-Glass.<sup>48</sup> Table 4.1 summarizes the composition of the prepared solutions and the nomenclature selected to refer to them, which will be kept in what follows.

Fn concentration spotted [µg/mL]	Ln concentration spotted [µg/mL]	BMP-2 concentration spotted [µg/mL]	Spot composition nomenclature
200	0	0	Fn200
200	0	100	Fn200 B100
360	0	0	Fn360 *
360	0	100	Fn360 B100 *
0	200	0	Ln200
0	200	100	Ln200 B100
0	360	0	Ln360 *
0	360	100	Ln360 B100 *
All spot compositions were printed in 5 and 10 drops, abbreviated as 5d and 10d in what follows.			
* These spot compositions were printed in PBS w/wo glycerol. When spotted with glycerol, the abbreviation used was PBS 2% glyc. If not specified, the spot composition was printed in PBS.			

**Table 4.1** Nomenclature adopted to refer to each spot composition printed. Besides the Fn, Ln and BMP-2 concentrations used for printing the solutions, all compositions were spotted in 5 and 10 consecutive drops, and some of them (indicated with an \* in the table) were spotted in PBS and PBS 2% glycerol.

A 10 µL volume of these solutions was placed in wells of a 384 wellplate. A robotic non-contact piezoelectric plotter (Nano-Plotter, GeSiM GmbH, Germany) was used to dispense the protein solutions onto the substrates in a square microarray format. The temperature of the workplate was set to 4 °C to delay protein dry out when printed. Two spot sizes were produced by overprinting 5 and 10 consecutive drops, 0.4 nL in volume each. Once spotted, the slides were incubated overnight at 4 °C to prevent evaporation and allow proteins to react with the AD-Glass surface chemistry. The layout of the protein microarray printed is depicted in Figure 4.2.

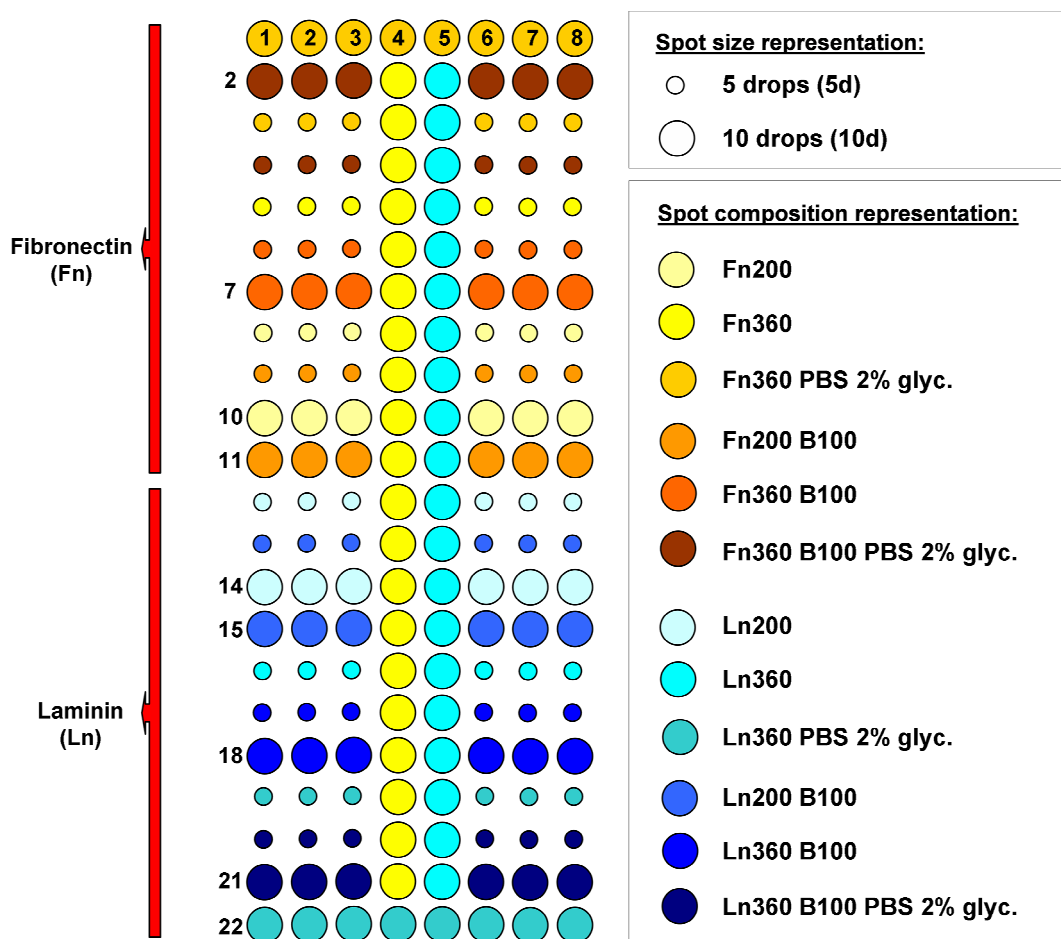


**Figure 4.2** Protein microarray layout printed for the cellular microarray experiments. The spot sizes and compositions are indicated in the caption on the right of the image. Nomenclature used is as indicated in Table 4.1. Distance between spots was 2 mm.

#### **Fabrication of control protein microarrays (no BMP-2 printed on the spots)**

With the objective of evaluating the effect of soluble BMP-2 on cells attached in control protein spots composed of immobilised Fn or Ln, but no BMP-2, control microarrays with 5 and 10 drop features were produced. This was accomplished by printing solutions composed only of Fn360 or Ln360 in PBS on AD-Glass slides following the same printing protocol described in the previous paragraph.

#### **Fabrication of cellular microarrays using the previously printed protein arrays**

Cellular microarray fabrication was based on the protocol previously exposed in Chapter 3, Section 3.3.2. However, slight differences were introduced and are listed in what follows:

- For passivation, the printed microarray slides were placed in Petri dishes (no FlexiPERM gasket was used in these experiments) and incubated with a 2% BSA solution prepared in PBS. In an attempt to reduce the smearing effect observed in Chapter 3 for some of the

spots, the printed microarray slides were first carefully placed upside down onto Petri dishes prefilled with a 2% BSA solution and incubated for 2 minutes. Afterwards the slides were placed, with the microarray face up again, in new Petri dishes and fresh 2% BSA solution was added. The slides were further incubated in this solution for 1 hour and then they were washed twice with PBS.

- The centrifugation step to remove unbound cells after seeding was eliminated, since it was found to be unnecessary for the cell line used. After passivation, C2C12 cells (resuspended in serum free medium) were seeded on the microarrays at a density of 20,000 cells/cm<sup>2</sup> for 15 minutes. Following the seeding, cells were cultured either in serum free medium (for Osx gene expression assessment) or low serum medium (as described in section 4.2.2 for ALP activity assays).

#### **4.2.4 Fabrication of substrates with large-area protein surfaces**

The effects of soluble BMP-2 on the C2C12 osteoblast differentiation have been widely reported. On the other hand, the effects of the BMP-2 factor on cell differentiation when this factor is immobilised on a surface (not in a microarray layout) have been only recently reported for BMP-2 dried on collagen-coated tissue culture wells.<sup>67</sup> Since the work presented here involved the use of additional ECM proteins (i.e. Fn and Ln) and a different substrate, it was considered necessary to perform these control experiments. For this purpose, AD-Glass slides with Fn or Ln and BMP-2 factor co-immobilised over large areas (> 5 mm<sup>2</sup>) were produced by dispensing volumes of 0.5 µL of Ln200, Ln200 B100, Fn200 and Fn200 B100 on AD-Glass slides using a micropipette.

It was previously found in Chapter 2 that, for spots printed from 1 up to 10 drops (resulting in spotted volumes from 0.4 nL to 4 nL), the amount of Fn and SA densities immobilised were mainly determined by the spotted protein concentration and not by the total volume of these solutions deposited. Indeed, the increase in the total volume of spotted solution produced an increase of the mass deposited but also an increase in the spot size and a change in the drying dynamics of the droplet. This yielded similar values of protein density immobilised after washing. Following these results, the solutions used to produce the large-area protein surfaces had the same protein concentrations that the solutions used for the production of the microarray. When compared to the microarray fabrication, these surfaces were produced by the deposition of much larger volumes of solution (0.5 µL), resulting in larger coated areas (5 to 7 mm<sup>2</sup>).

Therefore, the protein densities immobilised in these control slides were expected to be of the same order of magnitude to those immobilised on the microarray spots.

After the deposition of the protein solutions, the slides were incubated overnight at 4°C to prevent evaporation and allow proteins to react with the surface chemistry. The following day, the slides were passivated with a 2% BSA solution in PBS for 1 hour. Afterwards, they were washed twice with PBS and cells were seeded as indicated previously for cellular microarray fabrication. Cells attached on these slides were incubated for 24 h in serum free medium and cell differentiation was assessed by the evaluation of Osx gene expression.

#### **4.2.5 Protein microarray characterisation**

The fabricated protein microarrays were characterised by immunostaining of Ln, Fn and BMP-2 to check the microarray layout and the protein being effectively immobilised on the spots. For the immunostaining procedure, the protein printed slides were firstly blocked with BSA (1% in PBS-Gly) for 20 minutes. Afterwards, the slides were incubated for 1 h with primary antibodies: goat anti-BMP-2 (R&D, USA), rabbit anti-Ln and rabbit anti-Fn (Sigma, Spain), diluted 1:400. Then, they were incubated for 1 h with secondary antibodies: goat anti-rabbit Alexa Fluor 647 or donkey anti-goat Alexa Fluor 555, diluted 1:500. The samples were dried by centrifugation and scanned using a GenePix 4000B microarray scanner device (Molecular Devices Corp., USA). The Alexa Fluor 555 (green) and Alexa Fluor 647 signals (red) were successfully detected using the scanner excitation lasers at 532 nm and 635 nm with the ~557-592 nm and ~650-690 nm emission filters, respectively.

#### **4.2.6 Characterisation of cell cultures**

Cellular microarrays were characterised for the number of cells attached and their differentiation outcome.

To quantify the number of cells attached on the spots, cells were fixed (4% paraformaldehyde or 10% formalin) and nuclei were stained with Hoechst at days 0 (as seeded) and 4. The fixed cells were imaged using a standard fluorescence microscope. Cell counting was performed with the aid of ImageJ software (NIH, USA).

In order to assess the initiation of the osteoblast differentiation pathway, the expression of Osx was evaluated by applying an indirect immunostaining protocol (for further details of this technique refer to Appendix B.III). In this case, the immunostaining was based on the recognition of the Osx transcription factor, a protein which is expressed by C2C12 cells in

response to BMP-2 and remains inside the cell nucleus, by a primary antibody raised against this factor. For this purpose, cells were fixed in 4% paraformaldehyde, permeabilised for 4 minutes in Triton 100X (0,2% (v/v) solution in PBS-Gly) and blocked with goat serum (15% in PBS-Gly) for 45 min. Afterwards, the slides were incubated overnight at 4 °C with the primary antibody (rabbit anti-osterix diluted 1:100, Abcam, USA), followed by incubation with the secondary antibody (goat anti-rabbit Alexa Fluor 488 diluted 1:400, Molecular Probes, USA) for 1 hour at room temperature. Finally, samples were mounted using Fluoromount (Sigma, Spain) and imaged using standard or confocal fluorescence microscopes.

For ALP activity determination, at day 4 cells were fixed in 10% formalin for 1 hour, then a solution of naphtol AS-MX phosphate and fast blue RR in Milli-Q water was used to stain the cells according to the manufacturer instructions (Sigma Kit #85). Cells were incubated in the dark for 30 min and rinsed with water. Fixed cells were imaged using a bright field microscope.

#### **4.2.7 Statistics**

All experiments were repeated at least twice. Parametric one-way ANOVA tests were performed on the statistical analysis of variables plotted. Graphical data is reported as mean +/- standard deviation, and was calculated from spots of at least two independent experiments. Significance levels were set at p<0.05.

### **4.3 Results**

#### **4.3.1 Protein microarray characterisation**

##### *Characterisation of immobilised Fn and Ln*

The printed microarray layout (Figure 4.3A) was first characterised for the immobilisation of the ECM proteins (Fn and Ln). The specificity of the immunostaining was provided by the primary antibody used (raised against Fn or Ln), but the immunostaining images are both shown in red because the secondary labelled antibody used was the same in both stainings. Results for the immunostaining of Fn and Ln are shown in Figure 4.3B and Figure 4.3C, respectively. It was found that both printed protein microarray layouts remained identifiable after repeated washing steps, and the scanner images faithfully reproduced the intended layout spotted.

The areas of the spots printed with Fn and Ln were measured from the scanner images of the immunostained slides and the results are presented in Figure 4.4. A detailed analysis of these results showed that when Fn was spotted in 5 drops (Figure 4.4A), the spot area was not

significantly different for all the compositions assayed (i.e. Fn200 or Fn360 w/wo BMP-2 and in PBS w/wo glycerol, average area of  $0.073\text{ mm}^2$ ). However, when increasing the number of drops spotted per feature up to 10 drops, some differences were observed as a result of the smearing present in the features (Figure 4.5). In particular, it was found that spots containing BMP-2 had a tendency to yield larger spot areas (around 12% of increase in the area size).

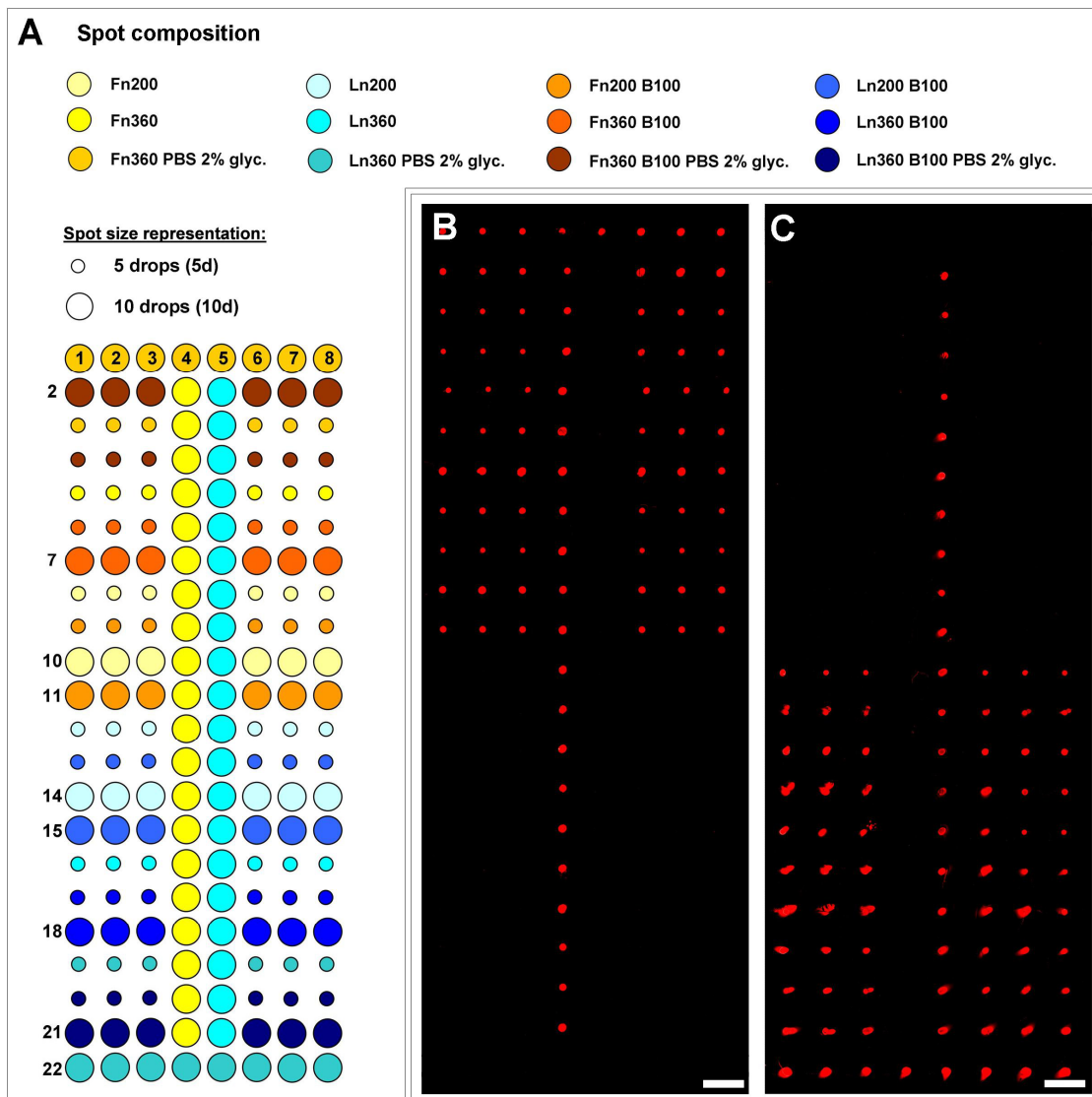


**Figure 4.3** Protein microarray characterisation. **A.** Protein microarray layout printed, adapted from Figure 4.2. **B, C.** Scanner images of the Fn (B) and Ln (C) immunostained slides. It can be observed that the signal detected from spots coincides with the intended layout, and no protein cross-contamination occurs. 2 mm scale bars are shown in white.

On the other hand, the spots containing Ln were measured to be larger than the equivalent spots containing Fn (compare the results presented in Figure 4.4A and B). This increase in area (up to threefold increments in some cases; e.g.  $0.075\text{ mm}^2$  for Fn360 B100 and  $0.224\text{ mm}^2$  for Ln360 B100 features spotted in 5 drops, Figure 4.4) was found to be variable, depending on the

spot composition and size, and was attributed to Ln spots being more smeared at the time of slide passivation and washing (Figure 4.5). An important difference in the spot area was found for Ln200 spots, which were significantly smaller than all other Ln compositions spotted (both when spotted in 5 and 10 drops, Figure 4.4) and was more similar to the spot areas obtained for Fn200 spots. Therefore, the smearing of the spots containing Ln was more important when the Ln concentration was increased, when BMP-2 was included in the spot composition or when the printing buffer used was PBS 2% glycerol.

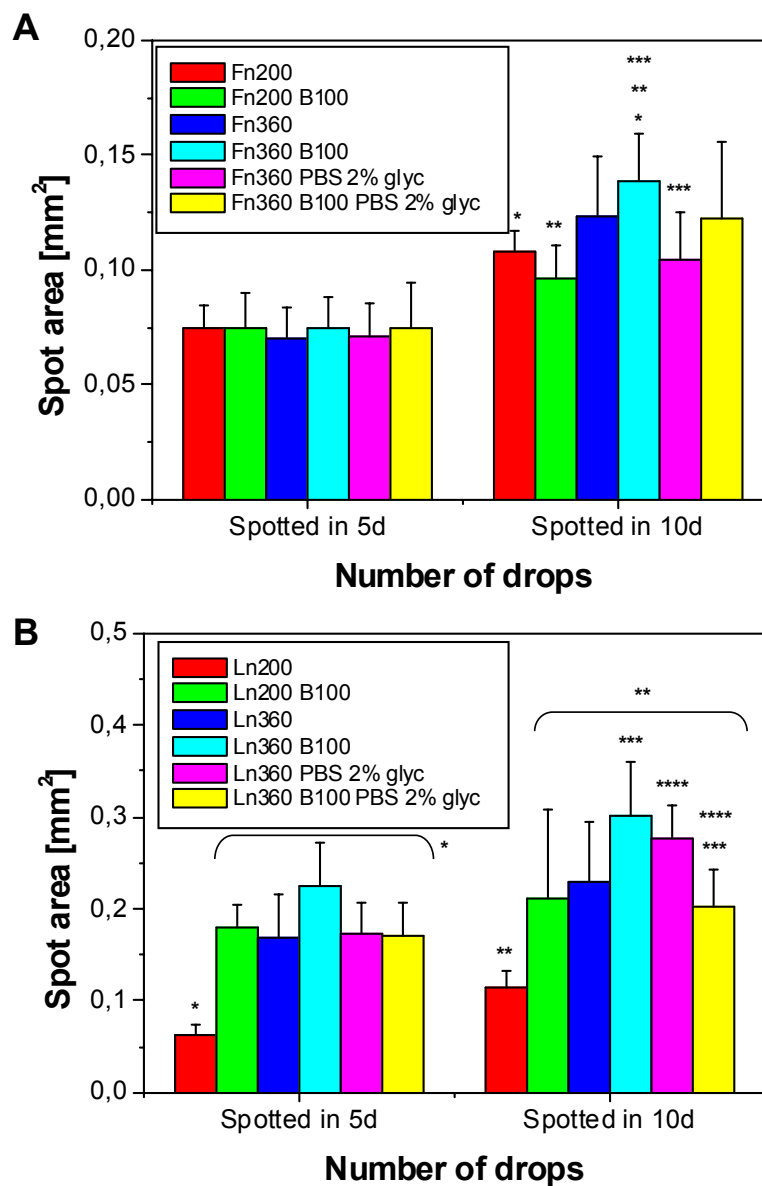


**Figure 4.4** Area values obtained for Fn (A) and Ln (B) features spotted. The values for the spot areas are indicated as mean  $\pm$  SD, calculated from 6 spots. Within each plot, bars marked with \*, \*\*, \*\*\* and \*\*\*\* are significantly different at the  $p<0.05$  level (One-way ANOVA test). In between plots, all bars representing equal compositions spotted with Fn or Ln were significantly different at the  $p<0.05$  level. The only exceptions were the areas obtained for Fn200 and Ln200 spots (both for 5 and 10 drops), which were not different when statistically evaluated.

Altogether, these observations suggested that the initial spot area (before any smearing occurred, i.e. before the passivation step) that is able to interact with the spotted proteins could be saturated by the Ln200 or, alternatively, by higher concentrated Fn360 solutions. Therefore, if BMP-2 (at 100 µg/mL, which also included BSA at 5 mg/mL) was included in the protein solution spotted, for Ln200 or Fn360, then the increase in area of the spots was more important due to the presence of larger amounts of protein that could not be able to interact with the saturated surface.

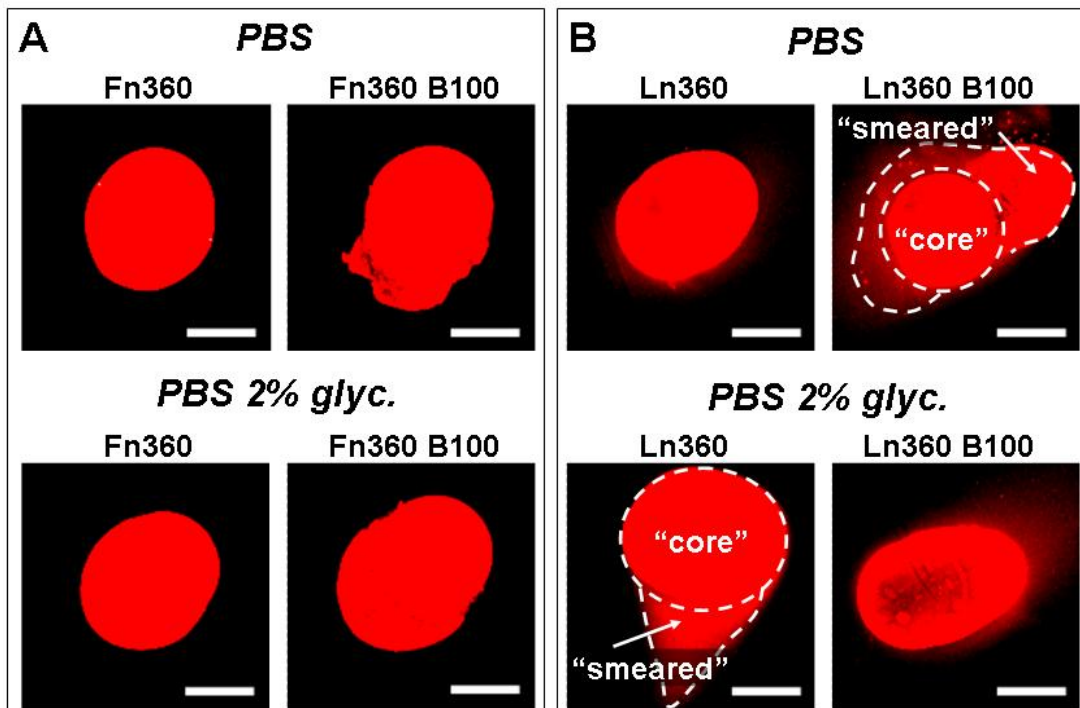


**Figure 4.5** Smearing effect observed in some of the features spotted in 10 drops for Fn (**A**) and Ln (**B**) spots. This effect is illustrated in the figure by the spots composed of Ln360 B100 and Ln360 in PBS 2% glycerol, for which the “core” of the spot (indicated by a dashed white circle) can be clearly distinguished from the “smear” part. The inclusion of BMP-2 in the solution printed also promoted (to a less extend) the smearing of the Fn360 spots. Brightness and contrast of the spot images has been forced to visualise spot morphology. 200 µm scale bars are shown in white.

Changes in the spot size when spotting Ln with different growth factors have been previously reported in the literature. In particular, Soen and co-workers reported that when Ln was spotted at 360 µg/mL with either BMP-4 or Wnt-3A (in concentrations up to 70 µg/mL) on AD-Glass slides, the inclusion of the later factor leaded to consistently larger spot sizes.<sup>48</sup> These authors, however, did not present a throughout study of the spot sizes. In the present case, the proteins used were Fn (molecular weight ~550 kDa), Ln (molecular weight ~ 800 kDa) and BMP-2 (molecular weight ~26 kDa). The latter protein is associated to BSA (molecular weight ~66 kDa)<sup>164</sup>, therefore yielding a protein complex of ~92 kDa. Despite there is not a clear

explanation to date for the changes in spot size observed, an explanation for the smearing of the spots can be attempted based on a combination of two phenomena:

- Proteins remaining in the bulk of the droplet, which were not able to interact with the surface because it was already saturated, would interact with the surroundings of the spot (at the time of passivation of the slides) leading to the smearing effect observed. Therefore, the smearing should be more important when larger amounts of protein remain in the bulk of the spotted droplet.
- Different proteins could have different affinity by the surface. It has been previously reported that the protein-surface affinity and the orientation of proteins adsorbed on a surface depend upon protein structure, protein size and concentration.<sup>128, 129</sup> The first step for protein immobilisation on AD-Glass consists of protein adsorption by means of hydrophobic or electrostatic interactions,<sup>128</sup> which will lead to the subsequent covalent bond formation. The differences in size and structure of the proteins spotted could affect the composition and amounts of proteins that either attach to the surface or remain in the bulk, ultimately leading to the differences observed in the area of features that were initially spotted with the same amounts of mass (e.g. Ln360 B100 and Fn360 B100).

Based on these assumptions, the smearing should be more important when larger amounts of protein remain in the bulk of the spotted droplet.

### ***Characterisation of immobilised BMP-2***

Regarding the immunostaining of BMP-2 on the microarrays, an extremely low signal was obtained after scanning the slides. This suggested that either BMP-2 was immobilised on the substrate at a low density or that most of the immobilised BMP-2 could not be accurately recognised by the antibody used due to partial denaturation of the growth factor or to being immobilised in a wrong orientation. However, other reasons that could difficult the recognition of the immobilised BMP-2 by the antibody are the covering of the BMP-2 by the BSA protein carrier (which is a 66 kDa protein, compared with the 26 kDa of the BMP-2) or by the much larger ECM proteins co-immobilised on the spots (i.e. Fn with 550 kDa or Ln with 800 kDa). These effects were difficult to evaluate and cannot be ruled out.

In order to visualise the BMP-2 in the microarray, the laser power had to be set to 100% and the PMT (i.e. the photomultiplier tube gain) to 725 (as a reference, in Chapter 2 the power used for the 532 nm excite laser was 10% and the PMT was in the range from 360 to 550). These settings allowed microarray visualisation, but the spots printed with BMP-2 could not be clearly

distinguished from the other microarray spots which did not contain BMP-2 (Figure 4.6A), probably due to a non-specific signal coming from the other proteins immobilised on the spots (i.e. Fn and Ln) as well as from salt aggregates from the PBS remaining in the features. In order to assess the specific staining in BMP-2 spots, a more detailed analysis was performed on the zoomed-in spot images (Figure 4.6B). It was found that bright green dots were present only in BMP-2 printed spots, which were assumed to be BMP-2 aggregates immobilised on these spots. Control spots, on the other hand, did not present this type of aggregates. The only exceptions were some control spots (e.g. Ln360 in PBS 2% glyc., Figure 4.6), which were located in the surroundings of 10 drop BMP-2 features spotted in PBS 2% glycerol (e.g. Ln360 B100 in PBS 2% glyc., Figure 4.6). This suggested that small amounts of the BMP-2 which were washed off from these spots could remain unspecifically attached on some of the neighbour spots and the surrounding passivated area. However, the signal coming from BMP-2 in these isolated cases was found to be much lower when compared with equal spot compositions in which BMP-2 was initially spotted (compare, as an example, Ln360 in PBS 2% glyc. and Ln360 B100 in PBS 2% glyc., Figure 4.6). Therefore, it was expected that this would not imply an important interference in the analysis of cell differentiation when cells were cultured on these spots.

It has been proposed that growth factors have the propensity to bind to laminins.<sup>165</sup> From the results presented here, it was noted that more bright green fluorescence dots (presumably indicating BMP-2 immobilisation) were detected when BMP-2 was co-spotted with Ln (Figure 4.6). In the same way, more green dot aggregates were detected when BMP-2 was co-spotted with the higher Fn and Ln concentrations (i.e. Fn360 B100 and Ln360 B100), suggesting that the growth factor was better retained on these spot compositions. Two possible explanations can account for this fact:

- On one hand, it has been previously reported that growth factors can be immobilised by the ECM proteins,<sup>166-168</sup> therefore enhancing its signalling effects. In this context, larger amounts of Fn or Ln immobilised on the spots (produced when spotting Fn360 and Ln360) could also lead to larger “indirect” immobilisation, mediated by the association of BMP-2 with the ECM proteins in these spots.
- On the other hand, it has been reported that the orientation of proteins adsorbed on a surface depends upon protein structure and concentration.<sup>128, 129</sup> As discussed previously in Chapter 2, at higher concentrations, large proteins such as Fn and Ln could leave more “space” for the immobilisation of small proteins such as BMP-2 or BMP-2-BSA complex

due to a “disordered” immobilisation. At a lower concentration, large proteins would elongate on the surface, therefore providing more contact points for anchorage and leaving less surface available for interaction with BMP-2.

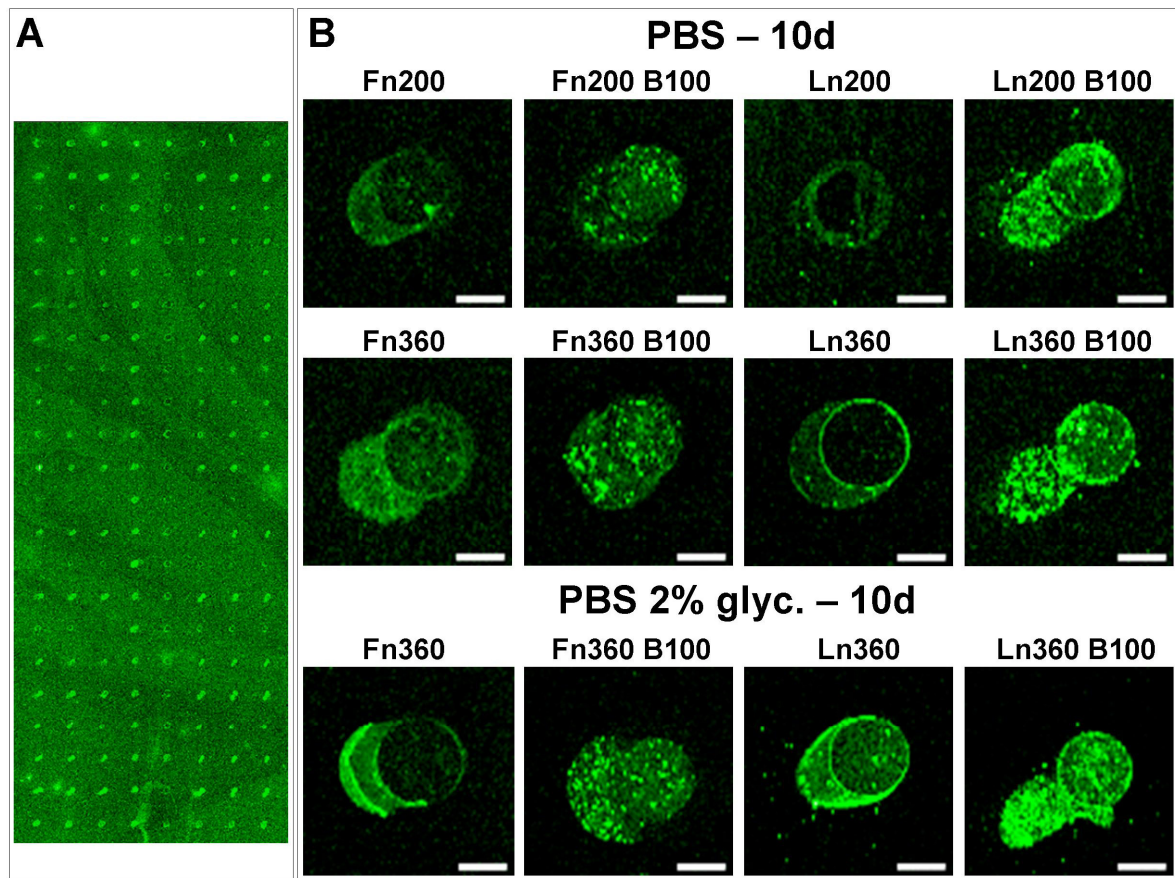


**Figure 4.6** Results obtained for the BMP-2 immunostained microarrays. **A.** Full scanner image of the immunostained microarray. In order to visualise the microarray spots, the scanner parameters had to be forced to a maximum. **B.** Detail of 10 drop spots for all the compositions assayed. Despite the high signal detected in control spots (i.e. those in which no BMP-2 was printed), brighter green dots (which were presumably BMP-2 aggregates immobilised on these spots) were only observed in the BMP-2 containing spots. Similar results were obtained for 5 drop spots. 200 µm scale bars are shown in white.

No quantitative analysis could be performed based on the indirectly immunostained slides due to the non-linear signal amplification taking place during the staining process (for more details on the indirect immunofluorescence technique refer to Appendix B.III). Alternative techniques usually reported for quantification of surface immobilised proteins, consist of direct immunostaining or radiolabelling of proteins. Neither of them, however, could be applied here to quantify the BMP-2 immobilised for different reasons. The direct immunostaining technique (in which each protein immobilised is recognised by only one antibody specific for that protein, which is fluorescently labelled, for further details refer to Appendix B.III) was discarded because in this technique no amplification of the signal is provided. Therefore, if BMP-2 was

barely detected from the immunostained images by the indirect immunostaining assay (in which signal amplification actually takes place), the direct approach of this technique would provide an even lower intensity signal. Regarding the radiolabelling of BMP-2, despite being an extremely sensitive approach for quantification, it was discarded due to the complexity of handling radiolabelled samples.

Summing up the results obtained in this section, a qualitative analysis allowed extracting interesting conclusions on the spotting process and microarray approach followed here to test the combination of Fn or Ln co-immobilised with BMP-2. Firstly, from an analysis the highly sensitive (i.e. those stainings which provided strong and specific fluorescence signals) Fn and Ln immunostaining, it resulted that the microarray layout spotted corresponded with the intended schematic and no cross-contamination between protein samples spotted took place during the printing process. Therefore, Fn and Ln were only detected in those spots in which these proteins were initially spotted. Secondly, a detailed qualitative analysis of the BMP-2 immunostained slides suggested that BMP-2 was only present in those spots in which this growth factor was initially spotted. Thirdly, in most cases, the effect of including BMP-2 in the spot resulted in an enlargement of the feature area due to an increase in the smearing of these spots at the time of passivation of the slide.

### 4.3.2 Cellular microarray fabrication and characterisation

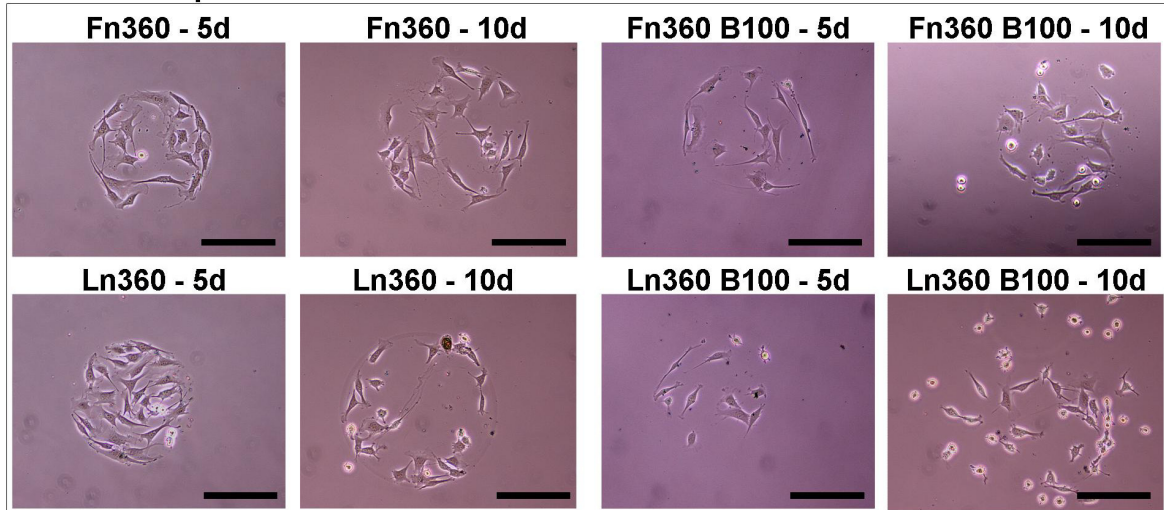
#### ***Cell attachment to the spots***

From the morphological evaluation of the cells attached on the spots immediately after cellular microarray fabrication (day 0), it was observed (for both printing buffers) that cells were well spread in spots composed of Fn and Ln only (Figure 4.7). When BMP-2 was included in the spot composition, it was noted that C2C12 cells had more difficulties for attachment to the spots when this growth factor was co-spotted with Ln. This can be seen in Figure 4.7 as, while cell attachment and spreading to Fn360 B100 spots was similar to the attachment of cells to Fn360 spots, cells attached on Ln360 B100 spots were less spread than cells on Ln360 spots. Therefore, cells were better spread on Fn360 B100 spots than on Ln360 B100 features. This was evidenced as more cells attached on Ln360 B100 spots had a round morphology.

This effect was extremely important when these spot compositions were printed in PBS with 2% glycerol. To quantify this evident difference, the cell spreading area was measured from the representative images presented in Figure 4.7, resulting in an average cell spreading area of  $1839 \pm 739 \mu\text{m}^2$  (for n=32 cells) for the Fn360 B100 spot and  $778 \pm 385 \mu\text{m}^2$  (for n=12 cells)

for the Ln360 B100 feature (both spotted in 10 drops and using PBS with 2% glycerol as printing buffer). These results were significantly different at the p<0.05 level (One-Way ANOVA Test).

#### A. Features spotted in PBS



#### B. Features spotted in PBS 2% glyc.

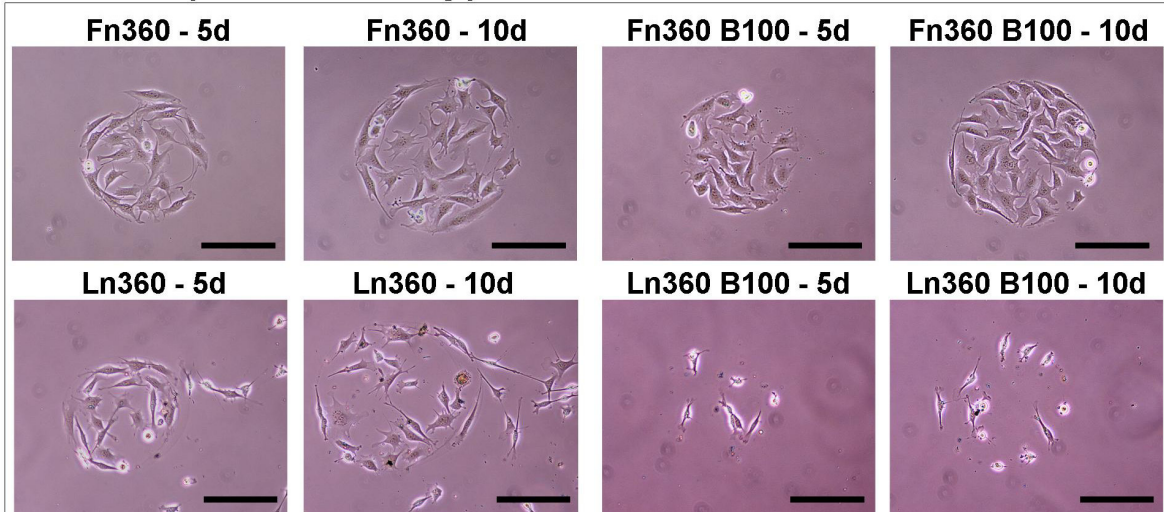


**Figure 4.7** Spot composition effect on cell attachment at day 0. Bright field images of cells attached in Ln360 and Fn360 spots (5 and 10 drops, with and without BMP-2 included in the protein mixture spotted) printed in PBS (**A**) or in PBS 2% glycerol (**B**). It can be observed that cells spread better in BMP-2 containing spots when this growth factor was co-spotted with Fn. 200  $\mu$ m scale bars are shown in black.

Also, as noted in the previous section, the smearing effect observed for the Ln spots deposited from glycerol containing solutions was significantly reduced when Ln360 features were spotted in PBS only and the cell attachment was then localised in a round spot area (Figure 4.8). However, smearing was not reduced by changing the printing buffer solution when BMP-2 was co-spotted in the features. Figure 4.8 allowed correlating the spot sizes and morphologies measured by fluorescence with optical microscopy pictures of cells attached on these areas.

Interestingly, more cells were attached on the “core” of the spot (indicated in Figure 4.8 by the dashed circles) than on the smeared part. This behaviour is clearly noted in Figure 4.8 for Ln360 in PBS 2% glycerol, and it appears to be related to the different protein densities immobilised in the core and the smeared parts of the spot.

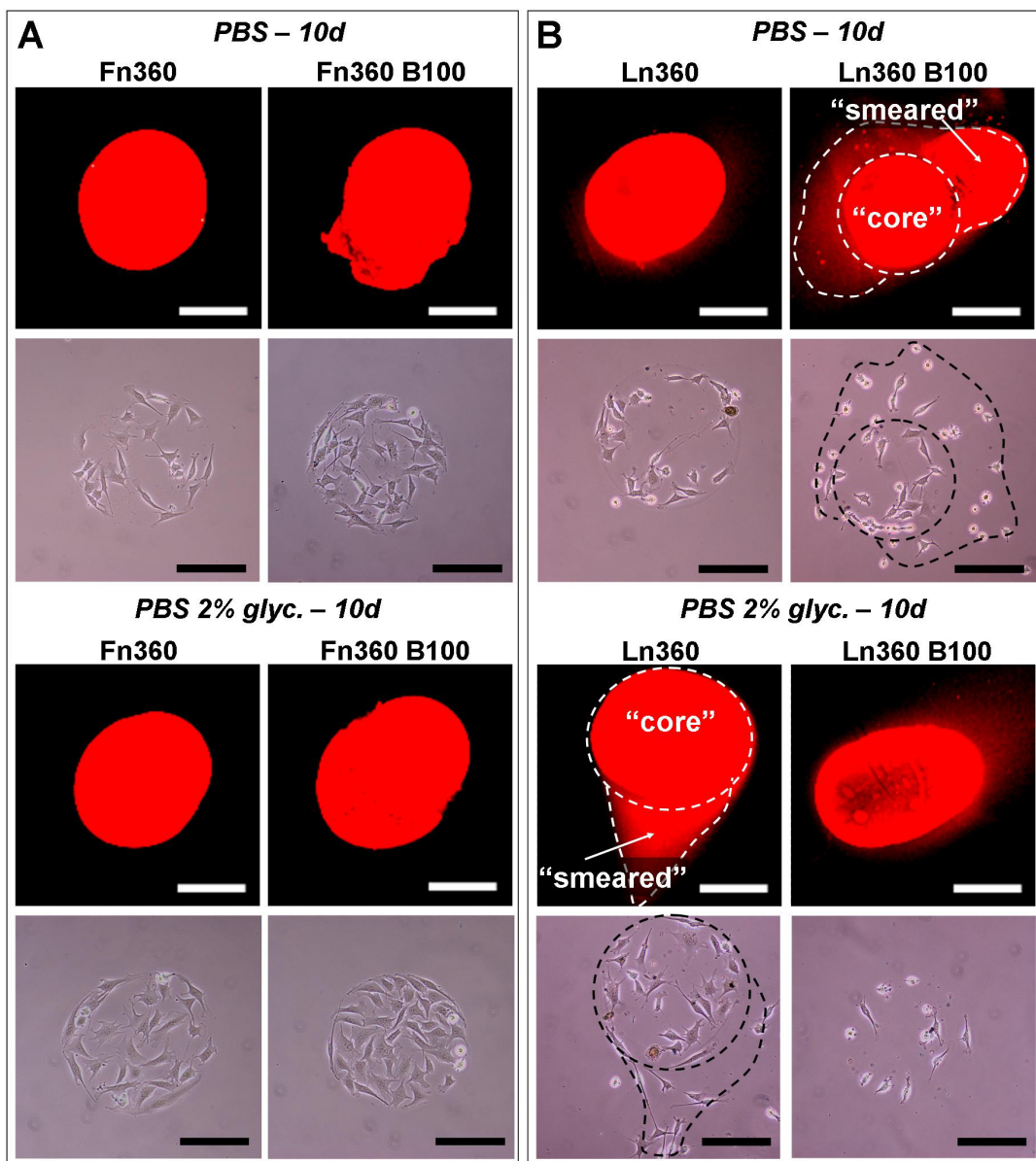


**Figure 4.8** Cell attachment on Fn (A) and Ln (B) features was correlated with the previously found spot morphology. **Top images for each spot composition:** Fluorescence images reproduced from the Fn and Ln immunostaining results presented in Figure 4.5. Dashed lines (in white) have been added to Ln spots to indicate the “core” and “smeared” parts of some of the features presented. **Bottom images for each spot composition:** Bright field images of cells attached on the corresponding spot compositions at day 0. Dashed lines (in black) indicating the “core” and “smeared” parts of some spots have also been added. Note that the smearing effect appearing for Ln spots when co-spotted with BMP-2 or when spotted in PBS 2 % glycerol correlates with cell adhesion on these areas. More cells were attached on the “core” of the spots, suggesting that a higher density of Ln was immobilised there. 200  $\mu\text{m}$  scale bars are shown in white (immunostaining images) or black (bright field images).

Next, the number of cells attached on the features at day 0 was quantified for each spot composition assayed. The results obtained are presented in Figure 4.9.

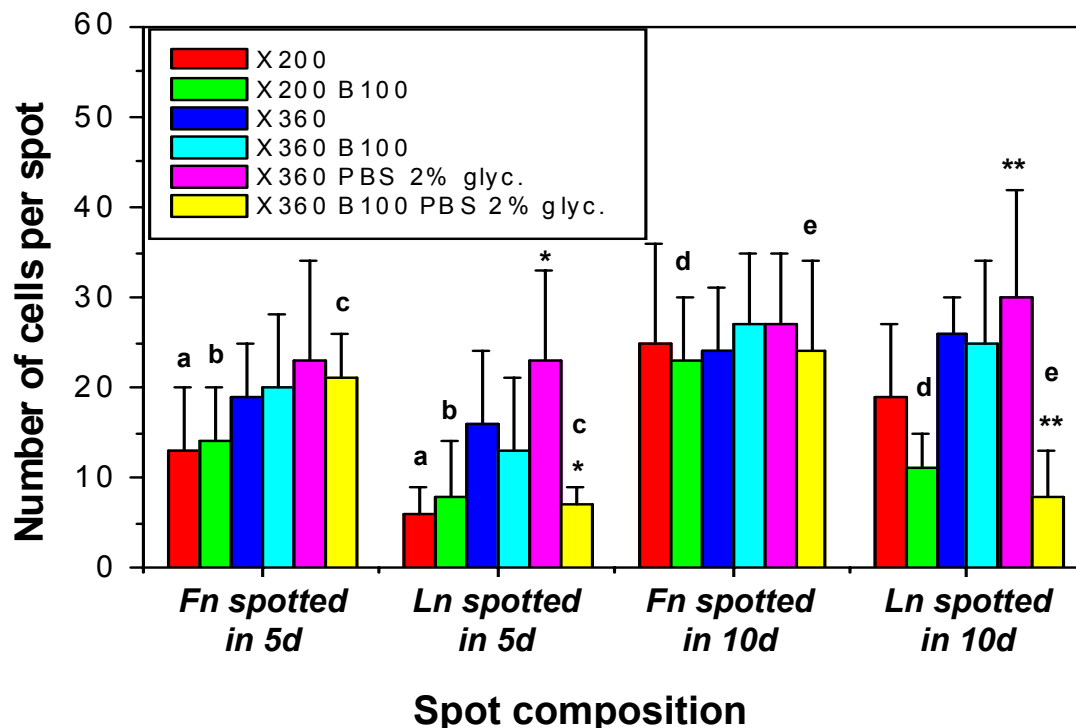


**Figure 4.9** Number of cells attached per spot composition assayed. The number of cells is indicated as mean  $\pm$  SD, calculated from 6 spots. For the bars nomenclature, an “X” represents either Fn o Ln composition, as indicated in the bottom label of the plot. For a comparison of the equivalent spot compositions spotted w/wo BMP-2 (i.e. for the same ECM protein and concentration, number of drops and printing buffer), bars marked with \* and \*\* were the only ones found to be significantly different at the p<0.05 level (One-way ANOVA test). For a comparison of the equivalent spot compositions spotted with either Fn or Ln (i.e. for the same ECM concentration, BMP-2 content spotted, number of drops and printing buffer), bars marked with a, b, c, d, and e were found to be significantly different at the p<0.05 level (One-way ANOVA test).

In general, it was observed that the inclusion of BMP-2 in the spot composition did not significantly affect the number of cells attached on the features for the same ECM protein and concentration, number of drops and printing buffer used. The only exception to this behaviour was found for Ln360 co-spotted with BMP-2 in PBS 2% glycerol, for both number of drops spotted. For these compositions, the number of cells attached on the spots was found to be significantly lower when BMP-2 was co-spotted with Ln (indicated by \* and \*\* in Figure 4.9). A detailed comparison is presented in what follows.

#### *Cell attachment to spots containing Fn*

For the Fn containing spots, it was observed that Fn360 features printed w/wo BMP-2 had a similar number of cells attached on them, and Fn200 spots (w/wo glycerol) yielded a slightly lower number of cells attached on them (yet while these Fn spots had the same area as Fn360 spots, Figure 4.4).

The results presented in the previous chapters of this thesis further support the results presented in Figure 4.9 for the number of cells attached on the spots containing Fn:

- In Chapter 2 (refer to section 2.3.6) it was demonstrated that the inclusion of a co-spotted protein (modelled by streptavidin) did not significantly affect the immobilisation of Fn, yielding similar amounts of Fn mass co-immobilised, which were in the range of 26 to 45% of the initial amount deposited. Since the spot sizes produced by solutions composed by one or two proteins did not vary either, **the overall Fn density immobilised on the spots was similar when it was spotted alone or with streptavidin.**
- In Chapter 3 (refer to section 3.4.2, Effects of the Fn concentration spotted) the cell spreading, targeted by the **Fn density immobilised on the spots**, in which cells spread better on more densely coated Fn features, **was found to affect the number of cells attached on the spots after the cell seeding and washing protocols.**

These observations supported that the inclusion of BMP-2 in the Fn spots did not significantly affect the Fn density immobilised and then the number of cells attached on these spots did not differ significantly (Figure 4.9) because cells spread similarly on both feature compositions (w/wo BMP-2). The variation of the Fn concentration spotted, on the other hand, introduced more important changes in the Fn density immobilised on the features and, therefore, fewer cells attached when Fn was spotted at the lowest concentration (Fn200 and Fn200 B100, Figure 4.9).

#### *Cell attachment to spots containing Ln*

When changing the composition of the spots by printing Ln instead of Fn, it was observed that the number of cells attached on Ln features was more dependent on the concentration of Ln spotted and the inclusion of BMP-2. In other words, larger differences were observed in the bars presented in Figure 4.9 (accounting for the number of cells per spot) for the feature compositions which included Ln as cell capture agent. In particular, it was found that fewer cells were attached on the Ln200 spots (w/wo BMP-2 in PBS, Figure 4.9) in comparison with Fn200 features. Since it was previously shown that these features yielded similar spot areas (Figure 4.4), the results presented here suggested that cells attached better to Fn than to Ln spots. The difference in the number of cells attached on the spots was not so evident when comparing the

results obtained for the Fn360 and Ln360 features (w/wo BMP-2 in PBS), suggesting that increasing the Ln concentration spotted facilitated cell attachment to these spots. The largest difference in cell attachment was found when comparing the results obtained for Fn360 B100 and Ln360 B100 features when spotted in PBS 2% glycerol (indicated as “c” and “e” in Figure 4.9). For both number of drops spotted, spots with Ln yielded less cells attached on the spots.

*Explanation assayed for the differences encountered in cell attachment*

The cell attachment mechanism to the microarray features was mediated by the spot content in Fn or Ln ECM proteins. These ECM proteins are known to interact with a specific set of cell surface receptors, called integrins, which are formed by  $\alpha\beta$  heterodimers. By integrin interactions, Fn and Ln provide cell adhesion and trigger intracellular signals which ultimately affect cell behaviour.<sup>169</sup> In fact, both Ln and Fn have been shown to be involved in cell adhesion, growth, migration and differentiation processes.<sup>50, 170</sup> A representative picture of the integrin receptor family and how they bind different ECM proteins is shown in Figure 4.10A.<sup>169</sup> The most widely described interactions for Fn involve the  $\alpha 5\beta 1$  and  $\alpha V\beta 3$  integrin receptors.<sup>171</sup> Laminin, on the other hand, binds to  $\alpha 3\beta 1$ ,  $\alpha 6\beta 1$ ,  $\alpha 6\beta 4$  and  $\alpha 7\beta 1$  integrin receptors, among others.<sup>172</sup> Noteworthy, integrin heterodimers binding to Fn (by means of its RGD receptors) differ from those binding to Ln, suggesting that different intracellular signals are modulated by integrin binding to these ECM proteins. Ultimately, when the integrin heterodimers (formed by the  $\alpha\beta$  clusters) bind to their corresponding ECM proteins, they trigger different intracellular signalling pathways that lead to the effects previously reported (Figure 4.10B).<sup>170, 173</sup>

An explanation to the differences found in the number of cells attached on the spots, when replacing Fn by Ln in the composition of the features, can be attempted based on the known fact that growth factors can affect the ECM protein/integrin interactions by modulating the production of integrin receptors and ECM proteins by cells.<sup>174</sup> The intracellular molecular signalling pathways triggered either by ECM proteins (by means of selective integrin binding) or by growth factors (by means of coupling to its receptors present in the cell membrane) are usually intercommunicated.<sup>169, 170</sup> Therefore, it was expected that cell adhesion and spreading were significantly affected by the different ECM /BMP-2 protein combinations assayed in this cellular microarray.

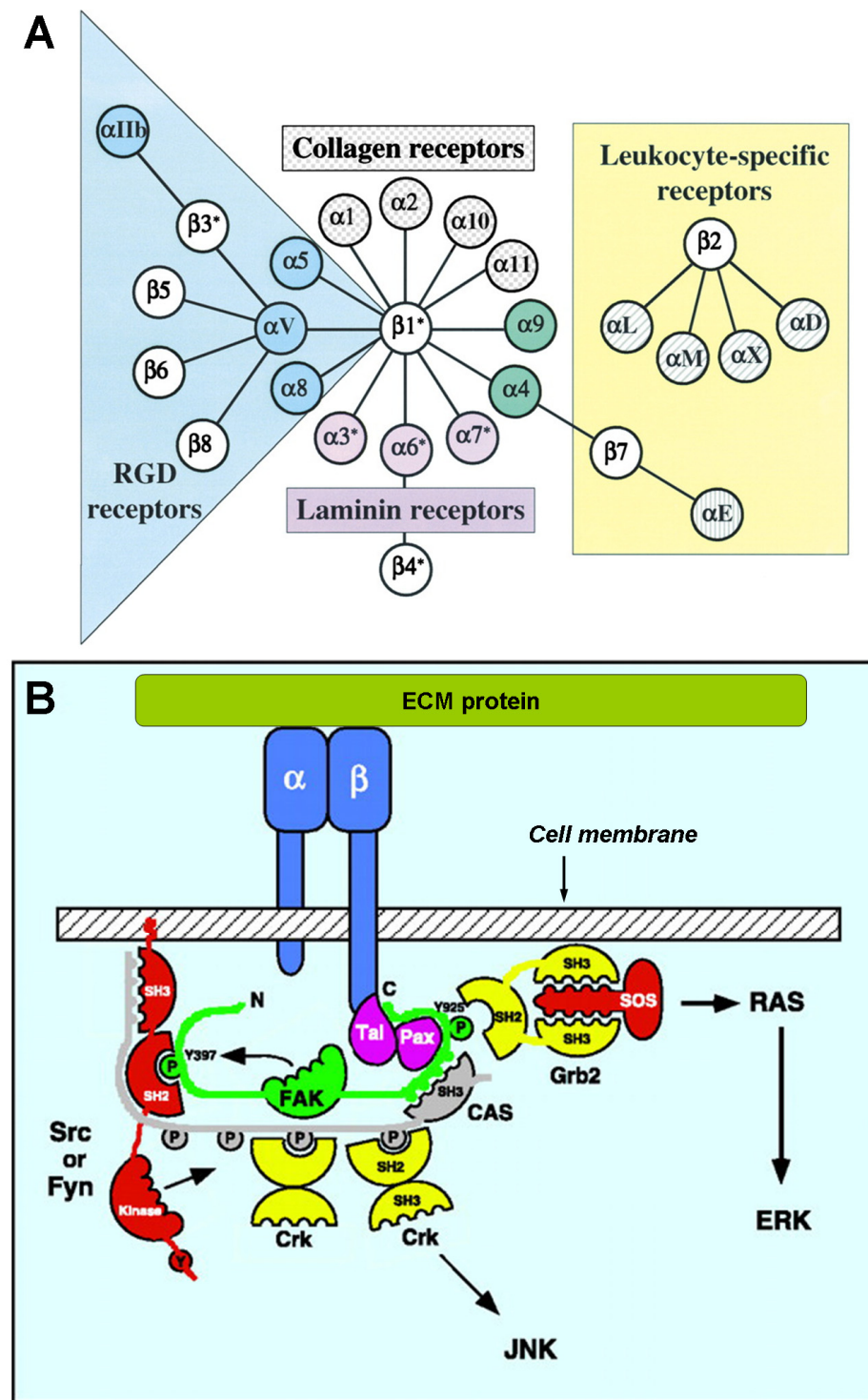


**Figure 4.10 A.** Integrin family of receptors and its associations to bind different ECM proteins, namely Collagen, Laminin and RGD containing proteins such as Fibronectin. Also, other integrin interactions with Leukocyte receptors are shown. The figure depicts the mammalian subunits and their  $\alpha\beta$  associations. Note that integrins cluster by specific  $\alpha$  subunits to the different ECM proteins shown. Asterisks denote alternatively spliced cytoplasmatic domains. Figure reproduced from cited reference.<sup>169</sup>

**B.** Proteins recruited intracellularly to the ECM protein/integrin binding site, related with the FAK pathway. Integrin heterodimers are indicated by the blue  $\alpha\beta$  cartoons. RAS, ERK and JNK are additional molecular pathways regulated by the set of proteins presented in this figure. Image adapted from cited reference.<sup>80</sup>

In particular, for BMP-2 it has been published that this growth factor can modulate cell-matrix interactions by modifying the expression of integrin-type receptors. In this case, it was found that while the expression of  $\alpha 3$  integrin (one of the mediators of cell adhesion to Ln) was downregulated in osteogenic cells, leading to a decreased number of these receptors available in the cell membrane, other types of integrins (including  $\alpha 5$  and  $\alpha V$ , involved in cell adhesion to Fn) were not affected.<sup>175</sup> A recent report showed that myogenic satellite cells did not spread on Ln coated areas when they were exposed to BMP-2 enriched medium. This behaviour was demonstrated to be caused by a novel role of BMP-2, which produced a rapid downregulation of  $\alpha 7$  integrin expression, one of the laminin receptors.<sup>176</sup>

On the other hand, cell spreading on Fn has been shown to be enhanced by cell treatment with BMP-2, and proposed to be due to an increased expression of  $\beta 1$  integrins, which was favoured by this growth factor.<sup>177</sup> Noteworthy, it was evidenced that the largest difference in cell spreading on Fn coated substrates (more rapid spreading when cells were simultaneously treated with BMP-2) took place between 10 and 20 minutes after cell seeding on the substrates. These seeding times are in the range of the ones used here.

The reports mentioned in the previous paragraphs demonstrate that BMP-2 can introduce differences in the expression (and therefore its availability on the cell membrane) of specific integrin subunits which ultimately result in differences in cell spreading, depending on the ECM protein which mediates cell anchorage to the substrate. These data is in accordance with the differences in cell spreading observed when comparing the cells attached on F360 B100 and Ln360 B100 spots (as previously noted in regard of Figure 4.7), in which the immobilised BMP-2 favoured cell spreading when co-spotted with Fn in the features. Ultimately, a rapid cell spreading during the cell seeding time, which has been associated in the previous chapter with a larger number of cells remaining on the Fn spots after the washing step, would increase the number of cells attached on the spots of the microarray presented here. In this context, the lower number of cells attached on the Ln360 B100 spots (when spotted in PBS 2% glycerol, Figure 4.9) is proposed to be due to cell detachment from these spots during the washing step, due to poor cell spreading on these features during the seeding time.

On the other hand, the difference in the number of cells attached between Fn360 B100 and Ln360 B100 (spotted in PBS) would not be so evident because cell detachment from Ln spots due to poor spreading could be compensated by a larger number of cells attached on Ln spots before the washing step (as a result of the larger spot areas produced by Ln360 B100 spots, in comparison with Fn360 B100 features, refer to Figure 4.4). This ultimately resulted in a similar

number of cells in the features after washing, and is further supported by the images presented in Figure 4.7, where it can be seen that cells attached on Ln360 B100 spots were distributed on a larger area when compared to cells attached on Fn360 B100 features.

Altogether, the data presented here suggested that co-immobilisation of Ln and BMP-2 make difficult cell attachment and spreading in the spots, and this effect was more important when the spot was printed using PBS with 2% glycerol. Therefore, the cell adhesion requirements for the cells used were better fitted by the Fn spots, which allowed to capture a similar number of cells on the spots printed with and without BMP-2.

### ***Cell proliferation on the spots***

Cellular microarrays were next characterised in terms of cell proliferation on the spots. For this purpose, cells were cultured for 24 h in serum free medium or, alternatively, in low serum medium for 4 days. The rationale for this choice was to reproduce the culture conditions that will be further assayed here for induction of osteoblast differentiation at 24 h (Osx gene expression) or at 4 days (ALP activity).

The following analysis was focused on the Fn360 and Ln360 features spotted in 10 drops in PBS, w/wo BMP-2. Similar outcome, however, was observed for all the other spot compositions assayed and was mainly dictated by the initial number of cells attached on the spots and whether it was composed of Fn or Ln. Cells were fluorescently stained, imaged by fluorescence microscopy and the number of cells per spot was evaluated at days 0, 1 and 4 of cell culture (Figure 4.11). For all the spot compositions, the number of cells attached on the spots at days 0 and 1, i.e. after being cultured for 24 h in the cellular microarray, was found to be not significantly different. However, when the microarrays were cultured during 4 days in low serum medium, it was found that cells proliferated, eventually exceeding the spot premises. In this case, the number of cells per spot showed important increases, from ~25 cells at day 0 to more than 300 cells at day 4 (Figure 4.11).

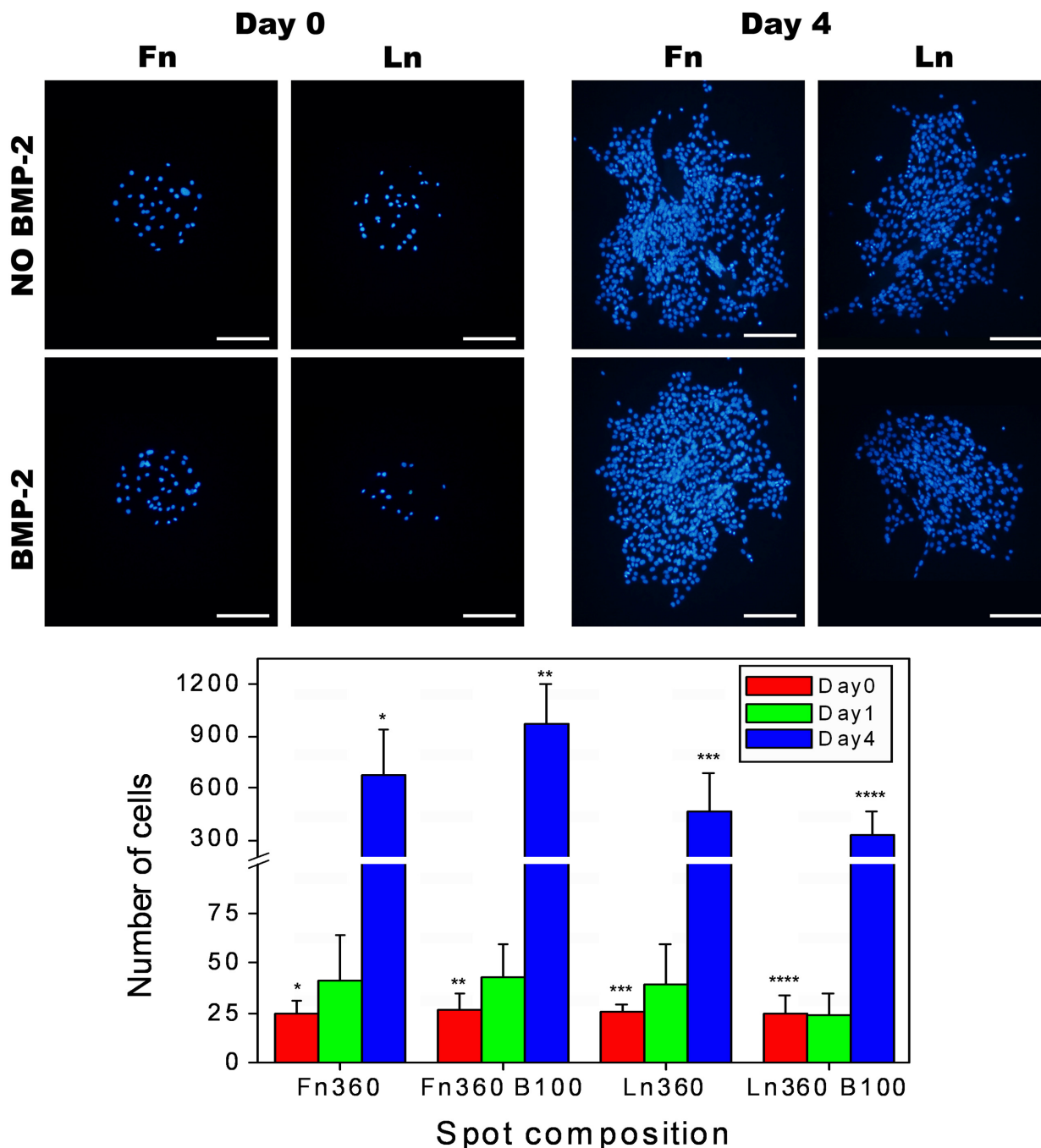


**Figure 4.11** Cell proliferation in the microarray spots. **A.** Immunostaining of cell nuclei (in light blue) at days 0 and 4 for spots composed of Fn and Ln in PBS (spotted at 360 µg/mL, prepared in PBS buffer) with and without BMP-2. Spot size is 10 drops. 200 µm scale bar is shown in white. **B.** Quantification of cell proliferation. Average number of cells on the microarray spots is shown for day 0, day 1 (for cell culture in serum free medium) and day 4 (for cell culture in low serum medium). Bars represent the mean values of 8 spots and the standard deviation associated. Bars marked with \*, \*\*, \*\*\* and \*\*\*\* are statistically different at the p<0.05 level (One-way ANOVA test).

The relatively high proliferation rate which led to the increase in the number of cells on the microarrays at day 4 was attributed in part to the small percentage of serum (i.e. 2% HS, which could include growth factors and hormones that enhance cell proliferation, even when present in

small quantities) in the medium as well as to the high proliferation rate typical of C2C12 cells. These cells have a doubling time of ~12 h when cultured in medium containing 10% serum.<sup>178</sup> Therefore, C2C12 cells seeded at low densities (i.e. being far from the confluent state) will double at least 8 times in 4 days (25 cells at day 0 would yield ~6400 cells after 4 days). However, it has been reported that variations in the cell doubling time are introduced by the amount of serum content in the culture medium. In particular, when cells were cultured in 2% serum, their doubling time was decreased to ~26 h.<sup>179</sup> With this doubling time, 25 cells would yield ~200 cells in 4 days. This value is much closer to the number of cells found here, especially for the Ln-containing spots at day 4. The Fn-containing spots, on the other hand, showed larger number of cells at day 4, suggesting an additional role of the Fn coating in cell proliferation.

It has been previously reported that Fn promotes myoblast proliferation, while Ln has been suggested to decrease cell proliferation by enhancing myoblast differentiation.<sup>82, 180</sup> These effects have been shown to be mediated by the  $\alpha 5$  and  $\alpha 6A$  integrin subunits, which increased the probability of proliferation or enhanced cell cycle withdrawal (decreasing the probability of proliferation) and promoted differentiation, respectively.<sup>173</sup> In fact, it has been widely reported that integrin signalling has profound effects in cell proliferation and differentiation.<sup>170</sup> These family of cell surface receptors was demonstrated also to mediate growth factor signalling, by enhancing or inhibiting their effects.<sup>80</sup> As previously exposed (refer to Figure 4.10), the  $\alpha 5$  integrin subunit clusters with  $\beta 1$  to bind to Fn while the  $\alpha 6A$  integrin subunit clusters to  $\beta 1$  or  $\beta 4$  to bind Ln.<sup>169</sup> In the cellular microarrays presented here, cells proliferated in both Fn and Ln-containing protein spots. However, higher proliferation was observed for the Fn containing spots, in agreement with the reported role of Fn in the enhancement of cell proliferation<sup>34</sup>. The effect of the spotted ECM proteins on cell proliferation, however, would mainly affect cell behaviour during the first 24-48 hours of cell culture. By that time, cells will have probably synthesised their own ECM.<sup>181, 182</sup>

#### 4.3.3 Cell differentiation at 24 h – Osterix gene expression analysis

In the previous section it was found that cell proliferation took place on the spots after 4 days of cell culture. For this reason, cell differentiation on the microarrays was evaluated in detail for the Osx gene expression at 24 h in this section. However, despite the spot composition is probably modified by the cells after several days of cell culture, the ALP activity of cells cultured in the microarrays for 4 days is shortly mentioned in the final experimental section of

this thesis. This was done to provide additional information regarding the effect of cell proliferation on cell differentiation.

#### ***Control cell cultures – BMP-2 added in the culture medium***

Before using the C2C12 cells for the study of cell differentiation in the cellular microarrays, their differentiation potential to the osteoblast fate was verified by means of standard cell differentiation assays. With this aim, cells were seeded at a high density to produce a semi-confluent cell culture after 1 or 2 days and allowed to spread in medium containing 10% serum, as usual for cell differentiation induction following standard protocols. After reaching the semi-confluent state, the medium was replaced with serum-free medium enriched with BMP-2 (50 ng/mL) and the cells were further cultured for 24 h.

For an earlier assessment of the effectiveness of the BMP-2 signalling, the expression of the Osx gene was analysed after 24 h of cell culture in serum free medium with and without BMP-2. It was found that, while more than 99% of the cells had green stained nuclei (indicative of Osx expression) in BMP-2 treated cultures (Figure 4.12A), cells on control cultures without the BMP2 did not expressed the marker (Figure 4.12B). According to these results, the C2C12 cells used in these experiments showed an early and measurable response to the BMP-2 factor when it was added in solution.

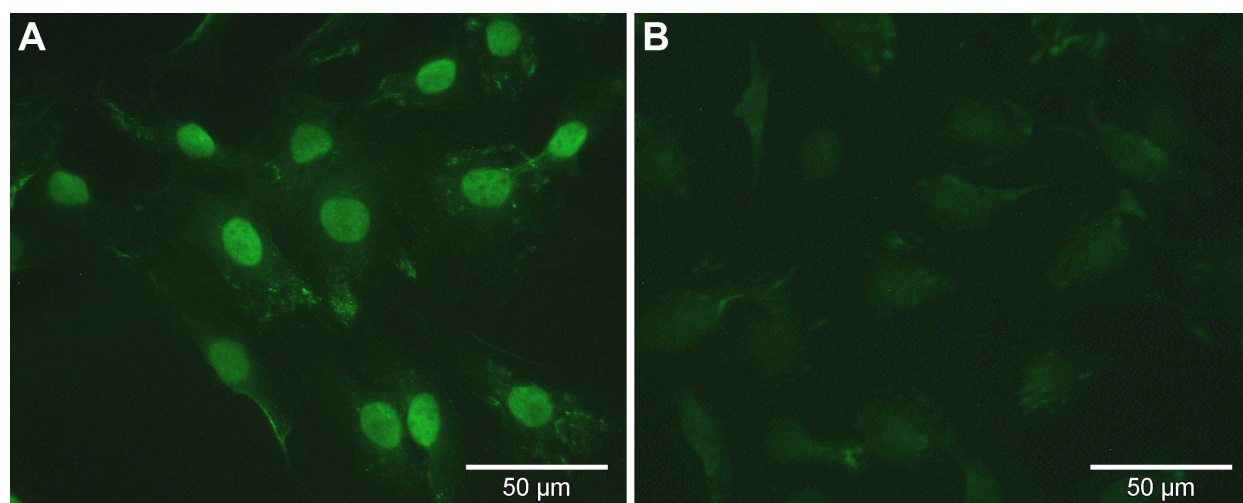


**Figure 4.12** Immuno fluorescence images for Osx expression (green nuclei immunostaining) in C2C12 cells cultured for 24 h in serum free medium supplemented with (A) or without (B) 50 ng/mL BMP-2.

#### ***Large-area protein surfaces – Cell response to BMP-2 factor immobilised on the surface***

Once it was verified that the cells used responded to the addition of BMP-2 in the culture medium by the expression of Osx, the next step was to assess whether the same response took

place when this factor was immobilised on the surface. The tests presented in this section had two aims:

- To evaluate the activity of the immobilised BMP-2.
- To assess this activity independent of the size constraints appearing when culturing cells on microarray spots and which could bias the cell differentiation response.<sup>48</sup>

For this purpose, blots of solutions composed of Fn or Ln, alone or mixed with BMP-2, were immobilised on AD-Glass surfaces and C2C12 cells were cultured on them in serum-free medium for 24 h. The concentration of the BMP-2 solution used to produce these surfaces (100 µg/mL) was the same that was used for the fabrication of the microarrays, but was lower than the concentration of the BMP-2 added in solution to the control wellplates (50 ng/mL). Considering a 26 kDa BMP-2 molecular weight ( $4.33 \times 10^{-12}$  pg), the BMP-2 concentration (100 µg/mL) and volumes (0.5 µL) used to produce the large-area protein surfaces resulted in  $1.15 \times 10^{12}$  molecules of BMP-2 deposited in each feature. On the other hand, the number of molecules that was added in the wellplate differentiation studies, in which the volume of cell culture medium (500 µL) was enriched with BMP-2 to yield a final concentration of 50 ng/mL, was  $0.58 \times 10^{12}$  BMP-2 molecules. However, since only part of the BMP-2 mass amounts deposited on the large-area protein surfaces would remain immobilised, a direct comparison based on the number of molecules used on each of these control experiments cannot be made.

Osx gene expression of the cells attached on the large-area protein surfaces was then evaluated and the results obtained are shown in Figure 4.13. For the samples where BMP-2 was immobilised, a large number of cells (~80%) showed green stained nuclei, indicating their positive Osx expression both for Fn and Ln containing surfaces. Cells growing on surfaces without BMP-2 did not show any Osx expression. It was also noticed that fewer cells attached and spread on the areas coated with Ln and BMP-2 (Figure 4.13, bottom right image) with respect to the areas coated with Ln only. This again confirms the previous results obtained with the cellular microarrays, where cell attachment was more difficult on spots of these compositions.

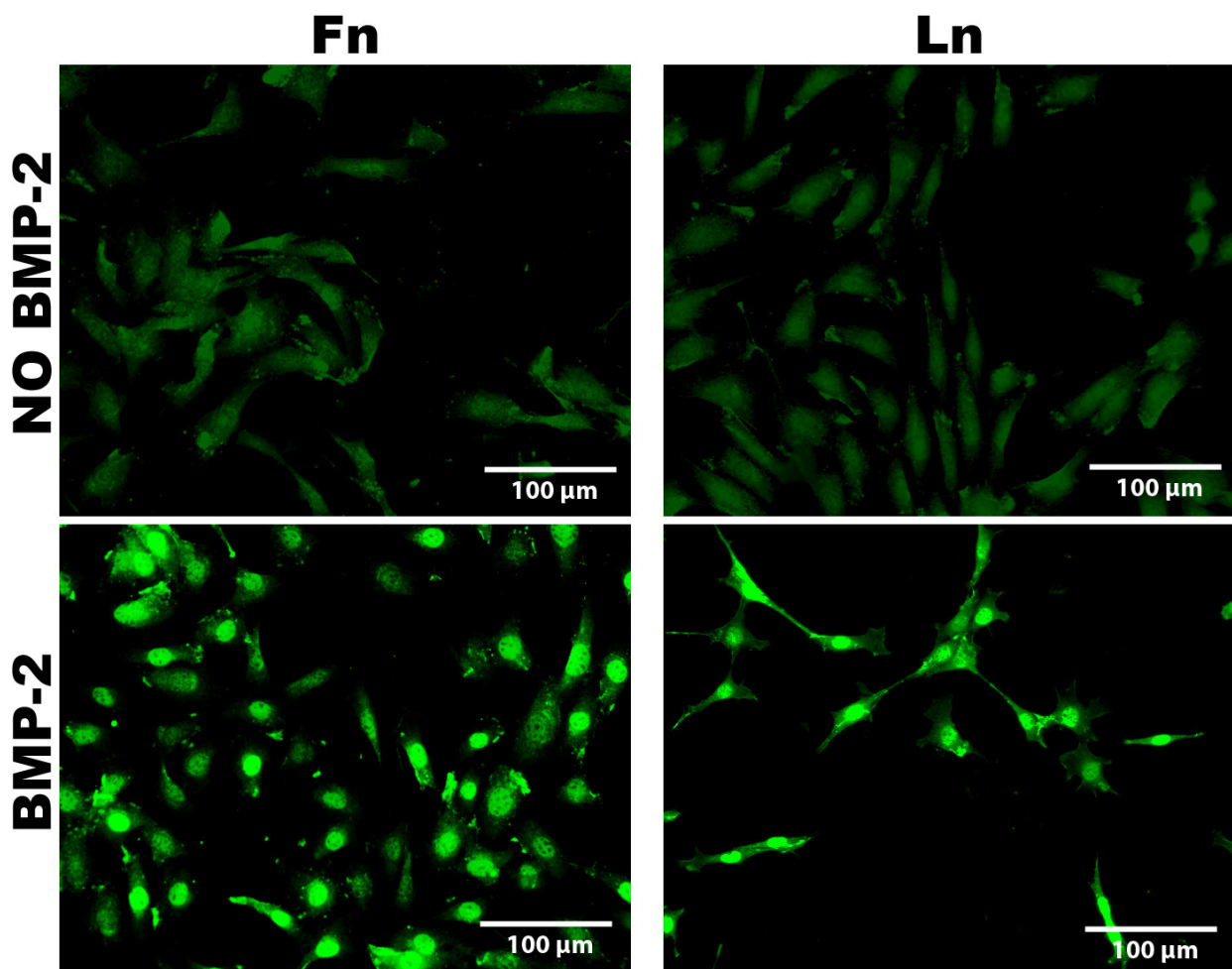


**Figure 4.13** Effect of BMP-2 immobilised in the large-area protein surfaces fabricated. Positive Osx expression was detected in BMP-2 containing surfaces (green nuclei immunostaining, bottom images).

Therefore, it was found that the BMP-2 was active when immobilised on these surfaces. Moreover, the number of cells expressing Osx was quite high (~80% of the attached cells). However, this figure was decreased when compared with the cell cultures in which the BMP-2 was added in solution (more than 99% of the cells expressed Osx). Several explanations can be proposed to account for this effect:

*1. Intercommunication of the intracellular pathways triggered by the ECM proteins and the BMP-2*

The diffusion on the cell membrane of the BMP-2 receptors bound to this growth factor can take place when the BMP-2 is added in the culture medium. The diffusion these receptors bounded to the immobilised BMP-2, on the other hand, would be highly restricted. Therefore, coupling of intracellular signals triggered by the ECM proteins and the BMP-2 could be restricted when the latter factor is immobilised.

It has been previously reported that the intracellular signals triggered by the ECM proteins are intimately coupled with the intracellular signals elicited by growth factors.<sup>169</sup> These signal transduction pathways are complex, but there is now a large body of evidence that an integrative response might be coordinated by the focal adhesion kinase (FAK) pathway and specific members of the mitogen-activated protein kinase (MAPK) cascades (including the extracellular-signal-regulated kinase, ERK, pathway, refer to Figure 4.10B).<sup>170</sup> These pathways have been demonstrated to be regulated both by ECM proteins, which generate intracellular signalling through its association with selected integrin clusters, as previously discussed, and growth factors, which generate intracellular signalling cascades by its association with the corresponding growth factor receptors present in the cell membrane.<sup>80, 160</sup> By these interactions, the recruitment of the growth factor receptors to the focal adhesions formed by integrins resulted in an enhanced phosphorylation and activation of the growth factor receptors, ultimately leading to an enhanced response to the growth factors added in the culture medium.<sup>183, 184</sup> Among other growth factors, these interactions have been suggested to take place between BMP-2 and signals elicited by integrins which bind collagen ECM proteins.<sup>185</sup>

One of the hypothesis assayed to explain how these interactions take place, involved the spatial coordination of cell receptors and intracellular signalling molecules through ECM-directed cell morphology and associated cytoskeletal changes (Figure 4.14).<sup>170</sup> By this, cell adhesion to the ECM via integrins (step 1 in Figure 4.14) activates the FAK pathway, leading to the actin cytoskeleton reorganization (steps 2 and 3) and subsequently to changes in cell shape. Since growth factor receptors and integrins are associated to the cytoskeleton, this reorganization allows its coupling in focal adhesions (step 4), ultimately leading to activation of the ERK signal transduction pathway (step 5).

Therefore, the decrease in the Osx expression observed here between cells cultured on wellplates (exposed to soluble BMP-2) and cells attached on areas with immobilised BMP-2 and Fn or Ln could be attributed to the difficulty in allowing the previously presented recruitment of integrins and BMP-2 receptors, once they have bound to its corresponding immobilised counterparts (i.e. Fn or Ln with integrins, and BMP-2 with its receptors).

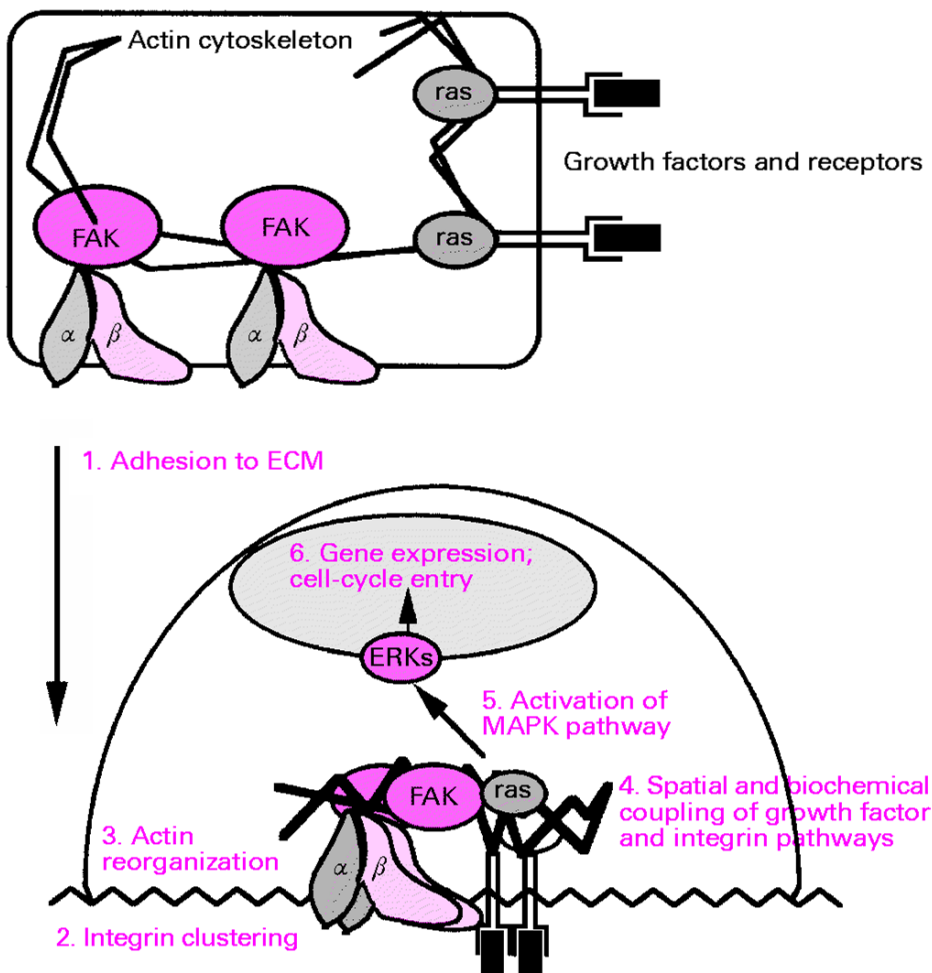


**Figure 4.14** Hypothetical model showing the coupling of the ECM/integrin and growth factor receptor pathways associated with integrin-dependent changes in cell shape. Growth factors binding to its receptors initiate the signalling pathway mediated by the ras protein. Cell adhesion to the ECM via integrins (1) activates the FAK pathway, leading to the actin cytoskeleton reorganization (2, 3) and subsequently to changes in cell shape. Since growth factor receptors and integrins are associated to the cytoskeleton, this reorganization allows its coupling in focal adhesions (4), ultimately leading to activation of the ERK signal transduction pathway (6). Image adapted from cited reference.<sup>170</sup>

## 2. More complex ECM matrix synthesised in the wellplate cell cultures

For the control wellplate experiments, the cells were cultured for 1 to 2 days before the addition of the BMP-2. In this case the cells did probably synthesise a complex ECM on which they were attached at the time of BMP-2 exposure.<sup>181</sup> On the other hand, cells cultured on the surfaces with immobilised BMP-2 received the factor stimulus right after cell seeding, and were therefore attached on a simplified ECM composed of Fn or Ln only. These differences in the ECM composition could additionally account for the enhanced Osx expression found in the wellplate cultures by forming more complex focal adhesions (i.e. composed of several distinct integrin ligands). This issue will be exposed in more detail in the following subsection.

### 3. Other effects related to the efficacy of the signalling by the immobilised BMP-2

Other issues such as low amounts of the growth factor immobilised, partial denaturation and incorrect orientation of the immobilised BMP-2 were difficult to evaluate that cannot be discarded. The effective density of the growth factor immobilised in an active conformation was difficult to assess. On the other hand, other effects could be related to the difficulty of the immobilised BMP-2 to interact with the BMP-2 receptors on the cell membrane due to the covering of the relatively small BMP-2 (26 kDa) by the much larger ECM proteins spotted (550 and 800 kDa for Fn and Ln, respectively), as well as by the BSA carrier protein (66 kDa).

All of the previously exposed reasons could lead to a decrease of the BMP-2 signalling when immobilised and would ultimately lead to a loss of efficiency in the induction of Osx expression when compared to the BMP-2 present in a soluble form.

Growth factors immobilised on AD-Glass have been previously reported to influence cell differentiation by Soen et al.<sup>48</sup> In this work the response of cells to surface immobilised growth factors as well as to the same factors solubilised in the culture medium was evaluated. The concentrations used for evaluation of these two presentation forms of the growth factor were much higher for the immobilisation of the factors than for the corresponding solubilised assays (e.g. immobilised BMP-4 was printed from a 70 $\mu$ g/mL solution and soluble BMP-4 was used at 250 ng/mL), as also assayed in the experiments presented here. These authors reported that the printed proteins were “generally functional, and able to induce cellular responses similar to those induced by the molecules in solution”. However, they found it difficult to make a quantitative comparison of the differentiation efficiency when exposing the cells to solubilised or immobilised growth factors, in part due to the complexity of characterising the “effective” (meaning the amount of growth factor immobilised in an active conformation and orientation) growth factor density immobilised on the spots, as also found in this chapter.

### **Control cellular microarrays – BMP-2 added in the culture medium**

To further analyse the effect of BMP-2 on Osx expression when the cell culture was restricted to the microarray spots, cellular microarrays with spots composed only of ECM proteins (Fn and Ln in PBS buffer) were exposed for 24 h to serum free medium containing BMP-2 (50 ng/mL). Then, the microarray was tested for Osx gene expression and the results are summarized in Figure 4.15.

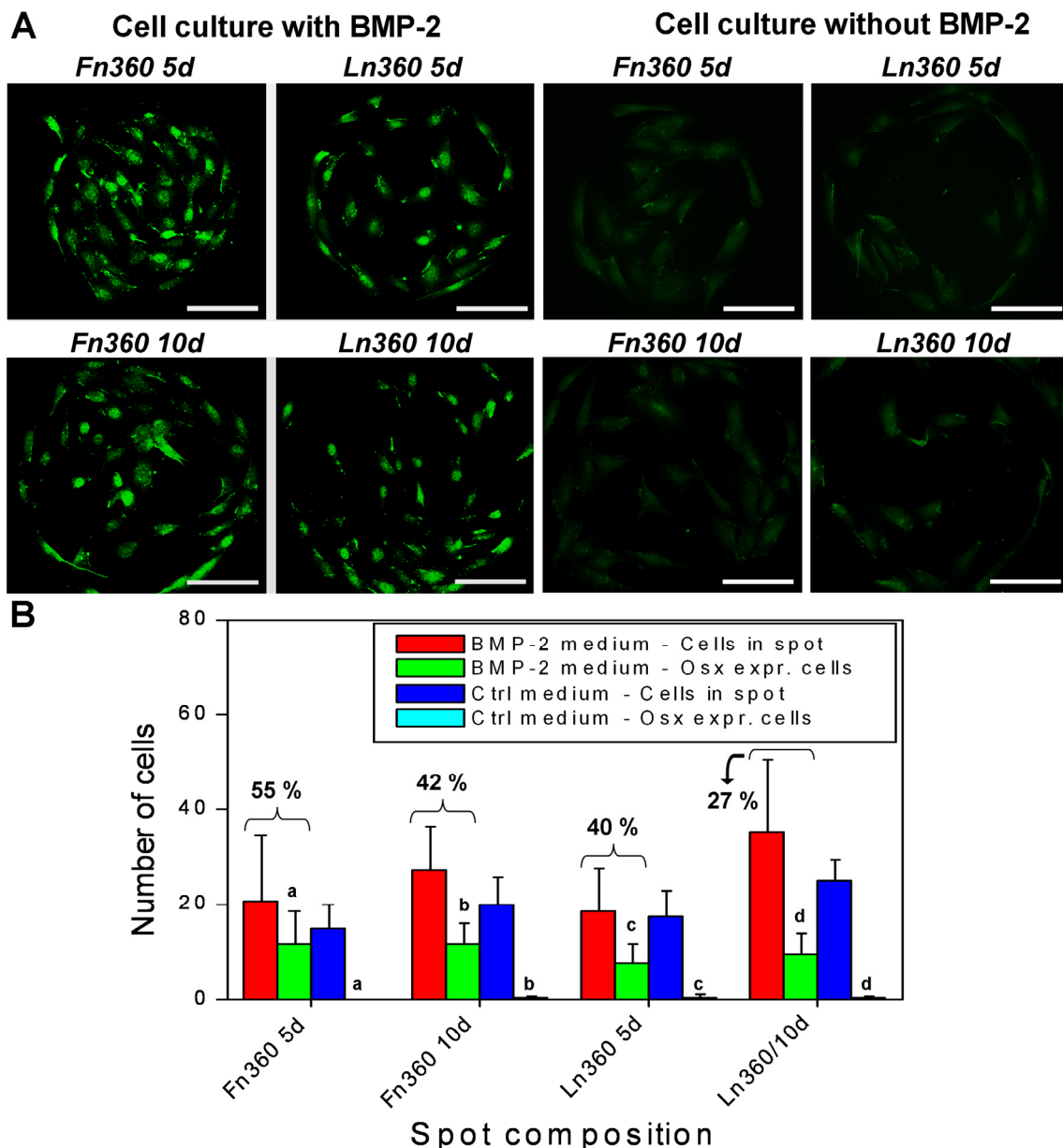


**Figure 4.15** Osx expression in cells attached on the Fn and Ln control features spotted in PBS. **A.** Osx immunostaining (nuclei in green) of cellular microarrays fixed after 24 h of cell culture in serum free medium with (left images) and without (images on the right) a BMP-2 supplement (50 ng/mL). Spot composition is indicated at the top of each image. 100 $\mu$ m scale bars are shown in white. **B.** Quantification of the total number of cells attached on the spots at day 1, and the number of these cells which showed Osx expression when the microarrays were cultured in serum free medium with (BMP-2 medium) or without (Ctrl medium) BMP-2. Percentage (of total number of cells in the spots) of Osx expression is also presented on top of each pair of bars for the microarrays exposed to BMP-2. Bars represent the mean values of 8 spots and the standard deviation associated. For Osterix expressing cells, bars labelled as a, b, c, d, denote a statistical difference of  $p < 0.05$  (One-way ANOVA test).

It was found that the number of cells with green stained nuclei (accounting for Osx expression) in response to the BMP-2 added in solution oscillated between 27 and 55% of the total number of cells per spot, depending on the spot composition (Figure 4.15B). When the

cells were cultured without BMP-2, they showed a negligible Osx expression. These data pointed out that Osx expression was induced by BMP-2 when added to the culture medium, independently of the spot composition (Fn or Ln). However, these results also showed that the culture of the cells on isolated spots produced a decrease in Osx expression when compared to the wellplate experiments.

The main differences between the wellplate cultures and cell culture on the control microarrays (schematised in Figure 4.16) reside in the restriction of cell spreading and the higher complexity of the ECM composition that aroused in the wellplate assays. These differences are explored in what follows.

### *1. Limitation of cell spreading in wellplate cultures*

As previously described for the wellplate assays, before adding the serum free medium supplemented with BMP-2, the cells were first seeded and cultured for 1-2 days in growth medium (10% FBS) to achieve a semi-confluent cell culture. In this state, cells have restrictions in their spreading as not much substrate area is available for them (Figure 4.16C).

On the other hand, cells attached on the microarray spots were cultured in small numbers (spreading was not restricted, Figure 4.16B). The cell culture medium in this case was the serum-free medium containing BMP-2 from day 0. Cell spots at day 0 (Figure 4.9) and at day 1 (Figure 4.15) showed that, during these time, cells attached and spread but did not proliferate on the spots. Therefore, cell-cell signalling, which is very relevant for semi-confluent cultures, was avoided and the main signalling to induce cell differentiation was coming only from the BMP-2 added in solution.

It has been published that spread cells induced osteogenesis, while spreading restrictions favoured adipocyte differentiation in MSCs in which cell proliferation was chemically inhibited.<sup>138</sup> In this report, the RhoA signalling pathway has been suggested as an integrator of cell spreading and growth factor signalling in the regulation of mesenchymal stem cell (MSC) differentiation. As exposed by the authors, RhoA signalling by cell shape could occur through multiple mechanisms, suggesting that cell spreading restriction could be integrated into different signalling pathways depending on the cell type and culture conditions assayed. This report underscores the importance that the integration of signals coming from cell spreading and growth factor signalling have on cell differentiation.

Therefore, for the cell type and culture conditions assayed in the work presented here, spread restrictions could elicit an enhanced osteoblast differentiation response in C2C12 semi-confluent

cultures exposed to BMP-2, which was diminished in cell cultures without limitations in their spreading possibilities.

## 2. Increased complexity of the ECM in the wellplate cultures

Another fact to be taken into account is that the cells seeded in wellplates were initially cultured in growth medium (10% FBS) for 1-2 days to achieve the semi-confluent state before adding the serum free medium enriched with BMP-2. The cells seeded on the microarrays, on the other hand, were cultured in the serum free medium enriched with BMP-2 from the very beginning after the seeding time was over.

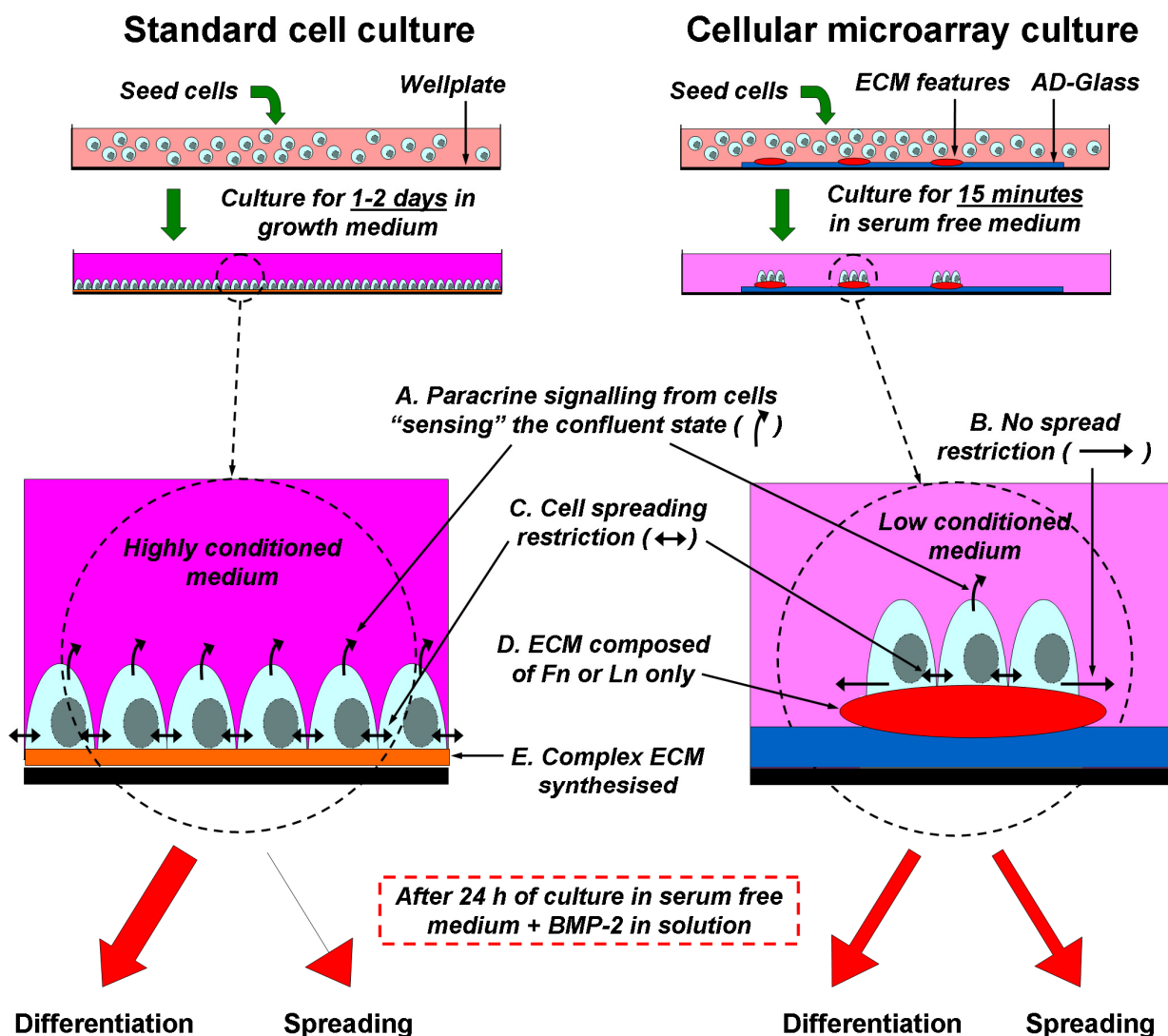


**Figure 4.16** Schematic showing the response of cells when cultured in standard wellplates or in the cellular microarrays and BMP-2 was added in the culture medium. In standard wellplate cultures, the highly enriched medium and the complex ECM produced by the cells can affect the BMP-2 signalling and therefore optimise the differentiation response.

Myoblasts cultured in standard wellplates have been shown to synthesise a complex ECM matrix microenvironment.<sup>181</sup> Therefore for the wellplate cultures previously assayed, the cells could be attached on a more complex ECM (Figure 4.16E) at the time of BMP-2 exposure. On the other hand, cells attached on the microarray spots were influenced by the Fn or Ln immobilised on the spots, this constituting a very simple ECM base (Figure 4.16D). As a result, the increase in complexity of the underlying ECM could optimise growth factor signalling by the recruitment of additional integrin types as well as by providing additional binding sites for BMP-2 due to the presence of other ECM proteins such as collagens.<sup>80, 185, 186</sup>

An additional issue adds complexity to the analysis presented here. When cells in the wellplates sense the semi-confluent state through cell-cell contact and cell spreading limitations, they could produce additional signalling through the secretion of factors to the culture medium (known as cell paracrine signalling, Figure 4.16A). This factor secretion would enrich the cell culture medium much faster when thousands of cells are cultured in wells of the wellplate (where the typical volume of medium used is ~500 µL) than when discrete numbers of cells (10s to 100s of cells) are cultured in the microarrays (where the typical volume of medium added to the Petri dishes, in which the microarray slide was placed, was 10 mL). In other words, the paracrine signalling was highly diluted in the culture medium for the microarray case. Ultimately, this signalling could give priority to a differentiation pathway when cells are in what is called a semi-confluent state.<sup>80</sup>

Altogether, the results obtained and the differences exposed among the cell differentiation experiments performed in wellplates or in microarray format, suggested that when few cells are cultured in isolated spots they can show a decrease in the Osx expression (larger than 50% in some cases) due to the lack of cell-cell additional signalling or complex microenvironments.<sup>186</sup>

### ***Cellular microarrays with BMP-2 immobilised on the spots***

The expression of Osterix was finally analysed in cells cultured for 24 h on microarrays with BMP-2 immobilised on the spots. The results obtained are shown in Figure 4.17.

It was detected that a small percentage (20 to 24%) of the cells attached on all spots containing BMP-2 showed Osx expression, whereas for all spots without BMP-2 a negligible Osx expression was detected. This unequivocally verified that Osx expression was produced by the BMP-2 factor immobilised on the substrate surface. No significant differences were found in the number of Osx expressing cells for the different spot compositions which included BMP-2, presented in Figure 4.17. This suggested that the BMP-2 signalling was not importantly affected

by the ECM protein co-spotted (i.e. Fn or Ln), when looking at the Osx differentiation marker at 24 h.

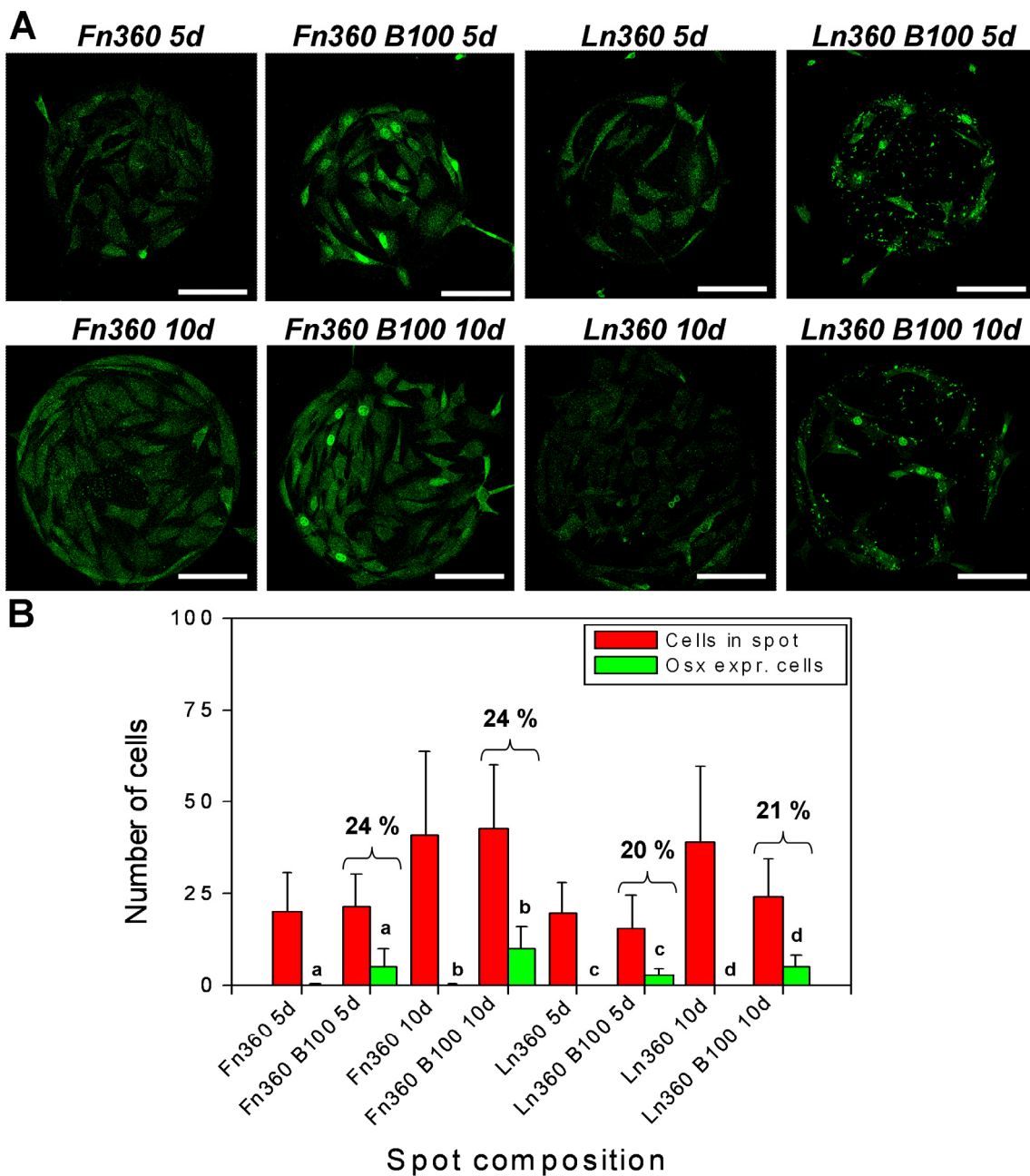


**Figure 4.17** Osx expression in Fn and Ln features spotted with and without BMP-2 in PBS buffer. **A.** Osx immunostaining of cellular microarrays fixed after 24 h of cell culture in serum free medium. Cells in spots printed with BMP-2 showed Osx expression (indicated by green nuclei staining) while control spots did not. Spot composition is indicated at the top of each image. 100 $\mu$ m scale bars are shown in white. **B.** Quantification of the total number of cells attached on the spots at day 1, and the number of these cells which showed Osx expression. Percentage (of total number of cells in the spots) of Osx expression is also presented on top of each pair of bars for the BMP-2 containing spots. Bars represent the mean values of 8 spots and the standard deviation associated. For Osterix expressing cells, bars labelled as a, b, c, d, denote a statistical difference of p<0.05 (One-way ANOVA test).

The relative amount of cells expressing Osx in the spots with immobilised BMP-2 was lower than the values found for cellular microarrays treated with BMP-2 in solution (from 27% to 55%, Figure 4.15). This decreasing can be attributed to the immobilisation of the BMP-2. As previously noted for the control experiments of BMP-2 immobilised on large-area protein surfaces, the immobilisation of BMP-2 could limit ECM/integrin and growth factor/receptor clustering or decrease the activity of the BMP-2 due to incorrect orientation or partial denaturation.

Regarding the effects of the buffer solution used for the protein printing, it was found that spots printed with Fn or Ln and BMP-2 in PBS 2% glycerol had much lower Osx expression (<12%, Figure 4.18) than spots printed with PBS only. Results from Chapter 2 showed that when PBS 2% glycerol was used as printing buffer, negligible amounts of SA were found immobilised on the surfaces. It could be argued, as noted in the previous chapter, that less BMP-2 was retained on the surface since glycerol decreased evaporation of the solution and part of the BMP-2 deposited could be washed off during the BSA passivation procedure. The low but measurable Osx expression detected in BMP-2 containing spots printed in PBS 2% glycerol solution can be accounted by the following rationales:

- The BMP-2 was better retained on the surfaces than the SA, probably due to a higher affinity of the BMP-2-BSA complex to react with the surface chemistry or by a higher affinity between the BMP-2 and the immobilised ECM proteins co-spotted. In the later case, the BMP-2 would be indirectly retained in the spots by its binding to the ECM proteins.
- An extremely low amount of BMP-2 immobilised, detected in section 4.3.1 by an indirect immunofluorescence approach (which produced an important amplification of the signal), would be able to induce a differentiation response.

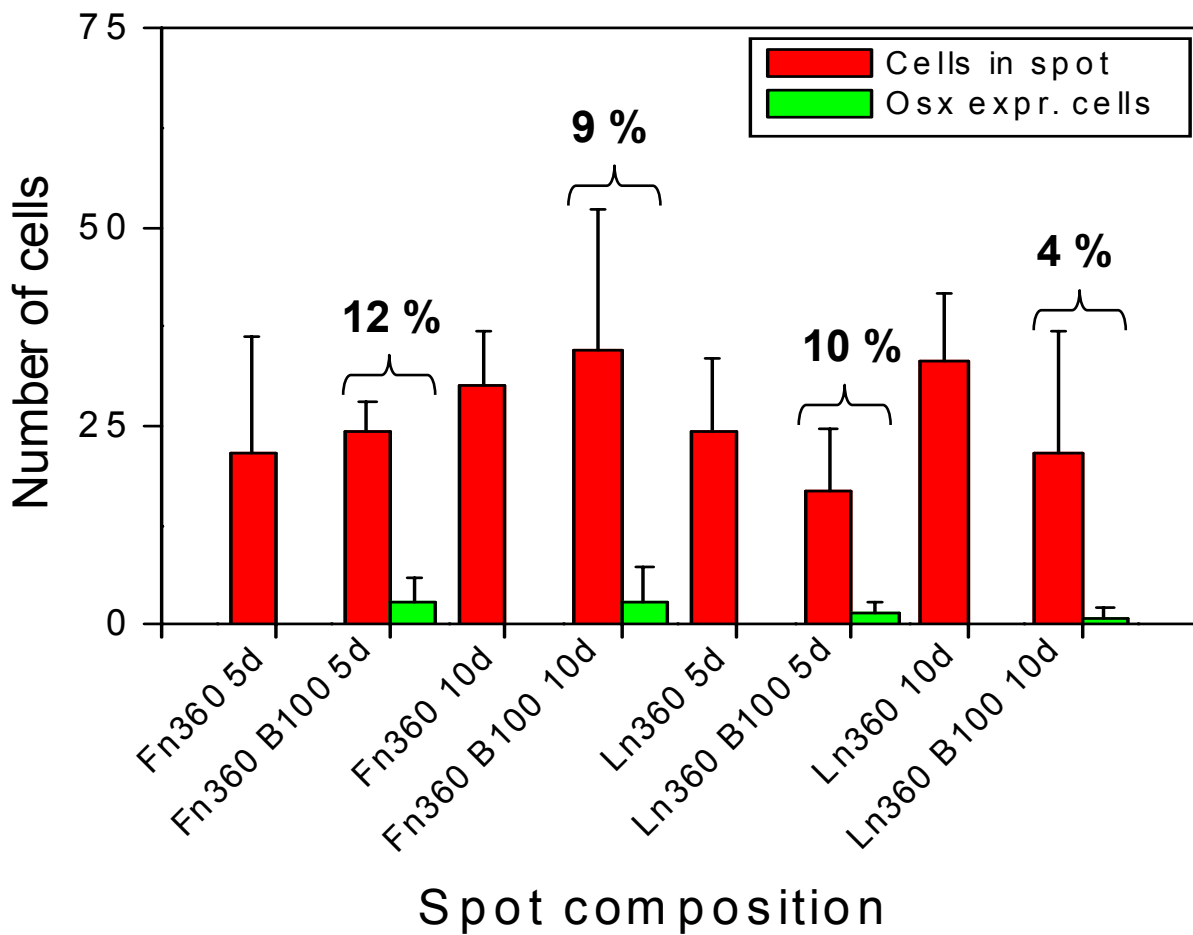


**Figure 4.18** Quantification of Osx expression in Fn and Ln features co-spotted with and without BMP-2 in PBS 2% glycerol buffer. Percentage (of total number of cells in the spots) of Osx expression is also presented on top of each pair of bars for the BMP-2 containing spots. Bars represent the mean values of 8 spots and the standard deviation associated

In an attempt to summarise the results presented in this section, Figure 4.19 shows a schematic of the cell differentiation response on the different cell culture conditions assayed: standard wellplates (A), cellular microarrays with soluble BMP-2 (B) and cellular microarrays w/wo immobilised BMP-2 (C and D). As previously noted, wellplate cell cultures yielded Osx expression in ~99% of the cells exposed to soluble BMP-2, while restricting the size of the cell culture to the microarray dimensions decreased Osx expression from 50 to 60% (for Fn spots). This was presumably due to the lack of signalling coming from semi-confluent cell cultures. When immobilising the BMP-2 on the microarrays (instead of delivering it in solution), the Osx expression additionally decreased down to 24%.

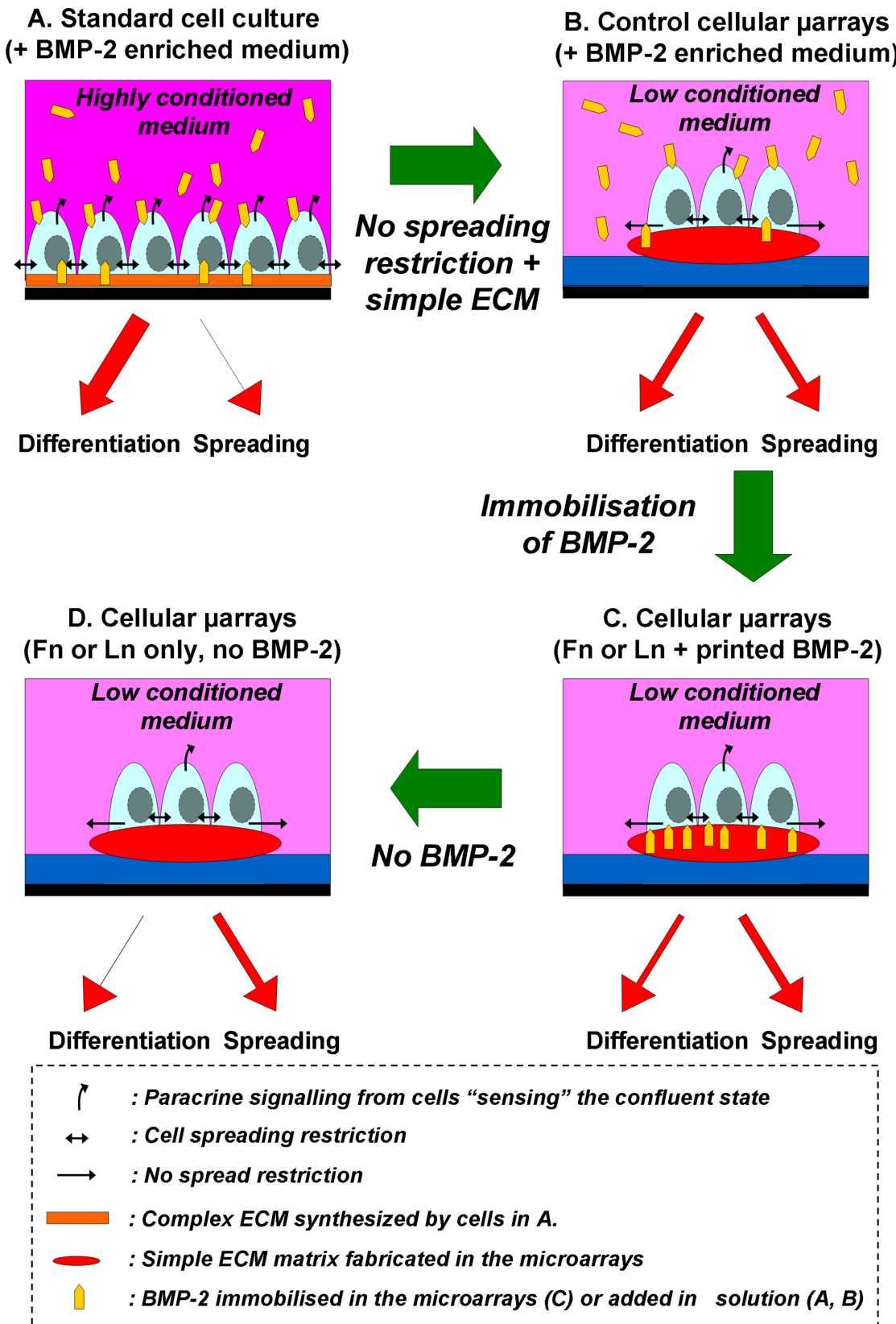


**Figure 4.19** Schematic showing the proposed cell differentiation integrative response for cells cultured in standard wellplates (A) and in control cellular microarrays (B), both exposed to BMP-2 enriched medium, and also for cells cultured in cellular microarray spots with (C) or without (D) BMP-2 included in the spot composition.

#### **4.3.4 Cell differentiation after 4 days – ALP activity analysis**

The ALP activity of C2C12 cells at day 4 was assessed to further evaluate the effect that the cell proliferation on the spots, described in the previous section, could have on the differentiation of these cells. It is known that cell proliferation and cell differentiation are mutually excluded pathways. An analysis of the ALP expression that could eventually take place in the cellular microarray platform developed here, however, could yield interesting insights into the future direction that the optimisation of this platform should follow. With this aim, in this section the ALP activity was studied only for the cells cultured for 4 days in the BMP-2 printed microarrays. A reference control experiment, consisting in evaluating the ALP activity induced by solubilised BMP-2 when cells were cultured in standard wellplates, was also included to discriminate the potential of the cells used to express this marker.

##### ***Control cell cultures – BMP-2 added in the culture medium***

For the analysis of a medium term cell differentiation response to BMP-2, ALP activity levels were assessed on cells cultured in wellplates, after 4 days of culture in low serum (2% HS) medium with and without BMP-2 (50 ng/mL) in solution.

After the staining for ALP, magnifying glass and microscopy pictures of the corresponding wellplates were taken and the results obtained are shown in Figure 4.20. ALP activity is observed as blue/violet staining of cells. C2C12 cells responded to BMP-2 in solution with a moderate ALP activity at day 4 (Figure 4.20A). On the other hand, the ALP activity was negligible in the culture control performed without the addition of BMP-2 (no staining in Figure 4.20B). This was expected since the C2C12 cells are myoblastic cells, and it has been widely reported that they differentiate to myocytes when cultured in low serum medium. From the results presented, it was shown that C2C12 were responding to BMP-2 by increasing their ALP activity, which can be detected from day 4. The activity of this marker was more difficult to quantify from the histological stainings. It was evaluated to be expressed in 10 to 20% of the cells, based on the area of the image presented in Figure 4.20A which showed at least some blue to violet staining.

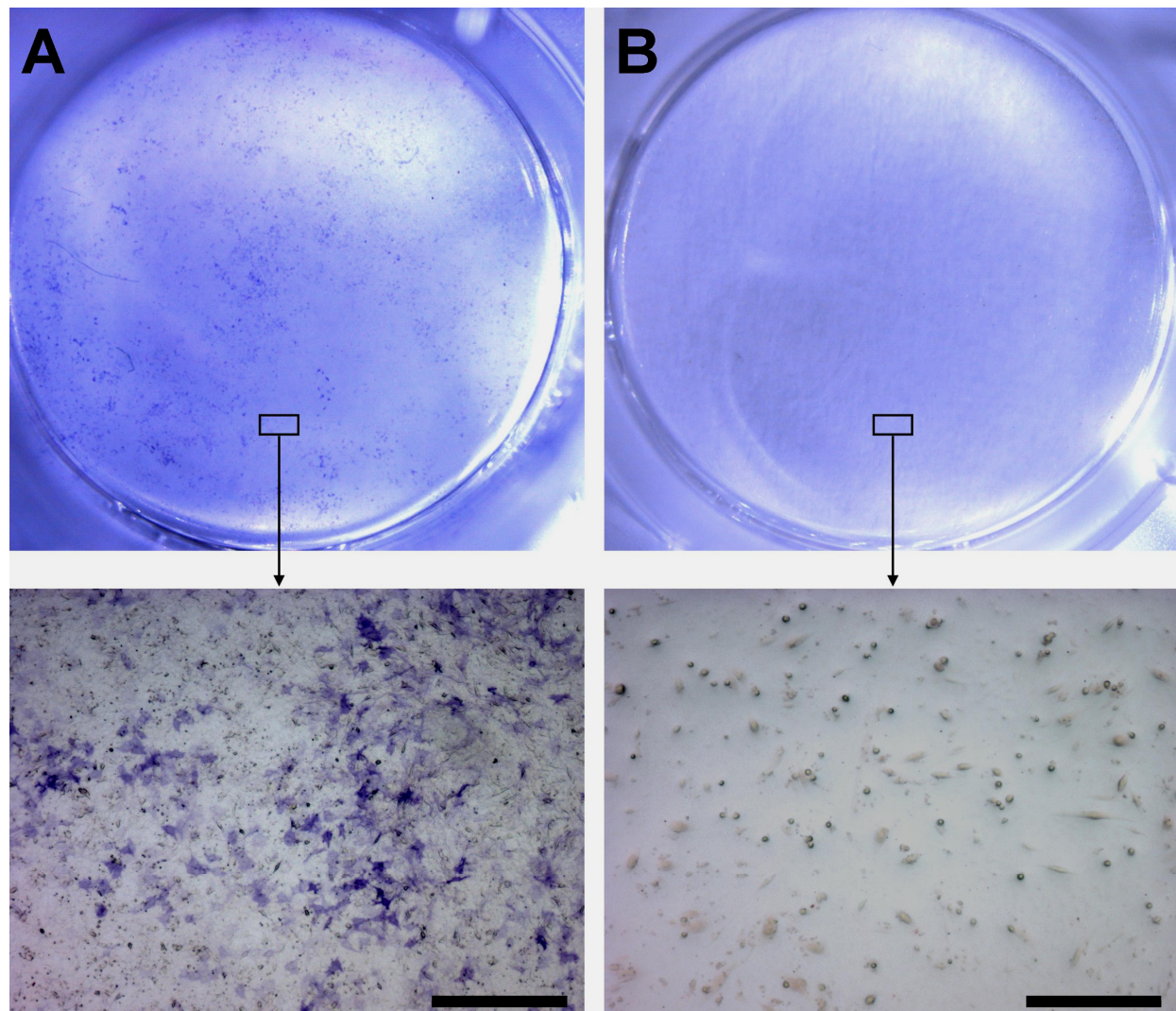


**Figure 4.20** ALP activity after 4 days of cell culture in low serum medium (2% HS) supplemented with (A) and without (B) 50 ng/mL BMP-2. Cells seeded in parallel wells of 48 wellplates. Top: images obtained with a magnifying glass. Bottom: detailed images obtained with a bright field microscope. 500  $\mu$ m scale bars are shown in black.

#### ***Cellular microarrays with BMP-2 immobilised on the spots***

With the aim of assaying whether the ALP activity results obtained with the wellplate cultures were reproduced through BMP-2 immobilised on the microarray spots, cellular microarrays were seeded with C2C12 cells as previously described and further cultured in low serum medium for 4 days.

When looking at the ALP activity of the cells cultured in the microarrays, results presented in Figure 4.21 exposed that few cells attached on spots printed with BMP-2 expressed this marker. Cells on control spots, with no BMP-2, were not positive at all for ALP staining.

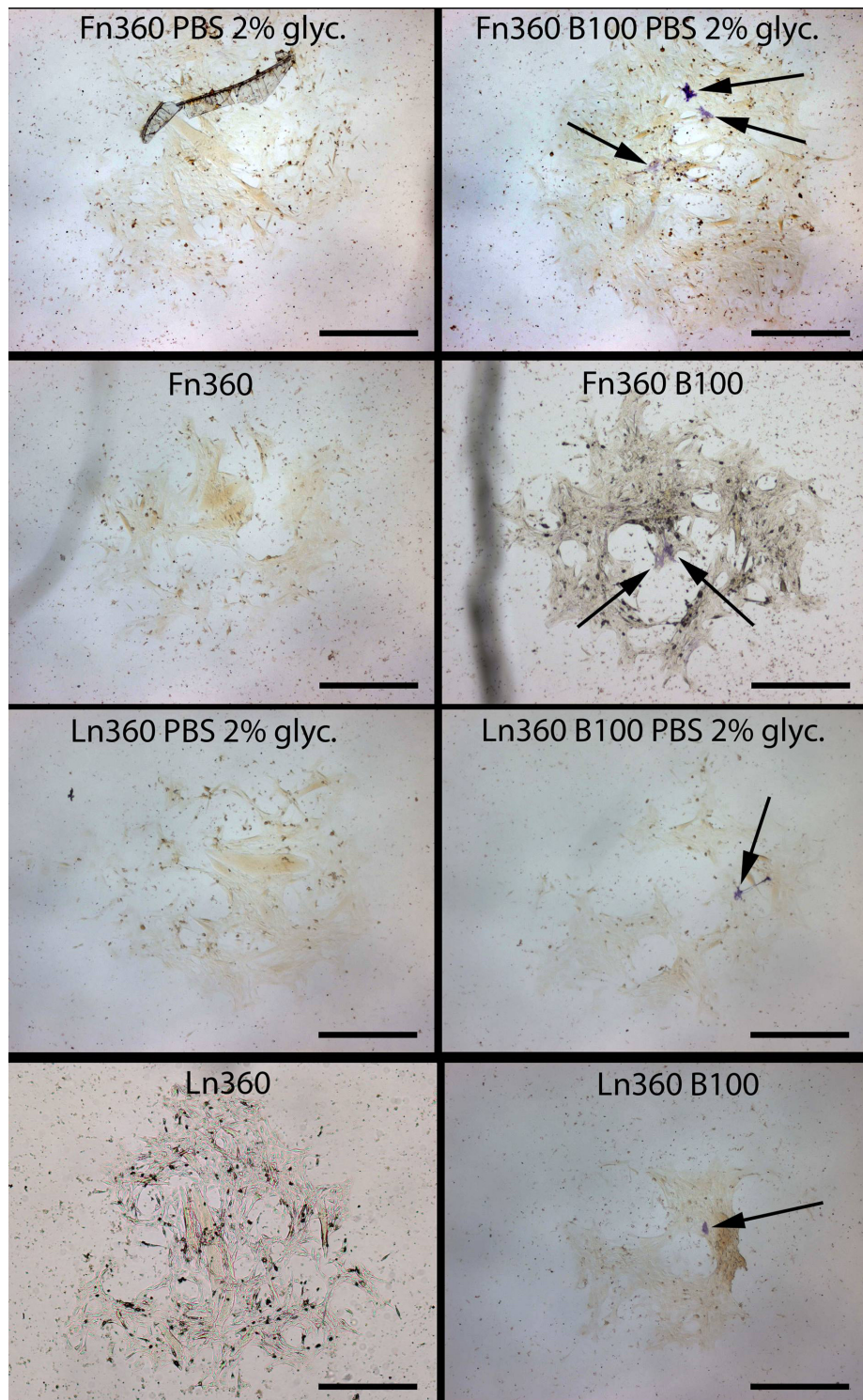


**Figure 4.21** ALP staining of cells in the cellular microarray, fixed after 4 days of culture in low serum medium. Spot size is 10 drops. Features printed with BMP-2 showed ALP staining in some of the cells at a very low rate (indicated by arrows) while control spots (only Fn or Ln) did not have ALP stained cells. Spot composition is indicated at the bottom of each image. 500  $\mu$ m scale bars are shown in black.

The ALP positive staining obtained for the BMP-2 containing spots was very low, with only 2 or 3 ALP stained cells from 300 to 1000 cells attached on the spot premises and its surroundings. As previously noted, an important rate of cell proliferation was detected in cells

attached on the spots after 4 days of cell culture, with cells eventually exceeding the spot premises. Therefore, not all the cells counted on the spots at day 4 were actually exposed to the signalling coming from the spot (at least not the cells that were attached beyond the spot premises). It was extremely difficult to evaluate the original limits of the spotted feature from the histological staining images presented. Therefore the 2 or 3 cells expressing ALP presented in Figure 4.21 could account for differentiated cells from a smaller cell population of ~25 cells which were initially attached on the spots at day 0, and which were exposed to BMP-2 from the beginning of the cell culture in the microarrays.

The quantification of the amount of BMP-2 immobilised on the spots appeared here as an extremely challenging task. Indirect immunostaining of the microarrays without cells (after passivation only) suggested that this factor was retained on the spots. However, to appropriately quantify the amounts of BMP-2 remaining on the spots after 4 days of cell culture on the microarrays, the implementation radioactive labelling of BMP-2 would be highly appreciated and is one of the main topics to deal with for the future optimisation of this platform. These results could allow decoupling whether the low rate of ALP expression obtained in these microarrays was due to BMP-2 detachment from the slides or by cell proliferation.

Despite the limitations found in this work to appropriately quantify the BMP-2 immobilised on the spots, another report using the same type of substrates (AD-Glass slides, obtained from the same manufacturer) and passivation strategy (2% BSA) has demonstrated that a similar growth factor (BMP-4 printed at 70 µg/mL and co-spotted with Ln at 360 µg/mL) induced differentiation on neural precursor cells after 4 days of cell culture.<sup>48</sup> In this report the amounts of growth factor immobilisation on the spots were not directly quantified, but evaluated through the effect produced in the cells cultured on them.

Other reasons that could further account for the low ALP activity detected in the microarrays presented here could include:

- The need of co-immobilisation of BMP-2 with other ECM proteins which were not assayed in this work (such as collagens)<sup>185</sup> or the need of a more complex ECM microenvironment.
- The need to stop cell proliferation. C2C12 cells continued to proliferate on the spots after cell seeding, and it is well-known that cell proliferation and differentiation are mutually excluded pathways which are ensured by several mechanisms.<sup>80</sup>

The low ALP activity detected on cells cultured for 4 days in the cellular microarray platform presented here contrasted with the previously reported by Phillipi et al (assessed as soon as 3 days after cell seeding on the BMP-2 patterns),<sup>67</sup> suggesting that cell differentiation in response to printed BMP-2 is decreased when culturing cells on individual and mutually isolated cell spots. Exit from the cell cycle is a prerequisite for cell differentiation. This is the reason why, usually, cell differentiation assays are performed in semi-confluent cell cultures. As previously noted, it could be argued that the effect of culturing cells in a semi-confluent monolayer (as reported by Phillipi et al.) could influence the rate of ALP activity by adequately providing additional signals, lacking in the case exposed in this work, which would allow exit from the cell cycle for the whole cell culture. Next, cells growing on BMP-2 arrays would successfully differentiate to osteoblasts while cells outside the array would follow the myoblast pathway, as reported by Phillipi et al.<sup>67</sup> Therefore, the difference in ALP response between the study presented here and the one reported by Phillipi et al. could be accounted, at least in part, by the proliferation of cells in the spots. Another possible effect for the ALP results reported here could be related to differences in the approach used for BMP-2 immobilisation (fibrin coated glass vs. AD-Glass). BMP-2 bound to fibrin on the substrates used by Phillipi and co-workers could remain in a better orientation and conformation to induce signalling to cells cultured on top of these surfaces.

As exposed here, the low ALP activity obtained with the microarray platform developed allowed speculating the probable causes for these results. This reasoning led to the proposal of some topics of the highest interest for future optimisation of the platform presented, that will be exposed in the final section of this chapter.

#### **4.4 Conclusions**

An approach to the study of osteoblast early differentiation stages based in myoblastic C2C12 cells was provided. It was demonstrated that BMP-2 was able to influence cells growing on them, when it was printed in combination with 2 ECM proteins (Fn and Ln) in a cellular microarray layout. This format allowed testing several BMP-2/Ln and BMP-2/Fn combinations in parallel on mutually isolated cell spots.

It was found that cells exposed to soluble or immobilised BMP-2 were early biased towards the osteoblast fate, assessed by means of Osterix expression at 24 h. However, the cell differentiation response was found to depend on the different culture conditions assayed. Cell differentiation was found to decrease in the following order: standard wellplates exposed to

soluble BMP-2 (>99% cells stained for Osx), cellular microarrays exposed to soluble BMP-2 (27 to 55% cells stained for Osx) and cellular microarrays with BMP-2 immobilised on the spots (20 to 24% cells stained for Osx). Most importantly, for the cellular microarrays in which BMP-2 was immobilised on some of the spots, it was observed that cells growing exclusively in BMP-2 containing spots were the only ones to express Osx. These findings allowed proposing a new model which accounted for an integrative cell differentiation response, which resulted from the changes introduced when varying the culture conditions.

On one hand, the restriction of the cell culture, appearing as a result of culturing small numbers of cells in isolated spots, was proposed to account for the decrease in the differentiation outcome from culturing cells in standard wellplates to cell culture in the cellular microarrays. On the other hand, the immobilisation of the BMP-2 was proposed to account for the additional decrease found when assaying the cell differentiation response in cellular microarrays exposed to soluble BMP-2 or to BMP-2 immobilised on the spots.

Culturing cells for longer periods (4 days) resulted in an extremely low osteoblast differentiation, according to ALP activity. This was attributed in part to the cell proliferation observed on the spots, which passed from having 25 cells attached at day 0 to more than 1,000 cells in some cases.

Summing up, the work presented in this chapter added to the state of the art in the development of cellular microarrays by analysing cell differentiation using a cell model (C2C12). The Osx expression was shown to be a suitable method to test the early cell response to the printed growth factor. New challenges to overcome when applying this platform for the study of stem cell differentiation were identified. The application presented demonstrated that platforms like the one exposed here are ideal tools to provide insights into the stem cell differentiation pathway based on cell response to ECM protein and growth factor combinations.

## **4.5 Future work**

The results presented in this chapter evidenced that the study of cell differentiation on the cellular microarrays turned out to be more complex than previously envisaged. Most of the previous literature reports describing the use of cellular microarrays for the study of cell differentiation were based on the use of robust and well established cell differentiation models (often including specific cell culture medium formulations) which were extensively characterised by standard in vitro cell biology approaches.

The cell differentiation model chosen for the experiments presented here evidenced an enhanced complexity for the induction of differentiation in the microarrays. In particular, the results presented after 4 days of cell culture served to open interesting new questions regarding the application of cellular microarrays for the study of cell differentiation. Based on these results, some topics of research appeared as very promising to develop as future work. In order to optimise and get an enhanced differentiation outcome, as well as a deeper understanding of the biology of cells when cultured on the microarrays, the topics that could derive in interesting results and which would further support the observations made here will be:

- 1- Integrin staining, together with BMP receptors staining, could provide insights to evaluate whether these cell receptors actually cluster (in the cells cultured on the BMP-2 containing spots, which expressed Osx) to trigger a common intracellular signalling pathway. The immunostaining of intermediate markers of intracellular signalling pathways (such as Smad proteins) would allow a more detailed evaluation of the pathways mediated by integrin binding only and the pathways mediated by the integrin clustering with the BMP-2 receptors. This could yield extremely interesting insights into how these events are combined to produce a common integrated cell response.
- 2- Artificially inhibiting cell proliferation on the microarray spots, by the addition of proliferation inhibitors such as aphidicolin or mitomycin C to the cell culture medium,<sup>138</sup> could yield further insights into the effect of cell proliferation on the differentiation of cells attached on the BMP-2 containing spots.
- 3- A more sensitive characterisation of the BMP-2 content of the spots, aided by the radioactive labelling of the BMP-2, could allow the quantification of the BMP-2 that actually remains immobilised on the spot surface, both after the passivation step as well as after several days of cell culture on the microarrays. This would therefore provide further insights into the reasons accounting for the low ALP activity observed on the BMP-2 containing spots after 4 days of cell culture.

Finally, further studies based on this platform are envisaged for the optimisation of the BMP-2 immobilisation and orientation in an active way, in order to improve the cell differentiation outcomes. These could include not only the assay of additional ECM proteins (such as collagens) and more complex ECM combinations, but also the indirect immobilisation of BMP-2 through printing BMP-2 antibodies and subsequent microarray incubation with soluble BMP-2 to promote site-specific binding.

## **Chapter 5      Conclusions of the thesis**

An integrative study comparing several substrates with cellular microarray-relevant proteins and concentrations has been presented in Chapter 2. The immobilised Fn and SA mass and density were qualitatively and quantitatively analysed for 4 substrates of interest in cellular microarray applications. The main objective of the chapter was to elucidate the best substrate for further analysis of cellular microarray fabrication. For this purpose, a number of crucial factors were considered and quantitatively evaluated. These included the amount of Fn and SA immobilised and the intra-slide reproducibility of the protein immobilisation results. Based on this study, it was concluded that AD-Glass substrates yielded the best intra-slide reproducibility and successfully immobilised variable amounts of Fn and SA (in the range from 25-45% of the total amount of Fn spotted, and ~10% of the total amount of SA mass spotted). For this reason, AD-Glass substrates were chosen to accomplish the following aims of this thesis. Additionally, a qualitative and quantitative analysis of the spot morphology and the protein density immobilised suggested the use of Fn spotted at 200 or 360 µg/mL for further optimisation of cellular microarray fabrication.

The results presented in Chapter 3 added to the literature state of the art by the fabrication of cellular microarrays on AD-Glass using Fn spots as cell adhesion agents that will capture MSCs and allow for variable periods of cell culture. For this purpose cellular microarray fabrication using five different spot sizes, three Fn concentrations, two buffer compositions and three different cell seeding densities was analysed. The results obtained leaded to an optimised set of parameters which were found when spotting 5 drops of Fn200 in PBS 2% glycerol, seeding cells at 11,000 cells/cm<sup>2</sup> density during 15 minutes, and cellular microarray culture in ITS medium. These parameters allowed for cell culture in the microarrays for periods up to 8 days. After this period of time, spontaneous cell differentiation to the osteoblast and adipocyte fates was detected in some of the spots at a very low rate, evidencing that under the adequate stimuli this platform would be viable to assess the differentiation of MSCs. These differentiation outcomes, however, were not expected in the experiments presented here (where all microarray spots were printed using Fn only) and were mainly attributed to the heterogeneity, in terms of differentiation potential, of the MSCs obtained as primary cultures.

Finally, an approach to the study of osteoblast early differentiation stages based in myoblastic C2C12 cells was presented in Chapter 4. Cell differentiation was assessed at two checkpoints of the differentiation pathway, evidencing Osx expression in 20 to 24% of the cells in response to signalling from spots printed with BMP-2 after 24 h, but a low ALP activity after several days of cell culture in these microarrays. Osx expression was found to be a suitable method to test earlier cell response to a printed growth factor. This marker allowed finding that the differentiation of C2C12 cells in response to printed BMP-2 depends on highly inter-correlated parameters and that its contribution to an effective growth factor signalling is quite complex. On one hand, the restriction of the cell culture, appearing as a result of culturing small numbers of cells in isolated spots, was proposed to account for the decrease found in the differentiation outcome from culturing cells in standard wellplates to cell culture in the cellular microarrays. On the other hand, the immobilisation of the BMP-2 was proposed to account for the additional decrease found when assaying the cell differentiation response in cellular microarrays exposed to soluble BMP-2 or to BMP-2 immobilised on the spots. As a result, new challenges to overcome when applying this platform for the study of stem cell differentiation were identified. The application presented demonstrated that platforms like the one exposed here are ideal tools to provide insights into the stem cell differentiation pathway based on cell response to ECM protein and growth factor combinations. Further studies based on this platform are envisaged for the optimisation of the growth factor signalling in order to improve the cell differentiation outcomes. These include the assay of additional ECM proteins (such as collagens) and the inhibition of cell proliferation on the spots.

## Appendix A Devices for microarray fabrication

Protein spotting onto the substrates is usually accomplished by either a contact pin or non-contact piezoelectric nozzle linked to a robotic microarray plotter device. Contact printing devices, such as the one presented in Figure A.1, consist of a workplate area where the slides to be printed are arranged. In this workplate there is also a space reserved for positioning wellplates which contain the working solutions to be spotted. In general, 384-wellplates are used and wells are filled with volumes as little as 10 µL. Also, a special sub device (the wash station) is integrated within the workplate area to provide the contact pins with an appropriate cleaning procedure between spotting of solutions. Since sample uptake in this kind of devices is usually driven by capillarity forces, the washing step usually involves sonication of the pin to better remove remaining solutions inside the pin (Figure A.1 also shows a detail of the contact pin). Connection of the device to a computer provides robot control and allows programming the pipetting cycle and microarray layout.

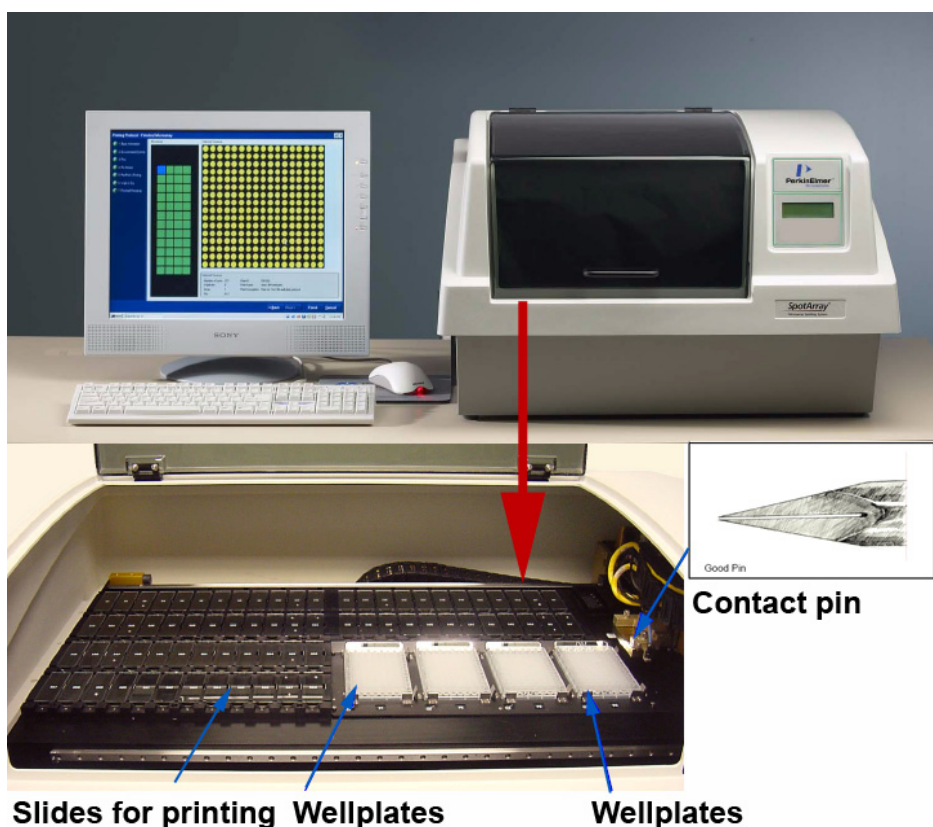


**Figure A.1** Spot array™ 24 microarray printing system from Pelkin Elmer. Image adapted from device user manual.

The non-contact printing devices, such as the one exposed in Figure A.2, share many similarities with contact printing ones in terms of workplate positioning of slides and wellplates, and computer control. The main difference is that in non-contact printing devices there is also an additional liquid handling system which fills or empties the piezoelectric pipette (Figure A.3). Sample uptake is driven by the fluidic system, while controlled drop release is driven by a very accurate piezoelectric crystal placed inside the pipette channel which creates drops of a few nanoliters in volume (usually from 0.1 nL to 3 nL).

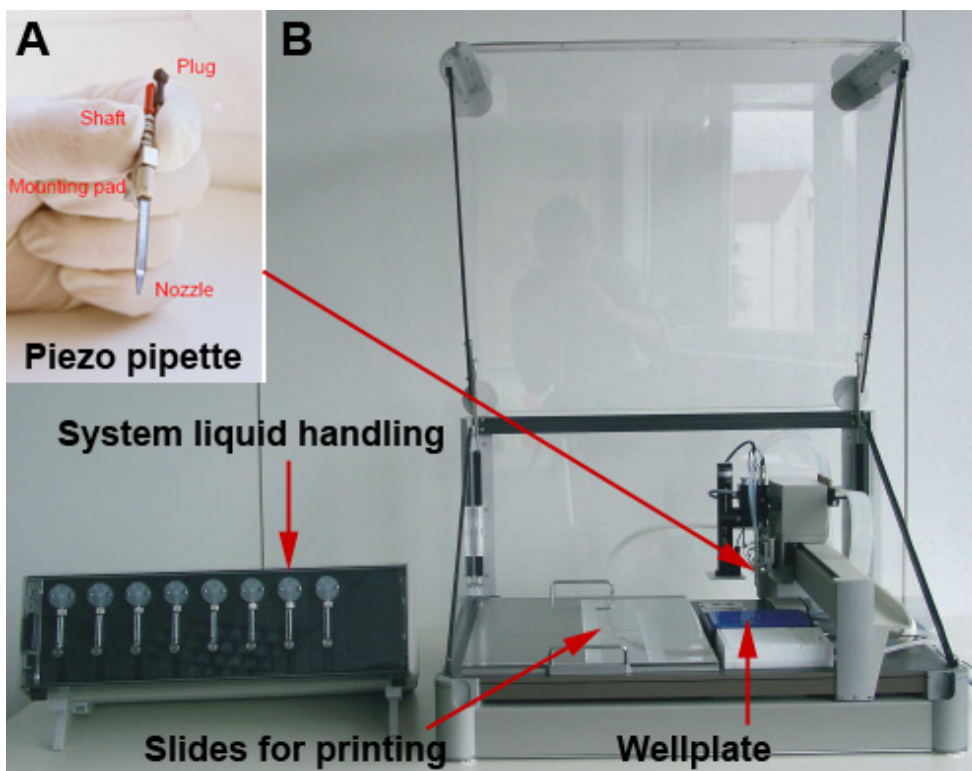


**Figure A.2** Nano-Plotter<sup>TM</sup> non-contact printing device from GeSIM. A. Piezoelectric pipette detail. B. Device workplate. Image adapted from device user manual.

The basic functioning of the piezoelectric pipette is exposed in Figure A.3.A. Sample uptake is governed by a difference in pressure ( $dp$ ) between the liquid pressure inside the pipette channel and the atmospheric pressure. Provided that the pipette is submerged in a solution, when  $dp < 0$  the solution uptake process takes place. In steps 3 to 5 of Figure A.3.A  $dp \approx 0$  because drop dispensing is produced by electrical excitation of the piezoelectric crystal. Figure A.3.B shows the general fluidic system. It can be seen that the pipette is operated by means of a dilutor (consisting on an electrically driven syringe) connected in the system, which fills or empties it and also controls sample uptake.

The wash station in this case involves system liquid (deionized water) ejection through the pipette and, at the same time, the pipette is usually submerged in a chamber which provides an

additional lateral liquid flow to efficiently remove waste solutions ejected from the pipette, and clean the pipette tip (Figure A.3.A, step 6).

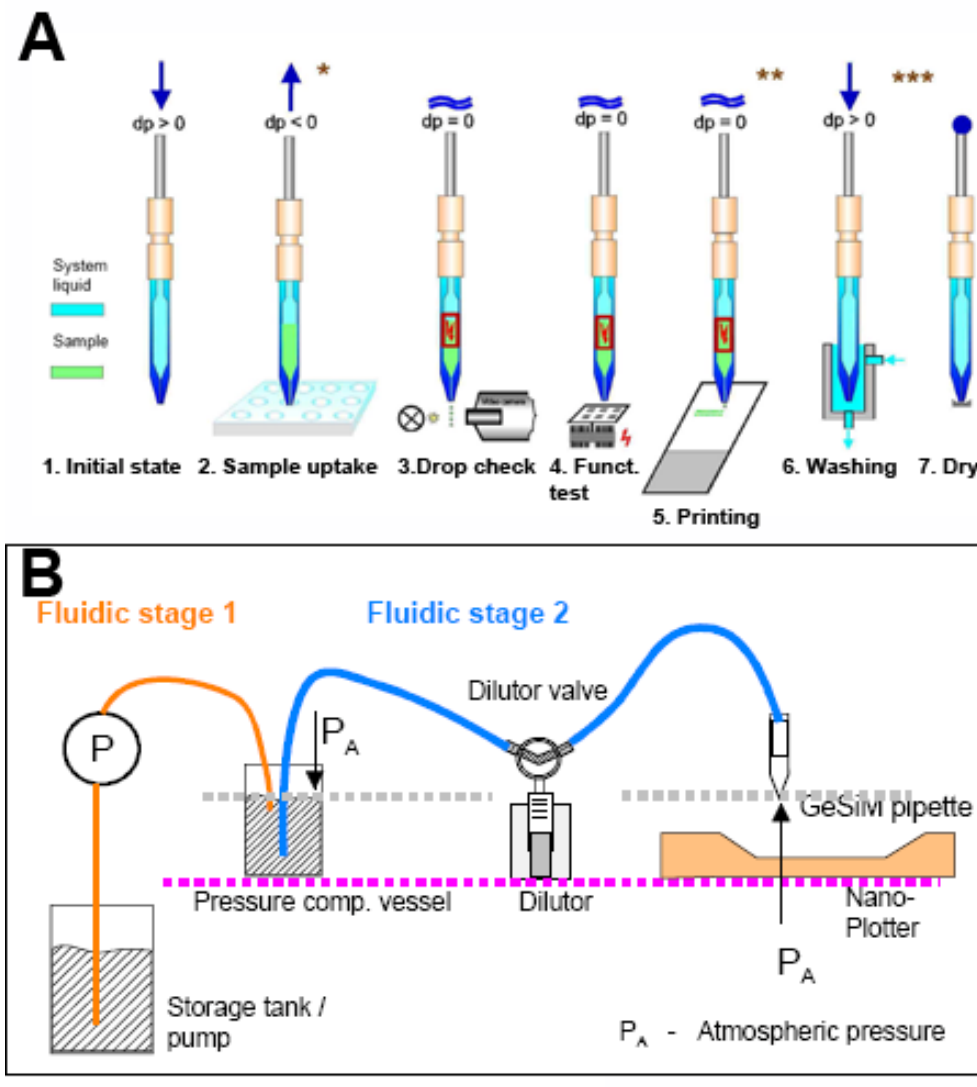


**Figure A.3** Nano-Plotter<sup>TM</sup> non-contact printing pipetting cycle. A. Principle of work for the piezoelectric pipette. B. Fluidic system of the system liquid in the Nano-Plotter<sup>TM</sup>. Image adapted from device user manual.

# Appendix B Devices and methods used for microarray characterisation

## Appendix B.I Fluorescence scanner device

The device used for scanning the fluorescently labelled microarrays was a GenePix 4000B (Molecular Devices, USA, Figure B.I.1), connected to a Personnal Computer.

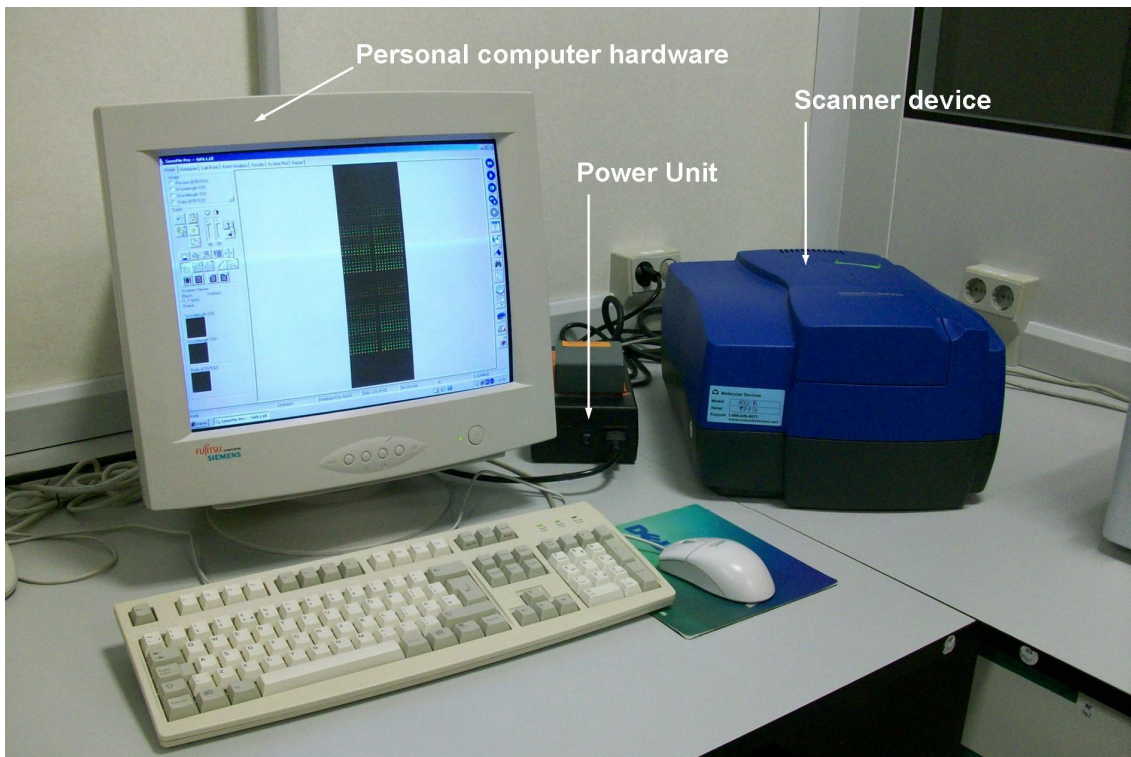


**Figure B.I.1** Device used for the fluorescence scanning of the slides.

This device allowed the simultaneous scan of the microarray slides at two wavelengths using a dual laser scanning system, aided by a 532 nm (17 mW) and a 635 nm (10 mW) excite lasers. These lasers, combined with the 575DF35 (green, ~557-592 nm) and 670DF40 (red, ~650-690 nm) emission filters, are optimised for the excitation of the Cy3 and Cy5 dyes, but also provide compatible detection of several other commercial dyes (Table B.I.1). As is observed in this table, the fluorophores used in the experiments presented in this Thesis work (Alexa Fluor 555, Alexa Fluor 568 and Alexa Fluor 647) were successfully detected using this scanner set-up.

Laser	Dye	Excitation Peak (nm)	Emission Peak (nm)
532	Alexa 532	531	554
	POPO-3	534	570
	PO-PRO-3	539	567
	Cy3	550	570
	Alexa 546	553	573
	Alexa 555	555	565
	Alexa 568	578	603
	Cy3.5	581	596
<hr/>			
635	BODIPY 630/650	625	640
	Alexa 633	632	647
	Cy5	649	670
	Alexa 647	650	668
	BODIPY 650/665	651	660
	Alexa 660	660	690
	Cy5.5	675	694
	Alexa 680	680	700

**Table B.I.1** List of dyes compatible with the fluorescence lasers and emission filters of the GenePix 4000B fluorescence scanner device. The emission and excitation peaks for each dye are also indicated in the table. Table reproduced from: [http://www.moleculardevices.com/pages/instruments/gn\\_genepix4000.html](http://www.moleculardevices.com/pages/instruments/gn_genepix4000.html) (updated as of October 2009).

The principle of measurement for the Genepix 4000B is the use of the two lasers previously described and a pair of high-sensitivity, low-noise photomultiplier tubes (PMTs) to detect the emitted fluorescent light.

The PMTs are optical components that convert the incident photons into electrons via the photoelectric effect (Figure B.I.2). Briefly, the photons emitted by the excited fluorophores impact into a photocathode, which is the element that transduces the energy carried by the photons into electrons. These electrons flow through a series of electron multipliers (called dinodes) to the anode. The current coming out of the PMT (at the anode) is directly proportional to amount of incident light at the photocathode.

The gain of the PMT depends on the voltage applied to the dinodes. These voltages accelerate the electrons to the dinodes. As the PMT voltage increases, the electrons gain more energy before impacting with the following dinode, and as a result more electrons are freed from the impact. Therefore, by an adequate choice of the voltage applied to each dinode, the electrons impacting into each dinode are amplified, ultimately resulting in the electric current that is collected at the anode.

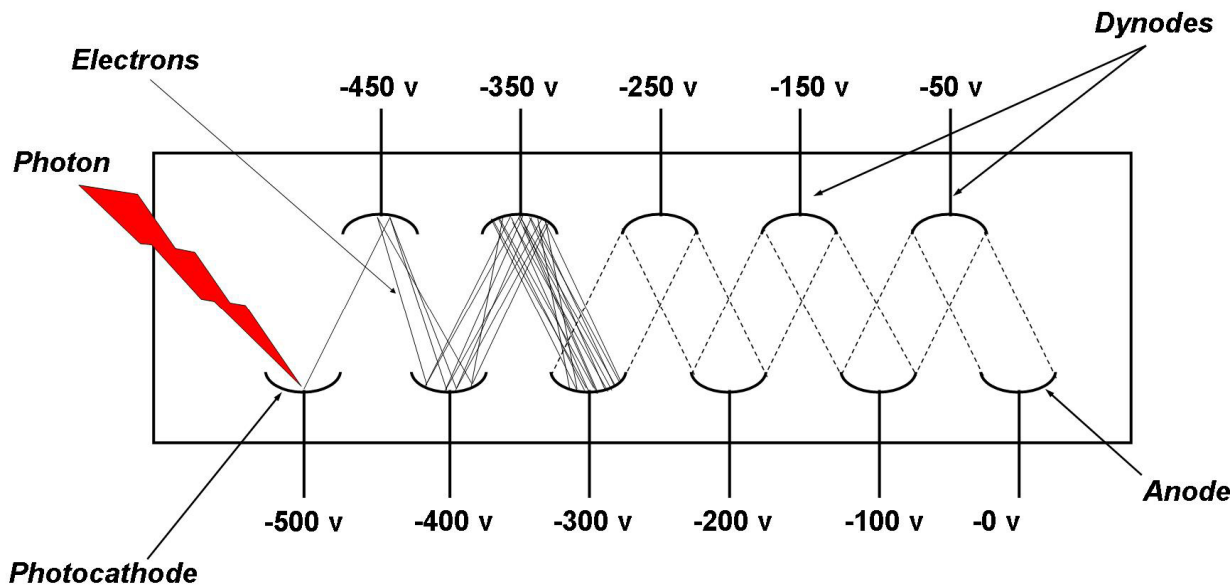


**Figure B.I.2** Diagram of a photomultiplier tube. The photons that impact on the photocathode are converted to an electric current that is amplified by a series of dynodes (electrodes), ultimately resulting in an electrical signal that is proportional to the flux of photons received by the photocathode.

When the PMT gain (voltage) setting in software provided by the scanner manufacturer is increased, the sensitivity of the PMT is increased. However, it is important to use the optimal PMT gain for each particular scan. Despite being true that a higher gain yields a brighter image, this is not always the best result. Setting high values for the PMT gain increase the noise as well as the signal intensity. If the gain is too low, on the other hand, the noise will increase more than the signal, and the signal-to-noise ratio will become worse. In the experiments presented in this Thesis, the PMT gain values were set by the scanner device, which performed several scans of each slide (using different PMTs) and automatically calculated the best PMT gain for each channel to optimise the signal-to-noise ratio.

## **Appendix B.II Hierarchical clustering analysis**

A cluster analysis consists in the assignment of a set of observations into subsets (called clusters), so that the observations in the same cluster are similar in some sense. Of the many types of the possible clustering algorithms, the results presented in Chapter 2 (Section 2.3.7) were obtained using a hierarchical clustering algorithm. This type of algorithm finds successive clusters using previously established clusters. In particular in Chapter 2, the agglomerative (“bottom up”) approach was followed. In this approach, the algorithm begins with each observation as a separate cluster and merges them into successively larger clusters.

To perform the hierarchical clustering, a **dissimilarity measure** is used to compare observations taken in pairs, and specific **linkage criteria** are used to allow the clustering of observations. These parameters are briefly described in the following subsections.

The example chosen for the following explanation (Figure B.II.1) is the hierarchical clustering of substrates in terms of immobilisation of Fn mass presented in Chapter 2, Section 2.3.7. In this particular case, the observations were the 14 microarray slides assayed (no distinction was made for the substrate type).

The data used to classify the slides (and therefore used for calculation of the dissimilarity measure between pairs of slides) were the values obtained for each of the variables assayed within each slide. These variables were defined by the combination of the number of drops, printing buffer, Fn concentration spotted and SA concentration spotted, yielding 40 individual spot compositions represented on the right of Figure B.II.1. The nomenclature followed to refer to these variables (i.e. spot compositions) is specified in the caption of the figure.

The outcome of a hierarchical clustering analysis is usually represented by a “heat map” (composed of colour coded cells according to the actual values obtained for each slide and spot composition, Figure B.II.1) and a phylogenetic-type tree (shown at the top side of the heat map in Figure B.II.1). This tree shows the grouping (or clustering) of slides based on similar outcome, where longer branches mean less similarity. The detailed analysis of the results presented in this example has been exposed in Chapter 2, Section 2.3.7.

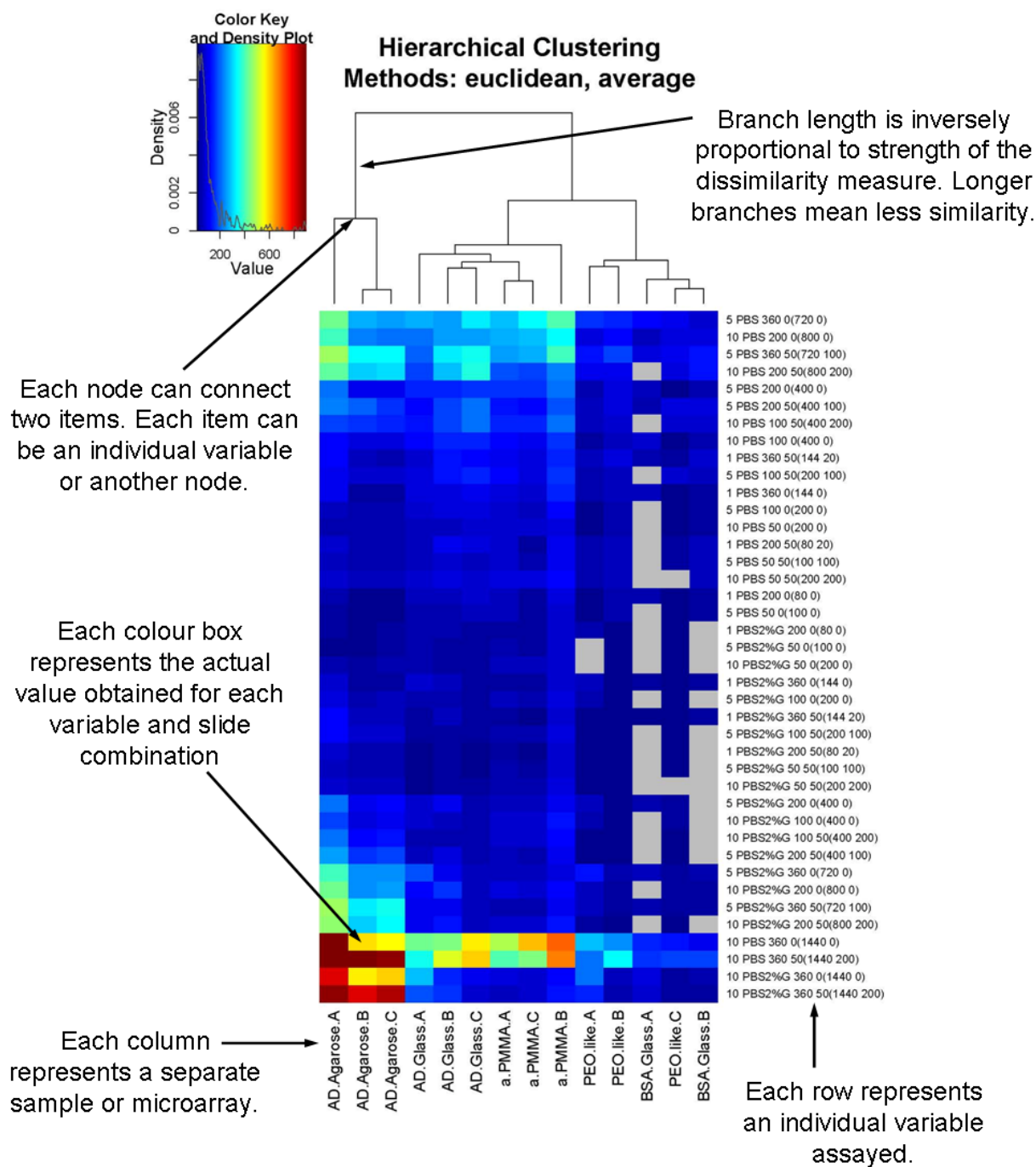


**Figure B.II.1** Hierarchical clustering graph generated using data for the immobilised Fn mass obtained from the protein microarrays assayed in Chapter 2. Three slides per substrate (two for BSA-Glass) are presented (A, B and C). Spot compositions on the right side of the image are indicated in the following order: number of drops, buffer, Fn concentration spotted, SA concentration spotted (Fn mass printed, SA mass printed). These compositions were used as the variable inputs to compare substrates based on the calculation of the Euclidean distance. Colour coding is indicated in the upper left box. The gray boxes represent unavailable values due to extremely low SNR for these conditions and substrates.

## Dissimilarity measure

The **dissimilarity measure** consists on a single calculated value which represents the difference (taken as a distance) in response between pairs of slides, and allows grouping microarray results according to affinity in performance.

The dissimilarity measure used in the experiments presented in Chapter 2 was the Euclidean distance, calculated by:

$$\|a - b\| = \sqrt{\sum_i (a_i - b_i)^2} \quad (\text{Eq. B.II.1})$$

Where:

$i$  : number of variables used to classify the observations

$a_i$  : data for observation a and the  $i^{\text{th}}$  variable, where  $i = 1$  to  $n$  ( $n$  being the number of variables or dimensionality)

$b_i$  : data for observation b and the  $i^{\text{th}}$  variable, where  $i = 1$  to  $n$  ( $n$  being the number of variables or dimensionality)

An illustrative example of how this metric is used to assess the distance between pairs of observations is the calculation of the distance between two points in a 2-dimensional space, for example between the points (1, 1) and the origin (0, 0). Using the Euclidean distance, the distance between these points is  $\sqrt{2}$ . The same reasoning can be extended to the evaluation of a distance in an  $n$ -dimensional space, used to compare the distance between two microarray experiments.

In the experiments presented in Chapter 2, the amount of Fn mass immobilised in response to 40 spot compositions was used to classify the slides (i.e.  $i = 40$ ), and “a” and “b” were the slides analysed by pairs (e.g.  $a = \text{AD.Agarose.A}$  and  $b = \text{AD.Agarose.B}$ ). Therefore, if the first parameter analysed (i.e.  $i = 1$ , arbitrarily chosen) was 5 PBS 360 0 (720 0) (refer to caption of Figure B.II.1 for the nomenclature used), then  $a_1 = 436$  and  $b_1 = 273$  were the amounts of mass immobilised (in pg) by AD.Agarose.A and AD.Agarose.B for this condition. Similarly, data for all the other spot compositions assayed (i.e.  $a_{2\dots 40}$  and  $b_{2\dots 40}$ ) was obtained. These data was used to calculate the Euclidean distance between AD.Agarose.A and AD.Agarose.B using Eq. B.II.1, yielding an overall distance of 640.6 (Figure B.II.2). Accordingly, when applying the same reasoning for AD.Agarose.B and AD.Agarose.C, the result obtained was 102.9 (Figure B.II.2,

red circle). These results allowed comparing AD.Agarose.B separately with AD.Agarose.A and AD.Agarose.C.

A similar calculation was performed by the algorithm taking all the other slides by pairs. The results of this first round of comparisons are presented in Figure B.II.2.

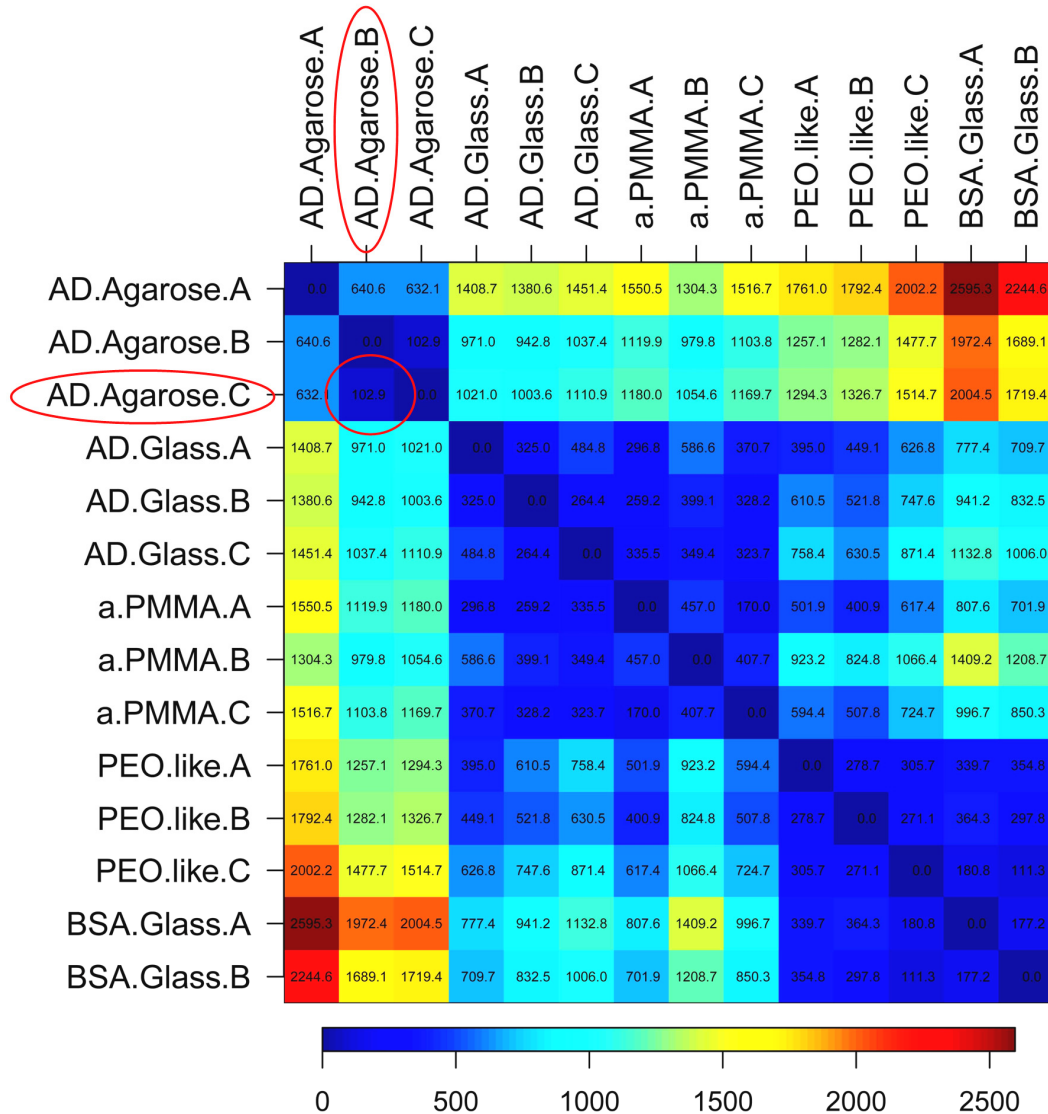


**Figure B.II.2** Heatmap representing the Euclidean distances calculated using Eq. B.II.1 for all the slides assayed taken in pairs. The lowest distance was found for AD.Agarose.B and AD.Agarose.C (102.9, marked with a red circle). Therefore this was the first pair of slides grouped together in Figure B.II.1, named from here on as C1 (cluster 1).

It was concluded that AD.Agarose.B and AD.Agarose.C were the pair of slides that yielded the most similar response (i.e. the lowest dissimilarity value). Therefore this was the first pair of slides grouped together in Figure B.II.1, named from here on as C1 (cluster 1).

### **Linkage criteria**

The newly formed C1 cluster was further used in the calculation of a new round of comparisons based on the Euclidean distance. In this new round, however, only 13 observations were compared, those obtained from AD.Agarose.B and AD.Agarose.C having been replaced by C1. In order to continue with the following clustering round, linkage criteria have to be used to allow calculating the Euclidean distances between C1 and all the other slides. In order to accomplish the following comparisons, in Chapter 2 the average linkage clustering was used. In this case, the linking distance is the average of all pair-wise distances between members of the two clusters.

Therefore, after C1 was found in the first place, new distance values were calculated between all other individual slides and cluster 1 using the average linking criterium. The results are presented in Figure B.II.3. Note that, in order to calculate the Euclidean distances between C1 (representing 2 slides) and all the other individual slides, the average of all pair-wise distances between members of C1 and the each of the other slides was used. As an example, to calculate the Euclidean distance between C1 and AD.Agarose.A, the average of the distances obtained for AD.Agarose.A and AD.Agarose.B (640.6, Figure B.II.2), and for AD.Agarose.A and AD.Agarose.C (632.1, Figure B.II.2) was used, resulting in the final value of 636.4 (Figure B.II.3).

From this new round of comparisons, it was found that the observations which yielded the lowest distance were PEO-like.C and BSA.Glass.B (111.3). Therefore, this pair of slides was the next one grouped together (Figure B.II.3, red circle, and Figure B.II.1). This procedure was followed until all newly formed clusters were grouped between them.

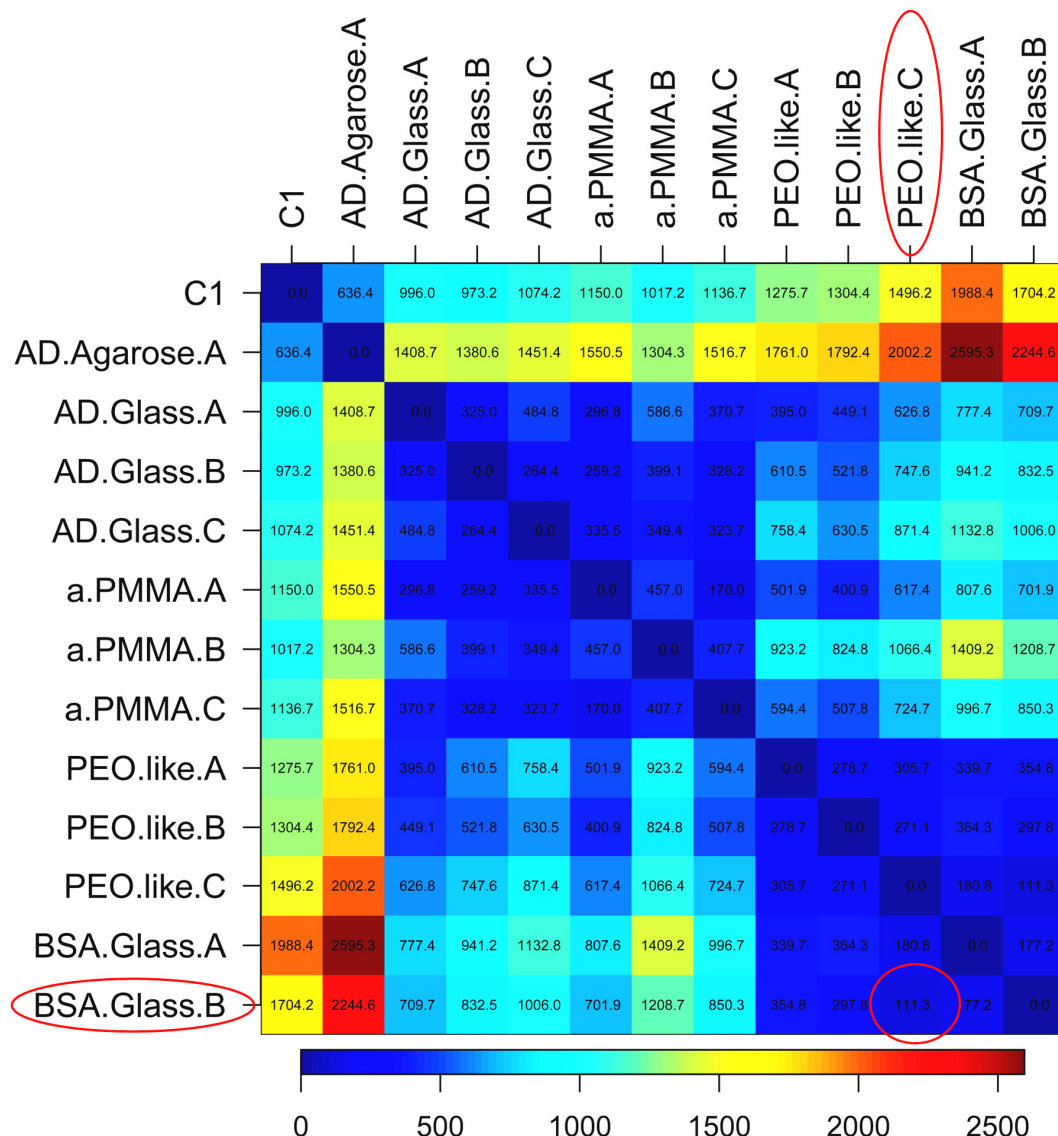


**Figure B.II.3** Heatmap representing the second round Euclidean distances calculated using Eq. B.II.1 for all the slides assayed taken in pairs. In this new round of calculation, AD.Agarose.B and AD.Agarose.C were replaced by C1 (cluster 1). The lowest distance was now found for PEO.like and BSA.Glass.B (marked with a red circle). Therefore this was the second pair of slides grouped together.

## References:

Kohane, I. S.; Kho, A. T.; Butte, A. J., Genomic Data-Mining Techniques. In *Microarrays for an integrative genomics*, MIT Press: Cambridge, Mass., 2003; pp 114-162.

### Appendix B.III Immunofluorescence stainings

The immunofluorescence staining protocols allow the detection of specific proteins in a fixed sample by the use of antibodies specific for that protein. These stainings can be accomplished in two different ways: the direct immunofluorescence and the indirect immunofluorescence approaches. Each of them has advantages and disadvantages that will be briefly exposed in the following subsections.

#### Direct immunofluorescence approach

The direct immunofluorescence approach consists in using a fluorescently labelled primary antibody, raised against the protein of interest (Figure B.III.1). In this approach, the unspecific binding events are only due to a single antibody. Additionally, different antibodies (raised against different proteins) can be used in the same incubation step. Using antibodies of the same species is not a problem, since each antibody will recognise its specific protein counterpart. The main inconvenient of this approach is that the amplification of the signal is extremely low. Additionally, the direct labelling of antibodies usually results inviable due to the extremely high cost of the antibody and the large amounts of it needed for the labelling procedure.

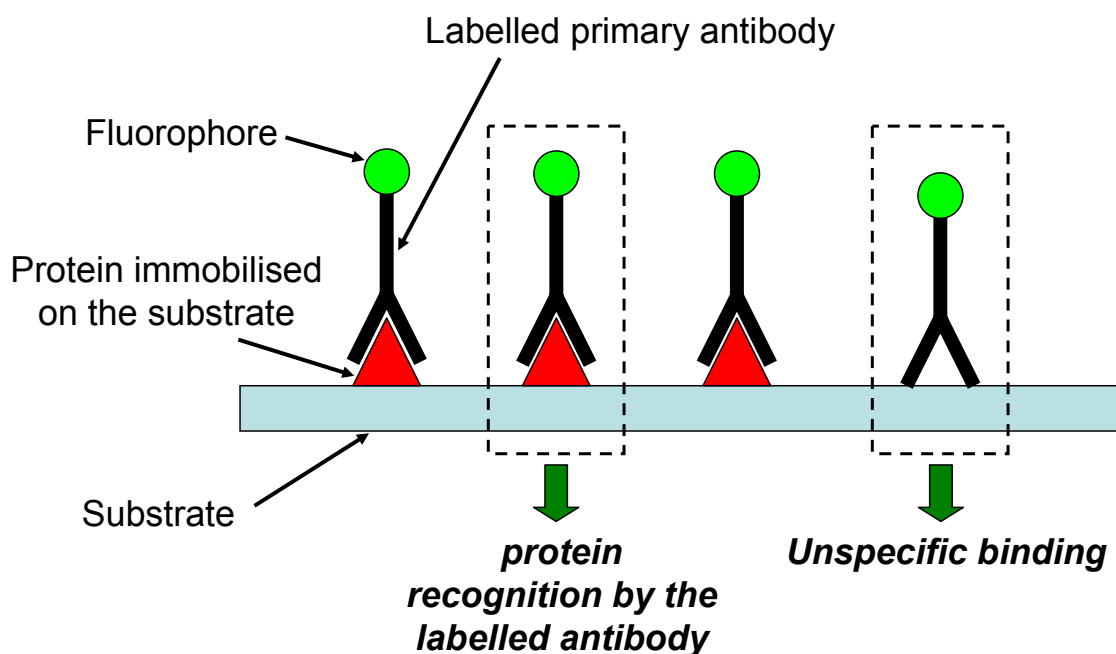


**Figure B.III.1** Schematic showing the direct approach for the immunofluorescence staining. In this approach, each protein is recognised by a single labelled antibody raised against that protein.

## Indirect immunofluorescence approach

The indirect immunofluorescence approach consists in using a fluorescently labelled secondary antibody, usually raised against the IgG of the primary antibody used to recognise the immobilised proteins (Figure B.III.2). The IgG of the primary antibody is given by the species in which it has been produced. In this approach, an important amplification of the signal is provided (much higher than in the direct immunofluorescence approach). Moreover, it is much easier to dispose of a set of secondary antibodies (labelled with different fluorophores) raised against the most commonly used IgGs (e.g. mouse, rabbit, goat IgGs). The main inconvenient is that it is not possible the use of primary antibodies obtained from the same species (which have the same IgG) without important inconveniences. Another inconvenient is that the possibilities of unspecific binding events are increased due to the combination of the unspecificity of the primary and the secondary antibodies (Figure B.III.2).

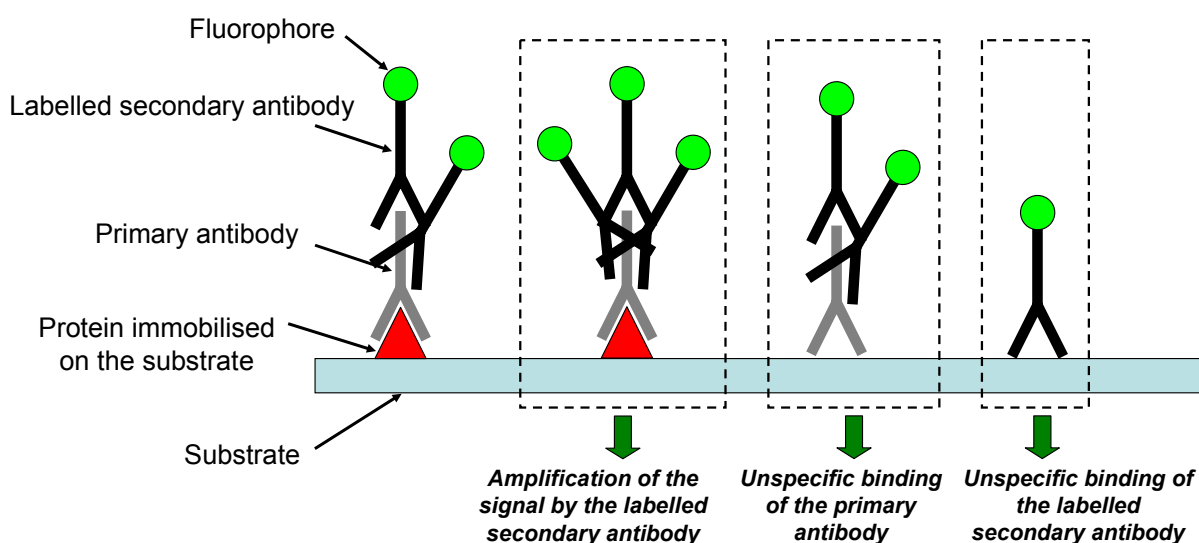


**Figure B.III.2** Schematic showing the indirect approach for the immunofluorescence staining. In this approach, each protein is recognised by a single primary antibody raised against that protein. Each of the immobilised primary antibodies is recognised, in a second incubation step, by several labelled secondary antibodies raised against the IgG of the primary antibody. Therefore, amplification of the signal takes place in this approach. Also, the unspecific binding of the antibodies is increased, since both unspecific recognition events (i.e. due to primary and secondary antibodies) can occur in this protocol.

## **Appendix C    Suitability of the substrates chosen for cellular microarray fabrication**

Protein microarrays composed of fluorescently labelled Fn (using the Alexa Fluor 555 labelling kit, Invitrogen, Spain) were produced as described in Chapter 2. In a preliminary approach, cellular microarray formation was demonstrated on the four substrates analysed (AD-Glass, AD-Agarose, a-PMMA and PEO-like) using C2C12 mouse cells (control slides were excluded from this test). Cells were seeded for 15 minutes (AD-Glass and a-PMMA) or 30 minutes (AD-Agarose and PEO-like) in the microarrays and incubated overnight in serum free medium.

The following day cell viability was assessed using a cell Viability/Cytotoxicity Assay Kit For Animal Live & Dead Cells (Biotium, Inc). This kit provides a two-colour fluorescence staining which allows identifying live and dead cells using two probes (calcein AM and ethidium homodimer-III (EthD-III)) that measure recognised parameters of cell viability, i.e. the intracellular esterase activity and the plasma membrane integrity. It is suitable to be applied to substrate attached cells. The principle of the viability measure resides in the intracellular esterase activity of live cells, which allows the conversion of the non-fluorescent cell-permeant Calcein AM to the intense fluorescent calcein. This converted dye is well retained within live cells, producing an intense uniform green fluorescence in live cells (with excitation peak at ~495 nm and emission peak at ~550 nm). EthD-III enters cells with damaged membranes and binds to nucleic acids, undergoing with this event a 40-fold fluorescence increase which produces a bright red fluorescence in dead cells (with excitation peak at ~530 nm and emission peak at ~635 nm). EthD-III is excluded by the intact plasma membrane of live cells. The protocol followed for applying the viability kit consisted in incubating the cellular microarrays, under culture conditions (i.e. in a humid incubator at 37 °C and 5% CO<sub>2</sub>), for 30 minutes in a 4 µM Eth-D and 2 µM calcein AM solution prepared in PBS.

After applying this kit, it was observed that cells were viable on most spots (with viability higher than 90%) on all substrates, as is presented in Figure C.1. In the figure, cells stained in green indicate good cell viability due to calcein staining (upper row of images in Figure C.1), and only few small red points could be distinguished in the bottom row of images in this Figure,

indicating EthD-III binding to DNA from the nuclei of dead cells. The number of live and dead cells was quantified from these images and is presented in Figure C.1 (bottom plot).

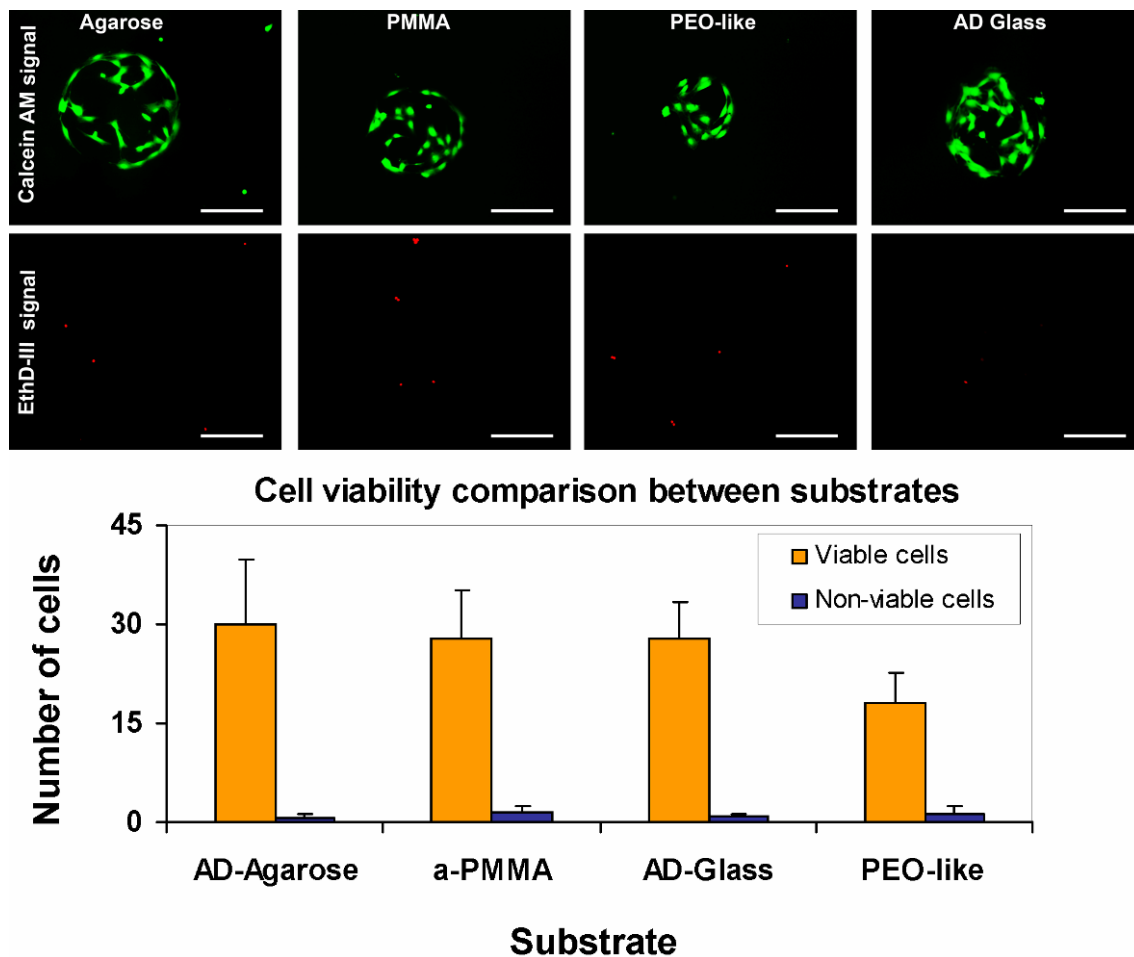


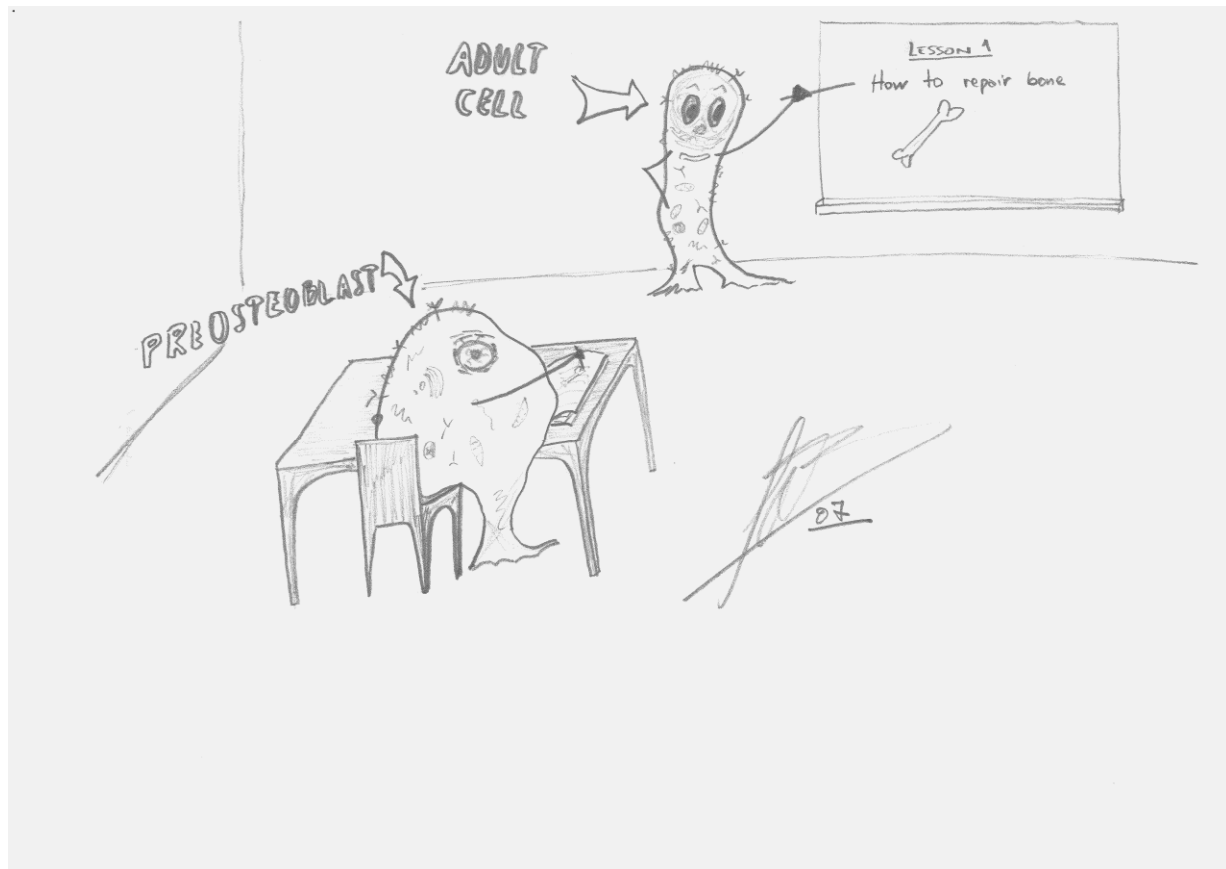
**Figure C.1** Fluorescence images of cell viability for cells growing on spots with Fn360 1% A555 in PBS (10 drops spot size) for the four substrates assayed (up) and plot for viable and non-viable cells (down). Bars represent the mean values from 10 spots, and the standard deviation associated. Calcein signal, in green, stains viable cells EthD-III signal, in red, indicates non-viable cells. Cell viability was similar in all spots with cells attached on them. 200  $\mu\text{m}$  scale bar is shown in white.

These results demonstrated that the substrates chosen for the assays in Chapter 2 were suitable for cellular microarray fabrication.

## Appendix D    Miscellaneous

**Appendix D.I Contribution presented for the Nano2Life Writing Contest celebrated in 2007, awarded the third prize for the public opinion.**

**“STEM CELLS DIFFERENTIATION AS A “NORMAL” HUMAN LIFE LINE”**



By now, almost everyone has heard something about stem cells, including the possible miraculous therapies that could arise from this new manipulation of biology, and in this context may have heard the words “differentiation” and “microenvironment”. But, what do the words “stem cells”, “differentiation”, and “microenvironment” really mean? What are stem cells useful for? What part does nanotechnology, another novel area of science, play?

Here, I will try to provide simple answers for these questions, based on a simplified comparison between differentiating stem cells and the course of a normal human life, from the point at which a child is born, until it grows up and takes up a profession. Only one exception has to be made for the sake of this comparison. While humans are usually most prepared for reproduction at the adult age, when they are fully educated and have a clear vision of what their place in the society will be, especially with regards his or her profession; we should imagine that instead of reproducing more easily at adult age, humans would reproduce more effectively when they are babies, giving rise to baby humans identical to its predecessor (and one another), and this capability is lost when it enters adulthood. In this comparison, a human “life line” is equivalent to a cell “life line”. Stem cells, in our comparison, are the equivalent to human babies, and cells that have already “differentiated” are the equivalent to adult humans. Moreover, we will compare the roles of cells in the human body with the roles of humans in the society, because in the end, our human body can be regarded as a society where cells live in harmony, they respect certain rules and they communicate with each other. Let’s enter a bit deeper into this comparison.

### ***The Human Body/The Cell***

Making a simplification of the human anatomy, humans are composed of skin (the “outer layer”), inside of which is blood and other biological fluids, muscles and bones, and the organs, including the brain. We can say that when humans are born, they all have inside the brain the same capability to learn any profession. Cells, on the other hand, are composed of a cell membrane (the cell’s “outer layer”), inside of which there is the cytoplasm (the cell’s blood), the cytoskeleton (the cell’s muscles and bones), and the cell organelles (the cell’s organs), including the nucleus (the cell’s brain) that contains all the information a cell must have to develop. All the cells inside the human body, independent of the cell type (neurons, skin cells, heart cells, retinal cells etc.), have the same information stored in the nucleus (they all have the same DNA sequence, i.e. the same genes). Yet, not all cells can access all this information at all times. In

fact, access to this information is restricted, and only cells that have “learned” how to use it are allowed to. This process is called “differentiation” of a cell. We will see how this happens.

### ***Information***

An adult knows how to fulfil a task related to its profession (for example an architect knows how to build a house), by adequately “using” the information stored in their brains. The same is applicable to cells; an adult differentiated cell knows how to fulfil a specific task (for example an osteoblast cell knows how to repair bone) by adequately using part of the information they have inside the nucleus. While a human stores the information, learned through its experiences and education, in its brain in the form of neuronal connections, a cell stores the information learned through its differentiation pathway in the form of protein and DNA interactions. These interactions restrict which parts of the DNA can be transcribed (used), and under which conditions each gene will be used.

### ***Pluripotency***

We said we can compare stem cells with human babies but, on what basis? Stem cells are pluripotent, meaning they can give rise to any kind of cells of a human body. These “differentiated” cells will then fulfil a specific function in the human body. Babies are similar to stem cells in the way that they can, as they grow up, learn any profession they want or are required to by the society, for example, as a doctor, an architect, a technician or a shop assistant. In other words, they have the same capability to turn into anything they want as they grow up (they are pluripotent). This allows them to “differentiate” from the fate other babies have chosen.

On the other hand, we can compare differentiated cells (for example adipocytes [fat cells], osteoblasts [bone cells] and lymphocytes [blood cells]) with adult humans, on the basis that both have a previous “pluripotent origin” (either stem cells or babies respectively) and they have followed a “differentiation pathway” (in cells as differentiation induced by biochemical signalling, or in humans as differentiation induced by means of education and experience). Taking this into account, we can say that adults, disregarding size differences, are specialized babies that can fulfil specific tasks in “the society”. They had to learn how to do this while growing up. In the same way, differentiated cells are specialized stem cells that can fulfil specific tasks in the human body that a stem cell cannot.

### ***Specialization***

We come now to an interesting point. How do human babies specialize, that is to say, how do they differentiate from other, similar babies? Are there any similarities with how stem cells specialize?

Human babies specialize as they grow up; they go to school, then high school and perhaps university. However, all these examples are just places. How do people learn inside these places? They have teachers; they read books and are subsequently expected to solve problems of increasing complexity. Taking this further, in the end, people learn a profession by interacting with others (teachers, classmates, colleagues etc.) using the senses. When we go to school, we listen to the teacher using our ears, we read the books using our “eyes”, and we create, or build things, using our hands. This basic simplification can be translated to cell biology through differentiation.

### ***Microenvironments***

What about stem cells? The environments analogous to schools are called “microenvironments”. This is where stem cells are “taught” what to do. Who are the teachers? At this point we are approaching what is considered the current state of the art in stem cell biology and some areas are to be decided on. However, there are scientists who say that stem cells have teachers, and they are nothing more than other, already differentiated, cells. What are the “senses” of these cells? Instead of having sight, hear, smell, taste and touch, cells interact with their environment and other cells by means of biochemical signals. We could say that biochemical signals are the “words” that make up the language a cell can understand. These biochemical signals are nothing more than proteins, or small molecules that are in the local environment and which can attach to proteins that are fixed in the cell membrane, therefore creating a signal. In this way, depending on the combination of biochemical signals, the stem cell has the ability to induce different differentiation pathways, just as different combinations of words have the ability to teach a human different things, from maths to history or french.

### ***Stimulated Differentiation***

Summing up; to teach children we have schools, in which are teachers. The children are taught by means of words in different combinations. For stem cells, we have microenvironments, in which there are specialized cells that control stem cell differentiation, by means of providing time-correlated biochemical signals. However, children, as well as stem

cells, are also responsive to signals in their environments. We could suppose that if the society needs doctors then the child will be influenced to be a doctor, by means of the adequate publicity campaigns or programs. If the human body needs lymphocytes, then a stem cell will be induced to differentiate into a lymphocyte by the body delivering the required biochemical signals.

### ***Embryonic vs Adult Stem Cells***

There is a marked difference between two different kinds (and sources) of stem cells, namely embryonic stem cells and adult stem cells. We can say that embryonic stem cells are the really pluripotent cells; equivalent to babies in our comparison (indeed, embryonic, means “of or relating to an embryo”, which represents the early stages of the baby). On the other hand, adult stem cells (mesenchymal stem cells being an example of these) are multipotent. What is the difference then? With respect to our comparison, if a child has completed intermediate “technical” training, then he will be more able to specialize in a “technical” profession (engineering, architecture, etc), but will find it difficult, although not impossible, to specialize in history or geography. The same is applicable to adult stem cells. They are the equivalent to children who have received some previous basic formation, causing them to differentiate into a cell of a predefined lineage. In this case the nomenclature is again explanatory: adult stem cell, suggests that these cells have a limited capacity for differentiation, just like the child (not the baby anymore) who has received prior training. For example, mesenchymal stem cells are adult stem cells, obtained from bone marrow, which can differentiate into any kind of cell belonging to the mesenchymal lineage, such as osteoblasts, adipocytes or chondrocytes, but not into cells of the neuronal lineage.

### ***A new revolution in biology?***

Lately, it has been reported that already committed adult cells can dedifferentiate under certain abnormal and specific stimuli, such as serious injury to an organ or tissue.<sup>1, 2</sup> These dedifferentiated cells turn into a kind of “stem cells” which can then follow another differentiation pathway. This is quite a revolution, since it means that our cells are capable of healing us from certain injuries, but, due to some reason, possibly evolution, the knowledge these cells require has been lost. An example can be myocardial infarction, a heart attack, where cardiac muscle cells die because of a lack of oxygen, and the cells that occupy their place could be proposed to be a kind of cardiac resident “stem” cells that differentiate into fibroblasts.<sup>1, 3</sup> This is believed to be due to the lack of adequate signalling to force the cells to commit into new

cardiac muscle cells. In future, however, we may be able to externally provide the required signals to initiate this behaviour. Amazingly, we can still apply our comparison here. The dedifferentiation coincides with the case, in society, when an adult who has studied a particular profession is forced into other work. For example, an engineer that has to retrain to work as a doctor because he is forced to by a society that needs doctors. This person will learn to be a doctor, although it will be much more difficult for him (as for the adult stem cell) than for a child (the real pluripotent stem cell).

### **Nanotechnology**

Finally, we will talk about the nano world. Why do we need nanotechnology to adequately control stem cell differentiation? My thesis work has to do with the induction of stem cell differentiation using nanotechnology tools. In particular, I use a technique to create different artificial microenvironments to direct stem cell differentiation. We have previously stated that humans “differentiate” as they use their senses to interact with the environment. We can roughly say that distances, between the senses in the human body, are measured in millimetres (for example, the distance between the eyes, or the ears, or the distance between nose and mouth). In the world of cells, on the other hand, distances are better measured in nanometres (one nanometre equals one millimetre divided by one million). The distances between receptor elements in the cell surface (its “senses”) are in the order of nanometres. Therefore, to adequately target specific receptors we would need, in principle, to deposit our biochemical signals (the Braille “words” for cells) with nano scale resolution. This is the ultimate aim of my work.

I hope you have been able to follow me on this short trip through stem cell differentiation. My final word is: let’s keep differentiating into stem cell researchers!

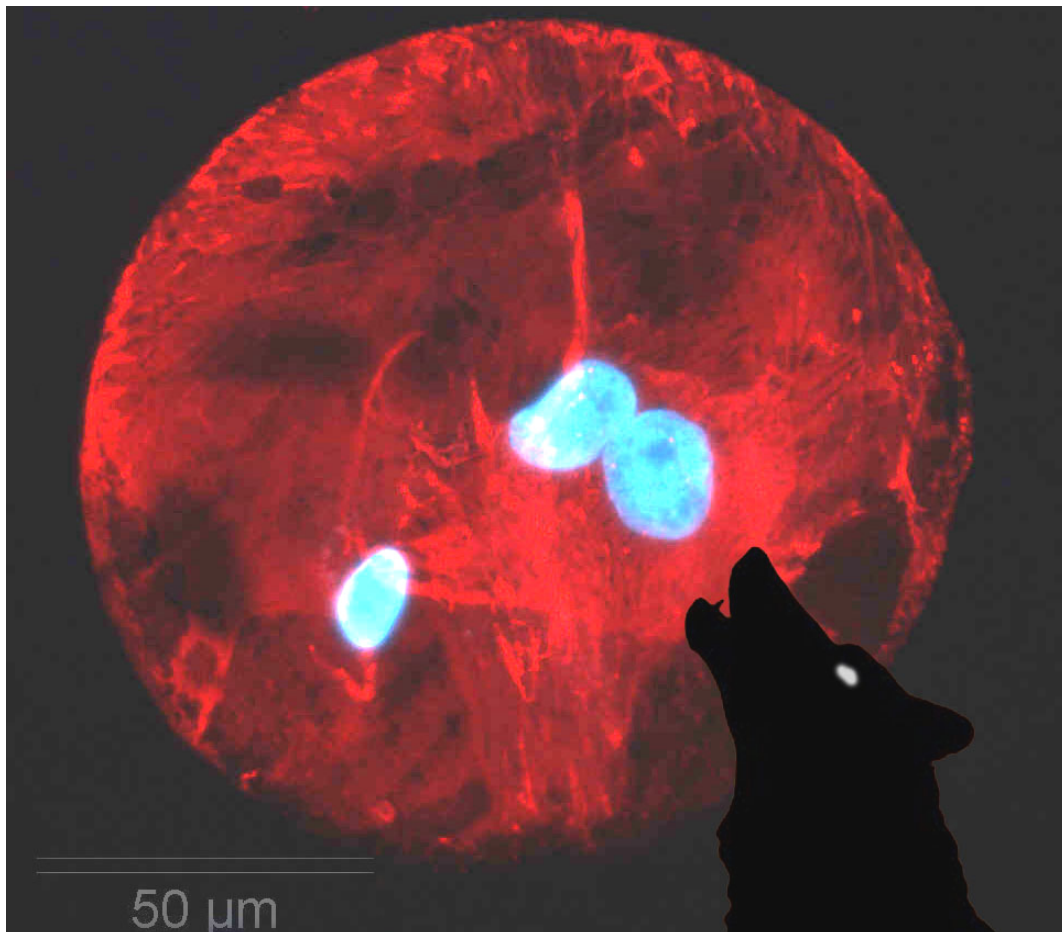
### **References:**

- [1] Smart, N., Risebro, C. A., Melville, A. A. D., Moses, K., Schwartz , R. J., Chien, K. R. and Riley, P. R. 2007. Thymosin beta4 induces adult epicardial progenitor mobilization and neovascularization. *Nature*. 445:177-182.
- [2] Song, L. and Tuan, R. S. 2004 Transdifferentiation potential of human mesenchymal stem cells derived from bone marrow. *FASEB J.* 18: 980-982.
- [3] Laflamme, M. A. and Murry, Ch. E. 2005. Regenerating the heart. *Nature Biotech.* 23 (7): 845-855.

Acknowledgements: The author would like to thank Dr. Chris A. Mills for kind revision and helpful comments on this manuscript.

**Appendix D.II Scientific images designed in an attractive “non conventional” way. Image contributions presented for the IBEC internal image competition.**

**Image 1**



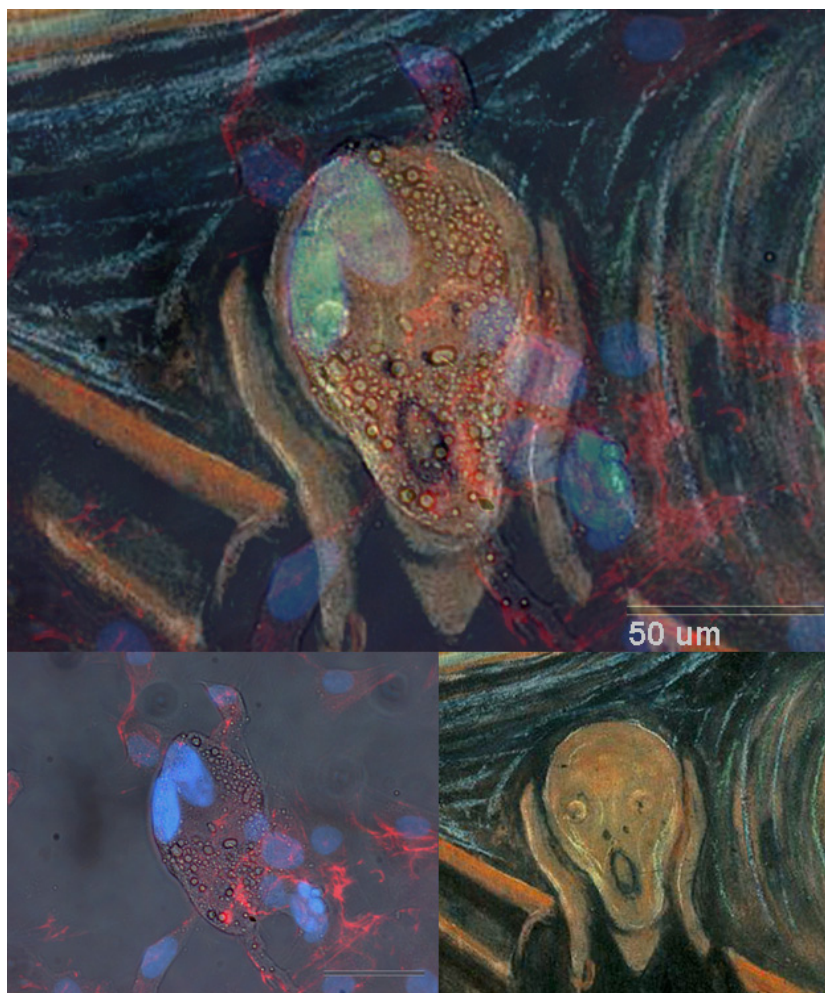
Howling at the moon:

Not everything is what it appears to be. It could be a wolf howling at the moon during a scary eclipse, but noticing the scale at the bottom left corner, the red spot is far smaller than the size of the moon.

It is in fact a fibronectin spot printed with a microarray plotter (GeSIM) on a chemically activated PMMA slide. The little blue balloons are mesenchymal stem cell's nuclei stained with Hoechst. The final aim of printing spots of protein mixtures with the Nanoplotter, is to be able to direct stem cells differentiation at the single cell level.

The wolf silhouette has been adapted from  
<http://media.photobucket.com/image/wolf%20howling%20at%20the%20moon/luvsvlph/the%20universe/Wolf-Moon.jpg>

## Image 2

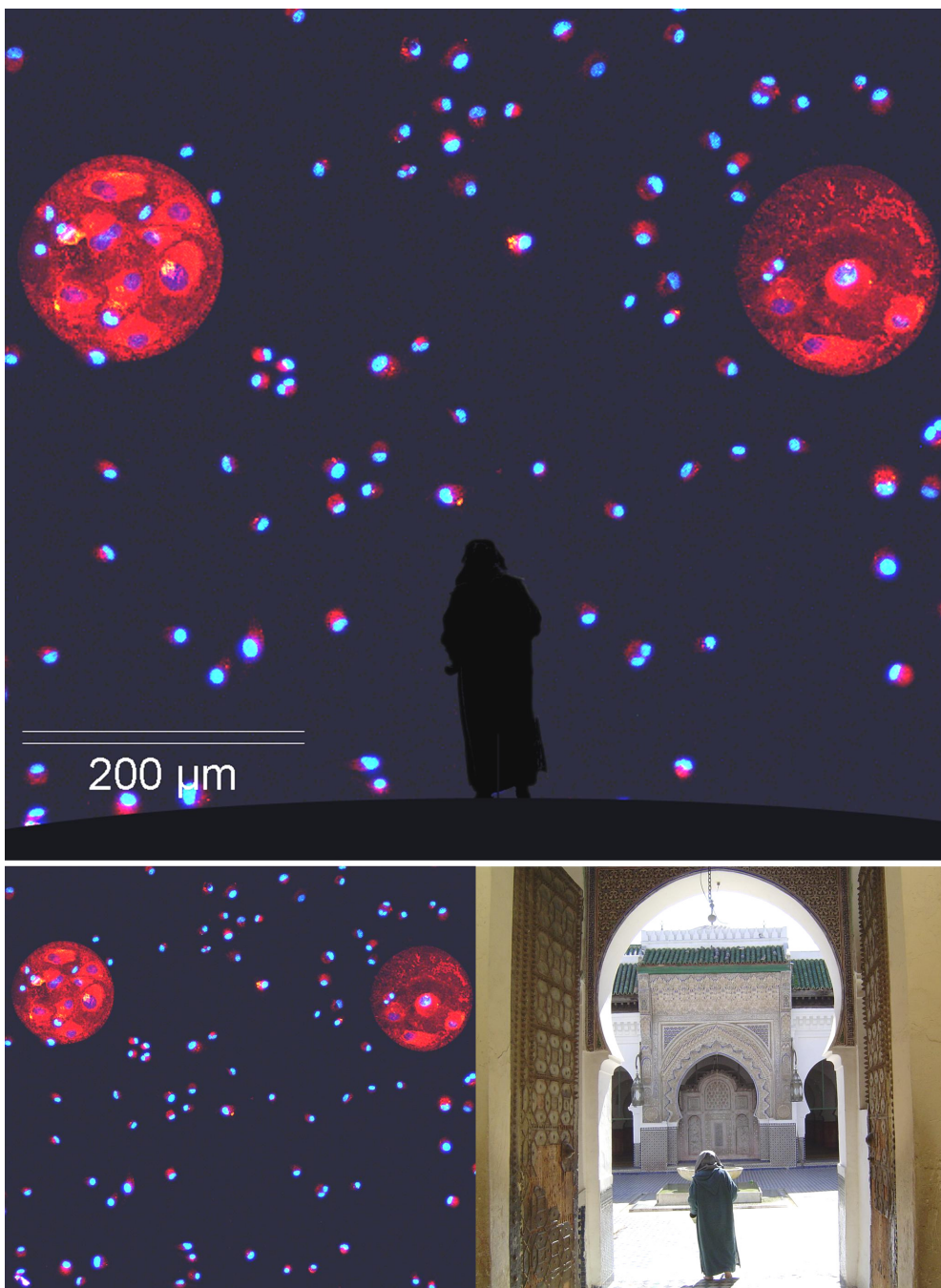


Intruders among us?

The base image for this composition is an immuno fluorescence image (blue: cells nuclei, red: fibronectin) superposed with a bright field image of a culture of mesenchymal stem cells (MSC, bottom left image). Rat MSC are cells purified from bone marrow. They are capable of differentiating into many cell types, including osteoblasts (bone cells) and adipocytes (fat tissue cells). The morphology of the cell in the center of the base image could resemble that of an adipocyte, nevertheless due to the staining of apparently two nuclei and the small size of the droplets inside it, we suspect it is in fact a blood cell known as megakaryocyte that has infiltrated in the culture. The second image (bottom right) could well represent our surprise for this finding. How can we be sure what this cell really is? Further characterisation is needed.

The bottom right image is part of the painting “The cry” (1893) by Norwegian painter Edvard Munch, whose intense, evocative treatment of psychological and emotional themes was a major influence on the development of German Expressionism in the early 20th century.

**Image 3**



Although one could dream about a Saturnian's scenario with two full red moons and a lot of stars on a clear night, the image is a composition of two different pictures. The bottom left image shows two Fn spots (immuno stained in red) seeded with mesenchymal stem cells (cell nuclei is stained in blue). This original image has been superimposed with the silhouette of a muslim man entering a the Al-Karaouine University in Fez, Morocco, recognised as the oldest continuously operating academic degree-granting university in the world. This original image (bottom right) was taken and modified by the author of this PhD thesis.

# Appendix E    Publications and conference communications

## Apppendix E.I Publications

Rodríguez-Seguí, S.A.; Pla-Roca, M.; Engel, E.; Planell, J.A.; Martínez, E.; Samitier, J., Influence of fabrication parameters in cellular microarrays for stem cell studies. *Journal of Materials Science-Materials in Medicine* 2009, 20, (7), 1525-1533.

Rodríguez-Seguí, S. A.; Pons Ximénez, J. I.; Sevilla, L.; Ruiz, A.; Colpo, P.; Rossi, F.; Martínez, E.; Samitier, J., Immobilized protein quantification and comparison in substrates for cellular microarray applications. *In preparation*.

Martinez, E.; Lagunas, A.; Mills, C. A.; Rodriguez-Segui, S.; Estevez, M.; Oberhansl, S.; Comelles, J.; Samitier, J., Stem cell differentiation by functionalized micro- and nanostructured surfaces. *Nanomedicine* 2009, 4, (1), 65-82.

E. Martínez, C.A. Mills, A. Lagunas, M. Estévez, S. Rodríguez-Segui, J. Comelles, S. Oberhansl and J. Samititer, Design and production of micro and nanostructured polymer substrates for cell culture applications. *NanoSpain Newsletter* 2008.

Akimov, V.; Alfinito, E.; Bausells, J.; Benilova, I.; Casuso Paramo, I.; Errachid, A.; Ferrari, G.; Fumagalli, L.; Gomila, G.; Grosclaude, J.; Hou, Y.; Jaffrezic-Renault, N.; Martelet, C.; Pajot-Augy, E.; Pennetta, C.; Persuy, M.; Pla-Roca, M.; Reggiani, L.; Rodriguez-Segui, S.; Ruiz, O.; Salesse, R.; Samitier, J.; Sampietro, M.; Soldatkin, A.; Vidic, J.; Villanueva, G., Nanobiosensors based on individual olfactory receptors. *Analog Integrated Circuits and Signal Processing* 2008, 57, 197–203.

Martinez E. ; Rios-Mondragon I. ; Pla-Roca M. ; Rodriguez-Segui S. ; Engel E. ; Mills C.A. ; Sisquella X. ; Planell J.A. ; Samitier J., **Cell-surface interactions studies to trigger stem cell differentiation.** *Nanomedicine : Nanotechnology, biology and medicine* 2007, 3, 346.

Rodríguez Seguí, S.; Pla, M.; Minic, J.; Pajot-Augy, E.; Salesse, R.; Hou, Y.; Jaffrezic-Renault, N.; Mills, C. A.; Samitier, J.; Errachid, A., Detection of Olfactory Receptor I7 Self-

Assembled Multilayer Formation and Immobilization Using a Quartz Crystal Microbalance.  
*Analytical Letters* 2006, 39, 1735-1745.

## **Appendix E.II Conference communications**

Poster presentation: "Cellular microarray design for the culture and differentiation study of mesenchymal stem cells"

Event: NanoBioEurope 2008 conference

Place: Barcelona, Spain.

Date: 9<sup>th</sup> - 13<sup>th</sup> June 2008.

Poster presentation: "Artificial microenvironments arranged in a microarray format to lead Mesenchymal Stem Cell differentiation"

Event: 8th World Biomaterials Congress

Place: Amsterdam, The Netherlands.

Date: 28<sup>th</sup> May - 1<sup>st</sup> June 2008.

Poster presentation: "Design of cellular microarrays to study mesenchymal stem cell differentiation"

Event: ESF-EMBO conference

Place: Sant Feliu de Gixols, Spain.

Date: 1<sup>st</sup> - 6<sup>th</sup> July 2007.

Organized by: European Science Foundation

Poster presentation: "Design of artificial niches to direct rat mesenchymal stem cells towards osteoblast or adipocyte fates"

Event: 5th annual meeting of the International Society for Stem Cell Research (ISSCR)

Place: Cairns, Australia.

Date: 17<sup>th</sup> – 20<sup>th</sup> July 2007.

Organized by: ISSCR

Poster presentation: "Application of a Bio-QCM to study carbohydrates self-interaction in presence of calcium"

Event: Eurosensors and Transducers Congress, 2007

Place: Lyon, France.

Date: 10<sup>th</sup> – 14<sup>th</sup> July 2007.

Organized by: IEEE

Poster presentation: "First characterization of a Biosensor for large DNA molecules using quartz crystal microbalance and impedance spectroscopy"

Event: Eurosensors and Transducers Congress, 2007

Place: Lyon, France.

Date: 10<sup>th</sup> – 14<sup>th</sup> July 2007.

Organized by: IEEE

Poster presentation: "Quartz Crystal Microbalance studies of olfactory receptors grafted on biotinylated surfaces"

Event: "Bionanotechnology: From self assembly to cell biology"

Place: Cambridge. UK.

Date: 3, 4 and 5th January 2007.

Organized by: Biochemical Society and Portland Press.

Event: "Cancer Nanotech". (Application of Nanotechnologies for the diagnosis and treatment of Cancer).

Place: Paris. France.

Date: 17<sup>th</sup> - 18<sup>th</sup> May 2006.

Organized by: Upperside Group.

Participation as: Conference assistance.

Poster presentation: "Hybrid Quartz Crystal Microbalance (QCM) sensor for the detection of pH"

Event: "International Workshop on Biosensors for Food Safety and Environmental Monitoring"

Place: Agadir. Morocco.

Year: 2005.

Organized by: Université Hassan II-Mohammedia.



# **Resumen en castellano - Desarrollo de microarrays celulares para el cultivo de células madre y la evaluación de estadios tempranos de diferenciación**

## **Prefacio**

Esta tesis involucra el desarrollo de una técnica relativamente nueva conocida como microarrays celulares. En particular, en lo referente al cultivo de células madre, los microarrays celulares han sido reportados a partir de 2004. Aunque una amplia gama de aplicaciones podría derivarse del uso de esta técnica aplicada al estudio de la diferenciación de células madre, en la práctica, al abordarse este tema se han encontrado ciertas limitaciones en el estado del arte del desarrollo de los microarrays celulares. Se llegó a la conclusión de que aún hacía falta investigación básica para comprender con mejor detalle la influencia de los parámetros tecnológicos que afectan la respuesta celular en este tipo de plataformas. Este hallazgo condujo a los objetivos planteados en la presente tesis doctoral.

Este trabajo está dividido en 5 capítulos. En la introducción (el capítulo 1) se provee una descripción general de las técnicas basadas en microarrays, con especial énfasis en los microarrays celulares. Los logros recientes y las limitaciones principales de esta técnica, reportadas en la literatura, se exponen para introducir la motivación de este trabajo. Los objetivos de esta tesis se presentan al final de este capítulo. Los capítulos siguientes describen el trabajo experimental realizado y los resultados obtenidos para lograr cada uno de los objetivos propuestos. En el capítulo 2, se presenta la caracterización de varios substratos con aplicaciones para microarray celulares. Esta caracterización se ha basado en la cantidad de proteína inmovilizada por cada uno de ellos después de la impresión y lavado. Esto constituye un aspecto importante con respecto a los microarrays celulares, ya que son las proteínas inmovilizadas en la superficie las que actúan sobre la señalización de las células adheridas sobre los spots. Por lo tanto, si luego de lavar los slides quedase poca o ninguna proteína, no se observarían las interacciones deseadas y la aplicación del microarray sería nula. Este análisis permitió elegir al

substrato mas adecuado para continuar con los siguientes objetivos de esta tesis. En el capítulo 3, los parámetros para la fabricación de los microarrays celulares fueron optimizados para el cultivo de células de madre mesenquimales en los microarrays por períodos de hasta 8 días. Dado que estas células son una fuente de células madre muy prometedora para su aplicación en terapias celulares diversas, la adaptación de los microarrays celulares para el futuro estudio de algunas de sus etapas de diferenciación resulta altamente atractiva. En el capítulo 4, se presenta un acercamiento al estudio de la diferenciación de células madre basándose en el protocolo celular previamente optimizado, demostrando que las células cultivadas en esta plataforma expresan marcadores de diferenciación temprana a osteoblastos en respuesta a un factor de crecimiento impreso. Adicionalmente, se han identificado nuevos desafíos a superar en el futuro para optimizar la aplicación de esta técnica. En el capítulo 5 se exponen las conclusiones de esta tesis.

## **Capítulo 1      Introducción**

Las técnicas de alto rendimiento (denominadas de aquí en adelante por su término en inglés, “high-throughput”, debido a la inexistencia de una traducción adecuada) basadas en microarrays han constituido un foco intensivo de investigación en la última década. La principal ventaja de estas técnicas es que permiten un tratamiento masivo, en paralelo y miniaturizado para el análisis y detección de múltiples analitos en una muestra, facilitado por las interacciones de unión específica entre moléculas en una interfase sólida. Los datos obtenidos en forma multiplexada a partir de un experimento de microarrays normalmente son el equivalente de cientos de experimentos realizados por medio del empleo de técnicas de biología molecular convencionales. Por consiguiente, las técnicas de microarrays proveen una alternativa más rápida para el análisis, al mismo tiempo que reducen considerablemente el consumo de las muestras a analizar, confiriendo también al análisis una mayor precisión y sensibilidad.

De forma general, un microarray esta formado por un substrato sobre el cual se han inmovilizado diferentes moléculas en puntos (denominadas de aquí en adelante por su término en inglés, “spots”, debido a la inadecuación de una traducción mas adecuada) individuales en un formato de matriz (denominado de aquí en mas por su termino en inglés, “array”). Cuando este substrato se incuba con la muestra en solución, reacciones paralelas específicas tienen lugar entre las moléculas inmovilizadas en la superficie y las moléculas presentes en la muestra. Debido a que usualmente la distancia entre spots es del orden de cientos de micrómetros, estos substratos impresos se suelen denominar por su termino en inglés, “microarrays”.

Según el tipo de moléculas que se inmovilizan en la superficie del substrato, los microarrays pueden clasificarse como microarrays de ADN (ácido desoxirribonucleico), microarrays de proteína, microarrays de tejido o microarrays celulares. En particular, los microarrays celulares involucran la impresión de proteínas (aunque también puede tratarse de otros factores, tales como polímeros) en formato de microarray sobre un substrato sólido y a continuación el cultivo celular exclusivamente en los spots impresos. La formación típica de un microarray celular involucra los siguientes pasos (Figura R. 1):

- Fabricación de los microarrays de proteína. Con este fin se imprimen soluciones de proteínas sobre los substratos, generalmente mediante el uso de robots trazadores (o plotter, por su término en inglés) de microarrays.
- Formación de los microarrays celulares y cultivo de las células. Este proceso involucra la pasivación, este término refiriéndose a la inactivación o bloqueo, de la superficie no impresa. El objetivo de la pasivación es aumentar la adhesión celular selectivamente en los spots impresos, y el subsiguiente sembrado de células. Después de un cierto tiempo, suficientemente extenso como para permitir la adhesión celular a los spots pero no tan largo como para promover la adhesión en las áreas pasivadas, las células no adheridas son removidas. El microarray celular así formado es luego cultivado por diversos períodos de tiempo.
- Caracterización de los microarrays celulares. El objetivo de este último paso en el proceso consiste en evaluar el efecto de las proteínas impresas sobre las células que se han cultivado encima. Con este fin, las células se fijan y se tiñen con los marcadores de interés, normalmente mediante técnicas de inmunofluorescencia. Finalmente, las células son observadas por medio de un microscopio de fluorescencia.

En contraste con las técnicas de microarrays de ADN o de proteína, la técnica de microarrays celulares no está aún bien establecida en los laboratorios de biología. Esto es debido a una serie de dificultades que aparecen como consecuencia del incremento en complejidad al pasar de imprimir ADN a imprimir proteínas (que deben permanecer en un estado funcional) y cultivar células encima de los spots por varios días. Como resultado, la elección de la estrategia para la implementación de los microarrays celulares es altamente dependiente del tipo de aplicación y problema a estudiar. En particular, el tipo de células empleadas, tiempo necesario de cultivo y el medio de cultivo requerido por las células son aspectos clave a tener en cuenta al momento de diseñar una aplicación de este tipo.

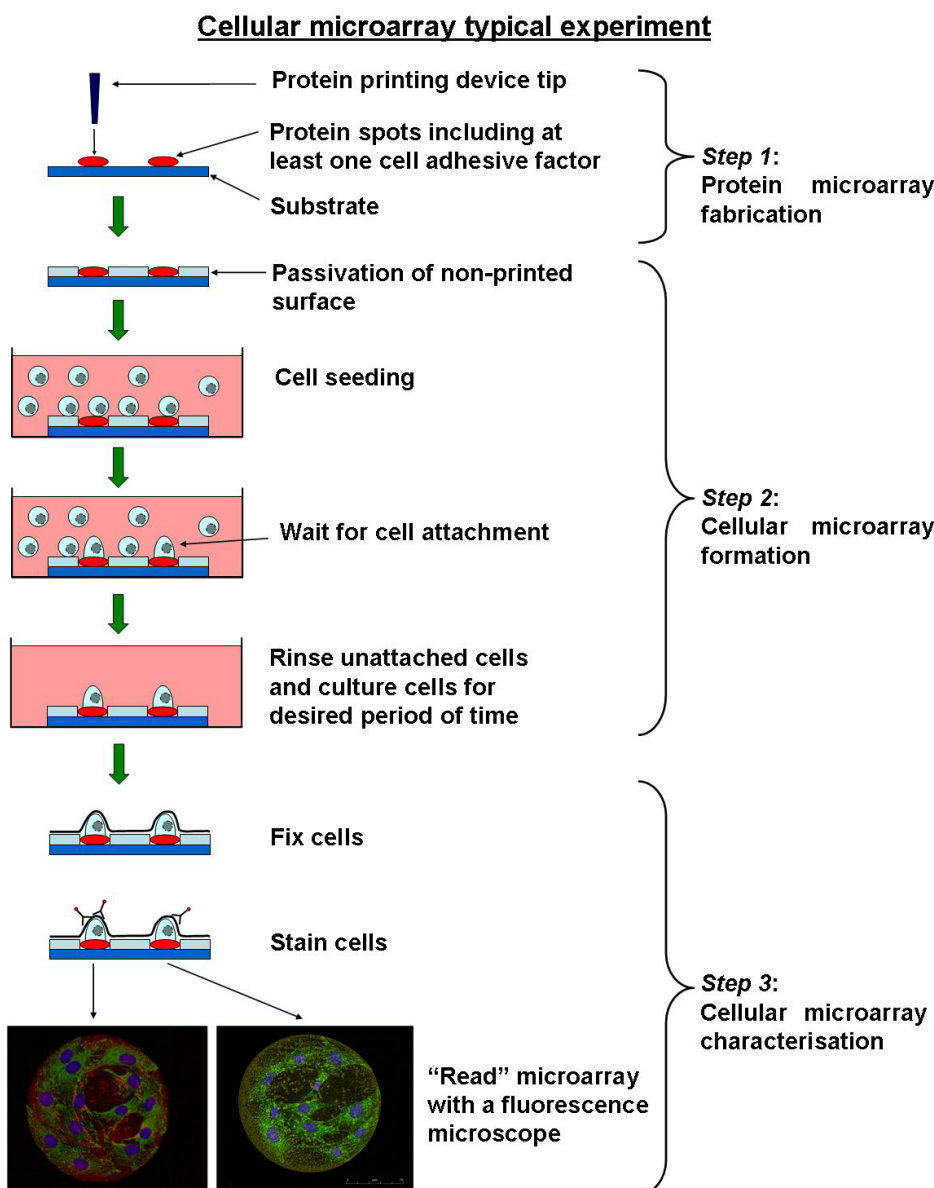


**Figura R. 1** Esquema representando un experimento tipo con microarrays celulares.

Actualmente no hay protocolos estándar que permitan el diseño de una aplicación universal de microarrays celulares. Una serie de desafíos ya han sido identificados como claves para el desarrollo de esta técnica. Estos involucran los siguientes:

- Evitar la adhesión celular fuera de los spots en los microarrays. Al mismo tiempo, los substratos empleados deberían permitir una eficiente inmovilización de las proteínas impresas. Para hacer posible este objetivo, se debe elegir una solución de compromiso entre el tipo de substrato a usar, la activación química de su superficie, y el método de pasivación a emplear.
- Mantener los spots, con células adheridas sobre ellos, aislados entre sí durante el tiempo completo que dure el cultivo celular. En este caso, los parámetros más

importantes que deben ser optimizados son la estrategia de pasivación y el medio de cultivo empleados. Los medios de cultivo que contienen proteínas (por ejemplo, el suero fetal bovino, FBS) tienden a degradar el cultivo en formato de microarray, mientras que los medios sin suero no están optimizados para la viabilidad celular.

- Mantener la viabilidad celular en los spots durante varios días, dependiendo del tiempo requerido para el experimento. Esto impone una adecuación del medio de cultivo usado y el aislamiento mutuo entre spots.
- Optimizar la cantidad y actividad de las proteínas inmovilizadas en el substrato. Este requerimiento es fuertemente afectado por la activación química de la superficie, en la cual una superficie activada químicamente para reaccionar con las proteínas impresas retendrá una mayor cantidad de proteína. La actividad de las propinas inmovilizadas también está influenciada por la solución tampón (referida de aquí en más por su término en inglés, “buffer”) en que se ha preparado las soluciones proteicas a imprimir. Por ejemplo, algunos buffers incluyen glicerol para retardar la evaporación de los spots al ser impresos.

Atendiendo a estos requerimientos, una serie de reportes recientes han aparecido sobre el estudio de la diferenciación de células madre mediante el empleo de microarrays. Estos han sido optimizados para evaluar la diferenciación de células madre de ratón en respuesta a distintas combinaciones de proteínas de matriz extracelular (ECM) y la respuesta de diferenciación de células precursoras neuronales en función de los factores de crecimiento impresos, entre otros. Cabe destacar que dichos reportes se han basado en substratos específicos, sobre los cuales se ha optimizado la composición de los spots y el medio de cultivo para permitir el estudio mediante microarrays empleando las líneas celulares elegidas.

## **Objetivos de esta tesis**

La gran variedad de substratos y parámetros de fabricación de los microarrays celulares descriptos en estas aplicaciones motivó el desarrollo de la presente tesis doctoral, cuyo objetivo general fue evaluar una serie de ellos para optimizar la plataforma para el cultivo de células mesenquimales y permitir la evaluación de estadios tempranos de diferenciación.

El primer objetivo consistió en realizar un estudio cuantitativo de la cantidad de proteína inmovilizada por una variedad de substratos con posibles aplicaciones en la técnica de microarrays celulares. Este análisis se enfocó en la eficiencia de inmovilización de proteínas por cada uno de los substratos evaluados, mediante la impresión de proteínas relevantes en

aplicaciones de microarrays celulares. Dichas proteínas fueron marcadas fluorescentemente e impresas a las concentraciones habitualmente empleadas en este ámbito. El substrato que permitió la inmovilización de una mayor cantidad de proteína, al tiempo que mostró la mejor repetitividad de los resultados, fue elegido para continuar con la optimización del protocolo de fabricación de microarrays celulares.

El segundo objetivo tuvo como meta optimizar los parámetros mas relevantes para la fabricación de microarrays celulares usando células mesenquimales (MSC). Estos parámetros incluyeron: el tamaño del spot, la composición del buffer de impresión, el medio de cultivo, el tiempo de sembrado celular y la concentración a la que las células son sembradas. Los spots impresos en este primer acercamiento estuvieron compuestos exclusivamente de fibronectina (Fn), una proteína de matriz extracelular que permite la adhesión de las células a los spots.

Dado que diferentes factores pueden producir diferentes respuestas, según el tipo celular empleado en los experimentos, el enfoque de este último objetivo consistió en evaluar un estadío temprano de diferenciación usando un modelo celular, en respuesta a un factor de crecimiento impreso en la plataforma optimizada previamente.

## **Capítulo 2 Caracterización y comparación cuantitativa de la inmovilización de proteínas en substratos para aplicaciones de microarrays celulares**

### **Introducción**

Varios substratos han sido previamente descriptos para aplicaciones en microarrays celulares: agarosa, poliacrilamida, oro, vidrio, nitrocelulosa, poli(metil metacrilato), poli(etilenglicol), entre otros. Los mecanismos de inmovilización de las proteínas en estos substratos son extremadamente variados, pasando desde la simple adsorción de proteínas (para los substratos de poli(etilenglicol), por ejemplo), hasta la inmovilización covalente de las proteínas mediante la activación química de substratos como vidrio u oro.

Actualmente pueden encontrarse varios reportes comparando la eficiencia de diversos substratos en aplicaciones de microarrays de ADN o microarrays de proteína. Sin embargo, el equivalente para microarrays de proteína con aplicación directa a la formación de microarrays celulares (es decir, usando proteínas y concentraciones relevantes en esta última técnica), no ha sido encontrado en la literatura. El principal desafío para cumplir este objetivo consiste en la

extrema dificultad existente para cuantificar, de forma precisa, la cantidad de proteína inmovilizada en una superficie.

El objetivo final de esta tesis consiste en desarrollar microarrays celulares basados en spots compuestos por mezclas de proteínas de matriz extracelular (para promover la adhesión celular a los spots) y un factor de crecimiento (para inducir diferenciación).

El trabajo presentado en este capítulo se basó en la evaluación de la eficiencia de una serie de substratos para inmovilizar dos proteínas marcadas fluorescentemente. Con este fin, una de las proteínas de matriz extracelular más comunes, la fibronectina (Fn), fue elegida como modelo de proteína de matriz extracelular, mientras que una proteína más pequeña, la streptavidina (SA), se eligió como un modelo conveniente para representar un factor de crecimiento. En el estudio presentado en este capítulo puntual no se emplearon factores de crecimiento reales debido a su elevado costo. Estas proteínas fueron impresas en diferentes tamaños de spot, y la Fn también fue ensayada impresa a distintas concentraciones. Adicionalmente, dos buffers de impresión fueron probados: PBS y PBS con un agregado de 2% de glicerol. El agregado de glicerol ha sido reportado en la literatura debido a que su inclusión retrasa el secado de los spots luego de impresos y, por consiguiente, podría favorecer la inmovilización de proteínas en una forma mas activa.

## Materiales y Métodos

Los substratos utilizados en este trabajo fueron elegidos de forma tal que cubriesen una variedad de propiedades distintas. Estos pueden clasificarse en 3 categorías:

- Substratos con superficies activadas químicamente para promover la inmovilización covalente de las proteínas impresas: Vidrio derivatizado con aldehído (**AD-Glass**), Agarosa derivatizada con aldehído (**AD-Agarose**) y PMMA derivatizado con PFP-COOH (**a-PMMA**).
- Substratos con una superficie modificada químicamente para proveerle propiedades de “non-fouling” (es decir, baja adsorción de proteínas cuando esta sumergida en un medio líquido): Vidrio recubierto con varios tipos de óxido de poli(etileno) (en inglés, Poly(ethylene) oxide-like, abreviado de aquí en mas como **PEO-like**).
- Substratos sin superficies modificadas químicamente (substratos control): Vidrio Control (no tratado, **Ctrl-Glass**), usado como referencia, y Vidrio recubierto

previamente con BSA (**BSA-Glass**) como control negativo (es decir de no adsorción de proteínas).

Con el objetivo de cuantificar la cantidad de proteína que queda inmovilizada en los substratos impresos, luego del tratamiento habitual que se sigue para la formación de microarrays celulares (que involucra varios pasos de lavado), se emplearon como modelo dos proteínas marcadas fluorescentemente: fibronectina marcada con el fluoróforo Alexa Fluor 555 (visualización en verde con el escáner) y streptavidina marcada con el fluoróforo Alexa Fluor 647 (visualización en rojo con el escáner).

Para la fabricación de los microarrays de proteína se empleó un Nanoplotter. Este equipo consiste en un robot trazador (“plotter”, por su término en inglés) conectado a una pequeña jeringa (operada por medio de un cristal de cuarzo que genera las nanogotas) que es capaz de dispensar gotas del orden de los nanolitros (0,4 nL en este caso) en posiciones arbitrarias sobre un substrato plano. Para este fin, el Nanoplotter toma las soluciones a dispensar de los pocillos de una placa (normalmente se preparan volúmenes de soluciones proteicas de aproximadamente 10 µL, que se depositan en pocillos de una placa de 386 pocillos). Con este dispositivo, se imprimieron diferentes concentraciones de Fn (50, 100, 200 y 360 µg/mL), con y sin SA (ensayada a una sola concentración: 50 µg/mL), en dos buffers de impresión (PBS y PBS con 2% glicerol) y en 3 tamaños de spot distintos. Los tamaños de spot se produjeron a partir de la sobre impresión, en la misma posición del microarray, de 1, 5 o 10 gotas.

La disposición de spots impresos en el microarray se diseñó de tal forma que permitió la evaluación de todos los parámetros de una forma paralela en cada substrato ensayado. Con este fin, cada combinación de los parámetros mencionados en el párrafo anterior fue impresa 20 veces en cada substrato. Esto permitió evaluar un parámetro adicional, la repetitividad intra-slide de los resultados de inmovilización. Este parámetro fue definido como la variación existente entre los spots replicas (es decir, aquellos impresos con igual composición y tamaño de spot) en cuanto al valor de proteína inmovilizada. El esquema impreso se presenta en la Figura R. 2.

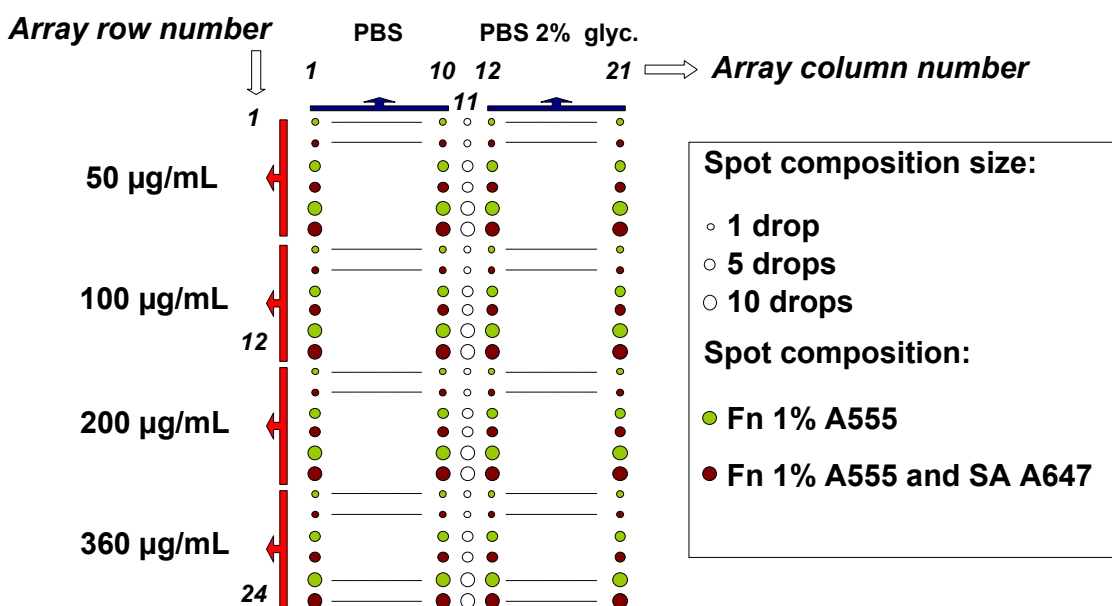


**Figura R. 2** Esquema mostrando la disposición de los spots impresos en formato de microarray. Cada composición de spot esta definida por el numero total de gotas impreso (1, 5 o 10 gotas), la composición del buffer (PBS o PBS 2% glicerol), la concentración de Fn marcada fluorescentemente (indicada como Fn 1% A555) y la inclusión o no de SA (a una única concentración: 50 µg/mL, indicada como SA A647) en la solución proteína impresa. Las condiciones de spot se imprimieron en 10 replicas en cada bloque, y dos bloques iguales fueron impresos por cada slide ensayado, resultando en un total de 20 condiciones de spot idénticas ensayadas en paralelo por cada experimento.

El principio fundamental en que se basa el método elegido para la cuantificación de proteína inmovilizada (explicado más abajo) consiste en que la señal de fluorescencia obtenida por el escáner para cada spot (es decir, la suma de la intensidad de todos los pixeles dentro del spot) es directamente proporcional a la cantidad de proteína marcada fluorescentemente que hay en ese spot. Mas aún, el método propuesto parte de que las cantidades de proteína depositadas inicialmente en cada spot son conocidas, y fueron calculadas a partir de los valores de concentración de proteína en la solución impresa y del volumen total de esta solución (que depende del numero total de gotas impresas) depositada en cada spot (se puede referir a la Tabla 2.6 de la tesis en inglés para consultar los valores concretos).

El protocolo seguido para cuantificar la cantidad de proteína que queda inmovilizada en los substratos se presenta en la Figura R. 3. Básicamente, luego de la impresión de los microarrays con las proteínas marcadas fluorescentemente (paso 1), se incubó dichos substratos durante toda la noche para facilitar la interacción de las proteínas con la superficie. El día siguiente, los substratos fueron escaneados antes (paso 2) y después (paso 5) de los pasos de lavado (que también incluyeron la pasivación previa de la superficie para los casos puntuales de los substratos AD-Glass, a-PMMA, BSA-Glass y Ctrl-Glass, paso 4). A partir de la cuantificación

de la intensidad de fluorescencia de las imágenes obtenidas con el escáner, antes de lavar los substratos, se trazaron curvas de calibración. Estas curvas de calibración, que son específicas para cada slide, fueron aproximadas por un modelo lineal (en el que mayor cantidad de proteína fluorescente impresa implicaba un aumento lineal de la intensidad de la señal de fluorescencia detectada con el escáner, paso 3). Los datos de intensidad de fluorescencia obtenidos para cada slide, después de los pasos de lavado, fueron traducidos a cantidad de masa inmovilizada en dicho slide mediante el empleo de la curva de calibración efectuada para el slide en cuestión (paso 6).

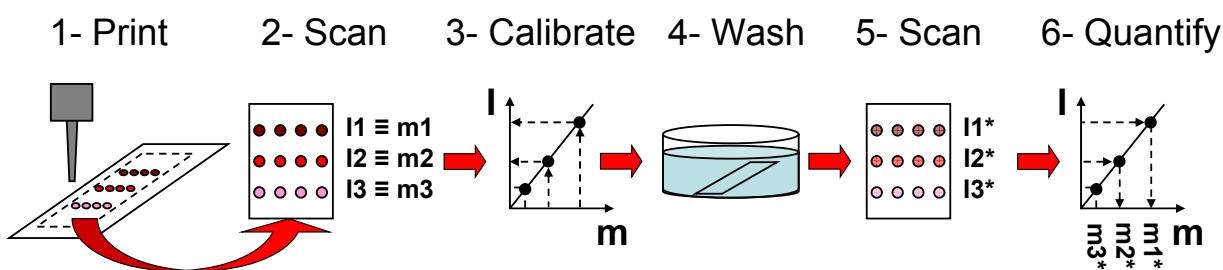


**Figura R. 3** Esquemático del protocolo experimental seguido para cuantificar la cantidad de proteína inmovilizada por cada substrato.

## Resultados

### Evaluación general

El formato de microarray impreso para estos experimentos se muestra en la Figura R. 4A. Algunas imágenes representativas de cómo se visualizaron los microarrays de proteína recién impresos y después de lavar se muestran en la Figura R. 4B y Figura R. 5B. Aquí se puede observar, por un lado, que el microarray revelado por las imágenes de fluorescencia coincide con el esquema del microarray impreso. Por otro lado, se observa también que la intensidad de los spots después de lavar disminuye considerablemente, indicando que efectivamente durante el proceso de lavado una parte de la proteína impresa fue removida de los spots. Nótese que la disminución en la fluorescencia de los spots tuvo importantes diferencias entre los substratos ensayados. Por un lado, mientras el microarray pudo ser identificado visualmente prácticamente en su totalidad para los substratos activados químicamente (Figura R. 4), la señal proveniente de muchos de los spots fue perdida luego de lavar los substratos que no fueron activados químicamente para promover la interacción de las proteínas (Figura R. 5). En particular, se observó que la señal proveniente de la SA (que da lugar a una fluorescencia amarillo a rojiza, según la cantidad de Fn co inmovilizada) desapareció prácticamente en su totalidad en estos

últimos substratos, los spots impresos con SA emitiendo fundamentalmente una señal verde (sugiriendo que solo se ha inmovilizado la Fn en estos spots).

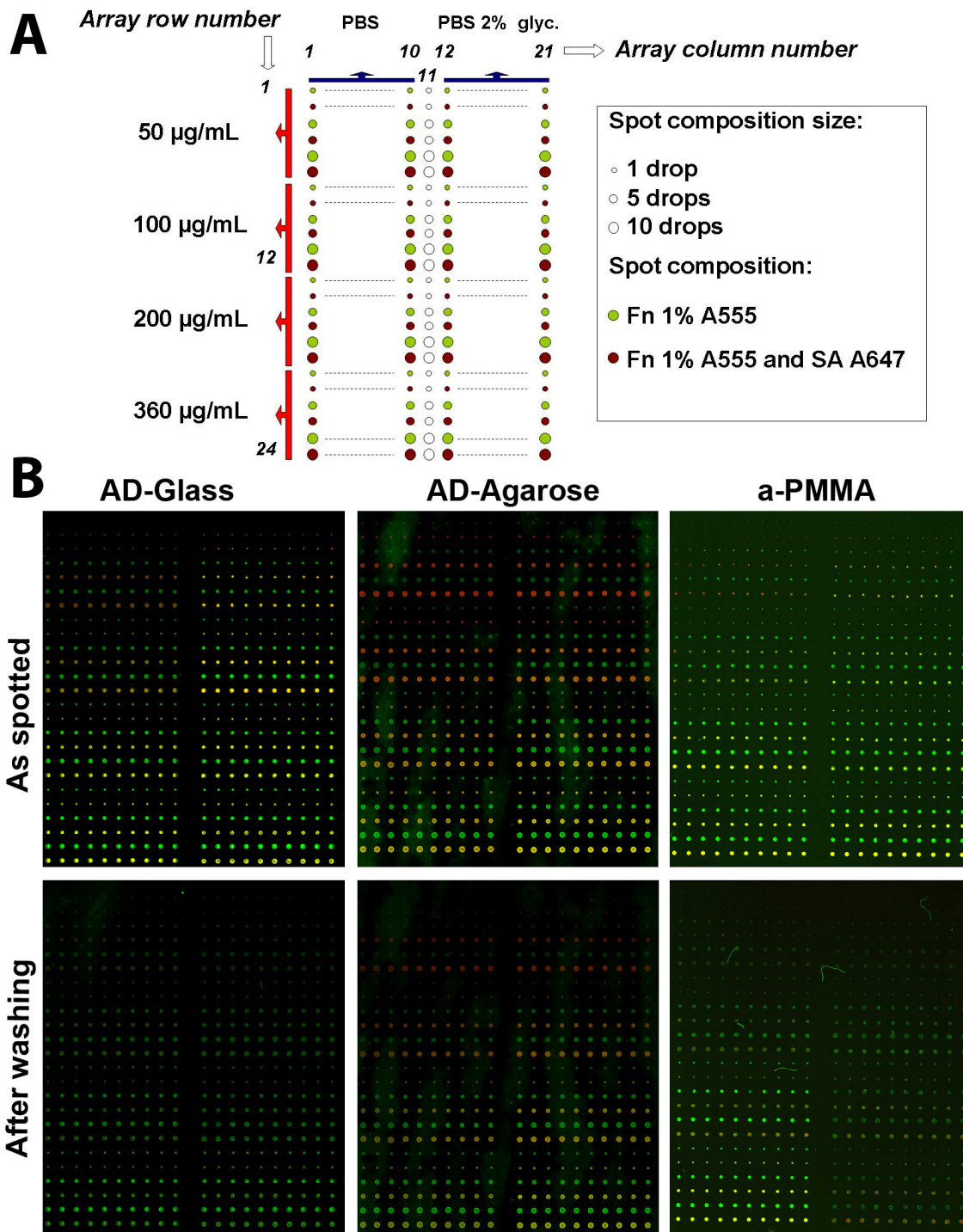


**Figura R. 4 A.** Esquema del microarray impreso. **B.** Imágenes representativas obtenidas con el escáner de fluorescencia antes (indicado como “as spotted”) y después (indicado como “after washing”) de lavar los slides, para AD-Glass, AD-Agarose y a-PMMA. Los spots verdes representan la Fn marcada en verde. Los spots de color amarillo a rojizo representan la SA (marcada en rojo) impresa conjuntamente con diferentes concentraciones de Fn (marcada en verde). La distancia entre spots es 1 mm.

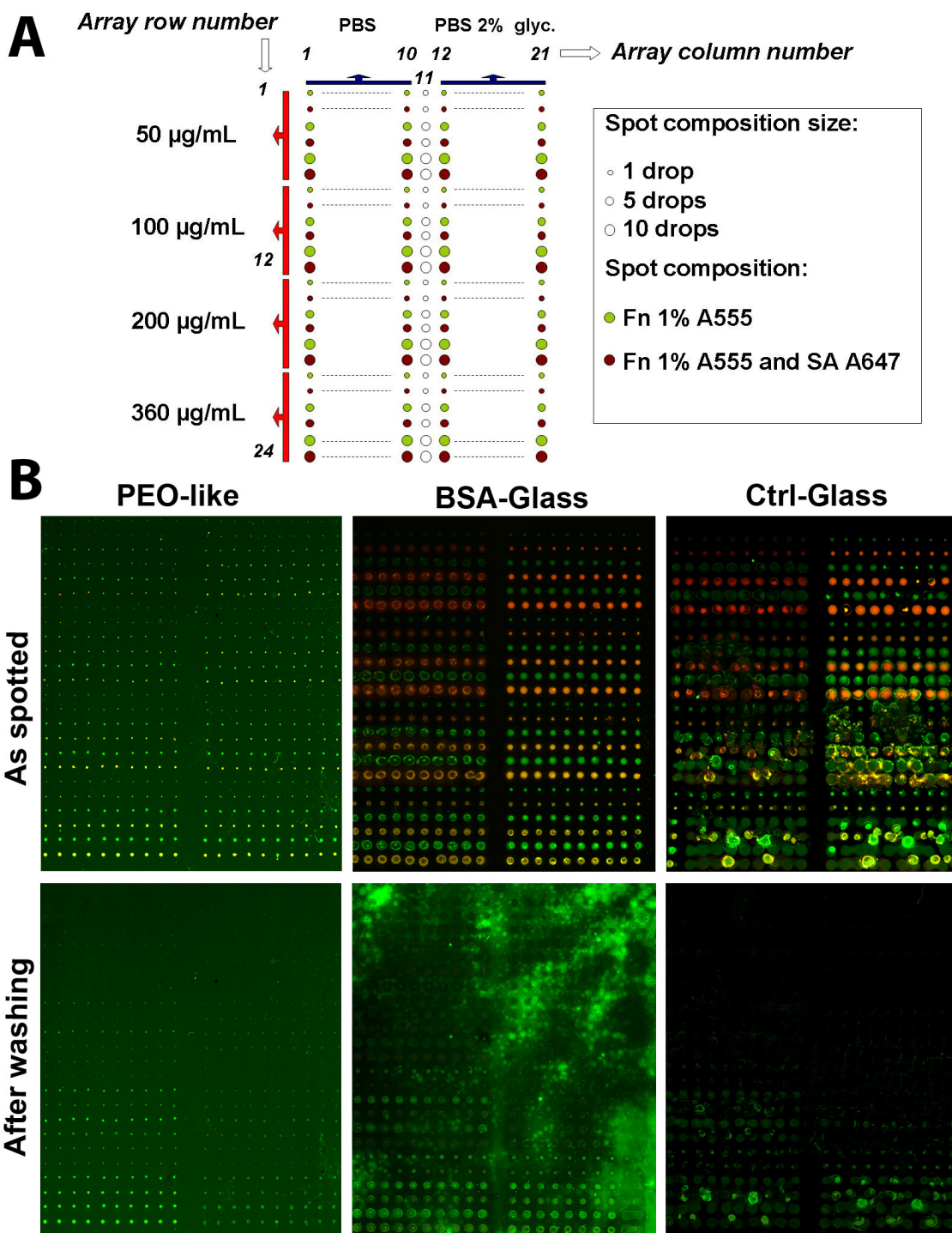


**Figura R. 5 A.** Esquema del microarray impreso. **B.** Imágenes representativas obtenidas con el escáner de fluorescencia antes (indicado como “as spotted”) y después (indicado como “after washing”) de lavar los slides, para PEO-like, BSA-Glass y Ctrl-Glass. Los spots verdes representan la Fn marcada en verde. Los spots de color amarillo a rojizo representan la SA (marcada en rojo) impresa conjuntamente con diferentes concentraciones de Fn (marcada en verde). La distancia entre spots es 1 mm.

### Inmovilización de Fn

Mediante la aplicación del protocolo para cuantificar la proteína descripto en el apartado de Materiales y Métodos, se generaron gráficos para representar la cantidad de proteína

inmovilizada luego de lavar, en función de la cantidad total de proteína impresa. A partir de estas representaciones, se halló que para la mayoría de los substratos (exceptuando Ctrl-Glass y BSA-Glass, que inmovilizaron cantidades ínfimas de proteína) esta relación fue extremadamente lineal y la pendiente de esta aproximación (que representa la cantidad de proteína inmovilizada según la cantidad impresa) dependió fundamentalmente del tipo de substrato. Tal y como se esperaba a partir de la observación hecha en las Figura R. 4B y Figura R. 5B, el orden de substratos en términos de mayor a menor cantidad de Fn inmovilizada fue: AD-Agarose, a-PMMA, AD-Glass, PEO-like y BSA-Glass (el Substrato Ctrl-Glass no pudo ser cuantificado debido a que una gran cantidad de los spots del microarray se unieron entre sí luego de la impresión, imposibilitando el trazado de la curva de calibración inicial, ver la imagen “alter washing” para este substrato presentada en Figura R. 5B). Dentro de los substratos que inmovilizaron cantidades importantes de Fn, el AD-Glass fue el que mostró la mayor repetitividad de resultados intra-slide (es decir, la cantidad de proteína inmovilizada para cada condición evaluada, que fue impresa en 20 spots replica en el mismo microarray, tuvo menores variaciones). Resultados similares fueron obtenidos al evaluar la cantidad de Fn inmovilizada cuando esta proteína fue impresa en PBS junto con SA en el mismo spot.

### **Inmovilización de SA y efectos del buffer de impresión**

En cuanto a la inmovilización de SA, cuando se imprimió junto con Fn y en PBS, se halló que después de lavar esta proteína sólo pudo ser detectada en los substratos AD-Agarose, a-PMMA y AD-Glass (Figura R. 6B, columnas marcadas como PBS). Es decir, solo fue inmovilizada en los spots por estos substratos. Los substratos que no tuvieron ningún tipo de activación química para promover la inmovilización covalente de las proteínas no fueron capaces de retener la SA. Esto se evidencia en las imágenes presentadas en la Figura R. 6C. Mientras que los spots impresos en PBS correspondientes a PEO-like y BSA-Glass mostraron una fluorescencia predominantemente verde después del lavado, los spots correspondientes al resto de los substratos exhibieron una fluorescencia amarillenta. El color amarillento resultó de la co-inmovilización de Fn (marcada en verde) y SA (marcada en rojo).

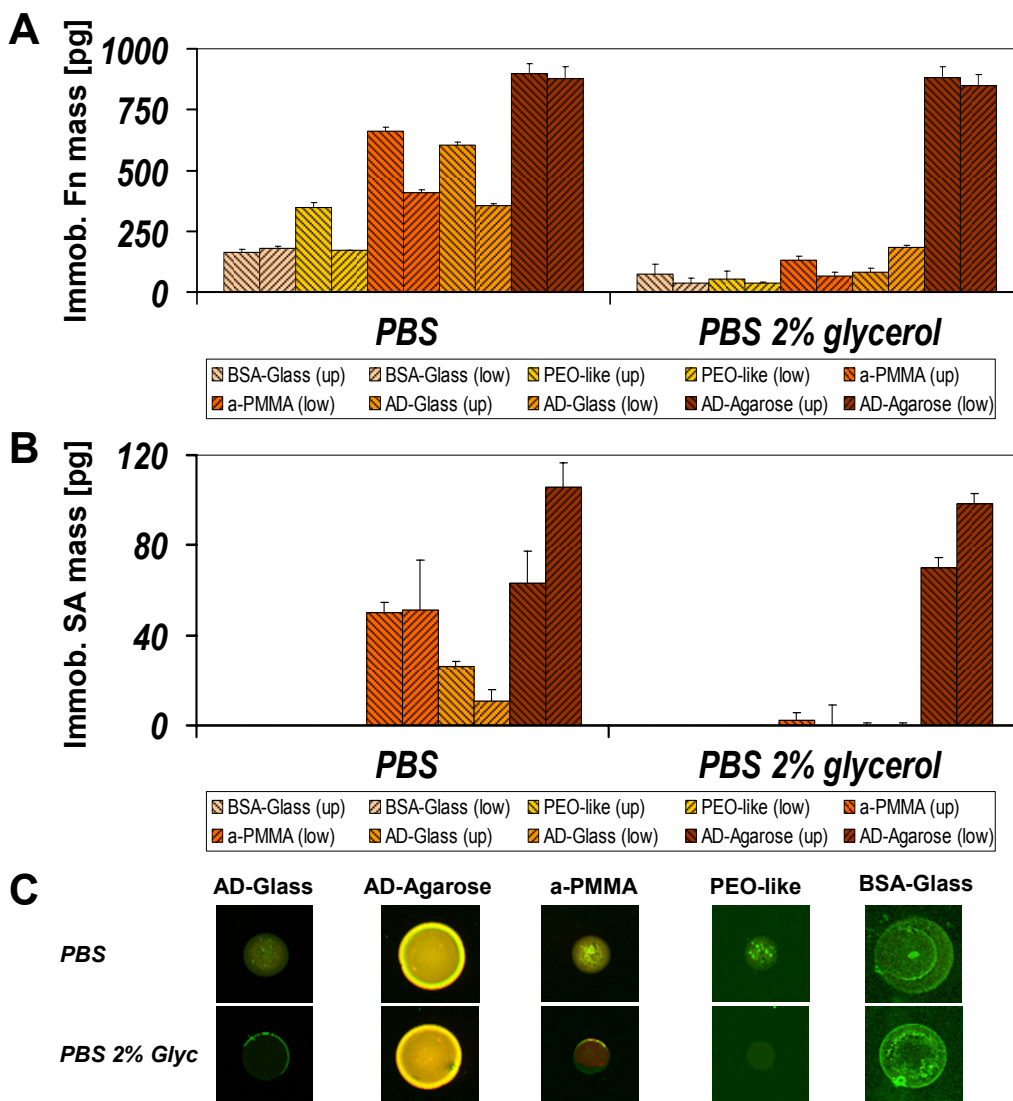


**Figura R. 6** Efecto del buffer de impresión sobre la cantidad de masa de Fn (A) y SA (B) inmovilizadas en los diferentes substratos ensayados. Datos presentados para la condición de spot Fn360 SA50 impresa en PBS con o sin glicerol, en 10 gotas. Los datos presentados corresponden a 2 experimentos independientes (indicados como *up* y *low* en la figura) realizados por cada substrato. C. Imágenes de fluorescencia representativas de los spots impresos usando la condición presentada en los gráficos superiores, obtenidas para cada substrato para los distintos buffer de impresión ensayados (PBS y PBS 2% Glyc.). La intensidad y contraste de las imágenes han sido optimizadas independientemente para cada substrato para permitir la visualización de los spots, por consiguiente sólo pueden realizarse comparaciones de intensidad entre los spots de un mismo substrato.

Por otro lado, al comparar los efectos de la inclusión del glicerol en el buffer de impresión, se observó que la cantidad de Fn retenida en los spots impresos con glicerol disminuyó en más del 50% para todos los substratos excepto AD-Agarose (Figura R. 6A). Por otro lado, al incluir el glicerol en los spots que también contenían SA, se halló que el único substrato capaz de retener la SA inmovilizada era AD-Agarose (Figura R. 6B). El resto de los substratos no llegaban a inmovilizar cantidades detectables de SA en los spots luego del lavado. Debido a que el

substrato AD-Glass fue el que mostró la mejor repetitividad de resultados intra-slide, se concluyó que la inclusión de glicerol en los spots no era conveniente de cara a aumentar la cantidad de proteína inmovilizada en los spots de este substrato, que permitió la inmovilización de cantidades relativamente altas de Fn y SA cuando estas fueron impresas en PBS.

## **Conclusiones**

En este estudio se analizaron, cualitativa y cuantitativamente, la masa y densidad de Fn y SA inmovilizada por 4 substratos de interés para su uso en microarrays celulares y, adicionalmente, se incluyeron dos substratos como controles negativos de adhesión de proteína.

El objetivo principal de este capítulo era hallar el substrato mas adecuado para continuar con el análisis de la fabricación de microarrays celulares. Con este fin, un número de factores cruciales fueron considerados y evaluados cuantitativamente, éstos incluyeron la cantidad de Fn y de SA inmovilizados y la reproductibilidad de intra-slide de los resultados de inmovilización de proteína.

El orden general hallado para los substratos ensayados, en términos de mayor a menor cantidad de Fn inmovilizada, fue: AD-Agarose, a-PMMA, AD-Glass, PEO-like y BSA-Glass. En particular, la inmovilización de Fn para el AD-Glass fue del 25-45%. Respecto a la cantidad de masa de SA inmovilizada, se hallo que tanto AD-Agarose como a-PMMA y AD-Glass fueron capaces de retener esta proteína. Sin embargo, en términos de reproductibilidad de intra-slide, los mejores resultados fueron obtenidos para AD-Glass, tanto para la inmovilización de Fn como de SA. Por este motivo, este fue el substrato elegido para continuar con el proceso de optimización en la fabricación de microarrays celulares.

## **Capítulo 3    Fabricación y optimización de los microarrays celulares**

### **Introducción**

Las células mesenquimales (referidas de aquí en adelante por su abreviación en inglés, MSCs, mesenquimal stem cells) son un tipo celular muy atractivo ya que pueden ser obtenidas de individuos adultos y tienen capacidad de diferenciarse en una amplia variedad de células especializadas tales como osteoblastos, condrocitos y adipocitos, entre otros.

Los reportes previos hallados en lo concerniente a microarrays celulares describen una gran variación en los parámetros clave para la fabricación de los mismos. Parámetros tales como la

pasivación de la superficie no impresa, el tiempo de sembrado celular, la concentración a la que las células son sembradas para formar el microarray y el medio usado para el cultivo de las células fueron optimizados para cada tipo particular de células y periodos de cultivo. Esto se debe a que no todos los tipos de células tienen el mismo comportamiento en lo concerniente a su adhesión al substrato. Propiedades celulares tales como su adhesión, migración, proliferación y habilidad para invadir el área pasivada de los microarrays deben tenerse en cuenta.

Este capítulo involucra la optimización de los parámetros de fabricación de los microarrays celulares con el objetivo de permitir el cultivo de células mesenquimales en el microarray durante varios días. Con este fin, se evaluaron microarrays con spots compuestos exclusivamente de Fn, que fue depositada a partir de soluciones preparadas en dos buffers de impresión: PBS y PBS con 2% glicerol. Otros parámetros evaluados fueron: la concentración de Fn usada en la impresión, la estrategia de pasivación de las áreas no impresas, el tamaño del spot de proteína impreso, la concentración de sembrado de células, el tiempo de sembrado y el medio empleado para el cultivo de células. Los resultados obtenidos para cada una de las condiciones experimentales evaluadas permitieron definir los mejores parámetros para el cultivo de células mesenquimales en los microarrays por periodos de hasta 8 días. Al cabo de este tiempo de cultivo, se evaluó la diferenciación de las células hacia osteoblastos y adipocitos.

## **Materiales y métodos**

Las células mesenquimales empleadas en los experimentos fueron obtenidas como cultivos primarios de fémures de rata. La diferenciación de estas células hacia osteoblastos o adipocitos se caracterizó mediante la actividad de alcalino fosfatasa (ALP de aquí en adelante, expresada por los osteoblastos) o mediante la presencia de vesículas con lípidos (en adipocitos).

El equipo y protocolos utilizados para la fabricación de los microarrays fueron los mismos que se describieron en el capítulo anterior. Para la formación del microarray celular, se siguieron los pasos que se presentaron en la introducción de esta tesis, referente a la Figura R. 1. En particular para los experimentos presentados en este capítulo, el paso de extracción de la solución con células no adheridas, una vez cumplido el tiempo de sembrado, fue realizado mediante la centrifugación de los microarrays celulares recientemente formados (el proceso se presenta en detalle en la Figura 3.8 de la tesis). Los parámetros ensayados, que fueron evaluados independientemente, son:

- La concentración de Fn impresa: 40, 100 y 200 µg/mL (referidas de aquí en adelante como Fn40, Fn100 y Fn200, respectivamente).

- El buffer de impresión: PBS y PBS 2% glicerol.
- El tamaño del spot: con este fin se sobre imprimieron 1, 3, 5, 7 o 10 gotas en la misma posición del microarray.
- El tipo de pasivación de la superficie no impresa: se evaluaron la pasivación mediante la inmersión del microarray impreso en una solución de 2% BSA (albúmina de suero bovino) o de 38 mg/mL de amino-PEG (poli(etilenglicol) con grupos amino en sus extremos, que reaccionaran con la química del AD-Glass, pasivando la superficie no impresa con proteínas).
- El tiempo de sembrado celular: con este fin se coloco el microarray impreso con proteínas (con las áreas no impresas ya pasivadas), y se agregó una solución con células en suspensión. El tiempo durante el que se expuso el microarray impreso a esta solución con células define el tiempo de sembrado. Los tiempos ensayados fueron 5, 15 y 45 minutos.
- La concentración de sembrado: análogamente al paso anterior, los microarrays impresos y pasivados fueron expuestos, de forma separada, a una solución con células en concentraciones de 5.500, 11.000 u 110.000 células/cm<sup>2</sup>.
- El medio de cultivo: se ensayaron un medio de cultivo con 10% FBS (medio usual para el cultivo y diferenciación de MSCs) y otro medio de cultivo en el que el porcentaje de FBS fue reemplazado con 1% ITS (suplemento compuesto principalmente por insulina, transferrina y selenita de sodio), dando lugar a un medio de cultivo con composición complemente conocida. Más detalles respecto a estos medios de cultivo se presentan en la correspondiente sección de la tesis.

## **Resultados**

### **Optimización de los parámetros empleados para la fabricación de los microarrays celulares**

De las distintas concentraciones de Fn ensayadas, el valor que dio los mejores resultados fue Fn200. Esta elección se baso en que para esta concentración los spots impresos presentaron un recubrimiento de Fn más uniforme, que produjo que las células se adhirieran mejor en ellos.

Respecto al tiempo y concentración de sembrado celular, los parámetros óptimos resultaron ser un tiempo de sembrado de 15 minutos y una concentración de sembrado de 11.000 células/cm<sup>2</sup> (Figura R. 7). Valores mayores produjeron spots saturados de células, en los que se

observó inclusive la adhesión de células unas encima de otras. Por otro lado, valores menores resultaron en una menor cantidad de células adheridas por spot, dando lugar también a una importante variación entre spots de igual composición.

Una vez formados los microarrays celulares, estos se cultivaron en medio con 10 % FBS o, alternativamente, en medio 1% ITS. Se hallo que al usar el medio con 10% FBS las células proliferaron e invadieron el área pasivada, resultando en la perdida del formato de cultivo en microarray a los 2 días. Por otro lado, uso de medio con 1% ITS permitió el cultivo en formato de microarrays hasta 8 días. Por este motivo, el medio con 1% ITS fue elegido como el mas apropiado de los ensayados para continuar con los experimentos.

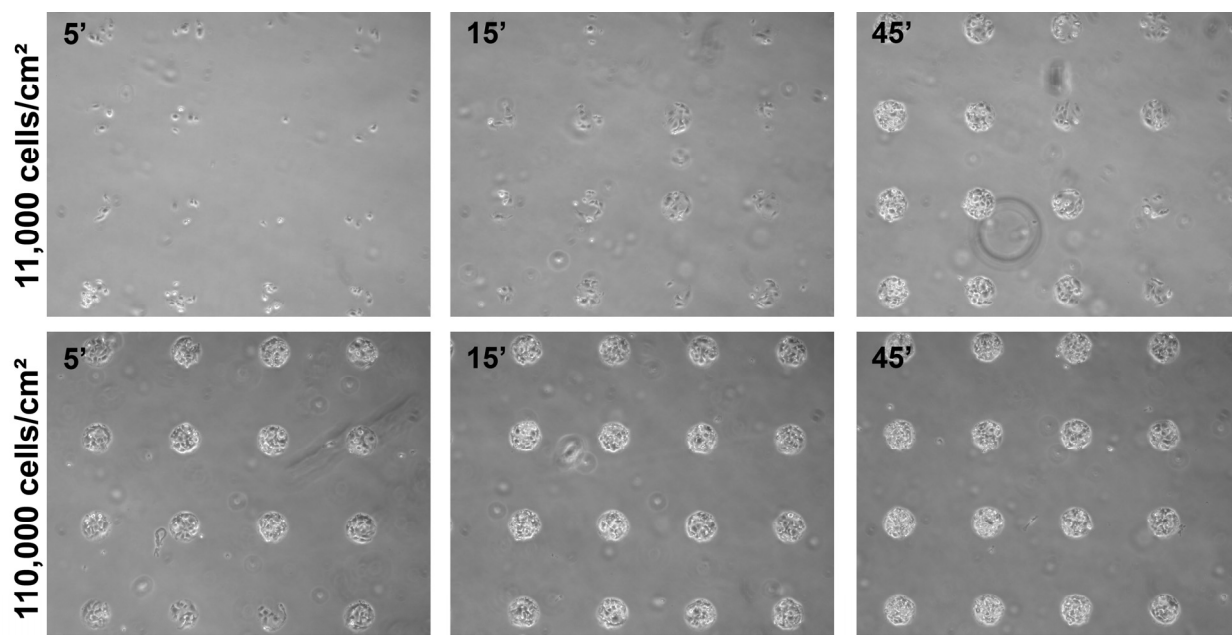


**Figura R. 7** Efecto en la formación del microarray de los distintos tiempos de sembrado celular, así también de dos de las concentraciones celulares utilizadas para el sembrado. Al aumentar el tiempo y la concentración de sembrado de las células, la cantidad de células adheridas por spot también aumenta, llegando a producir spots saturados con células para la densidad de sembrado más alta. Las imágenes presentadas son para spots compuestos por Fn200 en PBS 2% glicerol. El tamaño de spot impreso es 1 gota. La escala de 500 µm se muestra en negro.

En cuanto a los buffers de impresión probados, los mejores resultados fueron obtenidos para PBS con 2% glicerol. Los spots impresos con PBS fueron menos efectivos al momento de retener las células luego del sembrado y posterior extracción de la solución con células no adheridas (que en este capítulo se llevo a cabo mediante la centrifugación de los slides).

El tamaño de spot que permitió obtener un numero mas estable de células a lo largo del tiempo de cultivo ensayado (hasta 8 días) fue el generado por la sobre impresión de 5 gotas de la solución de Fn.

## Viabilidad y diferenciación celular a los 8 días en la plataforma optimizada

Finalmente, las MSC fueron sembradas en microarrays fabricados usando los parámetros previamente optimizados: Fn200 preparada en PBS con 2% glicerol, 5 gotas por spot, pasivación con BSA, sembrado celular a 11.000 células/cm<sup>2</sup> durante 15 minutos y cultivo en medio con 1% ITS durante 8 días. Al cabo de este tiempo se evaluó la viabilidad de las células adheridas a los spots, y se comprobó que la viabilidad es superior al 99% (Figura R. 8). Al mismo tiempo, también se observó que algunas células de las adheridas a los spots presentaban una morfología de adipocitos (indicado con las flechas blancas en la Figura R. 8).

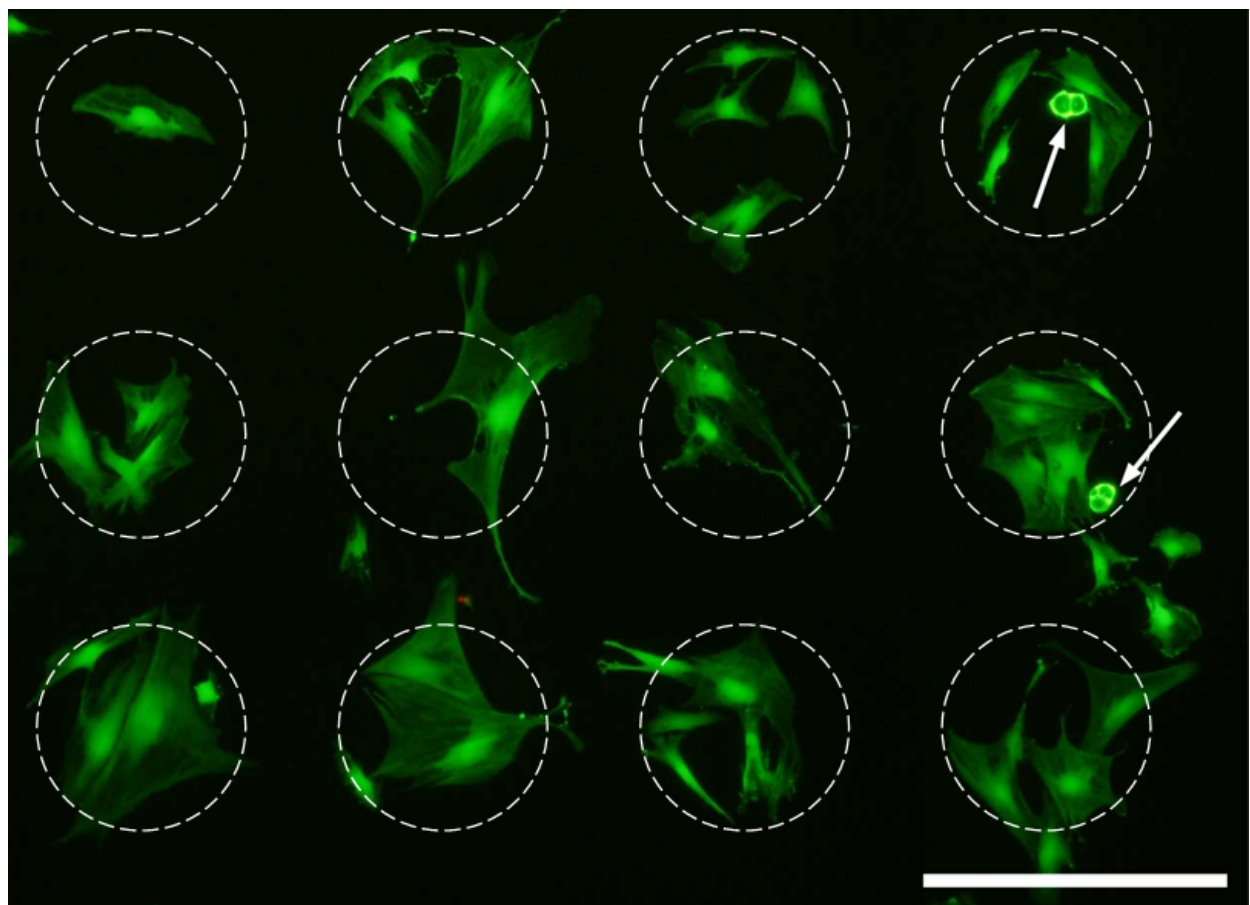


**Figura R. 8** La viabilidad de las células adheridas a los spots después de 8 días de cultivo en los microarrays es superior al 99%. La imagen muestra las células adheridas a 12 spots (cuya posición aproximada se indica por medio de los círculos blancos con línea discontinua). Se halló que las células mesenquimales eran viables en los spots (indicado por medio de la fluorescencia verde). Adicionalmente, se observó que algunas de las células en los spots mostraban una morfología correspondiente con los adipocitos (indicadas por las flechas blancas). La escala de 500 µm se muestra en blanco.

La caracterización de diferenciación a osteoblastos y adipocitos permitió confirmar que algunas de las células adheridas a los spots mostraron un fenotipo correspondiente con diferenciación a cada uno de estos destinos celulares (Figura R. 9). Sin embargo, este resultado no era de esperar, ya que la composición de todos los spots fue la misma (sólo Fn), y por

consiguiente se propuso que las MSCs empleadas en estos experimentos podrían estar constituidas por una población celular mas heterogénea, entre las cuales habría progenitores que se diferencian espontáneamente a osteoblastos y otros que tendrían una tendencia a diferenciarse en adipocitos bajo las mismas condiciones de cultivo.

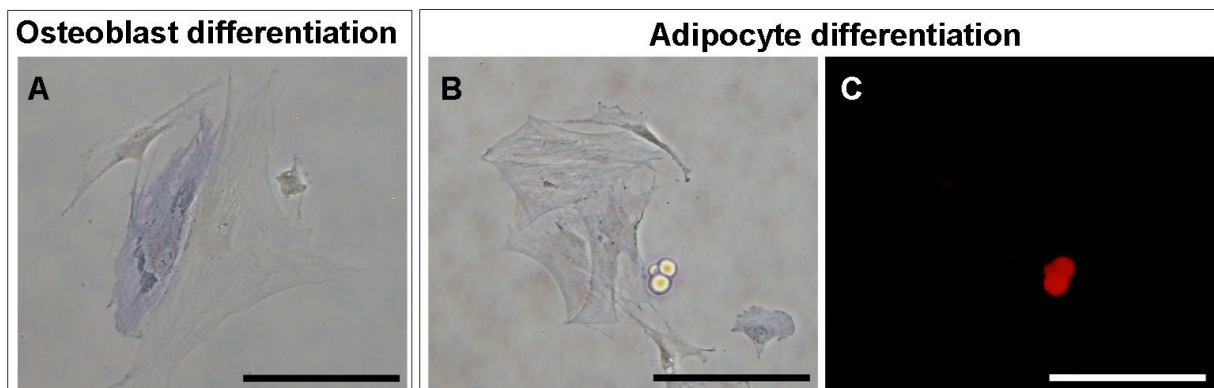


**Figura R. 9** Detalle de las células diferenciadas espontáneamente en los spots de los microarrays, después de 8 días de cultivo en medio con ITS. A. Imagen de contraste de fase mostrando la tinción celular para ALP en algunas de las células adheridas al spot. B. Imagen de contraste de fase obtenida para otro spot impreso con la misma condición inicial. En este caso, no hay células teñidas para ALP, pero se observa la morfología típica de adipositos en una de las células. C. Imagen de fluorescencia del mismo spot presentado en B. Las vesículas compuestas por lípidos han sido teñidas en rojo, indicando que la diferenciación espontánea hacia adipositos tuvo lugar en este spot. Las escalas de 200  $\mu\text{m}$  se muestran en negro (para imágenes de contraste de fase) o en blanco (para la imagen de fluorescencia).

## Conclusiones

El objetivo principal de este capítulo fue definir los parámetros óptimos para la fabricación de microarrays celulares con MSCs. Los resultados obtenidos condujeron a una serie de los parámetros optimizados: Fn200 preparada en PBS con 2% glicerol, 5 gotas por spot, pasivación con BSA, sembrado celular a 11.000 células/cm<sup>2</sup> durante 15 minutos y cultivo en medio con 1% ITS. Estos parámetros permitieron el cultivo celular en los microarrays por períodos de hasta 8 días. Al cabo de este tiempo de cultivo se detectó la diferenciación espontánea a osteoblastos y adipocitos de algunas de las células adheridas en los spots, evidenciando que bajo los estímulos apropiados esta plataforma permite la diferenciación de MSCs. Sin embargo, estos resultados de diferenciación no eran esperados en los experimentos presentados en este capítulo, el los cuales todos los spots del microarray fueron impresos usando únicamente Fn.

Según lo divulgado previamente, las MSCs obtenidas como cultivos primarios representan una población heterogénea en términos del potencial de diferenciación. Éste es un aspecto importante que debe ser considerado al analizar la diferenciación de células madre por medio de

microarrays celulares, puesto que la respuesta de las células adheridas a los spots de idéntica composición podría ser afectada según el estadio de diferenciación de las células adheridas inicialmente a cada spot (según lo sugerido por los resultados obtenidos en este trabajo). La mayoría de aplicaciones de microarrays celulares reportadas a la fecha se han centrado en tipos celulares extensamente caracterizados. Células bi-potentes, con una robusta respuesta de diferenciación a los factores ensayados, han sido hasta la fecha los modelos preferidos para probar las aplicaciones de microarrays celulares. Por este motivo, y con el fin de evaluar el efecto de la inclusión de un factor de crecimiento en la plataforma de microarrays celulares presentada aquí, es altamente deseable la utilización de una línea celular mejor caracterizada.

En resumen, los resultados obtenidos aquí fueron utilizados como base para la fabricación de microarrays celulares que se presenta en el capítulo siguiente, y que tiene como objetivo proporcionar una comprensión más detallada de cómo la inclusión de un factor de crecimiento en los spots del microarray puede afectar al proceso de diferenciación celular.

## **Capítulo 4    Aplicación: Análisis de estadios tempranos de diferenciación usando un modelo celular**

### **Introducción**

Los hallazgos expuestos en el capítulo anterior sugirieron, para el desarrollo de los experimentos presentados en este capítulo, el empleo de una línea celular con una respuesta de diferenciación muy bien caracterizada. Con este fin, la línea celular C2C12 fue elegida para estos estudios. La diferenciación de estas células ha sido ampliamente caracterizada mediante técnicas de biología convencionales. Se sabe que al usar un medio de cultivo con bajo contenido de suero, estas células se diferencian espontáneamente a miocitos (células musculares). Sin embargo, ante la presencia del factor de crecimiento BMP-2 (bone morphogenetic protein 2) solubilizada en el medio de cultivo, estas células cambian su destino de diferenciación hacia osteoblastos. Esta diferenciación puede ser evaluada a las 24 hs mediante la expresión del gen Osterix (Osx) o bien después de 4 días mediante la detección de actividad ALP (Figura R. 10). Recientemente, también se ha demostrado que la BMP-2 impresa en un substrato también es capaz de generar la respuesta de diferenciación en estas células. Sin embargo, este reporte en cuestión ha demostrado la diferenciación de esta línea celular en respuesta a los patrones de BMP-2 impresa cuando las células se cultivan en monocapa sobre los substratos impresos. El desafío expuesto en el presente capítulo de tesis consiste en evaluar si la diferenciación de las

células C2C12 también puede influenciarse por medio de la BMP-2 impresa cuando el formato de cultivo de estas células se restringe a los spots del microarray.

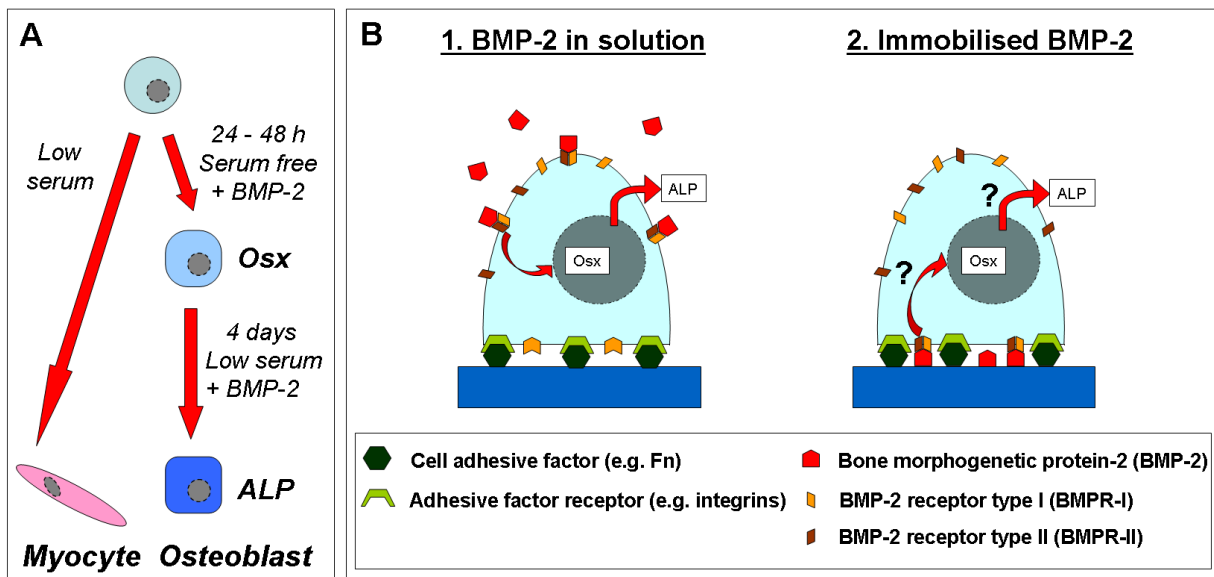


**Figura R. 10 A.** Esquema representando el cambio del camino de diferenciación, de miocitos hacia osteoblastos, de las células C2C12. **B.** Esquema representando una célula adherida a un spot del microarray (a través de factor de adhesión celular). La interacción de la BMP-2, soluble (1) o inmovilizada (2), con sus respectivos receptores, inicia una cascada de señalización intracelular que induce la expresión del gen Osterix (Osx) en el núcleo (a 24 hs) y la producción de alcalino fosfatasa (ALP) después de 4 días.

Basándose en los resultados presentados en los capítulos anteriores, la plataforma de microarray celular desarrollada fue evaluada en este capítulo con respecto a la respuesta de diferenciación celular cuando se incluye BMP-2 inmovilizada en los spots. Se ha puesto especial énfasis en la comparación de la respuesta de diferenciación celular luego de 24 hs de exposición (por medio del análisis de expresión de Osx) al factor de crecimiento cuando este esté inmovilizado en los spots del microarray y cuando este es agregado en solución al medio de cultivo.

## Materiales y métodos

La diferenciación de las células C2C12 hacia osteoblastos fue caracterizada mediante la expresión del gen Osx, en el núcleo celular, después de 24 hs en medio de cultivo sin suero, o bien mediante la actividad de alcalino fosfatasa al cabo de 4 días de cultivo en medio con 2% de suero de caballo (de aquí en adelante referido como 2% HS, del inglés horse serum).

El protocolo usado para la impresión de los microarrays de proteínas fue el mismo que el especificado en el capítulo 2. Los microarrays de proteína impresos fueron caracterizados por tinciones inmunofluorescentes usando anticuerpos específicos para detectar cada una de las

proteínas impresas. El proceso seguido para la formación de los microarrays celulares fue el mismo que se ha descripto en el capítulo anterior. En particular para los experimentos presentados en este capítulo, el paso de extracción de la solución con células no adheridas, una vez cumplido el tiempo de sembrado, no requirió la centrifugación de los microarrays celulares y simplemente consistió en el recambio de medio con células por medio de cultivo sin células. Por otro lado, se evaluaron dos proteínas de matriz extracelular de forma separada, fibronectina (Fn) y laminina (Ln), que fueron impresas con y sin BMP-2 en los spots. Los parámetros ensayados en este capítulo fueron:

- La concentración de Fn y Ln impresas: 200, y 360 µg/mL (referidas de aquí en adelante como Fn200, Fn360, Ln200 y Ln360, respectivamente).
- La inclusión o no de BMP-2 en los spots, a una concentración fija de 100 µg/mL.
- El buffer de impresión: PBS y PBS 2% glicerol. Ambas opciones continuaron siendo evaluadas aquí debido a que, si bien en el capítulo 3 se escogió PBS con 2% glicerol como la mejor opción basándose en la adhesión celular a los spots de Fn, en el capítulo 2 se sugirió que la inclusión de glicerol en los spots podría disminuir considerablemente la inmovilización de otros factores distintos de proteínas de matriz extracelular, tales como SA en el capítulo 2 o la BMP-2 en el presente capítulo.
- El tamaño del spot: con este fin se sobre imprimieron 5 y 10 gotas en la misma posición del microarray.

El resto de los parámetros empleados para la formación de los microarrays celulares fueron:

- Concentración de sembrado celular: 20.000 células/cm<sup>2</sup>.
- Tiempo de sembrado celular: 15 minutos.
- Pasivación de la superficie no impresa: se utilizó una solución de 2% BSA.
- Medio de cultivo: medio sin suero para cultivo a 24 hs y evaluación de expresión de Osx, o medio con 2% HS para cultivo a 4 días en evaluación de actividad de ALP.

La elección de dichos parámetros fue hecha en función de los parámetros previamente optimizados, adaptándolos al nuevo tipo celular empleado en este capítulo. Además de la diferenciación celular en los microarrays con BMP-2 impresa, se incluyeron varios controles para comprender de una forma más completa la respuesta de diferenciación. Estos controles fueron diseñados:

- Para validar la respuesta de diferenciación a osteoblastos previamente reportada en la literatura se probó el efecto de BMP-2 soluble en el medio de cultivo cuando las células C2C12 fueron cultivadas de manera convencional en placas de cultivo.
- Para evaluar el efecto de inmovilizar la BMP-2 *per se*, las células fueron cultivadas sobre áreas (de superficie considerablemente mayor a los spots del microarray) recubiertas con soluciones de Fn y BMP-2 o Ln y BMP-2.
- Para evaluar independientemente el efecto de cultivar las células en pequeñas áreas aisladas (constituidas por los spots impresos) del efecto de la inmovilización de la BMP-2, microarrays celulares control (con spots compuestos exclusivamente por Fn o Ln, en los cuales no se imprimió BMP-2) fueron expuestos a BMP-2 solubilizada en el medio de cultivo.

## **Resultados**

### **Caracterización de los microarrays de proteína fabricados**

Tanto la presencia de Fn como de Ln fue detectada en los spots de los microarrays impresos, correspondiendo su detección con las posiciones del microarray en las cuales dichas proteínas fueron depositadas. De esta forma se comprobó que el método de impresión empleado permitió depositar selectivamente las proteínas de interés en cada posición del microarray y no hubo efectos de contaminación cruzada entre la impresión de distintas soluciones proteicas.

La presencia de BMP-2 en los microarrays resultó más difícil de evaluar ya que la señal resultante de la tinción inmunofluorescente fue demasiado débil y por lo tanto solo pudo hacerse una evaluación cualitativa. Este análisis permitió concluir que la BMP-2 estaba presente exclusivamente en los spots en los que este factor había sido impreso, pero que la BMP-2 estaba inmovilizada en muy baja cantidad.

### **Caracterización de la fabricación de los microarrays celulares**

Por un lado, se observó que las células se adherían bien a los spots impresos con Fn y Ln. Sin embargo, cuando se incluyó la BMP-2 en la composición de los spots, la adhesión celular a los spots compuestos por Ln y BMP-2 disminuyó considerablemente. Por otro lado, cuando la BMP-2 fue impresa junto con la Fn, la adhesión celular no fue afectada en gran medida. Un análisis del número de células adheridas por spot luego de la formación del microarray demostró que la adhesión fue mejor y más repetitiva (es decir, similar entre las distintas composiciones del spot) para los spots con Fn, impresos con y sin BMP-2. Como ejemplo, todas las

condiciones ensayadas para los spots impresos con Fn (Fn200 y Fn360, con y sin BMP-2, preparadas en PBS con o sin glicerol) inmovilizaron aproximadamente unas 25 células por spot.

Un análisis de la proliferación celular en estos spots, cuando las células eran cultivadas en los microarrays durante 1 o 4 días, usando medio sin suero o con 2% HS, respectivamente, dio como resultado que si bien no había proliferación importante luego de 1 día de cultivo en medio sin suero, las células adheridas a los spots mostraron un índice de proliferación importante al cabo de 4 días en cultivo con medio con 2% HS. Al cabo de este tiempo de cultivo, el numero de células en los spots aumento de aproximadamente 25 células por spot al día 0 (es decir, recién formado el microarray) a mas de 300 células luego de 4 días de cultivo. Esto se atribuyó a la inclusión del pequeño porcentaje de suero incluido en el medio de cultivo.

### **Caracterización de la diferenciación celular**

El análisis del numero de células que expresaron Osx luego de 24 hs de exposición a BMP-2, ya sea en solución o impresa, permitió demostrar que en todos los casos la BMP-2 fue capaz de inducir la expresión de este marcador de diferenciación a osteoblastos. No obstante, una cuantificación de este efecto mostró el numero de células que en respuesta a la BMP-2 expresaban Osx dependía fuertemente del tipo de cultivo empleado. En este aspecto, los cultivos control en placas convencionales, en las cuales las células fueron expuestas a BMP-2 en solución, mostraron una expresión muy alta, en el que más del 99% de las células expresaron Osx. Al inmovilizar la BMP-2 en áreas grandes (de aproximadamente 5 mm<sup>2</sup>, considerablemente mayores que las producidas por los spots del microarray, que oscilaron entre 0.075 y 0.3 mm<sup>2</sup>), se hallo que este factor de crecimiento continuaba induciendo la expresión de Osx en un numero considerablemente alto de células (alrededor del 80%). La disminución del número de células que expresaron Osx, respecto del control en placas, fue atribuida principalmente a efectos propios de la inmovilización de la BMP-2. Entre otros, podría incluirse la restricción de interacción entre los receptores de BMP-2, presentes en la membrana celular, con las integrinas, también presentes en la membrana celular. En este aspecto, al unirse los primeros con la BMP-2 inmovilizada no podrían asociarse adecuadamente con los receptores de adhesión celular formados por las integrinas, que a su vez estarían unidas a las proteínas de matriz extracelular inmovilizadas en el substrato. Esta interacción, sin embargo, no sería restringida en el caso de la exposición del cultivo celular a BMP-2 en solución.

Por otro lado, al exponer los microarrays control (es decir, con spots compuestos exclusivamente por Ln o Fn, en los que no se imprimió la BMP-2) a BMP-2 en solución, se

observo que el numero de células que expresaron Osx fue de entre el 27% y el 55%, dependiendo principalmente de la composición del spot. En este caso, la disminución del numero de células que expresaron Osx fue atribuida principalmente al efecto causado al cultivar células exclusivamente en spots de áreas muy pequeñas y aislados entre si. Mientras que en los cultivos en placa las células cultivadas fueron primero llevadas a semi-confluencia (es decir, que prácticamente toda la superficie disponible para la adhesión de células estuviese cubierta), en el caso de los microarrays las células no detectaron una limitación para continuar expandiéndose. La diferencia de señalización entre células (ya sea por contacto directo entre membranas celulares, o bien mediante la señalización paracrína entre células mas distantes) en ambos casos fue atribuida como la principal causante de la disminución de diferenciación en los microarrays expuestos a BMP-2 en solución.

Por ultimo, cuando los microarrays impresos con BMP-2 fueron cultivados con células durante 24 hs, se observo que el numero de células que expresaron Osx osciló entre el 20 y 24% (Figura R. 11). Este resultado fue explicado como una combinación de las disminuciones de diferenciación provenientes del cultivo celular en microarray, por un lado, y de la inmovilización de la BMP-2, por el otro, tal como se ha expuesto en los párrafos anteriores.

Resumiendo los hallazgos presentados en este capítulo, la Figura R. 12 muestra un diagrama esquemático de la respuesta de diferenciación de las células cuando estas fueron cultivadas bajo las diversas condiciones ensayadas: las placas de cultivo estándar (A), los microarrays celulares con BMP-2 soluble (B) y los microarrays celulares con y sin BMP-2 inmovilizada en los spots (C y D). De acuerdo a lo observado previamente, los cultivos celulares en placas de cultivo estándar generaron la expresión de Osx en ~99% de las células expuestas a BMP-2 soluble, mientras que la restricción del tamaño del cultivo celular a las dimensiones del microarray disminuyó la expresión de Osx entre el 50 y el 60% (para los spots con Fn). Esto fue atribuido principalmente a la falta de señalización proveniente de cultivos celulares semi-confluentes. Al inmovilizar el BMP-2 en los microarrays (en vez de agregarla en solución), la expresión de Osx disminuyó al 24% de las células en los spots. Esto se atribuyó al efecto combinado de cultivar las células en spots aislados y a la inmovilización de la BMP-2.

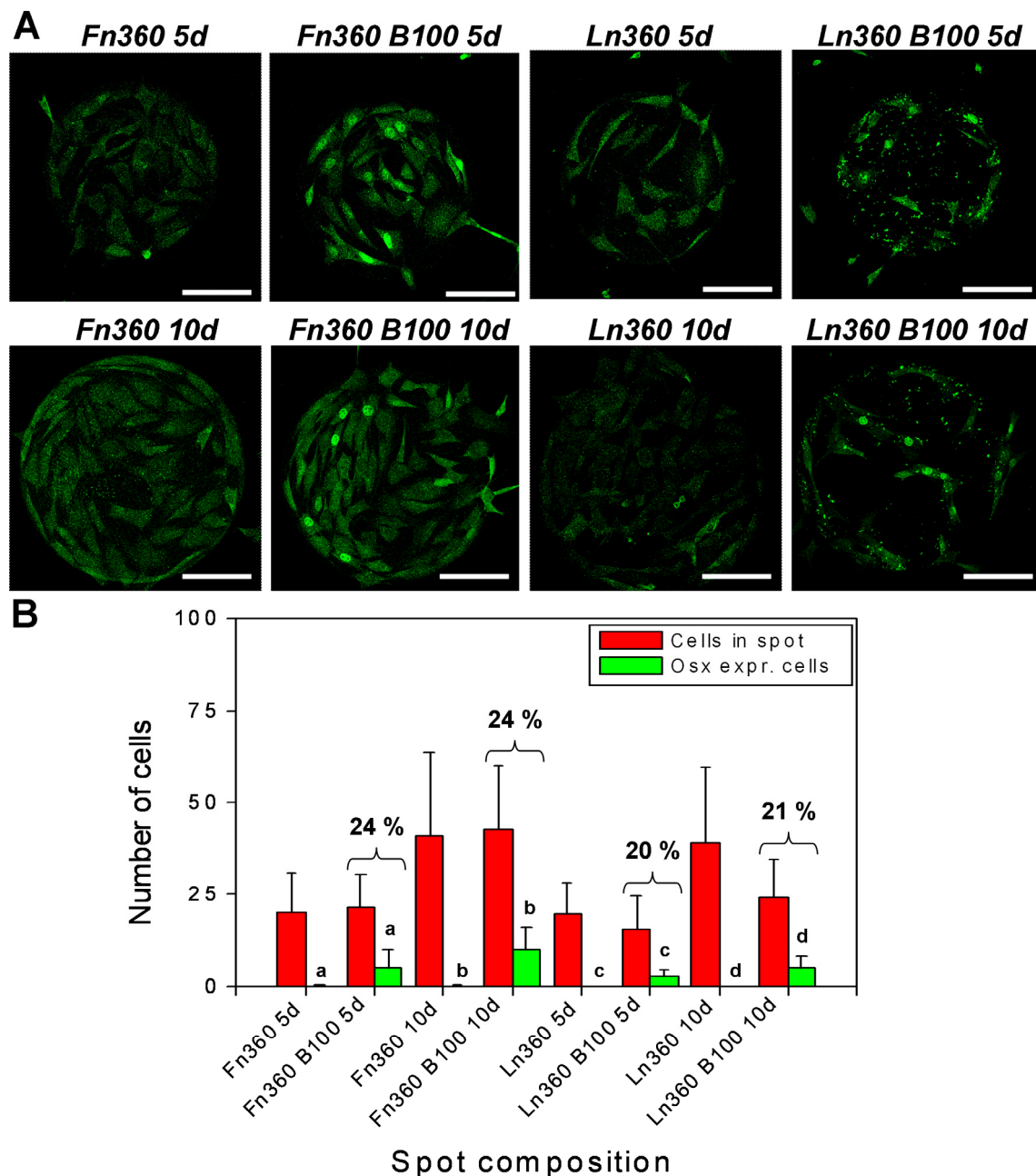


**Figura R. 11** Expresión de Osx en las células adheridas a spots impresos con y sin BMP-2, en buffer PBS. **A.** Marcaje inmunofluorescente para Osx de las células cultivadas en los microarrays durante 24 hs. Las células en los spots impresos con BMP-2 mostraron expresión de Osx (indicada por la tinción en verde de sus núcleos), mientras que las células en los spots control no. **B.** cuantificación del numero de células totales en los spots (*Cells in spot*) adheridas a día 1, y el numero de estas células que expresaron Osx cuando las células fueron cultivadas en los microarrays durante 24 hs. El porcentaje de células que expresaron Osx respecto al del número total de células en el spot también se presenta para los spots impresos con BMP-2. Las barras representan el promedio y la desviación estándar de 8 spots. Para las barras de células que expresaron Osx (*Osx expr. cells*), a, b, c, d, indican diferencias significativas de  $p < 0.05$ .

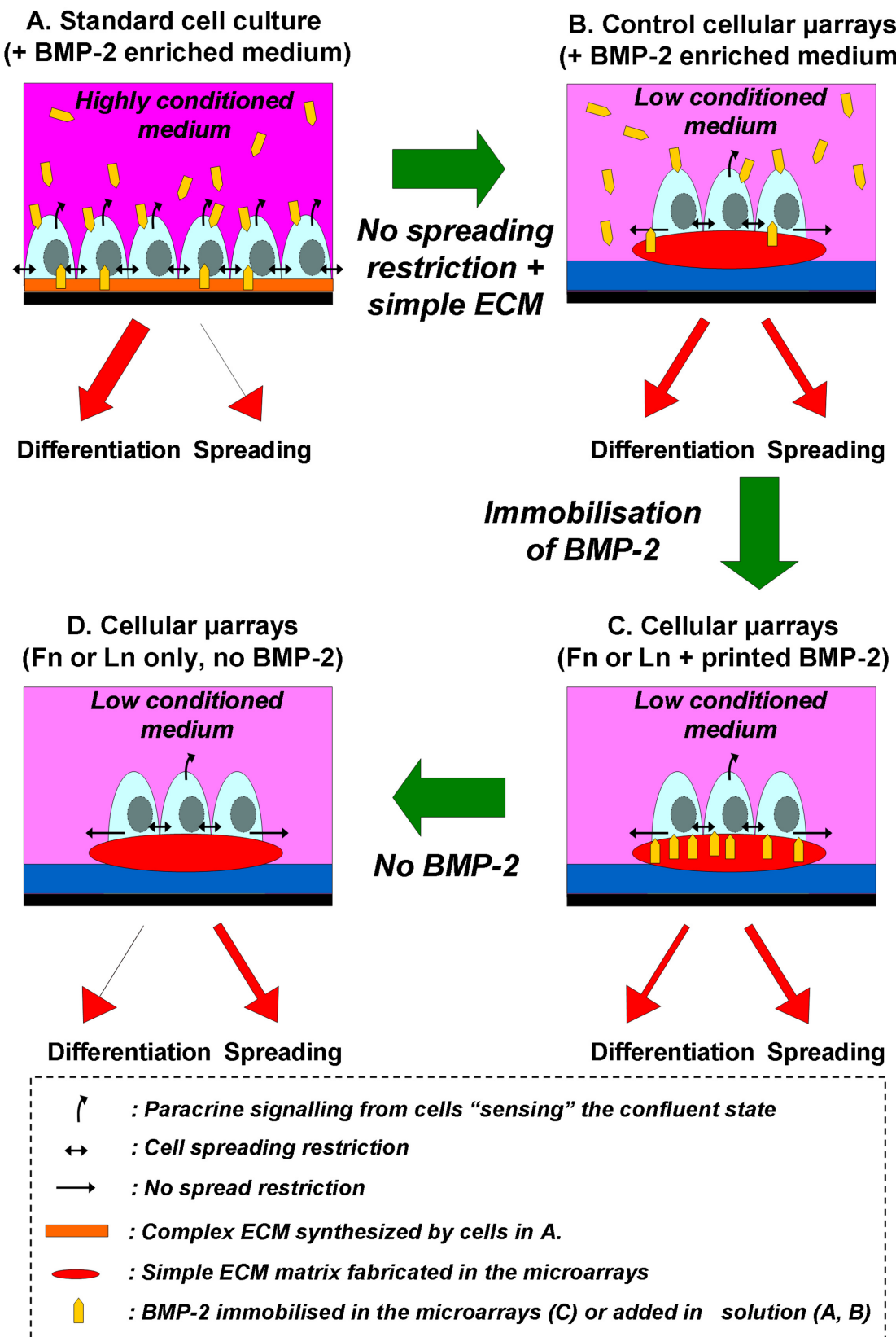


**Figura R. 12** Esquema presentando la respuesta integrativa, en cuanto a su diferenciación, de las células cultivadas en placas de pocillos estándar (A) y en microarrays celulares usados como control (B), cuando ambos fueron expuestos a BMP-2 en solución. También se presenta la respuesta de diferenciación de las células cultivadas en los microarrays con (C) y sin (D) BMP-2 impresa.

Por último, la detección de ALP en las células cultivadas en los microarrays durante 4 días fue extremadamente baja. Esto se atribuyó, en parte, a la observación previamente mencionada de que las células cultivadas durante 4 días bajo estas condiciones proliferaron en una forma significativa. En este aspecto, ha sido ampliamente reportado que la proliferación y diferenciación celulares son procesos mutuamente excluyentes. No obstante, otras causas tales como la perdida de señalización de la BMP-2 debido a desnaturización o desprendimiento del spot fueron difíciles de evaluar y no pueden ser descartadas.

## **Conclusiones**

En este capítulo se demostró que las células C2C12 expuestas a BMP-2, en forma soluble o inmovilizada, fueron dirigidas tempranamente hacia su diferenciación a osteoblastos, que se evaluó por medio de la expresión de Osx a 24 hs. Sin embargo, se halló que la respuesta de diferenciación celular dependió de las diversas condiciones de la cultivo ensayadas. El número de células que iniciaron su diferenciación hacia osteoblastos disminuyó en el siguiente orden: cultivos en placas estándar expuestos a BMP-2 soluble (más del 99% de las células expresaron Osx), los microarrays celulares expuestos a BMP-2 soluble (entre el 27 y el 55% de las células expresaron Osx) y los microarrays celulares con BMP-2 inmovilizada en los spots (entre el 20 y el 24% de las células expresaron Osx). Vale la pena destacar que, para los microarrays celulares en los cuales BMP-2 fue inmovilizada tan solo en algunos de los spots, las únicas células que expresaron Osx fueron aquellas que estaban adheridas sobre los spots que fueron impresos con BMP-2. Estos resultados permitieron el proponer una explicación en la cual la respuesta de diferenciación celular resultó como una integración de las diferentes variables que se introdujeron al variar las condiciones de cultivo.

Por un lado, la restricción del cultivo celular, resultante de cultivar una pequeña cantidad de células en spots aislados, fue el motivo atribuido para explicar la disminución en la diferenciación de las células que fueron cultivadas en placas estándar y el cultivo celular en los microarrays celulares. Por otro lado, la inmovilización de la BMP-2 explicaría la disminución adicional encontrada cuando se evaluó la diferenciación celular en los microarrays expuestos a BMP-2 soluble o inmovilizada en los spots.

El cultivo de células en los microarrays por períodos más largos (4 días) dio lugar a una diferenciación a osteoblastos extremadamente baja (evaluada por la expresión de ALP). Esto fue atribuido en parte a la proliferación celular observada en los spots, que pasaron de tener 25 células adheridas a día 0, a más de 1.000 células a día 4, en algunos casos.

En resumen, el trabajo presentado en este capítulo ha contribuido al estado del arte en el desarrollo de microarrays celulares por medio del análisis de diferenciación usando un modelo celular (C2C12). Se demostró que la expresión de Osx es un método adecuado para evaluar la respuesta de diferenciación celular temprana al factor de crecimiento impreso (BMP-2). Además, se identificaron nuevos desafíos a superar para aplicar esta plataforma en el estudio de la diferenciación de células madre. La aplicación presentada permitió demostrar que plataformas como la expuesta aquí son herramientas ideales para proporcionar información clave en los caminos de diferenciación de células madre, basados en la respuesta celular a combinaciones de proteínas de matriz extracelular y un factor de crecimiento.

## **Capítulo 5 Conclusiones de la tesis**

Un análisis cualitativo y cuantitativo de la cantidad de proteína inmovilizada por 4 substratos de interés en aplicaciones de microarrays celulares, no descripto hasta la fecha, permitió identificar al substrato AD-Glass (vidrio derivatizado con grupos aldehído) como la mejor opción para la fabricación de los microarrays celulares. Esta elección se basó en la relativamente alta capacidad para retener las proteínas impresas, así como la repetitividad intra-slide de los resultados de inmovilización.

Una optimización de los parámetros empleados para la fabricación de los microarrays celulares usando células mesenquimales permitió el cultivo de estas células en el formato de microarray hasta 8 días. Los parámetros que dieron los mejores resultados fueron: Fn200 preparada en PBS con 2% glicerol, 5 gotas por spot, pasivación con BSA, sembrado celular a 11.000 células/cm<sup>2</sup> durante 15 minutos y cultivo en medio con 1% ITS.

Finalmente, la plataforma desarrollada fue evaluada acerca de su adecuación para el estudio de estadios tempranos de diferenciación en un modelo celular. En este aspecto, se demostró que un factor de crecimiento impreso en el formato de microarray fue capaz de iniciar el camino de diferenciación en el modelo celular elegido. Sin embargo, la respuesta de diferenciación de las células empleadas en este estudio disminuyó conforme las condiciones de cultivo variaron desde el cultivo celular en placas estándar y la exposición a BMP-2 en solución hasta el cultivo en los microarrays celulares con BMP-2 impresa en los spots. Un análisis detallado demostró que el hecho de cultivar células en pequeñas cantidades en los spots aislados entre sí produjo una disminución en los resultados de diferenciación, probablemente como consecuencia de la falta de señalización adicional entre células (por contacto celular directo, señalización paracrína o

bien por la restricción en la posibilidad de expandirse y proliferar), que sí tuvo lugar cuando estas se cultivaron en placas estándar.



## References

1. Stoughton, R. B., Applications of DNA microarrays in biology. *Annu. Rev. Biochem.* **2005**, 74, 53-82.
2. Seidel, M.; Niessner, R., Automated analytical microarrays: a critical review. *Anal. Bioanal. Chem.* **2008**, 391, (5), 1521-44.
3. Angenendt, P., Progress in protein and antibody microarray technology. *Drug Discov. Today* **2005**, 10, (7), 503-11.
4. Humphrey-Smith, I., Protein Biochips and Array-Based Proteomics. In *Protein arrays, biochips and proteomics : the next phase of genomic discovery*, Albala, J. S.; Humphrey-Smith, I., Eds. Marcel Dekker, Inc.: New York, 2003; pp 1-82.
5. Heller, M. J., DNA microarray technology: devices, systems, and applications. *Annu. Rev. Biomed. Eng.* **2002**, 4, 129-53.
6. Hartmann, M.; Roeraade, J.; Stoll, D.; Templin, M.; Joos, T., Protein microarrays for diagnostic assays. *Anal. Bioanal. Chem.* **2009**, 393, (5), 1407-1416.
7. Southern, E. M., DNA microarrays. In *DNA arrays : methods and protocols*, Rampal, J. B., Ed. Human Press: Totowa, NJ, 2001; Vol. 170, pp 1-15.
8. Kafatos, F. C.; Jones, C. W.; Efstratiadis, A., Determination of nucleic acid sequence homologies and relative concentrations by a dot hybridization procedure. *Nucleic Acids Res.* **1979**, 7, (6), 1541-52.
9. Maskos, U. A novel method of nucleic acid sequence analysis. Thesis (D Phil ), University of Oxford, Oxford, UK, 1991.
10. Maskos, U.; Southern, E. M., A novel method for the analysis of multiple sequence variants by hybridisation to oligonucleotides. *Nucleic Acids Res.* **1993**, 21, (9), 2267-8.
11. Fodor, S. P.; Read, J. L.; Pirrung, M. C.; Stryer, L.; Lu, A. T.; Solas, D., Light-directed, spatially addressable parallel chemical synthesis. *Science* **1991**, 251, (4995), 767-73.
12. Pease, A. C.; Solas, D.; Sullivan, E. J.; Cronin, M. T.; Holmes, C. P.; Fodor, S. P., Light-generated oligonucleotide arrays for rapid DNA sequence analysis. *Proc. Natl. Acad. Sci. USA* **1994**, 91, (11), 5022-6.
13. McGall, G. H.; Fidanza, J. A., Photolithographic Synthesis of High-Density Oligonucleotide Arrays In *DNA arrays : methods and protocols*, Rampal, J. B., Ed. Human Press: Totowa, NJ, 2001; Vol. 170, pp 71-101.
14. Lashkari, D. A.; DeRisi, J. L.; McCusker, J. H.; Namath, A. F.; Gentile, C.; Hwang, S. Y.; Brown, P. O.; Davis, R. W., Yeast microarrays for genome wide parallel genetic and gene expression analysis. *Proc. Natl. Acad. Sci. USA* **1997**, 94, (24), 13057-62.
15. Alizadeh, A. A.; Eisen, M. B.; Davis, R. E.; Ma, C.; Lossos, I. S.; Rosenwald, A.; Boldrick, J. G.; Sabet, H.; Tran, T.; Yu, X.; Powell, J. I.; Yang, L. M.; Marti, G. E.; Moore, T.; Hudson, J.; Lu, L. S.; Lewis, D. B.; Tibshirani, R.; Sherlock, G.; Chan, W. C.; Greiner, T. C.; Weisenburger, D. D.; Armitage, J. O.; Warnke, R.; Levy, R.; Wilson, W.; Grever, M. R.; Byrd, J. C.; Botstein, D.; Brown, P. O.; Staudt, L. M., Distinct types of diffuse large B-cell lymphoma identified by gene expression profiling. *Nature* **2000**, 403, (6769), 503-511.
16. van't Veer, L. J.; Dai, H. Y.; van de Vijver, M. J.; He, Y. D. D.; Hart, A. A. M.; Mao, M.; Peterse, H. L.; van der Kooy, K.; Marton, M. J.; Witteveen, A. T.; Schreiber, G. J.; Kerkhoven, R. M.;

- Roberts, C.; Linsley, P. S.; Bernards, R.; Friend, S. H., Gene expression profiling predicts clinical outcome of breast cancer. *Nature* **2002**, 415, (6871), 530-536.
17. Weinstein, J. N.; Myers, T. G.; OConnor, P. M.; Friend, S. H.; Fornace, A. J.; Kohn, K. W.; Fojo, T.; Bates, S. E.; Rubinstein, L. V.; Anderson, N. L.; Buolamwini, J. K.; vanOsdol, W. W.; Monks, A. P.; Scudiero, D. A.; Sausville, E. A.; Zaharevitz, D. W.; Bunow, B.; Viswanadhan, V. N.; Johnson, G. S.; Wittes, R. E.; Paull, K. D., An information-intensive approach to the molecular pharmacology of cancer. *Science* **1997**, 275, (5298), 343-349.
18. Jones, S.; Zhang, X.; Parsons, D. W.; Lin, J. C.; Leary, R. J.; Angenendt, P.; Mankoo, P.; Carter, H.; Kamiyama, H.; Jimeno, A.; Hong, S. M.; Fu, B.; Lin, M. T.; Calhoun, E. S.; Kamiyama, M.; Walter, K.; Nikolskaya, T.; Nikolsky, Y.; Hartigan, J.; Smith, D. R.; Hidalgo, M.; Leach, S. D.; Klein, A. P.; Jaffee, E. M.; Goggins, M.; Maitra, A.; Iacobuzio-Donahue, C.; Eshleman, J. R.; Kern, S. E.; Hruban, R. H.; Karchin, R.; Papadopoulos, N.; Parmigiani, G.; Vogelstein, B.; Velculescu, V. E.; Kinzler, K. W., Core signaling pathways in human pancreatic cancers revealed by global genomic analyses. *Science* **2008**, 321, (5897), 1801-6.
19. Hughes, T. R.; Marton, M. J.; Jones, A. R.; Roberts, C. J.; Stoughton, R.; Armour, C. D.; Bennett, H. A.; Coffey, E.; Dai, H.; He, Y. D.; Kidd, M. J.; King, A. M.; Meyer, M. R.; Slade, D.; Lum, P. Y.; Stepaniants, S. B.; Shoemaker, D. D.; Gachotte, D.; Chakraburty, K.; Simon, J.; Bard, M.; Friend, S. H., Functional discovery via a compendium of expression profiles. *Cell* **2000**, 102, (1), 109-26.
20. McMillian, M.; Nie, A. Y.; Parker, J. B.; Leone, A.; Kemmerer, M.; Bryant, S.; Herlich, J.; Yieh, L.; Bittner, A.; Liu, X.; Wan, J.; Johnson, M. D., Inverse gene expression patterns for macrophage activating hepatotoxicants and peroxisome proliferators in rat liver. *Biochem. Pharmacol.* **2004**, 67, (11), 2141-65.
21. Behr, M. A.; Wilson, M. A.; Gill, W. P.; Salamon, H.; Schoolnik, G. K.; Rane, S.; Small, P. M., Comparative genomics of BCG vaccines by whole-genome DNA microarray. *Science* **1999**, 284, (5419), 1520-1523.
22. MacBeath, G., Protein microarrays and proteomics. *Nat. Genet.* **2002**, 32 Suppl, 526-32.
23. Chang, T. W., Binding of cells to matrixes of distinct antibodies coated on solid surface. *J. Immunol. Methods* **1983**, 65, (1-2), 217-23.
24. Ekins, R.; Chu, F.; Micallef, J., High specific activity chemiluminescent and fluorescent markers: their potential application to high sensitivity and 'multi-analyte' immunoassays. *J. Biolumin. Chemilumin.* **1989**, 4, (1), 59-78.
25. Haab, B., Practical Approaches to Protein Microarrays. In *Protein arrays, biochips and proteomics : the next phase of genomic discovery*, Albala, J. S.; Humphery-Smith, I., Eds. Marcel Dekker, Inc.: New York, 2003; pp 127-144.
26. Hanash, S., Disease proteomics. *Nature* **2003**, 422, (6928), 226-232.
27. Templin, M. F.; Stoll, D.; Schrenk, M.; Traub, P. C.; Vohringer, C. F.; Joos, T. O., Protein microarray technology. *Trends Biotechnol.* **2002**, 20, (4), 160-166.
28. Kusnezow, W.; Jacob, A.; Walijew, A.; Diehl, F.; Hoheisel, J. D., Antibody microarrays: an evaluation of production parameters. *Proteomics* **2003**, 3, (3), 254-64.
29. Afanassiev, V.; Hanemann, V.; Wolf, S., Preparation of DNA and protein micro arrays on glass slides coated with an agarose film. *Nucleic Acids Res.* **2000**, 28, (12), E66.
30. Wingren, C.; Borrebaeck, C. A. K., Antibody-Based Microarrays. In *Microchip methods in diagnostics*, Bilitewski, U., Ed. Humana: New York, 2009; Vol. 509, pp 57-84.
31. Peluso, P.; Wilson, D. S.; Do, D.; Tran, H.; Venkatasubbaiah, M.; Quincy, D.; Heidecker, B.; Poindexter, K.; Tolani, N.; Phelan, M.; Witte, K.; Jung, L. S.; Wagner, P.; Nock, S., Optimizing antibody immobilization strategies for the construction of protein microarrays. *Anal. Biochem.* **2003**, 312, (2), 113-24.

32. Zhu, H.; Bilgin, M.; Bangham, R.; Hall, D.; Casamayor, A.; Bertone, P.; Lan, N.; Jansen, R.; Bidlingmaier, S.; Houfek, T.; Mitchell, T.; Miller, P.; Dean, R. A.; Gerstein, M.; Snyder, M., Global analysis of protein activities using proteome chips. *Science* **2001**, 293, (5537), 2101-5.
33. Chen, C. S.; Zhu, H., Protein microarrays. *BioTechniques* **2006**, 40, (4), 423, 425, 427, 429.
34. Zhu, H.; Bilgin, M.; Snyder, M., Proteomics. *Annu. Rev. Biochem.* **2003**, 72, 783-812.
35. MacBeath, G.; Schreiber, S. L., Printing proteins as microarrays for high-throughput function determination. *Science* **2000**, 289, (5485), 1760-1763.
36. Chen, D. S.; Davis, M. M., Molecular and functional analysis using live cell microarrays. *Curr. Opin. Chem. Biol.* **2006**, 10, (1), 28-34.
37. Mei, Y.; Goldberg, M.; Anderson, D., The development of high-throughput screening approaches for stem cell engineering. *Curr. Opin. Chem. Biol.* **2007**, 11, (4), 388-93.
38. Fernandes, T. G.; Diogo, M. M.; Clark, D. S.; Dordick, J. S.; Cabral, J. M. S., High-throughput cellular microarray platforms: applications in drug discovery, toxicology and stem cell research. *Trends Biotechnol.* **2009**, 27, (6), 342-349.
39. Underhill, G. H.; Bhatia, S. N., High-throughput analysis of signals regulating stem cell fate and function. *Curr. Opin. Chem. Biol.* **2007**, 11, (4), 357-66.
40. Folch, A.; Toner, M., Microengineering of cellular interactions. *Annu. Rev. Biomed. Eng.* **2000**, 2, 227-56.
41. Ito, Y., Covalently immobilized biosignal molecule materials for tissue engineering. *Soft Matter* **2008**, 4, (1), 46-56.
42. Nelson, C. M.; Raghavan, S.; Tan, J. L.; Chen, C. S., Degradation of micropatterned surfaces by cell-dependent and -independent processes. *Langmuir* **2003**, 19, (5), 1493-1499.
43. Fernandes, T. G.; Kwon, S. J.; Lee, M. Y.; Clark, D. S.; Cabral, J. M.; Dordick, J. S., On-chip, cell-based microarray immunofluorescence assay for high-throughput analysis of target proteins. *Anal. Chem.* **2008**, 80, (17), 6633-9.
44. Lee, M. Y.; Kumar, R. A.; Sukumaran, S. M.; Hogg, M. G.; Clark, D. S.; Dordick, J. S., Three-dimensional cellular microarray for high-throughput toxicology assays. *Proc. Natl. Acad. Sci. USA* **2008**, 105, (1), 59-63.
45. Bailey, S. N.; Ali, S. M.; Carpenter, A. E.; Higgins, C. O.; Sabatini, D. M., Microarrays of lentiviruses for gene function screens in immortalized and primary cells. *Nat. Methods* **2006**, 3, (2), 117-22.
46. Campbell, P. G.; Miller, E. D.; Fisher, G. W.; Walker, L. M.; Weiss, L. E., Engineered spatial patterns of FGF-2 immobilized on fibrin direct cell organization. *Biomaterials* **2005**, 26, (33), 6762-70.
47. Lee, J. Y.; Shah, S. S.; Zimmer, C. C.; Liu, G. Y.; Revzin, A., Use of Photolithography to Encode Cell Adhesive Domains into Protein Microarrays. *Langmuir* **2008**, 24, (5), 2232-2239.
48. Soen, Y.; Mori, A.; Palmer, T. D.; Brown, P. O., Exploring the regulation of human neural precursor cell differentiation using arrays of signaling microenvironments. *Mol. Syst. Biol.* **2006**, 2, 37.
49. Jones, C. N.; Tuleuova, N.; Lee, J. Y.; Ramanculov, E.; Reddi, A. H.; Zern, M. A.; Revzin, A., Cultivating liver cells on printed arrays of hepatocyte growth factor. *Biomaterials* **2009**, 30, (22), 3733-3741.
50. Flaim, C. J.; Chien, S.; Bhatia, S. N., An extracellular matrix microarray for probing cellular differentiation. *Nat. Methods* **2005**, 2, (2), 119-25.
51. Flaim, C. J.; Teng, D.; Chien, S.; Bhatia, S. N., Combinatorial signaling microenvironments for studying stem cell fate. *Stem Cells Dev.* **2008**, 17, (1), 29-39.

52. Chen, D. S.; Soen, Y.; Stuge, T. B.; Lee, P. P.; Weber, J. S.; Brown, P. O.; Davis, M. M., Marked differences in human melanoma antigen-specific T cell responsiveness after vaccination using a functional microarray. *PLoS Med.* **2005**, 2, (10), e265.
53. Kuschel, C.; Steuer, H.; Maurer, A. N.; Kanzok, B.; Stoop, R.; Angres, B., Cell adhesion profiling using extracellular matrix protein microarrays. *BioTechniques* **2006**, 40, (4), 523-31.
54. Nakajima, M.; Ishimuro, T.; Kato, K.; Ko, I. K.; Hirata, I.; Arima, Y.; Iwata, H., Combinatorial protein display for the cell-based screening of biomaterials that direct neural stem cell differentiation. *Biomaterials* **2007**, 28, (6), 1048-60.
55. Jones, C. N.; Lee, J. Y.; Zhu, J.; Stybayeva, G.; Ramanculov, E.; Zern, M. A.; Revzin, A., Multifunctional protein microarrays for cultivation of cells and immunodetection of secreted cellular products. *Anal. Chem.* **2008**, 80, (16), 6351-7.
56. Zhu, H.; Stybayeva, G.; Macal, M.; Ramanculov, E.; George, M. D.; Dandekar, S.; Revzin, A., A microdevice for multiplexed detection of T-cell-secreted cytokines. *Lab Chip* **2008**, 8, (12), 2197-205.
57. Ceriotti, L.; Buzanska, L.; Rauscher, H.; Mannelli, I.; Sirghi, L.; Gilliland, D.; Hasiwa, M.; Bretagnol, F.; Zychowicz, M.; Ruiz, A.; Bremer, S.; Coecke, S.; Colpo, P.; Rossi, F., Fabrication and characterization of protein arrays for stem cell patterning. *Soft Matter* **2009**, 5, (7), 1406-14016.
58. Kurkuri, M. D.; Driever, C.; Johnson, G.; McFarland, G.; Thissen, H.; Voelcker, N. H., Multifunctional Polymer Coatings for Cell Microarray Applications. *Biomacromol.* **2009**, 10, (5), 1163-1172.
59. Roth, E. A.; Xu, T.; Das, M.; Gregory, C.; Hickman, J. J.; Boland, T., Inkjet printing for high-throughput cell patterning. *Biomaterials* **2004**, 25, (17), 3707-15.
60. Monchaux, E.; Vermette, P., Bioactive microarrays immobilized on low-fouling surfaces to study specific endothelial cell adhesion. *Biomacromol.* **2007**, 8, (11), 3668-73.
61. LaBarge, M. A.; Nelson, C. M.; Villadsen, R.; Fridriksdottir, A.; Ruth, J. R.; Stampfer, M. R.; Petersen, O. W.; Bissell, M. J., Human mammary progenitor cell fate decisions are products of interactions with combinatorial microenvironments. *Integr. Biol.* **2009**, 1, (1), 70-79.
62. Anderson, D. G.; Levenberg, S.; Langer, R., Nanoliter-scale synthesis of arrayed biomaterials and application to human embryonic stem cells. *Nat. Biotechnol.* **2004**, 22, (7), 863-6.
63. Anderson, D. G.; Putnam, D.; Lavik, E. B.; Mahmood, T. A.; Langer, R., Biomaterial microarrays: rapid, microscale screening of polymer-cell interaction. *Biomaterials* **2005**, 26, (23), 4892-7.
64. Benoit, D. S.; Schwartz, M. P.; Durney, A. R.; Anseth, K. S., Small functional groups for controlled differentiation of hydrogel-encapsulated human mesenchymal stem cells. *Nat. Mater.* **2008**, 7, (10), 816-23.
65. Peterbauer, T.; Heitz, J.; Olbrich, M.; Hering, S., Simple and versatile methods for the fabrication of arrays of live mammalian cells. *Lab Chip* **2006**, 6, (7), 857-63.
66. Miller, E. D.; Fisher, G. W.; Weiss, L. E.; Walker, L. M.; Campbell, P. G., Dose-dependent cell growth in response to concentration modulated patterns of FGF-2 printed on fibrin. *Biomaterials* **2006**, 27, (10), 2213-21.
67. Phillipi, J. A.; Miller, E.; Weiss, L.; Huard, J.; Waggoner, A.; Campbell, P., Microenvironments engineered by inkjet bioprinting spatially direct adult stem cells toward muscle- and bone-like subpopulations. *Stem Cells* **2008**, 26, (1), 127-34.
68. Rodriguez-Segui, S. A.; Pla-Roca, M.; Engel, E.; Planell, J. A.; Martinez, E.; Samitier, J., Influence of fabrication parameters in cellular microarrays for stem cell studies. *J. Mater. Sci. Mater. Med.* **2009**, 20, (7), 1525-1533.
69. Falconnet, D.; Csucs, G.; Grandin, H. M.; Textor, M., Surface engineering approaches to micropattern surfaces for cell-based assays. *Biomaterials* **2006**, 27, (16), 3044-63.

70. Doyle, A.; Mather, J. P., Culture environment. In *Cell and tissue culture: laboratory procedures in biotechnology*, Doyle, A.; Griffiths, J. B., Eds. John Wiley & Sons: New York, 1998; pp 83-91.
71. Belov, L.; de la Vega, O.; dos Remedios, C. G.; Mulligan, S. P.; Christopherson, R. I., Immunophenotyping of leukemias using a cluster of differentiation antibody microarray. *Cancer Res.* **2001**, 61, (11), 4483-4489.
72. Keller, G., Embryonic stem cell differentiation: emergence of a new era in biology and medicine. *Genes Dev.* **2005**, 19, (10), 1129-1155.
73. Phinney, D. G.; Prockop, D. J., Concise review: mesenchymal stem/multipotent stromal cells: the state of transdifferentiation and modes of tissue repair--current views. *Stem Cells* **2007**, 25, (11), 2896-902.
74. Pittenger, M. F.; Mackay, A. M.; Beck, S. C.; Jaiswal, R. K.; Douglas, R.; Mosca, J. D.; Moorman, M. A.; Simonetti, D. W.; Craig, S.; Marshak, D. R., Multilineage potential of adult human mesenchymal stem cells. *Science* **1999**, 284, (5411), 143-147.
75. Kajstura, J.; Rota, M.; Whang, B.; Cascapera, S.; Hosoda, T.; Bearzi, C.; Nurzynska, D.; Kasahara, H.; Zias, E.; Bonafe, M.; Nadal-Ginard, B.; Torella, D.; Nascimbene, A.; Quaini, F.; Urbanek, K.; Leri, A.; Anversa, P., Bone marrow cells differentiate in cardiac cell lineages after infarction independently of cell fusion. *Circul. Res.* **2005**, 96, (1), 127-37.
76. Fuchs, E.; Tumbar, T.; Guasch, G., Socializing with the neighbors: Stem cells and their niche. *Cell* **2004**, 116, (6), 769-778.
77. Yamanaka, S., A Fresh Look at iPS Cells. *Cell* **2009**, 137, (1), 13-17.
78. Takahashi, K.; Tanabe, K.; Ohnuki, M.; Narita, M.; Ichisaka, T.; Tomoda, K.; Yamanaka, S., Induction of pluripotent stem cells from adult human fibroblasts by defined factors. *Cell* **2007**, 131, (5), 861-72.
79. Wilson, A.; Trumpp, A., Bone-marrow haematopoietic-stem-cell niches. *Nat. Rev. Immunol.* **2006**, 6, (2), 93-106.
80. Giancotti, F. G.; Ruoslahti, E., Integrin signaling. *Science* **1999**, 285, (5430), 1028-32.
81. Hughes, F. J.; Turner, W.; Belibasakis, G.; Martuscelli, G., Effects of growth factors and cytokines on osteoblast differentiation. *Periodontology 2000* **2006**, 41, 48-72.
82. Adams, J. C.; Watt, F. M., Regulation of development and differentiation by the extracellular matrix. *Development* **1993**, 117, (4), 1183-98.
83. Pittenger, M. F.; Martin, B. J., Mesenchymal stem cells and their potential as cardiac therapeutics. *Circul. Res.* **2004**, 95, (1), 9-20.
84. Ziauddin, J.; Sabatini, D. M., Microarrays of cells expressing defined cDNAs. *Nature* **2001**, 411, (6833), 107-10.
85. Yoshikawa, T.; Uchimura, E.; Kishi, M.; Funeriu, D. P.; Miyake, M.; Miyake, J., Transfection microarray of human mesenchymal stem cells and on-chip siRNA gene knockdown. *J. Controlled Release* **2004**, 96, (2), 227-32.
86. Angenendt, P.; Glokler, J.; Murphy, D.; Lehrach, H.; Cahill, D. J., Toward optimized antibody microarrays: a comparison of current microarray support materials. *Anal. Biochem.* **2002**, 309, (2), 253-60.
87. Seurynck-Servoss, S. L.; White, A. M.; Baird, C. L.; Rodland, K. D.; Zangar, R. C., Evaluation of surface chemistries for antibody microarrays. *Anal. Biochem.* **2007**, 371, (1), 105-15.
88. Guilleaume, B.; Buness, A.; Schmidt, C.; Klimek, F.; Moldenhauer, G.; Huber, W.; Arlt, D.; Korf, U.; Wiemann, S.; Poustka, A., Systematic comparison of surface coatings for protein microarrays. *Proteomics* **2005**, 5, (18), 4705-12.

89. Castner, D. G.; Ratner, B. D., Biomedical surface science: Foundations to frontiers. *Surf. Sci.* **2002**, 500, (1-3), 28-60.
90. Bretagnol, F.; Lejeune, M.; Papadopoulou-Bouraoui, A.; Hasiwa, M.; Rauscher, H.; Ceccone, G.; Colpo, P.; Rossi, F., Fouling and non-fouling surfaces produced by plasma polymerization of ethylene oxide monomer. *Acta Biomater.* **2006**, 2, (2), 165-72.
91. Ruiz, A.; Buzanska, L.; Gilliland, D.; Rauscher, H.; Sirghi, L.; Sobanski, T.; Zychowicz, M.; Ceriotti, L.; Bretagnol, F.; Coecke, S.; Colpo, P.; Rossi, F., Micro-stamped surfaces for the patterned growth of neural stem cells. *Biomaterials* **2008**, 29, (36), 4766-74.
92. Roach, P.; Shirtcliffe, N. J.; Farrar, D.; Perry, C. C., Quantification of surface-bound proteins by fluorometric assay: Comparison with quartz crystal microbalance and amido black assay. *J. Phys. Chem. B* **2006**, 110, (41), 20572-9.
93. Vertegel, A. A.; Siegel, R. W.; Dordick, J. S., Silica nanoparticle size influences the structure and enzymatic activity of adsorbed lysozyme. *Langmuir* **2004**, 20, (16), 6800-7.
94. Rodríguez Seguí, S.; Pla, M.; Minic, J.; Pajot-Augy, E.; Salesse, R.; Hou, Y.; Jaffrezic-Renault, N.; Mills, C. A.; Samitier, J.; Errachid, A., Detection of Olfactory Receptor 17 Self-Assembled Multilayer Formation and Immobilization Using a Quartz Crystal Microbalance. *Anal. Lett.* **2006**, 39, 1735-1745.
95. Tengvall, P.; Lundstrom, I.; Liedberg, B., Protein adsorption studies on model organic surfaces: an ellipsometric and infrared spectroscopic approach. *Biomaterials* **1998**, 19, (4-5), 407-22.
96. Hook, F.; Voros, J.; Rodahl, M.; Kurrat, R.; Boni, P.; Ramsden, J. J.; Textor, M.; Spencer, N. D.; Tengvall, P.; Gold, J.; Kasemo, B., A comparative study of protein adsorption on titanium oxide surfaces using in situ ellipsometry, optical waveguide lightmode spectroscopy, and quartz crystal microbalance/dissipation. *Colloids Surf. B. Biointerfaces* **2002**, 24, (2), 155-170.
97. Mrksich, M.; Sigal, G. B.; Whitesides, G. M., Surface Plasmon Resonance Permits in Situ Measurement of Protein Adsorption on Self-Assembled Monolayers of Alkanethiolates on Gold. *Langmuir* **1995**, 11, (11), 4383-4385.
98. Silin, V. V.; Weetall, H.; Vanderah, D. J., SPR Studies of the Nonspecific Adsorption Kinetics of Human IgG and BSA on Gold Surfaces Modified by Self-Assembled Monolayers (SAMs). *J. Colloid Interface Sci.* **1997**, 185, (1), 94-103.
99. Browne, M. M.; Lubarsky, G. V.; Davidson, M. R.; Bradley, R. H., Protein adsorption onto polystyrene surfaces studied by XPS and AFM. *Surf. Sci.* **2004**, 553, (1-3), 155-167.
100. Lowe, A. M.; Ozer, B. H.; Wiepz, G. J.; Bertics, P. J.; Abbott, N. L., Engineering of PDMS surfaces for use in microsystems for capture and isolation of complex and biomedically important proteins: Epidermal growth factor receptor as a model system. *Lab Chip* **2008**, 8, (8), 1357-1364.
101. Hynd, M. R.; Frampton, J. P.; Dowell-Mesfin, N.; Turner, J. N.; Shain, W., Directed cell growth on protein-functionalized hydrogel surfaces. *J. Neurosci. Methods* **2007**, 162, (1-2), 255-63.
102. McQuain, M. K.; Seale, K.; Peek, J.; Levy, S.; Haselton, F. R., Effects of relative humidity and buffer additives on the contact printing of microarrays by quill pins. *Anal. Biochem.* **2003**, 320, (2), 281-291.
103. Wu, P.; Grainger, D. W., Comparison of hydroxylated print additives on antibody microarray performance. *J. Proteome Res.* **2006**, 5, (11), 2956-2965.
104. Lv, L. L.; Liu, B. C.; Zhang, C. X.; Tang, Z. M.; Zhang, L.; Lu, Z. H., Construction of an antibody microarray based on agarose-coated slides. *Electrophoresis* **2007**, 28, (3), 406-13.
105. Hyun, J.; Zhu, Y. J.; Liebmann-Vinson, A.; Beebe, T. P.; Chilkoti, A., Microstamping on an activated polymer surface: Patterning biotin and streptavidin onto common polymeric biomaterials. *Langmuir* **2001**, 17, (20), 6358-6367.

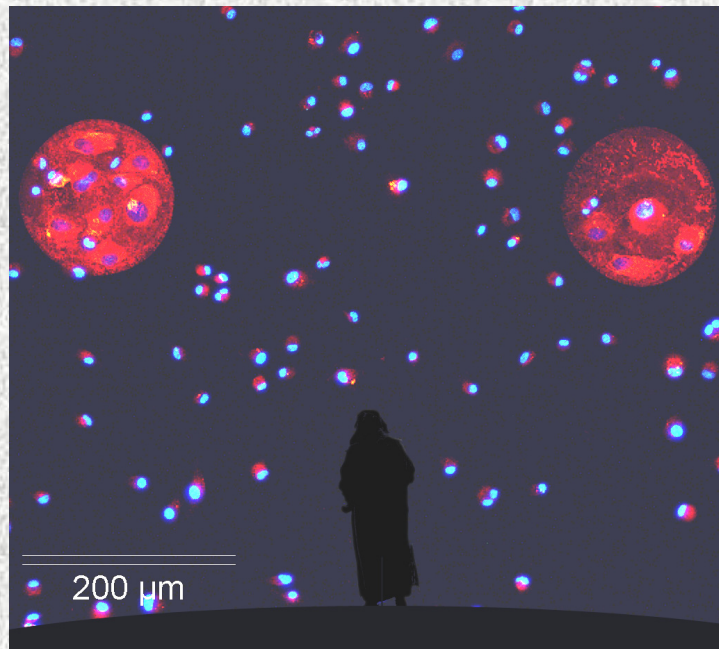
106. Belegrinou, S.; Mannelli, I.; Lisboa, P.; Bretagnol, F.; Valsesia, A.; Ceccone, G.; Colpo, P.; Rauscher, H.; Rossi, F., pH-dependent immobilization of proteins on surfaces functionalized by plasma-enhanced chemical vapor deposition of poly(acrylic acid)- and poly(ethylene oxide)-like films. *Langmuir* **2008**, 24, (14), 7251-61.
107. Horcas, I.; Fernandez, R.; Gomez-Rodriguez, J. M.; Colchero, J.; Gomez-Herrero, J.; Baro, A. M., WSXM: a software for scanning probe microscopy and a tool for nanotechnology. *Rev. Sci. Instrum.* **2007**, 78, (1), 013705.
108. R\_Development\_Core\_Team. *R: A language and environment for statistical computing*. R Foundation for Statistical Computing, Vienna, Austria, 2008.
109. Smith, J. T.; Viglianti, B. L.; Reichert, W. M., Spreading diagrams for the optimization of quill pin printed microarray density. *Langmuir* **2002**, 18, (16), 6289-6293.
110. Roach, P.; Eglin, D.; Rohde, K.; Perry, C. C., Modern biomaterials: a review-bulk properties and implications of surface modifications. *J. Mater. Sci. Mater. Med.* **2007**, 18, (7), 1263-1277.
111. Denis, F. A.; Hanarp, P.; Sutherland, D. S.; Gold, J.; Mustin, C.; Rouxhet, P. G.; Dufrene, Y. F., Protein adsorption on model surfaces with controlled nanotopography and chemistry. *Langmuir* **2002**, 18, (3), 819-828.
112. Velzenberger, E.; El Kirat, K.; Legeay, G.; Nagel, M. D.; Pezron, I., Characterization of biomaterials polar interactions in physiological conditions using liquid-liquid contact angle measurements Relation to fibronectin adsorption. *Colloids Surf. B. Biointerfaces* **2009**, 68, (2), 238-244.
113. Guo, Z. G.; Fang, J.; Hao, J. C.; Liang, Y. M.; Liu, W. M., A novel approach to stable superhydrophobic surfaces. *Chemphyschem* **2006**, 7, (8), 1674-7.
114. Dufrene, Y. F.; Marchal, T. G.; Rouxhet, P. G., Influence of substratum surface properties on the organization of adsorbed collagen films: In situ characterization by atomic force microscopy. *Langmuir* **1999**, 15, (8), 2871-2878.
115. Han, M.; Sethuraman, A.; Kane, R. S.; Belfort, G., Nanometer-scale roughness having little effect on the amount or structure of adsorbed protein. *Langmuir* **2003**, 19, (23), 9868-9872.
116. Rechendorff, K.; Hovgaard, M. B.; Foss, M.; Zhdanov, V. P.; Besenbacher, F., Enhancement of protein adsorption induced by surface roughness. *Langmuir* **2006**, 22, (26), 10885-10888.
117. Ruiz, A.; Buzanska, L.; Ceriotti, L.; Bretagnol, F.; Coecke, S.; Colpo, P.; Rossi, F., Stem-cell culture on patterned bio-functional surfaces. *J. Biomater. Sci.-Polym. Ed.* **2008**, 19, (12), 1649-57.
118. Ruiz, A.; Valsesia, A.; Ceccone, G.; Gilliland, D.; Colpo, P.; Rossi, F., Fabrication and characterization of plasma processed surfaces with tuned wettability. *Langmuir* **2007**, 23, (26), 12984-9.
119. Koblinski, J. E.; Wu, M.; Demeler, B.; Jacob, K.; Kleinman, H. K., Matrix cell adhesion activation by non-adhesion proteins. *J. Cell Sci.* **2005**, 118, (Pt 13), 2965-74.
120. Deng, Y.; Zhu, X. Y.; Kienlen, T.; Guo, A., Transport at the air/water interface is the reason for rings in protein microarrays. *J. Am. Chem. Soc.* **2006**, 128, (9), 2768-2769.
121. Razumovsky, L.; Damodaran, S., Surface activity-compressibility relationship of proteins at the air-water interface. *Langmuir* **1999**, 15, (4), 1392-1399.
122. Pereira, L. G. C.; Johansson, C.; Radke, C. J.; Blanch, H. W., Surface forces and drainage kinetics of protein-stabilized aqueous films. *Langmuir* **2003**, 19, (18), 7503-7513.
123. Harnett, E. M.; Alderman, J.; Wood, T., The surface energy of various biomaterials coated with adhesion molecules used in cell culture. *Colloids Surf. B. Biointerfaces* **2007**, 55, (1), 90-7.
124. Absolom, D. R.; Vanoss, C. J.; Zingg, W.; Neumann, A. W., Determination of surface tensions of proteins. 2. Surface-Tension of serum-albumin, altered at the protein-air interface. *Biochim. Biophys. Acta* **1981**, 670, (1), 74-78.

125. Sengupta, T.; Razumovsky, L.; Damodaran, S., Phase separation in two-dimensional alpha(s)-casein/beta-casein/water ternary film at the air-water interface. *Langmuir* **2000**, 16, (16), 6583-6589.
126. Koteliansky, V. E.; Glukhova, M. A.; Bejanian, M. V.; Smirnov, V. N.; Filimonov, V. V.; Zalite, O. M.; Venyaminov, S. Y., A study of the structure of fibronectin. *Eur. J. Biochem.* **1981**, 119, (3), 619-624.
127. Hendrickson, W. A.; Pahler, A.; Smith, J. L.; Satow, Y.; Merritt, E. A.; Phizackerley, R. P., Crystal structure of core streptavidin determined from multiwavelength anomalous diffraction of synchrotron radiation. *Proc. Natl. Acad. Sci. USA* **1989**, 86, (7), 2190-2194.
128. Nath, N.; Hyun, J.; Ma, H.; Chilkoti, A., Surface engineering strategies for control of protein and cell interactions. *Surf. Sci.* **2004**, 570, (1-2), 98-110.
129. Nakanishi, K.; Sakiyama, T.; Imamura, K., On the adsorption of proteins on solid surfaces, a common but very complicated phenomenon. *J. Biosci. Bioeng.* **2001**, 91, (3), 233-244.
130. Haeberli, A., *Human protein data*. VCH: Weinheim [etc.], 1992.
131. Mace, C. R.; Yadav, A. R.; Miller, B. L., Investigation of Non-Nucleophilic Additives for the Reduction of Morphological Anomalies in Protein Arrays. *Langmuir* **2008**, 24, (22), 12754-12757.
132. Akiyama, S. K.; Yamada, K. M., Fibronectin and fibronectin fragments. In *Extracellular matrix : a practical approach*, Haralson, M. A.; Hassell, J. R., Eds. Oxford University Press: Oxford, 1995; p 183.
133. Humphries, M. J.; Newham, P., The structure of cell-adhesion molecules. *Trends Cell Biol.* **1998**, 8, (2), 78-83.
134. Muraglia, A.; Cancedda, R.; Quarto, R., Clonal mesenchymal progenitors from human bone marrow differentiate in vitro according to a hierarchical model. *J. Cell Sci.* **2000**, 113, (7), 1161-1166.
135. Celil, A. B.; Campbell, P. G., BMP-2 and insulin-like growth factor-I mediate Osterix (Osx) expression in human mesenchymal stem cells via the MAPK and protein kinase D signaling pathways. *J. Biol. Chem.* **2005**, 280, (36), 31353-9.
136. Celil, A. B.; Hollinger, J. O.; Campbell, P. G., Osx transcriptional regulation is mediated by additional pathways to BMP2/Smad signaling. *J. Cell. Biochem.* **2005**, 95, (3), 518-28.
137. Gori, F.; Thomas, T.; Hicok, K. C.; Spelsberg, T. C.; Riggs, B. L., Differentiation of human marrow stromal precursor cells: bone morphogenetic protein-2 increases OSF2/CBFA1, enhances osteoblast commitment, and inhibits late adipocyte maturation. *J. Bone Miner. Res.* **1999**, 14, (9), 1522-35.
138. McBeath, R.; Pirone, D. M.; Nelson, C. M.; Bhadriraju, K.; Chen, C. S., Cell shape, cytoskeletal tension, and RhoA regulate stem cell lineage commitment. *Dev. Cell* **2004**, 6, (4), 483-95.
139. Flaim, C. J.; Chien, S.; Bhatia, S. N., An extracellular matrix microarray for probing cellular differentiation. *Nat. Methods* **2005**, 2, (2), 119-25.
140. Maniatopoulos, C.; Sodek, J.; Melcher, A. H., Bone formation in vitro by stromal cells obtained from bone marrow of young adult rats. *Cell Tissue Res.* **1988**, 254, (2), 317-30.
141. McCulloch, C. A.; Strugurescu, M.; Hughes, F.; Melcher, A. H.; Aubin, J. E., Osteogenic progenitor cells in rat bone marrow stromal populations exhibit self-renewal in culture. *Blood* **1991**, 77, (9), 1906-11.
142. Gregory, C. A.; Prockop, D. J.; Spees, J. L., Non-hematopoietic bone marrow stem cells: molecular control of expansion and differentiation. *Exp. Cell Res.* **2005**, 306, (2), 330-5.
143. Tontonoz, P.; Hu, E.; Graves, R. A.; Budavari, A. I.; Spiegelman, B. M., mPPAR-Gamma-2 - Tissue-specific regulator of an adipocyte enhancer. *Genes Dev.* **1994**, 8, (10), 1224-1234.

144. Tong, Q.; Tsai, J.; Tan, G.; Dalgin, G.; Hotamisligil, G. S., Interaction between GATA and the C/EBP family of transcription factors is critical in GATA-mediated suppression of adipocyte differentiation. *Mol. Cell. Biol.* **2005**, 25, (2), 706-15.
145. Bilgen, B.; Orsini, E.; Aaron, R. K.; Ciombor, D. M., FBS suppresses TGF-beta1-induced chondrogenesis in synoviocyte pellet cultures while dexamethasone and dynamic stimuli are beneficial. *J. Tissue Eng. Regen. Med.* **2008**, 1, (6), 436-442.
146. Mackay, A. M.; Beck, S. C.; Murphy, J. M.; Barry, F. P.; Chichester, C. O.; Pittenger, M. F., Chondrogenic differentiation of cultured human mesenchymal stem cells from marrow. *Tissue Eng.* **1998**, 4, (4), 415-28.
147. Dennis, J. E.; Fau - Carbillot, J.-P.; Carbillot, J. P.; Fau - Caplan, A. I.; Caplan, A. I.; Fau - Charbord, P.; Charbord, P., The STRO-1+ marrow cell population is multipotential. *Cells Tissues Organs* **2002**, 170, (2-3), 73-82.
148. Greenspan, P.; Mayer, E. P.; Fowler, S. D., Nile red - A selective fluorescent stain for intracellular lipid droplets. *J. Cell Biol.* **1985**, 100, (3), 965-973.
149. Unsworth, L. D.; Sheardown, H.; Brash, J. L., Polyethylene oxide surfaces of variable chain density by chemisorption of PEO-thiol on gold: Adsorption of proteins from plasma studied by radiolabelling and immunoblotting. *Biomaterials* **2005**, 26, (30), 5927-5933.
150. Malmsten, M.; Emoto, K.; Van Alstine, J. M., Effect of chain density on inhibition of protein adsorption by poly(ethylene glycol) based coatings. *J. Colloid Interface Sci.* **1998**, 202, (2), 507-517.
151. Barrett, D. G.; Yousaf, M. N., Rapid patterning of cells and cell co-cultures on surfaces with spatial and temporal control through centrifugation. *Angew. Chem.* **2007**, 46, (39), 7437-9.
152. Doyle, A.; Mather, J. P., In *Cell and tissue culture: laboratory procedures in biotechnology*, Doyle, A.; Griffiths, J. B., Eds. John Wiley & Sons: New York, 1998; pp 83-91.
153. Chen, C. S.; Mrksich, M.; Huang, S.; Whitesides, G. M.; Ingber, D. E., Geometric control of cell life and death. *Science* **1997**, 276, (5317), 1425-1428.
154. Wagner, W.; Feldmann, R. E., Jr.; Seckinger, A.; Maurer, M. H.; Wein, F.; Blake, J.; Krause, U.; Kalenka, A.; Burgers, H. F.; Saffrich, R.; Wuchter, P.; Kuschinsky, W.; Ho, A. D., The heterogeneity of human mesenchymal stem cell preparations--evidence from simultaneous analysis of proteomes and transcriptomes. *Exp. Hematol.* **2006**, 34, (4), 536-48.
155. Chen, X. D.; Dusevich, V.; Feng, J. Q.; Manolagas, S. C.; Jilka, R. L., Extracellular matrix made by bone marrow cells facilitates expansion of marrow-derived mesenchymal progenitor cells and prevents their differentiation into osteoblasts. *J. Bone Miner. Res.* **2007**, 22, (12), 1943-1956.
156. Baksh, D.; Song, L.; Tuan, R. S., Adult mesenchymal stem cells: characterization, differentiation, and application in cell and gene therapy. *J. Cell. Mol. Med.* **2004**, 8, (3), 301-316.
157. Gronthos, S.; Graves, S. E.; Ohta, S.; Simmons, P. J., The STRO-1+ fraction of adult human bone marrow contains the osteogenic precursors. *Blood* **1994**, 84, (12), 4164-4173.
158. Katagiri, T.; Yamaguchi, A.; Komaki, M.; Abe, E.; Takahashi, N.; Ikeda, T.; Rosen, V.; Wozney, J. M.; Fujisawa-Sehara, A.; Suda, T., Bone morphogenetic protein-2 converts the differentiation pathway of C2C12 myoblasts into the osteoblast lineage. *J. Cell Biol.* **1994**, 127, (6 Pt 1), 1755-66.
159. Lopez-Rovira, T.; Chalaux, E.; Massague, J.; Rosa, J. L.; Ventura, F., Direct binding of Smad1 and Smad4 to two distinct motifs mediates bone morphogenetic protein-specific transcriptional activation of Id1 gene. *J. Biol. Chem.* **2002**, 277, (5), 3176-85.
160. Ryoo, H. M.; Lee, M. H.; Kim, Y. J., Critical molecular switches involved in BMP-2-induced osteogenic differentiation of mesenchymal cells. *Gene* **2006**, 366, (1), 51-57.
161. Katagiri, T.; Imada, M.; Yanai, T.; Suda, T.; Takahashi, N.; Kamijo, R., Identification of a BMP-responsive element in Id1, the gene for inhibition of myogenesis. *Genes Cells* **2002**, 7, (9), 949-60.

162. Vinals, F.; Ventura, F., Myogenin protein stability is decreased by BMP-2 through a mechanism implicating Id1. *J. Biol. Chem.* **2004**, 279, (44), 45766-72.
163. Chen, D.; Zhao, M.; Mundy, G. R., Bone morphogenetic proteins. *Growth Factors* **2004**, 22, (4), 233-41.
164. Hirayama, K.; Akashi, S.; Furuya, M.; Fukuhara, K., Rapid confirmation and revision of the primary structure of bovine serum-albumin by ESIMS and FRIT-FAB LC MS. *Biochem. Biophys. Res. Commun.* **1990**, 173, (2), 639-646.
165. Aumailley, M.; Smyth, N., The role of laminins in basement membrane function. *J. Anat.* **1998**, 193, 1-21.
166. Suzawa, M.; Takeuchi, Y.; Fukumoto, S.; Kato, S.; Ueno, N.; Miyazono, K.; Matsumoto, T.; Fujita, T., Extracellular Matrix-Associated Bone Morphogenetic Proteins Are Essential for Differentiation of Murine Osteoblastic Cells in Vitro. *Endocrinology* **1999**, 140, (5), 2125-2133.
167. Zhu, Y.; Oganesian, A.; Keene, D. R.; Sandell, L. J., Type IIA procollagen containing the cysteine-rich amino propeptide is deposited in the extracellular matrix of prechondrogenic tissue and binds to TGF-beta 1 and BMP-2. *J. Cell Biol.* **1999**, 144, (5), 1069-1080.
168. Ruppert, R.; Hoffmann, E.; Sebald, W., Human bone morphogenetic protein 2 contains a heparin-binding site which modifies its biological activity. *Eur. J. Biochem.* **1996**, 237, (1), 295-302.
169. Hynes, R. O., Integrins: Bidirectional, allosteric signaling machines. *Cell* **2002**, 110, (6), 673-687.
170. Boudreau, J.; Jones, P. L., Extracellular matrix and integrin signalling: the shape of things to come. *Biochem. J.* **1999**, 339, 481-488.
171. Leiss, M.; Beckmann, K.; Giros, A.; Costell, M.; Fassler, R., The role of integrin binding sites in fibronectin matrix assembly in vivo. *Curr. Opin. Cell Biol.* **2008**, 20, (5), 502-507.
172. Colognato, H.; Yurchenco, P. D., Form and function: The laminin family of heterotrimers. *Dev. Dyn.* **2000**, 218, (2), 213-234.
173. Sastry, S. K.; Lakonishok, M.; Wu, S.; Truong, T. Q.; Huttenlocher, A.; Turner, C. E.; Horwitz, A. F., Quantitative changes in integrin and focal adhesion signaling regulate myoblast cell cycle withdrawal. *J. Cell Biol.* **1999**, 144, (6), 1295-1309.
174. Sastry, S. K.; Horwitz, A. F., Adhesion-growth factor interactions during differentiation: An integrated biological response. *Dev. Biol.* **1996**, 180, (2), 455-467.
175. Nissinen, L.; Pirila, L.; Heino, J., Bone morphogenetic protein-2 is a regulator of cell adhesion. *Exp. Cell Res.* **1997**, 230, (2), 377-385.
176. Ozeki, N.; Jethanandani, P.; Nakamura, H.; Ziober, B. L.; Kramer, R. H., Modulation of satellite cell adhesion and motility following BMP2-induced differentiation to osteoblast lineage. *Biochem. Biophys. Res. Commun.* **2007**, 353, (1), 54-59.
177. Sotobori, T.; Ueda, T.; Myoui, A.; Yoshioka, K.; Nakasaki, M.; Yoshikawa, H.; Itoh, K., Bone morphogenetic protein-2 promotes the haptotactic migration of murine osteoblastic and osteosarcoma cells by enhancing incorporation of integrin beta 1 into lipid rafts. *Exp. Cell Res.* **2006**, 312, (19), 3927-3938.
178. Bardouille, C.; Lehmann, J.; Heimann, P.; Jockusch, H., Growth and differentiation of permanent and secondary mouse myogenic cell lines on microcarriers. *Appl. Microbiol. Biotechnol.* **2001**, 55, (5), 556-562.
179. Liu, J. M.; Burkin, D. J.; Kaufman, S. J., Increasing alpha(7)beta(1)-integrin promotes muscle cell proliferation, adhesion, and resistance to apoptosis without changing gene expression. *Am. J. Physiol. Cell Physiol.* **2008**, 294, (2), C627-C640.

180. von der Mark, K.; Ocalan, M., Antagonistic effects of laminin and fibronectin on the expression of the myogenic phenotype. *Differentiation* **1989**, 40, (2), 150-7.
181. Beach, R. L.; Burton, W. V.; Hendricks, W. J.; Festoff, B. W., Extracellular-matrix synthesis by skeletal-muscle in culture - Proteins and effect of enzyme degradation. *J. Biol. Chem.* **1982**, 257, (19), 1437-1442.
182. Laping, N. J.; Grygielko, E.; Mathur, A.; Butter, S.; Bomberger, J.; Tweed, C.; Martin, W.; Fornwald, J.; Lehr, R.; Harling, J.; Gaster, L.; Callahan, J. F.; Olson, B. A., Inhibition of transforming growth factor (TGF)-beta 1-induced extracellular matrix with a novel inhibitor of the TGF-beta type I receptor kinase activity: SB-431542. *Mol. Pharmacol.* **2002**, 62, (1), 58-64.
183. Miyamoto, S.; Teramoto, H.; Gutkind, J. S.; Yamada, K. M., Integrins can collaborate with growth factors for phosphorylation of receptor tyrosine kinases and MAP kinase activation: Roles of integrin aggregation and occupancy of receptors. *J. Cell Biol.* **1996**, 135, (6), 1633-1642.
184. Miyamoto, S.; Akiyama, S. K.; Yamada, K. M., Synergistic roles for receptor occupancy and aggregation in integrin transmembrane function. *Science* **1995**, 267, (5199), 883-885.
185. Xiao, G. Z.; Gopalakrishnan, R.; Jiang, D.; Reith, E.; Benson, M. D.; Franceschi, R. T., Bone morphogenetic proteins, extracellular matrix, and mitogen-activated protein kinase signaling pathways are required for osteoblast-specific gene expression and differentiation in MC3T3-E1 cells. *J. Bone Miner. Res.* **2002**, 17, (1), 101-110.
186. Stern, M. M.; Myers, R. L.; Hammam, N.; Stern, K. A.; Eberli, D.; Kritchevsky, S. B.; Soker, S.; Van Dyke, M., The influence of extracellular matrix derived from skeletal muscle tissue on the proliferation and differentiation of myogenic progenitor cells ex vivo. *Biomaterials* **2009**, 30, (12), 2393-2399.



U  
B

UNIVERSITAT DE BARCELONA